The cellular and molecular basis of defects in Down syndrome fetal bone marrow B-lymphopoiesis



Caitlin Murnane

St Edmund Hall

University of Oxford

A thesis submitted for the degree of

Doctor of Philosophy

Long Vacation, 2022

Abstract

Background

Trisomy of the chromosome 21 (T21) causes a broad clinical syndrome called Down syndrome (DS). Children with DS have an increased risk of acute lymphoblastic leukaemia of DS (DS-ALL) and reports show qualitative and functional abnormalities in B-cells within trisomic individuals as young as neonatal stages, which indicates these abnormalities begin before birth. Our lab has shown that T21 perturbs haematopoiesis in fetal liver (FL), causing a bias toward the megakaryocytic and erythroid lineages at the expense of B-progenitors. Preliminary work suggests this is also the case in fetal bone marrow (FBM), the main site of B-lymphopoiesis before birth. Thus far, most work on lymphoid defects of DS, particularly in fetal tissue, has focused on B-cell development despite reports that T21 disrupts both T/NK lymphocytes. Therefore, it is unclear whether impairments are specific to the B-lineage or the result of disrupted pan-lymphoid differentiation. The exact mechanisms for how T21 impacts haematopoiesis are unknown. Several genes which have roles in haematopoiesis including *RUNX1, BACH1, ERG* and *DYRK1A*, are encoded on chromosome 21 and their altered expression may disrupt haematopoiesis. More recent evidence suggests that epigenetic mechanisms may also play a role.

Aim

The aim of this project was to refine the existing model fetal B-lymphopoiesis use this as a reference point to i) identify the specific immunophenotypic and functional differences in B-progenitor differentiation between normal and DS FBM and ii) to understand these changes at the molecular level.

Results

Discovery of new lymphomyeloid progenitors in FBM helps refine the fetal B-lymphopoiesis model:
Immunophenotypic profiling of normal and DS FBM revealed the existence of 3 newly described progenitors: CD10-/+ LMPP and Pre-ELP/GMP. Extensive functional characterisation places CD10- LMPP upstream of both CD10+LMPP and Pre-ELP/GMP in the differentiation hierarchy and reveals these populations support the expansion of B-cells in FBM. Whilst CD10- LMPP and Pre-ELP/GMP

also show myeloid potential, CD10+LMPP are comparatively lymphoid primed. Preliminary immunophenotyping of cord blood (CB), suggests that Pre-ELP/GMP are enriched in FBM, like other CD10- progenitors: ELP and PreProB, and the frequency of CD10+LMPP is significantly expanded in CB relative to FBM.

The functional impact of T21 on B-lymphopoiesis in FBM: Immunophenotyping of DS FBM shows large-scale alterations to HSPC frequencies including a significant depletion of B-progenitors, most severely the CD10- ELP and PreProB and a significant expansion of HSCs and MEPs. Interestingly, CD10+ LMPP, which are rare in FBM, are significantly expanded in DS and ProB show a less severe reduction, suggesting that CD10-/+ HSPCs are affected differently in DS. Functional assays reveal a severe B-cell defect in upstream and intermediate DS HSPCs. T-cell differentiation is also impaired, but less markedly and CD10-LMPP and Pre-ELP/GMP appear to be junctions through which myeloid biasing is propagated. Interestingly, almost all of the DS FBM HSPCs showed an NK bias, which is the first time this has been described in fetal tissue. DS FBM HSCs and MPPs showed a significant erythroid bias on methylcellulose.

Understanding the impact of T21 on FBM HSPCs at the molecular level: Gene expression and chromatin accessibility profiles demonstrate that CD10-LMPP and Pre-ELP/GMP are distinct populations. Clustering based on gene expression and chromatin accessibility profiles resolves the proposed lineage hierarchies in FBM, but these are altered in DS where Pre-ELP/GMP and MPP show greater similarity to GMP and MEP respectively. RNA sequencing of several DS FBM HSPCs including the newly described progenitors revealed significantly reduced expression of several B-cell genes and elevated expression of genes associated with the myeloid, mega-erythroid and – to a lesser degree- NK lineages.

Conclusions

The identification and characterisation of new progenitor populations in FBM has facilitated existing models of fetal B-lymphopoiesis to be refined. In DS FBM, lymphopoiesis is disrupted with a severe block in B-cell differentiation that appears to occur upstream and is propagated through the newly described progenitors, as well as moderately impaired T-cell development and a skew toward NK lymphopoiesis. These findings were validated at the molecular level, with T21 causing broad changes in both the transcriptome and chromatin accessibility of FBM HSPCs.

Acknowledgements

First and foremost, I want to thank the women who donated fetal samples to this work. This project would not have been possible without this deeply personal and for many, emotional sacrifice.
I also want to give pause to recognise the millions of people living with Down syndrome today, hopefully living fuller lives than the generations before them. For me, this project has been one of fascination and passion, but for people with Down syndrome facing the risks of leukaemia and living with a disrupted immune system are day to day, sometimes fatal struggles. As scientists it's easy to get caught up in running experiments and forget why we are here and who we are working for.
To add my efforts to the many others who have made far greater contributions to our field in the hope of finding life-changing therapies, has been an immense privilege.

This work would not have been possible without my supervisors Professors Irene Roberts and Andi Roy. To say that I stand on the shoulders of giants would be the greatest understatement. Having access to Irene and Andi's (many) ideas, advice and support, has been invaluable. I know few students who have benefited from such engaged supervision. It was during my PhD that my determination to study medicine blossomed, and I thank my supervisors for their practical support during those applications. I can only hope I have given the lab half as much as you have both given me.
I would also like to thank my supervisor Prof. Claus Nerlov for his useful ideas and suggestions which have helped guide my project.

I am also very grateful for the encouragement and support during my thesis committees and both transfer and confirmation milestones. Thank you to Prof. Doug Higgs, Prof. Catherine Porcher and Prof. Beth Psaila, whose collective input helped guide me toward submission.

This work would not have been possible and my PhD would have been far less enjoyable without the camaraderie of my lab. Special thanks go to Siobhan, Natalina and Lucy for their help (and patience) with my experiments. Thanks to Tom, Lena, Marcela and Rebecca for looking out for me and helping me find reasons to smile on challenging days. Siobhan Rice and Joe Harman were immensely helpful when I was learning to code, thank you both for helping me believe in myself and for making this new virtual world feel less daunting!

Within the wider WIMM, I want to warmly thank all of the members of the flow cytometry facility. Paul, Kevin, Sally and Craig not only helped me learn the wizardry of FACS, but became my friends over the pain-staking 10 hour sorts I roped them into. We are so lucky to have you here at the WIMM.

Thanks to Zoe, Philip and Ryan within the genome-engineering team who welcomed me to the WIMM in my first year and have kept an eye out for me ever since.
Otherwise, I'd like to thank my WIMM friends and colleagues. These include Jenni and Nigel who I loved sharing a lab space with, Sue for the giggles, Shams and my WIMMies cohort- especially Grigore, Spencer and Ali.

Outside of work, there are too many people to mention that have fortified me during this PhD which has been extremely academically and personally challenging. Megan, thank you for being the best inspiration I could ask for, I look forward to following in your footsteps. Thank you to my amazing extended Oxford family who have made this magical, bizarre place less daunting. Special mention goes to Nina and Conrad, thank you for nurturing my spark to finally pursue medicine and for making my dreams feel like a possibility. Thank you to Ruth, Dan, Rich, Franci, Kate, Bruce, Esme, Shams, Robin, Oli, Katie, Helen, Alice, Shannon, Sian, Mo and many others for always being there for a pep talk.

Finally, I want to thank the most important people within this journey: my loved ones. Thank you to my mum and John for the jokes during days when I felt woefully inadequate and for constantly checking in on me. Thank you to Kieran and Lou for helping me let off some much-needed steam through the medium of Plush and wild swimming. Thank you to Cheryl, Lucy and Jay, auntie Dee, Uncle Nath, Ash and Grandma for loving me through this process. I wish my wonderful dad, who's words spurred me on during dark times, could have been here to see me carry the science baton forward. I think he would be proud.

Finally, thank you to Gabriel for being my constant source of love, sunshine and magic. I couldn't have written this thesis without you. You mean more to me than you can ever know. I look forward to seeing where our next adventure takes us.

Publications

Laura Jardine, Simone Webb, Issac Goh, Mariana Quiroga Londoño, Gary Reynolds, Michael Mather, Bayanne Olabi, Emily Stephenson, Rachel A. Botting, Dave Horsfall, Justin Engelbert, Daniel Maunder, Nicole Mende, **Caitlin Murnane**, et al. 2021. "Blood and Immune Development in Human Fetal Bone Marrow and Down Syndrome." *Nature* 598 (7880): 327–31.

Conferences and awards

As a presenter:

Caitlin Murnane, Unravelling impaired fetal B-lymphopoiesis in Down syndrome, June 2020, Oxford Centre of Haematology Conference. (Was awarded the inaugural Doug Higgs prize for my research poster).

As a participant:

Translational and Personalized Medicine: from bench to the bedside, June 2019, University of Padua.

MRC DTP Global Postgraduate Retreat: Engaging with Health Policy, July 2019, Imperial College London.

List of abbreviations

α-MEM	α-Minimum Essential Medium
10-B	CD10- PreB cell
10+B	CD10+PreB cell
ABM	Adult bone marrow
ALL	Acute Lymphoblastic Leukaemia
ANOVA	Analysis of Variance
ATAC-Seq/ ATACSeq	Assay for transposase-accessible chromatin-sequencing
BM	Bone Marrow
CB. . . .	Cord Blood
CLP	Common Lymphoid Progenitor
CMP	Common Myeloid Progenitor
Chr21. . . .	Chromosome 21
DAR. . . .	Differentially Accessible Region
DE	Differentially Expressed
DEG	Differentially Expressed Gene(s)
DS	Down Syndrome
DS-ALL	Down Syndrome Acute Lymphoblastic Leukaemia
ELP	Early Lymphoid Progenitor
FACS	Fluorescence Activated Cell Sorting
FBM	Fetal Bone Marrow
FBS	Fetal Bovine Serum

FC. . . .	Fold change
FDR	False Discovery Rate
FL	Fetal Liver
GMP	Granulocyte/Macrophage Progenitor
HDBR	Human Developmental Biology Resource
HI	Heat Inactivated
Hsa21	Human chromosome 21
HSC	Haematopoietic Stem Cell
HSPC	Haematopoietic Stem and Progenitor Cells
iALL	infant ALL
iPSC	induced Pluripotent Stem Cell
IFN	Interferon
LMPP	Lymphoid-primed Multipotent Progenitor
CD10- LMPP / 10-LMPP. . . .	CD10- Lymphoid-primed Multipotent Progenitor
CD10+ LMPP/ 10+LMPP. . . .	CD10+ Lymphoid-primed Multipotent Progenitor
MEP	Megakaryocyte/Erythroid Progenitor
MLP	Multi-Lymphoid Progenitor
MNC	Mononuclear Cells
MPP	Multipotent Progenitor
ML-DS	Myeloid Leukaemia of Down Syndrome
MS-5	Murine Stromal-5 cell line
non-DS	Non-Down Syndrome
N	Normal (non-DS)
OP9-DL1. . . .	murine bone-marrow-derived stromal cell line that expresses

	the Notch ligand, Delta-like 1
PBMCs	Peripheral Blood Mononuclear Cells
PBS	Phosphate Buffered Saline
PBM	Paediatric bone marrow
PCA	Principal Component Analysis
PCR	Polymerase Chain Reaction
Pre-ELPGMP	Pre- Early Lymphoid Progenitor/ Granulocyte/ Macrophage progenitor
RNA-Seq/ RNASeq. . . .	RNA-Sequencing
RT	Reverse Transcription
SEM	Standard Error of Mean
Sc	single cell
T21	Trisomy 21
TSS	Transcriptional start site
CPM	Counts Per Million mapped reads
UMAP	Uniform Manifold Approximation and Projection
VST	Variance Stabilising Transformation

The impact of COVID-19 and other extenuating circumstances on this project

There have been two major disruptions which impacted my DPhil: changing lab groups and the lab closure (and subsequent disruption) during the COVID-19 pandemic.

The detailed impact of these events on my work are described in the table below.

I joined the Roberts/Roy labs in January 2020, having started my PhD in September 2018 within the Nerlov group. As a consequence, my time to complete the entire DPhil (experiments, data analysis, Transfer/ Confirmation milestones, thesis writing and submission) was reduced to 33 months. With the additional COVID-19 lab closure (March - July 2020), and time taken outside the lab to write my thesis (July 2022-September 2022), in reality I had approximately 24 months to generate and analyse the data presented in this thesis.

The direct impact of moving lab was that I had to adjust very quickly and learn new protocols specific to the Roberts/Roy groups including: fetal dissection and processing, three new culture systems (MS-5, OP9-DL1, methylcellulose) and new molecular techniques (small bulk ATAC/ RNASeq. There was no time for a detailed literature review due to the urgent need to start experiments, so I had to quickly establish the current literature and develop achievable research questions with my supervisors' support.

By March 2020, I had completed my first large-scale co-culture experiment and had developed and optimised a new comprehensive FACS panel to sort 14 populations simultaneously.

During COVID-19 pandemic lab closure between March – July, I was unable to do any lab work which was a significant obstacle having already lost 15 months due to moving lab. Aside from having to delay my major DPhil milestones (Transfer and Confirmation of status) by the maximum number of terms, there were several knock-on effects of this combined disruption, **which are described in the table below**. During the closure, I was able to analyse my new functional data and prepare for my Transfer of Status but the lack of lab access considerably impacted the experiments I could do when the lab re-opened.

I was not in a position to take an extension due to both my personal financial circumstances, and my place on the Graduate-Entry Medicine programme starting September 2022.

Nature of Disruption	Detailed impact
Loss of lab time	Lab closures of approximately 5 months prevented me doing experiments. Ordinarily this time would have been used to complete the MS-5 co-culture dataset (3-4 time course experiments for normal and DS in parallel).
Reduced primary samples	During this the COVID-19 lockdown, we received reduced human samples from the HDBR, which meant that there were loss opportunities to obtain particularly rare DS samples for my experiments which reduced the number of potential samples available to me when lab work resumed. This meant I had to very carefully prioritise both whole experiments and time points of experiments, which directly impacted the number of biological replicates I was able to generate, especially for DS.
Reduced working hours/ shift work when labs re-opened	The experiments presented in this DPhil are labour intensive and time consuming mainly due to the highly complex FACS (up to 15 populations being simultaneously sorted) and accordingly the number of readouts across a time course as well as performing normal and DS in parallel, doubling the work load. Having restricted lab hours and working around a strict rota both for the lab space and facilities (e.g. flow cytometry, PCR clean room), directly limited my access and the time available to perform these experiments, leading to difficult choices about how many populations to assess, numbers of time points and numbers of replicates.
Forced cancellation of experiments leading to amended project aims and rescheduling ongoing work	<u>Cancelled Methylation studies</u>: I initiated a new collaboration, to perform some small bulk/ single cell whole genome methylation assays on fetal HSPCs with the Song group (Ludwig institute). I performed some pilot experiments with this group however these experiments had to be foregone due to the lack of sufficient time to allow for the necessary optimisation of these protocols. <u>Rescheduling:</u> During the pandemic and post-pandemic period, I was unable to access certain supplies needed for experiments including Tapestation and Kapa QC reagents for the ATAC sequencing experiments and I had to delay the OP9-DL1 T-cell assays for several months due to blocked supply chains of necessary culture

	reagents. This meant I had to perform the T-cell experiments in the final 6 months of my DPhil between February- June 2022, when my preference for this time would have been solely data analysis.
Bioinformatics	Prior to joining the lab, I had no bioinformatics skills. I was unable to dedicate sufficient time for the 12-week CCB course, so I attended a series of online short courses through the University of Cambridge Bioinformatics training centre: Introduction to working with UNIX and BASH, Introduction to R for Biologists, Analysis of bulk RNA-seq data, Analysis of mapped NGS data with SeqMonk, Extracting biological information from gene lists Due to COVID-related delays to my starting the both RNA and ATAC sequencing experiments, I had limited time to apply the skills I had learned to my own RNA sequencing and ATAC sequencing data (3-4 months). This particularly limited analysis of the ATAC seq data due to this being more complex and time intensive.

Contents

Abstract **1**

Acknowledgements **3**

Publications and presentations **5**

List of abbreviations **6**

The impact of COVID-19 and other extenuating circumstances on this project **9**

1 Introduction **16**

1.1. Human haematopoiesis throughout ontogeny 16

1.1.1. Haematopoietic maturation adapts to meet physiological properties 16

1.1.2. Regulation of haematopoietic maturation throughout ontogeny 23

1.1.3. The classical haematopoietic hierarchy model 25

1.1.4. Advances in the haematopoietic hierarchy model 26

1.1.5. Current models for human B-lymphoid differentiation 31

1.1.6. Transcriptional control of B-cell development 38

1.1.7. Cytokine regulation of B-lineage specification and differentiation 39

1.1.8. Current models for human T/NK-lymphoid differentiation 41

1.2. Fetal haematopoiesis 43

1.2.1. Origins of fetal haematopoiesis 43

1.2.2. Primitive versus definitive haematopoiesis 44

1.2.3. Human fetal B-lymphopoiesis 48

1.3. Down syndrome and haematopoiesis 53

1.3.1. Trisomy 21, aneuploidy and disease 53

1.3.2. Abnormal haematopoiesis in DS 56

1.3.2.1. Abnormal adult haematopoiesis in DS 59

1.3.2.2. Abnormal fetal haematopoiesis in DS 59

1.3.3. DS-associated leukaemias 60

1.3.3.1. Myeloid leukaemia of DS (ML-DS) 61

1.3.3.2. DS-ALL 62
1.3.4. The molecular mechanism for T21-mediated perturbation of B-lymphopoiesis and DS-ALL 66
1.3.5. An altered progenitor compartment in DS FBM underlies perturbed haematopoiesis of DS and may provide clues as to the unique characteristics of DS-ALL 70
1.4. Hypothesis and aims 72

2 Methods 74
2.1. Samples 74
2.2. Sample processing and cryopreservation 75
2.3. Sample thawing 76
2.4. Fluorescently-activated-cell-sorting (FACS) of HSPCs by immunophenotype and flow cytometry 77
2.5. MS-5 co-cultures to assess multi lineage output potential 81
2.6. Single cell methocult assays to assess myeloid/erythroid/MK output 83
2.7. OP9-DL1 stromal co-cultures to assess T-cell output 84
2.8. Small bulk RNA sequencing of FBM HSPCs 86
2.9. RNA sequencing analysis 89
2.10. Small bulk ATAC-sequencing of FBM HSPCs 93
2.11. ATAC-sequencing analysis 95
2.12. Statistics 98

3 Immunophenotypic and functional characterisation of fetal bone marrow haematopoiesis to understand alternative pathways of human fetal B-lymphopoiesis 100
3.1. Background and aims 100
3.2. Discovery of novel fetal lympho-myeloid progenitors in normal FBM through immunophenotypic characterisation of FBM HSPC 102
3.3. Functional characterisation of novel fetal lympho-myeloid progenitors in normal FBM 110
3.4. Functional characterisation of normal FBM HSPCs to refine the fetal B cell developmental hierarchy 118

3.5. Summary and discussion 130

4 Immunophenotypic and functional characteristics of B-cell differentiation in DS FBM 136

4.1. Background and aims 136

4.2. Immunophenotypic characterisation of DS FBM shows striking differences in HSPC frequencies, especially CD10- and CD10+ populations 140

4.3. DS FBM HSPCs show altered lineage potential in vitro 144

4.3.1. DS FBM HSPCs show an intrinsic B-cell defect and a myeloid/ NK bias from the HSC-level 145

4.3.2. DS FBM HSPCs show increased clonogenicity in methylcellulose, with HSCs and MPPs showing megakaryocyte-erythroid bias. 158

4.3.3. Early and intermediate DS FBM HSPCs exhibit impaired T-cell differentiation 163

4.4. Summary and discussion 168

5 The impact of trisomy 21 on the transcriptome and chromatin accessibility of fetal bone marrow B lymphopoiesis 178

5.1. Background and aims 178

5.2. Molecular characterisation of normal fetal bone marrow HSPCs by bulk RNA sequencing and ATAC sequencing 181

5.3. The impact of T21 on the transcriptome and chromatin accessibility of FBM HSPCs 205

5.4. Summary and discussion 230

6 Discussion 237

6.1. Background 237

6.2. Refining existing models of human fetal BM B-lymphopoiesis 240

6.3. The functional impact of T21 on multi-lineage haematopoiesis in FBM 247

6.4. The impact of T21 on the transcriptome and chromatin accessibility of FBM HSPCs 253

6.5. Future work 256

6.6. Conclusions 259

Bibliography 260

Chapter 1

Introduction

1.1 Human haematopoiesis throughout ontogeny

1.1.1 Haematopoietic maturation adapts to meet physiological priorities

Haematopoiesis is the process by which mature blood cells are produced during a series of differentiation steps of progressive lineage restriction, originating with a self-renewing multipotent haematopoietic stem cell (HSC) (Orkin, 2000; Orkin and Zon, 2008).
Normal development requires temporally controlled ontogenic remodeling and accompanying divergence of stem and progenitor fates to meet the changing demands of distinct stages of life and their respective physiological priorities. Prior to birth, the naïve fetal immune system remains relatively unchallenged and primed toward immune tolerance and anti-inflammatory signatures, whilst there is a drive towards HSC self-renewal and erythropoiesis to help establish definitive haematopoiesis and promote survival within the hypoxic intrauterine environment (Finne and Halvorsen, 1972; Burt, 2013; Rowe et al, 2016; Bunis et al, 2021). An important immunomodulatory transition occurs as the fetus approaches birth, whereby the comparatively tolerant fetal immune system switches to a more activated and defensive-like state in order to protect against pathogenic threats in the early years of life (Burt, 2013). To support this transition, after birth, haematopoiesis continues to be predominantly lymphoid biased in order to develop and prime the adaptive

immune system (Mackinney, 1978; Basha et al, 2014). In later life there is an increase in long-term HSCs (LT-HSCs) in an attempt to restore homeostasis in response to 'Inflamm-aging' which is defined as an increase in inflammatory cytokine concentration in the peripheral blood (PB) and bone marrow (BM) produced by the expanded myeloid compartment in older individuals (Young et al, 2016; SanMiguel et al, 2020; Young et al, 2021).

Researchers have long sought to identify and define the molecular regulators and mechanisms underpinning haematopoietic maturation during development and throughout life. For many years, the predominant school of thought, supported by seminal publications of the time, was that the developing and adult immune system, and haematopoietic differentiation more widely, arose through a layered model (Herzenberg and Herzenberg, 1989). In terms of layered haematopoiesis, this meant temporally-restricted and distinct populations of fetal HSCs and HSPCs were superseded at defined developmental timepoints by new 'adult' HSPCs with their own distinct patterns of differentiation (Cumano and Godin, 2007).

In terms of the immune system, the layered model proposes that there is no discrete separation between embryonic, fetal and adult immune systems (see new Figure 1.1). Instead, alterations to fetal immune development are proposed to have downstream ramifications for later adult immunity (Hadland and Yoshimoto, 2018; Elsaid et al, 2020).

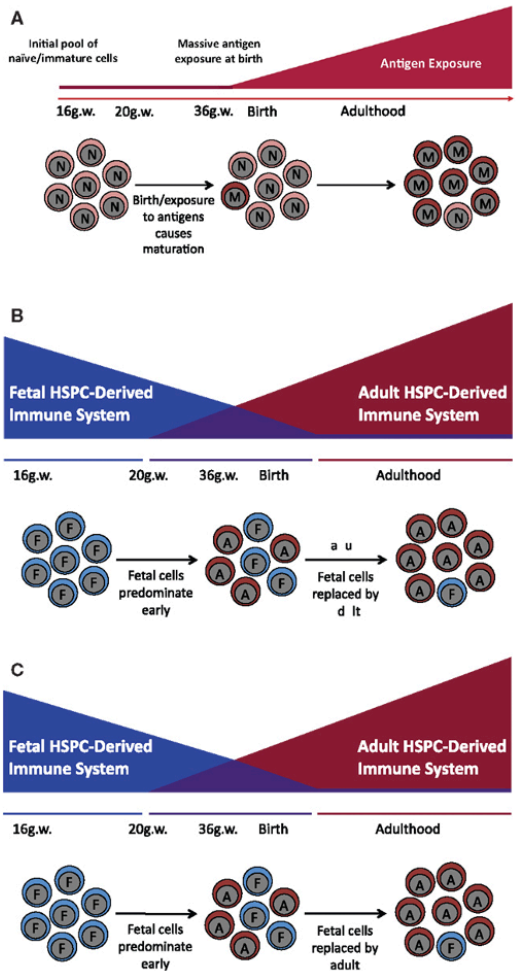


Figure 1.1 Models of human immune development
(A) Linear model of immune development argues that the fetal immune system is completely naïve and after birth is exposed to exogenous antigens, prompting maturation into the adult immune system.

(B) The layered model of immune development argues that HSPCs emerge sequentially and function in developmentally-defined waves. These waves give rise to unique layers of HSPC-derived cells with different functional outcomes.
During gestation, haematopoietic cells originate from fetal HSPCs, while in the adult, most cells come derive from an adult HSPC. This model suggests that during the transition between fetal and post-natal life, there is a mixture of fetal and adult-derived cells with different functional properties that contribute toward the neonatal immune system.

(C) The maturation model of immune development.
Fetal cells directly mature into adult cells, meaning that at birth there are cells with a mixture of both fetal and adult characteristics.

Adapted from (Krow-Lucal and McCune, 2014).

Supporting the layered hypothesis, Hardy's work on murine B-cells, suggests that early waves of B-cell during development can support and regulate later B-cell subsets, however these studies also showed, importantly, that murine fetal and adult B-lymphopoiesis are somewhat distinct.

Briefly, Hardy's classification of B-cells and their progenitors in mice, enabled the delineation of typical B-cell differentiation into fractions (Hardy and Hayakawa, 1991), with the distinct fractions possessing different characteristics (Figure 1.2).

In particular, the distinctions between B-1 and B-2 B-cells have drawn interest. B-1 cells are a small and unique B-cell subset found before birth that mainly derives from the fetal liver and lesser so from adult bone marrow (Hardy and Hayakawa, 2001; Hardy et al, 2007). These cells spontaneously and rapidly produce natural antibodies without the need for exogenous or artificial immunization (Rodriguez-Zhurbenko et al, 2019). By contrast, B-2 cells or Conventional B-cells, are a more common subset which support T-cell responses within the germinal centre and themselves mount highly specific and high-affinity antibody responses (De Silva and Klein, 2015).

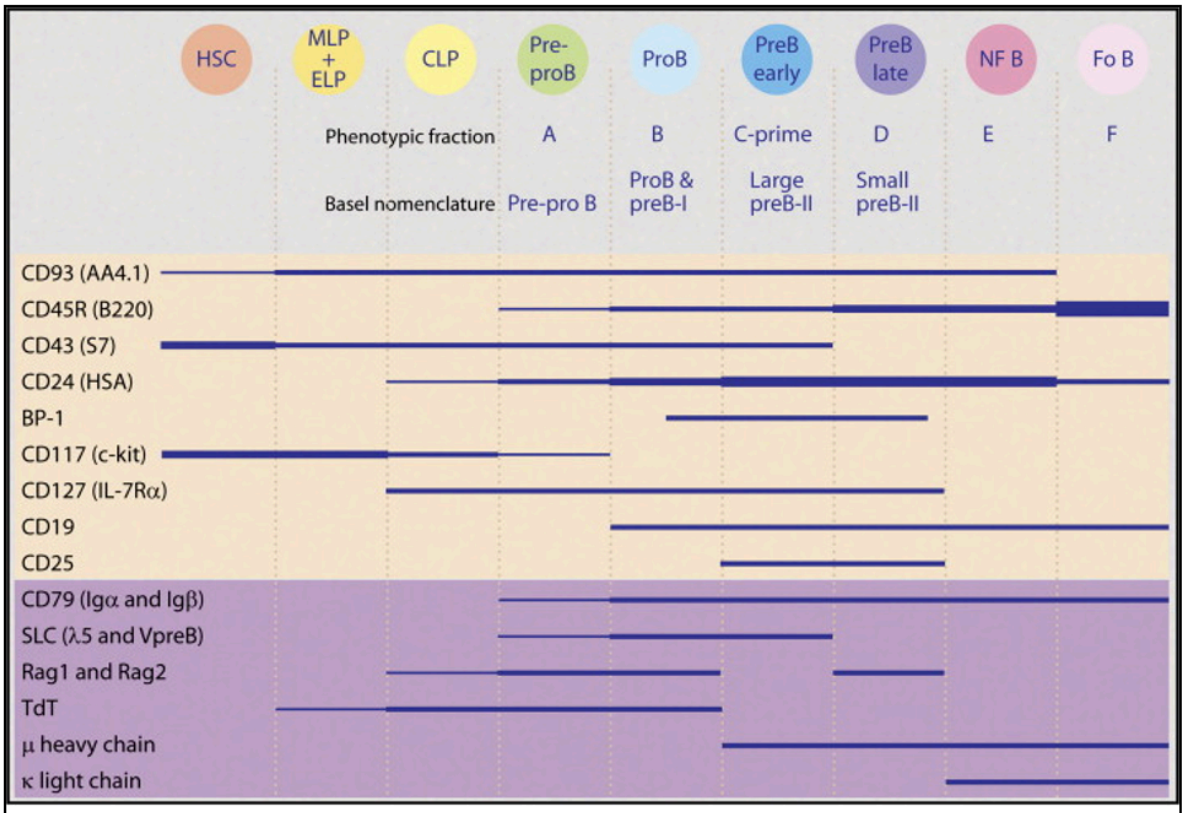


Figure 1.2 The original Hardy B-cell fractions.
Delineated by Cluster of Differentiation (CD) cell surface markers (Hardy and Hayakawa, 1991). Along with changes in cell surface protein expression, discrete B-cell fractions have been characterized by their gene expression and intracellular protein expression profiles.
Figure adapted from Hardy et al, 2007.

The observation that B-1 cells present early in development, before B-2 cells, especially those secreting IgM, has led to the argument that these are important in establishing immediate protective natural antibody defences during ontogeny (Rodriguez-Zhurbenko et al, 2019).

The layered hypothesis argues that the existence of B-1 (innate) and B-2 (classical) lymphocytes (Hardy and Hayakawa, 1991), could be explained by two temporally distinct origins involving different progenitors (Herzenberg and Herzenberg, 1989; Montecino-Rodriguez and Dorshkind, 2012), rather than a drive of immature B-progenitors toward B-1 or B-2 fates based on antigen specificity of the BCR, as the selection model had proposed (Berland and Wortis, 2002). It has been suggested that the emergence of B-1 cells during early ontogeny, and production of natural IgM by this population, supports the subsequent development of further B-1 and B-2 cells, supporting the layered hypothesis argument that alterations to fetal immune development have downstream ramifications for later adult immunity (Hadland and Yoshimoto, 2018; Elsaid et al, 2020).

Greater support for the layered immune hypothesis came after the discovery of unique innate-like immune cells, namely B1-a and γδ T cells within mice, which arise in a HSC-independent manner before the establishment of definitive fetal HSCs (Haas et al, 2012; Montecino-Rodriguez et al, 2016; Elsaid et al, 2019).

One of the arguments for the existence of a layered immune system, is that it makes evolutionary sense, because it offers important, protective biological functions. Within mice, both B1-a and γδ T cells are believed show a less diverse antigen repertoire, allowing them

to serve broader, protective innate functions until full adaptive immunity is later established (Elsaid et al, 2020).

Moreover, it was recently reported that embryonic HSC-like progenitors showed a higher capacity than both fetal and adult HSCs, to generate innate B/T-like cells (Beaudin et al, 2016), whilst definitive fetal liver (FL) HSCs failed to do so (Ghosn et al, 2016). However, in a separate study, it was separately demonstrated that murine FL HSC could in fact give rise to B-1a cells (Kristiansen et al, 2016), challenging the idea that B1-a cells originate from a distinct progenitor (Elsaid et al, 2020).

One consistent observation is that Lin28B, a master regulator of fetal haematopoiesis only expressed in fetal life (Copley et al, 2013; Zhou et al, 2015), is necessary for the production of both B-1 (Zhou et al, 2015; Kristiansen et al, 2016; Vanhee et al, 2019) and γδ T cells (Yuan et al, 2012) and a low IL-7 microenvironment also favours the production of B-1 cells (Wong et al, 2019). Whilst these observations support the view that these innate cells are preferentially produced during development, it leads to speculation as to whether these cells actually arise from distinct origins, or simply the same progenitors which are subject to stage-specific regulation.

Several studies in mice have shown the persistence of embryonically-derived cells into adult life, for example the existence of tissue-resident macrophages within adult mice which were shown to develop from yolk sac erythro-myeloid progenitors (Gomez Perdiguero et al, 2015). Paradoxically, these populations cannot be *de novo* generated by HSCs derived from adult haematopoietic sites without fetal-like reprogramming (Kristiansen et al, 2016). Altogether this has led supporters of the layered immune system model to propose that

these progenitors may possess non-redundant functions with their timely establishment during development, and their subsequent persistence, being important for immunity within adult life.

Within humans however, the existence of B-1 cells within human fetal tissue remains controversial (Jackson et al, 2021). There have been reports of cells satisfying the characteristics of B-1cells within human cord blood (CB) and adult PB (Griffin et al, 2011), whilst others within the field contest these findings due to discrepancies of CD3 positivity within the proposed B-1 population (Descatoire et al, 2011; Perez-Andres et al, 2011). During our own investigations, we did not record any CD5+ B-1-like cells within FL or bone marrow, (Roy et al, 2017). This led some to conclude that B-1 cells and their progenitors were species-specific, or alternatively that a human equivalent expresses currently unknown surface markers, preventing our detecting them. However, a recent extensive study of multiple human fetal tissues including FBM, spleen and FL has provided evidence of human pre-natal B-1 cells for the first time, validated by functional and molecular profiling and the comparative assessment of the known characteristics of murine B-1 cells (Suo et al, 2022).

Given the current evidence, it is probably accurate to say that fetal HSPCs have unique characteristics and features (Montecino-Rodriguez, 2016; Hadland and Yoshimoto, 2018) and for the most part, the progression from fetal to adult blood development arises via progressive maturational changes and a continuum of intermediate cellular phenotypes, rather than via a discrete transition (Bunis et al, 2021).

One of the main motivations to identify and characterise the regulators and drivers of normal blood maturation, is that age-related shifts in haematopoiesis are mirrored by incidence rates of haematological diseases in different age groups, such as a propensity toward infant and childhood lymphoblastic leukaemias in early life (Greaves, 1999) or clonal haematopoiesis and myeloproliferative neoplasms during aging (Shlush, 2018).

1.1.2 Regulation of haematopoietic maturation throughout ontogeny

Emerging research over the past 20 years indicates that appropriate haematopoietic maturation is ensured by marked changes in haematopoietic stem and progenitor cells (HSPCs) at the transcriptomic, epigenetic and chromatin organisation level, in tightly regulated developmental windows.

Several examples of haematopoietic maturation processes exist, but perhaps the best resolved is globin switching during fetal development. Humans sequentially express embryonic, fetal or adult haemoglobin. After the advent of definitive haematopoiesis (see 2.2.1) fetal haemoglobin becomes the predominant haemoglobin for the majority of gestation and shortly after birth there is a switch to adult haemoglobins (Sankaran and Orkin, 2013). Extensive molecular studies have revealed this switch is orchestrated through exquisitely timed transcriptomic and epigenetic changes (Xu et al, 2013; Liu et al, 2018; Shen et al, 2021).

A key regulator of haematopoietic maturation is *LIN28B,* an onco-fetal gene specifically expressed during embryonic and fetal development, which acts through a range of

molecular mechanisms to control several aspects of haematopoietic maturation including fetal B and T-cell differentiation, HSC renewal, myelopoiesis and globin switching (Yuan et al, 2012; Copley et al, 2013; Zhou et al, 2015; Wang et al, 2022). A major mechanism through which *LIN28B* exerts its effects is via repression of the Let-7 family of miRNAs and their many downstream targets, the identity of which depends on the cell context, e.g. B-lineage specific transcription factors *PAX5* and *ARID3A* within B-cell progenitors (Zhou et al, 2015; Wang et al, 2019), or the self-renewal regulator *HMGA2* in HSCs (Copley et al, 2013; Cesana et al, 2018). A recent study comparing fetal and adult murine HSCs showed that *LIN28B* coordinates a shift in the differentiation potential each HSC subset. Specifically, *LIN28B* ensures that fetal HSCs differentiate predominantly into erythroid- and lymphoid-biased multi-potent progenitors (MPPs), designated MPP-2 and MPP-4 respectively, and by contrast, promotes the differentiation of adult HSCs toward myeloid-biased MPPs, designated MPP-3, via mechanisms involving the let-7 target and polycomb family member Cbx2 (Wang et al, 2022).

More broadly, the polycomb family, and the Polycomb Repressor Complexes (PRCs) they form with other effector proteins, perform with varying roles in distinct stages of haematopoietic development. For example, during the shift from primitive to definitive haematopoiesis, (discussed in 1.2 Human Fetal Haematopoiesis*)*, Ezh1, a PRC2 component which represses its target genes via histone methylation (Shen et al, 2008), is itself downregulated to prevent silencing of key genes involved in initiating murine definitive HSC development programmes (Vo et al, 2018). Throughout both definitive fetal and adult haematopoiesis, PRCs are further regulated to maintain normal blood production in a developmental-stage-specific manner (Xie et al, 2014).

1.1.3 The classical haematopoietic hierarchy model

Within developmental biology, differentiation, or the specialisation of stem cells toward cell fates, has been thought to follow Waddington's landscape model (Waddington, 1957). Within the context of haematopoiesis, HSPCs were thought to differentiate in a stepwise manner from multi-potent HSPCs to oligo-, bi and uni-potent progenitors through increasingly intricate branching points illustrated within an immunophenotypically described hierarchal tree-like model (Morrison et al, 1997; Akashi et al, 2000; Laurenti and Gottgens, 2018). However, recent advances indicate that the degree of HSPC multipotency differs by developmental stage. Fetal HSPCs show greater multipotency compared with adult bone marrow (ABM), where a greater proportion of ABM are unipotent or oligopotent (Notta et al, 2016). In addition, the balance of HSC subsets also changes with age for instance, a greater proportion of lymphoid-deficient HSCs dominate the overall HSC pool in adult mice compared with fetal (Benz et al, 2012; Laurenti and Gottgens, 2018).

According to the classical model (New Figure 1.3, A), which was largely resolved through studies of murine haematopoiesis, HSCs are subdivided into CD34- long term (LT-HSCs) and CD34+ short term HSCs (ST-HSCs) (Reya et al, 2001; Seita and Weissman, 2010). Studies investigating the phenotype and capacities of these sub-populations show that LT-HSCs are rarer and comparatively quiescent, with expanded long term reconstituting capacity (the ability to sustainably generate all of the possible haematopoietic lineages, i.e. throughout life), compared to ST-HSCs which show short term reconstituting potential and very limited or no self-renewal (Wagenblast et al, 2019).

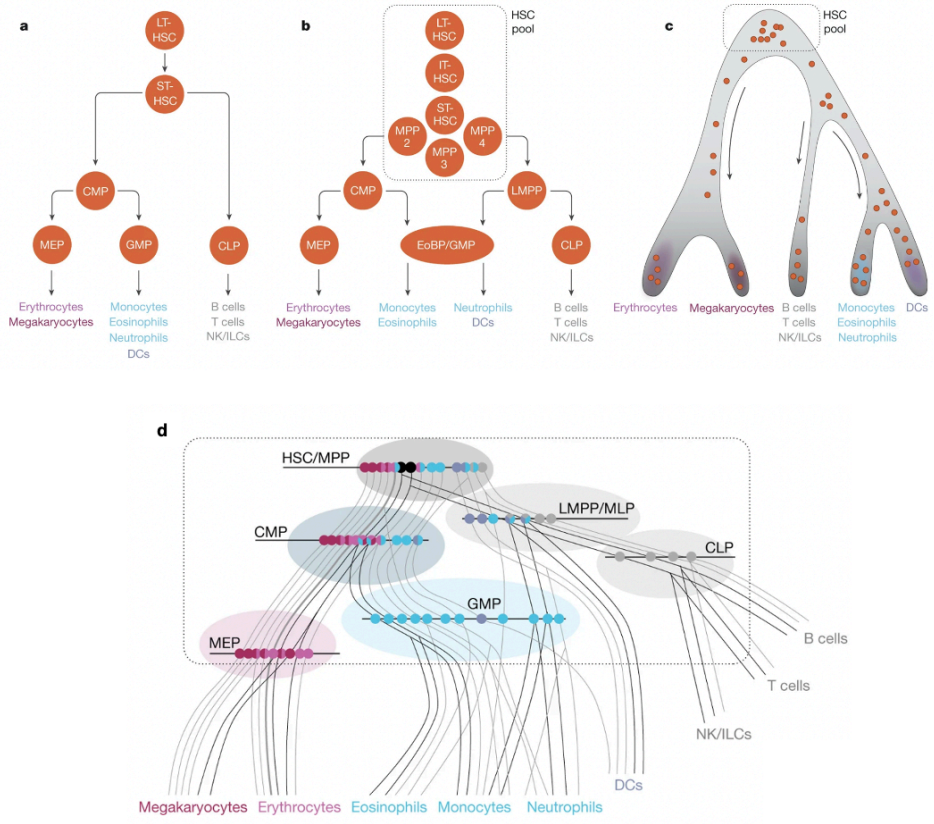
Within the model, a proportion of LT-HSCs differentiate into to ST-HSCs which have the potential to give rise to lymphoid and myeloid progenitors via an intermediate multipotent progenitors (MPP), which themselves do not self-renew (Reya et al, 2001; Orkin and Zon, 2008). Within this conventional model, lineage branching down the myeloid and lymphoid was considered separate solely downstream of the HSC and MPP level (Reya et al, 2001). Briefly, the first post-MPP bifurcation occurs between the common myeloid progenitors (CMPs) (Akashi et al, 2000) and common lymphoid progenitors (CLP) (Kondo et al, 1997). CMPs were thought to facilitate the production of megakaryocyte, erythrocytes and granulocytes/monocytes via lineage-restricted progenitors called granulocyte-macrophage progenitors (GMPs) and megakaryocytic-erythrocyte progenitors (MEPs) (Akashi et al, 2000). In contrast, progression down the lymphoid pathway via CLPs leads to the formation of B and T lymphocytes as well as natural killer cells (NK) (Orkin, 2000; Orkin and Zon, 2008).

1.1.4 Advances in the haematopoietic hierarchy model

Whilst Waddington's landscape and the classical haematopoietic tree are useful for conveying the basic principles of differentiation, they are simple and reductive models. The classical haematopoietic model was developed predominantly by the Weissman group and their affiliates within mice using immunophenotypic definitions, and accompanying transplantation experiments (Morrison et al, 1997; Akashi et al, 2000; Manz et al, 2002). Unfortunately, this early work faces limitations on several fronts (Nerlov and Jacobsen, 2019). Firstly, the emergence of new lineage markers since the development of this model, has enabled researchers to identify new sub-populations and refine the model (New Figure 1.3).

Secondly, despite flow cytometry (FC) and Fluorescent-activated cell sorting (FACS) being invaluable for researchers, these techniques involve gating positive and negative populations based on arbitrary points along a fluorescent marker continuum. Paradoxically, this means that biologically relevant nuance can be lost e.g. HSPCs transitioning from one differentiation stage to the next, or very rare populations fail to be adequately detected and characterised. Mass cytometry (Cytof) - in which antibodies are conjugated to heavy metal isotopes rather than fluorophores - has enabled the simultaneous appraisal of a greater number of surface markers (Leipold et al, 2015; Gadalla et al, 2019).

The greatest challenge to the hierarchal model, is the implicit assumptions that sub-populations which share the same immunophenotype are molecularly identical and functionally homogeneous (Laurenti and Gottgens, 2018; Jacobsen and Nerlov, 2019). However, emerging evidence from studies utilising single-cell technologies indicates that immunophenotypically defined HSPC populations are more heterogeneous than previously appreciated, and that lineage restricted unipotent progenitors might reside within populations that were previously thought to be multipotent, prompting a re-evaluation over the stage at which HSCs and their progenitors become lineage biased (New Figure 1.3 C,D) (Sanjuan-Pla et al, 2013; Notta et al, 2016; Drissen et al, 2016; Velten et al,2017; Carrelha et al, 2018; Drissen et al, 2019). For the purposes of discussing advances in the hierarchy model, I have outlined definitions of relevant terms in Table 1.1.



<u>Figure 1.3</u> Classic and revised models of human haematopoietic differentiation.

Refinements to the human haematopoietic hierarchy model over the past 25 years. In all models, self-renewing HSCs sit at the apex of the hierarchy and are able to give rise to all haematopoietic cell types through a series of progressively lineage restricted progenitors.

(a) Classic model (circa 2000): Long-term HSCs (LT-HSCs) lose self-renewal capacity to become ST-HSCs which can then differentiate to MPPs which are able to generate all major lineages, but themselves possess reduced self-renewal. MPPs differentiate down the myelo-erythroid trajectory via a CMP, or toward a lymphoid fate via the CLP.

(b) A greater appreciation for HSPC heterogeneity (2005-2016): HSCs are accepted to be more heterogeneous both in terms of self-renewal (vertical axis, Long/ Intermediate/ Short term HSC) and differentiation potential (horizontal axis). HSCs give rise to distinct MPP subsets (MPP 2-4) which show different properties such as lineage output. Myeloid and lymphoid branches remain more associated than previously thought via the LMPP. The EoBP/GMP compartment is also fairly heterogeneous.

(c) and (d) Single cell snapshots indicate a continuum of differentiation (current models). Red dots / coloured circles represent single cells and their localization along a differentiation trajectory with continuous lines **(d)** or tracks **(c)** denoting differentiation trajectories of single cells which involve cells and their progeny passing through progenitor compartments which all possess considerable heterogeneity. **(d)** Horizontal lines represent the lineage potential of the cells present in each phenotypic compartment (single-colour circles denote unilineage cells; two-colour circles denote bilineage cells; three-colours circles denote trilineage cells; black circles denote multipotent cells). For the most part, unipotent cells outnumber bi- or trilineage-potent cells.

Figure adapted from Laurenti and Gottgens, 2018.

<u>Key:</u>
HSC, haematopoietic stem cell (short, intermediate and long term as indicated); **MPP**, multipotent progenitor; **LMPP**, lymphoid-primed multipotent progenitor, **MLP, m**ulti-lymphoid progenitor, **CMP**, common myeloid progenitor; **CLP**, common lymphoid progenitor, **MEP**, megakaryocyte-erythroid progenitor, **EoBP**, eosinophil–basophil progenitor, **GMP**, granulocyte-macrophage progenitor, **ILCs**, innate lymphoid cells.

Table 1.1 Glossary of terms relevant to haematopoietic differentiation	
Term	Definition
Lineage specification	The process by which multipotent cells are initially directed toward a specific lineage and associate cell fate.
Lineage priming	Molecular alterations, such as at the transcriptomic level, which progressively restrict and bias progenitors toward specific lineages, is accompanied by a loss of functional plasticity. Within an immunophenotypically-defined progenitor population, cells can be differentially primed e.g. lymphoid-primed LMPP vs myeloid-primed LMPP.
Lineage commitment	The process by which HSPCs are irreversibly directed down a specific lineage trajectory e.g. the myeloid lineage, as a result of sufficient specification, priming. Lineage commitment is accompanied by a loss in plasticity and stem-like qualities.
Cell fate	The terminal, mature cell type that a progenitor differentiates to become e.g. erythrocyte.

Specifically, in contrast to the previously held view that a single Common Myeloid Progenitor (CMP) gives rise to all human myeloid cells, recent work suggests there are two pathways of myeloid development supplied by distinct progenitors, which generate the neutrophil/monocyte and basophil/eosinophil/mast cell lineages, respectively. Investigation of the early lineage commitment of index-sorted human bone marrow (BM)-derived CMPs using single cell expression analyses, reveals that the neutrophil/monocyte skewed CD131- CMPs co-segregate with the lymphoid lineage, whilst the basophils/eosinophil/mast cell skewed CD131+ CMP align more closely with megakaryocyte/erythroid lineages (see New Figure 1.3 D) (Drissen et al, 2016; Drissen et al, 2019).

Other work within both mice and humans revealed the existence of progenitors, designated ‘LMPPs’, that possess lymphoid potential and the ability to give rise to granulocytes and monocytes but not megakaryocytes (MKs) or erythrocytes (Adolfsson et al., 2005; Yoshida et

al, 2006; Lai and Kondo, 2006, Arinobu et al, 2007; Goardon et al, 2011; Gorgens et al, 2013; Karamitros et al, 2018; Drissen et al, 2019).

Furthermore, lineage tracing within mice has revealed biased sub-populations of HSCs (and likely MPPs) which are primed toward specific lineages (Sanjuan-Pla et al, 2013; Carrelha et al, 2018, see New Figure 1.3 D) and earlier this year came first definitive evidence of platelet-biased HSCs in humans (Aksoz et al, 2022). Whilst much of the work on lineage-biased HSCs has focused on those that preferentially give rise to platelets, lymphoid and myeloid biased HSCs have also been reported in mice (Muller-Sieburg et al 2004, Challen et al, 2010; Belluschi et al, 2018). Moreover, work in the downstream progenitors has also identified lineage primed MPP and LMPP subsets (Pietras et al, 2015; Karamitros et al, 2018)

Evidence suggests these primitive cells may be induced to selectively give rise to specific cell types as a result of extrinsic stimulation, such as the 'activation' of megakaryocyte-primed HSC-like progenitors in response to inflammation (Haas et al, 2015).

A recent comprehensive single cell (sc) transcriptomic analysis of FL, fetal BM (FBM), paediatric BM (PBM) and ABM has profiled changes in lineage biasing that were shown to present at the level of HSCs (Roy et al, 2021), building upon evidence of lineage priming within FL HSCs and MPPs (Popescu et al, 2019). The priming of HSCs and HSPCs was shown to underpin the broad changes in lineage composition at each stage of human ontogeny from an early drive toward megakaryo-erythropoiesis in the embryonic liver, followed by a marked expansion of lymphoid cells in the FBM which then declined gradually after birth and into adult life (Roy et al, 2021). Comparison of HSPCs from these stages of ontogeny with age-related haematopoietic abnormalities has enabled us to gain a better

understanding of how the molecular circuitry in primitive cells at these stages of development can be hijacked and exploited to drive the pathology of JMML in PBM and primary myelofibrosis (PMF) in ABM (Roy et al, 2021).

1.1.5 Current models for human B-lymphoid differentiation

Studies exploring lymphoid differentiation have led to widespread debate with the sub-populations along the continuum of lymphoid development incompletely characterised. This is in part due to the increasingly complex picture painted by studies which reveal the full extent of heterogeneity at all levels of the lymphoid differentiation trajectory (Karamitros et al, 2018; Sigvardsson, 2018). In addition, much of our current understanding of lymphoid development came from early studies in mice, however the discrepancies between murine and human lymphopoiesis have limited how much we can infer from these models (Mestas and Hughes, 2004; Ichii et al, 2014).

The following review of the literature focuses on lymphoid restriction within the context of the B-lineage, starting with the CD38- multipotent progenitor compartment and subsequently the CD38+ lymphoid progenitors and B-progenitors. The schematic for B-lymphopoiesis in post-natal life is shown in Figure 1.4.

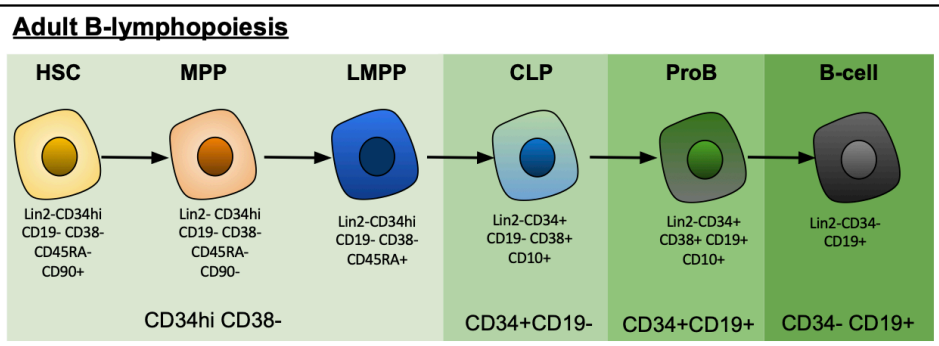


Figure 1.4 Human adult B-lymphopoiesis pathway
Schematic illustrating the human B-differentiation pathway within post-natal life.

HSC, haematopoietic stem cell; **MPP**, multipotent progenitor; **LMPP**, lymphoid-primed multipotent progenitor **CLP**, common lymphoid progenitor.
Lin2= CD2/3/14/16/56/235a

CD38- compartment: multipotent progenitors and multi-lymphoid progenitor (MLP)

Our current understanding of the steps that lead to the generation of LMPPs within humans involves HSCs losing CD90 to give rise to MPPs and the subsequent generation of CD45RA+ LMPPs. The immunophenotypic definition of HSCs was further refined after the identification of CD49f, an integrin that mediates niche: HSC interactions, as a potentially unique marker for long term engrafting HSCs (Notta et al, 2011). Subsequent studies have shown that downregulation of surface CD49f accompanies the transition from HSC to MPP, or at least LT-HSC to ST-HSC (Notta et al, 2016; Belluschi et al, 2018). Recent studies have argued that the low expression level of CD49f could impede its use to readily detect HSCs (Anjos-Afonso et al, 2022). Moreover, recent work within human CB indicates that considerable heterogeneity exists within the CD49f+ fraction which indicates that the idea of a unified CD49f+ HSC population is an over-simplification (Knapp et al, 2018; Belluschi et al, 2018). Therefore, whilst CD49f has become a common HSC marker, other markers such

as endothelial protein C receptor (EPCR) have been presented as an alternative (Anjos-Afonso et al, 2022).

Downstream, MPPs acquire CD45RA+, giving rise to LMPPs; intermediate progenitors that exhibit pan-lymphoid priming whilst still retaining residual myeloid-monocytic potential with an absence of erythroid and megakaryocytic potential (Adolfsson et al, 2005). Originally discovered and studied in mice, (Adolfsson et al, 2005; Mansson et al, 2007; Ramond et al, 2014), the evidence for human immunophenotypic LMPPs (CD34+CD38-CD90-CD45RA+) came first within CB and bone marrow mononuclear cells (Majeti et al, 2007), and have since been characterised within fetal and adult tissues (Doulatov et al, 2010; Goardon et al, 2011; Roy et al, 2012; Gorgens et al 2013; Karamitros et al, 2018; O'Byrne et al, 2019; Jardine et al, 2021). LMPPs were considered to be the earliest HSPC population that exhibits lymphoid priming, though reports of lymphoid-primed ST-HSCs in CB (Belluschi et al, 2018) and MPPs in mice (Pietras et al, 2015), challenge this belief.

One of the key markers in the earliest stages of lymphoid priming is CD62L (L-Selectin). Studies in mice had indicated that the upregulation of CD62L was associated with a loss of myeloid and erythroid potential (Perry et al, 2006; Cho et al, 2011), and subsequently a CD34+CD10-CD62L^{high} progenitor discovered in human BM was shown to produce all of the major lymphoid lineages but with no functional myeloid or erythroid output in vitro, however they did give rise to both myeloid and B-cells within NOD-SCID recipients (Kohn et al, 2012). Transcriptomic profiling revealed a lack of a B-cell specific signature, and indicated that these cells were more representative of an intermediate between MPPs and a downstream CD10+ B-progenitors, placing CD62L as an earlier stage in lymphoid priming than CD10, a key determinator of B-cell commitment (Ichii et al, 2010). The loss of CD62L

expression has also been considered a key step in the transition from an early/intermediate NK to a terminally differentiated state (Luetke-Eversloh et al, 2013).

CD10 has been identified as important marker in HSPC differentiation in humans, specifically in lymphoid priming and B-cell commitment. Originally detected in the sera of patients diagnosed with acute lymphoblastic leukaemia (ALL), CD10 is a membrane-bound endopeptidase and has also been shown to impact cellular migration (Carrel et al, 1984; Malfroy et al, 1988; Maguer-Satta et al, 2011; Mishra et al, 2016). Extensive studies have explored the prognostic implications of CD10 expression in ALL (Pui et al, 1993; Consolini et al, 1998; Bene, 2005; Gleissner et al 2005; Jackson et al, 2021).

The early observations that CD10+ cells (since designated CLPs), failed to produce non-lymphoid output (Galy et al, 1995) whilst CD10- cells showed dual lymphomyeloid potential (Berardi et al, 1997), led to subsequent studies which showed concordance between the expression of CD10 and lymphoid surface markers such as CD7, CD19 and CD24 (Ichii et al, 2010). Transcriptomic data reflect this, with several B-cell genes e.g. *EBF1* and *PAX5* being upregulated in CD10+ cells, whilst known myeloid TFs such as MPO and *CEBPA* were downregulated (Ichii et al, 2010; Kohn et al, 2012; Sorcha O'Byrne DPhil thesis). Upregulation of CD10 is one of the last markers to be acquired during B-cell maturation and CD10 is likely to be a marker of B-lineage commitment rather than pan-lymphoid priming (Kohn et al, 2012).

Within the B-differentiation hierarchy, MLPs and CLPs have been proposed as the earliest CD10+ progenitor.

As discussed above, CLPs (CD34+Lin+CD38+CD10+CD19-) are thought to sit downstream of LMPPs and upstream of ProB progenitors and B-cells (Figure 1.4).

By contrast MLPs reside within the CD38- compartment (CD34+CD38^{low}CD45RA+CD7-CD10+) and were first described in human CB and adult BM as cells which showed lymphoid, monocytic and dendritic potential but an absence of erythroid potential (Doulatov et al, 2010). This work argued that MPPs could gain CD10 (and CD45RA) to become MLPs and then undergo further gradual lineage specification toward lymphoid, monocytic or dendritic lineages, including losing CD10 altogether at a GMP stage, which could then produce granulocytes (Doulatov et al, 2010; Doulatov et al, 2012).

The best characterisation of MLPs came from Karamitros and colleagues (2018), who compared the lineage output of LMPPs, MLPs and GMPs and their underlying molecular profiles, with the bulk of this work being performed in CB and to a lesser extent, ABM. During these experiments, it was shown that MLPs are heavily lymphoid primed, showing very minimal residual monocytic potential, which was mirrored in the transcriptomic profiling of these cells (Karamitros et al, 2018). The description of MLPs within this study highlighted the significant extent to which MLPs appeared to have almost entirely lost myeloid potential, in contrast to original claims that MLPs were more balanced in their lymphomyeloid potential (Doulatov et al, 2012).

Importantly, these experiments also revealed the high heterogeneity of the LMPP compartment for the expression of CD45RA and CD10. Functional assays showed that LMPP^{Ly}, LMPPs highly expressing CD10 and CD45RA, showed greater lymphoid output than the LMPP^{mix} which was moderate/low for CD10 and CD45RA (Karamitros et al, 2018). Overall, the model presented within this study argued that LMPP^{mix} are comparatively less

lymphoid primed with the potential to give rise to both myeloid and lymphoid output, lay upstream of an intermediate $LMPP^{Ly}$ population followed by the most lymphoid-primed MLP (Karamitros et al, 2018).

CD38+ progenitors (CLP and committed B-cell progenitors)

Downstream of LMPPs are more restricted lymphoid progenitors lacking myeloid potential, known as CLPs which were first discovered in the ABM CD34+ compartment and were shown to give rise to B, NK, T-and Dendritic cells but reduced myeloid output in vitro (Galy et al, 1995). Since then, the existence of CLPs has been validated in human CB, (Canque et al, 2000; Hao et al, 2001; Haddad, et al, 2004; Hoebeke et al, 2007; Su et al, ASH Abstract, 2010; Jardine et al, 2021) and ABM (Pang et al, 2011; Saxena et al, ASH Abstract, 2016), as well as within mouse bone marrow (Kondo et al, 1997; Perry et al, 2007; Mansson et al, 2010; Ghaedi et al, 2016). Within humans, the proportion of CLP in the human bone marrow was shown to decrease throughout adulthood, in line with age-related immune decline (Pang et al, 2011). Within mice, CLPs (and HSCs) from neonates were shown to produce greater numbers of B-1 cells than adult-derived cells (Barber et al, 2011).

Whilst FL CLPs have been reported in mice (Mebius et al, 2001; Tsuneto et a, 2013; Iida et al, 2016; Malouf and Ottersbach, 2018), data for them in human fetal development has been limited (Liu et al, 2021; Jardine et al, 2021).

The current immunophenotypic definition for CLP used by ourselves and many others is CD34+CD38+CD19-CD10+ (Galy et al, 1995; Kondo et al, 1997; Haddad et al, 2004). Others have incorporated *CD127* (IL-7R) and CD7 into immunophenotypic definitions (Canque et al,

2000; Hao et al, 2001; Hoebeke et al, 2007; Su et al, ASH Abstract, 2010; Pang et al, 2011; Saxena et al, ASH Abstract, 2016). Given that fetal-specific ELPs express IL-7R and are CD10- (CD34+CD38+CD19-CD10-CD127+) (Roy et al, 2012; Hussen et al, 2017; O'Byrne et al, 2019), has led to inclusion of CD10 within our studies of human fetal tissue to enable us to separate CD10-CD127+ ELPs and CD10+CD127$^{-/+}$ CLPs. Overall, CD7 positivity is associated with lymphoid progenitors that are primed toward T/NK output, whilst the classical CD10+CLPs described by Galy and colleagues, can generate all lymphoid lineages but appear biased toward B-cell output (Canque et al, 2000; Haddad et al, 2004; Hoebeke et al, 2007).

Downstream of CLPs are CD34+CD19+ ProB-progenitors which have been reported in human FL, FBM, CB and ABM (LeBien et al, 2000; Reynaud et al, 2003; Yang et al, 2007; LeBien and Tedder, 2008; Sanz et al, 2010; Roy et al, 2012; O'Byrne et al, 2019; Sorcha O'Byrne ASH Abstract, 2019). ProB progenitors show a clear B-lineage signature including elevated expression of key early and late B-cell genes including *PAX5, RAG1, CD72* and readily give rise to B-cells within functional assays (Yang et al, 2007; Sanz et al, 2010; Roy et al, 2012; O'Byrne et al, 2019). Sanz et al, 2019 offer a comprehensive review of the downstream human mature B-cell subsets.

Given that CD10+ ProB progenitors comprise the majority of the B-progenitors in ABM, whilst ELPs and PreProB progenitors are much more common in FBM (O'Byrne et al, 2019), the enrichment of CD10+CLPs in CB may indicate a shift toward a more CD10+ phenotype for B-cell precursors after birth.

1.1.6 Transcriptional control of B-cell development

There are several transcription factors which regulate the specification and later commitment to the B-lineage (Hardy and Hayakawa, 2001), reviewed extensively by LeBien and Tedder, 2008, O'Riordan and Grosschedl, 2000 and Rothenberg, 2014. While new players in B-cell development continue to emerge, such as the growing family of ZBTB transcription factors (Zhu et al, 2018), the best-established transcription factors include E2A (encoded by *TCF3*), EBF1 and PAX5, which all play vital roles in ensuring commitment to the B-lineage and subsequent normal differentiation to produce mature B-cells (Nutt et al, 1999; Nutt and Kee, 2007). Altogether, the expression of these transcription factors occurs in a stepwise process: once a sufficient threshold of E2A expression has been reached, EBF1 is then upregulated from which point it can cooperate with E2A to upregulate PAX5 (Rothenberg, 2014). Upstream, the sufficient expression of these integral and early determinators of B-lymphopoiesis is ensured by background E2A and collaborating FoxO1, Runx/CBFβ activities (Rothenberg, 2014).

Work has consistently indicated that B-progenitors at distinct stages of the B-differentiation hierarchy express varying levels of B-lineage associated transcription factors, reflective of their degree of B-lymphoid commitment. Whilst the expression B-cell transcripts (*TCF3, EBF, BCL11A* and *PAX5)* is high within earlier B-progenitors, they retain expression of T/NK (e.g. *CD2, NOTCH1*) and even myeloid genes (e.g. *MPO*) (Hystad et al, 2007; Kohn et al, 2012). By contrast within more B-committed progenitors, there is reduced expression of genes associated with early lymphoid priming (*CD62L*) and higher expression of genes that are associated with a terminal B-cell phenotype CD72, CD79A, CD44, CD20) (Hystad et al, 2007; Sanz et al, 2010; Kohn et al, 2012; O'Byrne et al, DPhil thesis, 2019).

1.1.7 Cytokine regulation of B-lineage specification and differentiation

Many cytokines act to regulate B-cell production, both in a stimulatory and repressive manner including members of the Interleukin and Interferon families (Vazquez et al, 2015). Some of the cytokines which have been identified, mainly through murine studies, as playing major roles in B-cell development are IL-7, FLT3-L and TSLP.

After IL-7 was shown to be vital for B-lymphopoiesis in mice, it has also been shown to be important during human B-cell differentiation and proliferation (Ryan et al, 1997; Puel et al, 1998; Nutt et al, 1999; Johnson et al, 2005; Taguchi et al, 2007; Parrish et al, 2009), with some work indicating a greater dependence on IL-7 for B-lymphopoiesis later in ontogeny (Parrish et al, 2009). In addition to IL-7, FLT3-L, which acts by binding its cognate tyrosine kinase receptor Flt3 on many haematopoietic progenitors (Gilliand and Griffin, 2002), has also been shown to play an integral role in B-lymphopoiesis in both humans and mice (Namikawa et al, 1996; Vosshenrich et al, 2003; Vosshenrich et al, 2004; Jensen et al, 2007; Jensen et al, 2008; Parrish et al, 2009).

Thymic stromal-derived lymhopoietin (TSLP) also signals via the IL-7Ra receptor and has been explored most extensively within the context of fetal B-lymphopoiesis (Vosshenrich et al, 2003; Vosshenrich et al, 2004; Jensen et al, 2007). Despite claims that TSLP can rescue B-lymphopoiesis in the absence of IL7 (Vosshenrich et al, 2003; Vosshenrich et al, 2004; Montecino-Rodriguez et al, 2006), separate work within mice suggests that whilst TSLP can augment IL-7 independent B-differentiation, it does not play a central role (Jensen et al, 2008). The main difficulty in concluding whether TSLP does display a level of redundancy for IL-7 or is simply an important cooperating cytokine, has been that some of the data

supporting this claim failed to distinguish impaired signalling during deficiencies in the IL-7Ra chain (which is the receptor for both IL-7 and TSLP signalling) compared to the IL-7Rγ which is involved in IL-7 but not TSLP signalling (Vosshenrich et al, 2003; Vosshenrich et al, 2004; Jensen et al, 2007). Subsequent to these works, Scheeran and colleagues showed that TSLP supports the proliferation and differentiation of human fetal B-cells in vitro (Scheeren et al, 2010), however there have been few other direct reports of the TSLP function in human B-lymphopoiesis (Savino and Izraeli, 2016). Recent xenograft models which express human TSLP should be useful in clarifying the role of TSLP in human B-differentiation (Francis et al, 2016).

Several other cytokines have been implicated in B-cell differentiation including IL-2, IL-3, IL-4 and IL-21 (Crooks et al, 2000; Hipp et al, 2017; Cyster and Allen, 2019). More comprehensive, recent reviews on the cytokines which support B-lymphopoiesis include those by Vazquez and colleagues, 2015 or Cyster and Allen, 2019.

1.18 Current models for human T/NK-lymphoid differentiation

Aside from B-lymphocytes, the CLP can also give rise to NK cells and T-cells. T-lymphocytes are a vital component of the adaptive immune response, with different subsets offering specialised functions (Kumar et al, 2018). Briefly, CD4+ T-helper cells support B-cell humoral responses, whilst CD8+ killer T-cells mount protective cytotoxic responses against pathogens and tumor cells. Fetal tissues exhibit an increased frequency of Treg cells compared to any other human developmental stage, highlighting the importance of modulating the immune response and promoting immune tolerance toward maternal allo-antigens and to prevent damage to the fetal host (Burt et al, 2013).

T-cells derive from BM-resident progenitors which undergo maturation and selection within the thymus before being released to lymph nodes for antigen presentation during infection or tumor-exposure (Kumar et al, 2018). Unlike mice, the majority of human T-cell production occurs during development; with both conventional and regulatory T-cells emerging from the fetal thymus around 12-14 weeks of gestation (Rackaityte and Halkias, 2020), where they begin to migrate to the peripheral lymph nodes and can be detected in circulation from 15-16 weeks onward (Rechavi et al, 2015). After birth, these fetal-derived naïve T-cells become exposed to antigens after birth and memory is gradually developed throughout childhood (Kumar et al, 2018; Rackaityte and Halkias, 2020).

Natural killer cells are innate, cytotoxic lymphocytes which specialise in anti-tumor and anti-viral responses. During fetal development, the fetus is exposed to considerable allogenic maternal cells, maternal antibodies and extrinsic pathogens and for this reason, NK cells play important roles in balancing immune reactivity and tolerance at the fetal: maternal

interface to prevent rejection of the fetus or complications during pregnancy (Papuchova et al, 2019). Current models suggest that in post-natal life, the adult BM is the primary site of NK production and that to a lesser degree, extramedullary sites including tonsil, thymus and the liver may play a supportive secondary role (Renoux et al, 2015). Recent work has led to the identification of NK progenitors (NKPs) in fetal BM, fetal liver, CB, Adult BM and adult tonsil. NKPs give rise exclusively to NK cells in vitro and in vivo and represent the earliest NK-lineage committed progenitor in fetal and adult life, unlike CLPs can give rise to T, B and NK-lineages (Renoux et al, 2015). Recent work in fetal tissues indicates that NK cells emerge early within gestation, and can be detected by 6 weeks post-conception in fetal liver, and that 2 waves of NK development occur, with terminal NK differentiation stabilising within the second trimester (Ivarsson et al, 2013). Comparative studies of cord blood and fetal NK cells indicates that the transition to a more adult-like NK phenotype occurs in the third trimester (Ivarsson et al, 2013).

1.2 Fetal haematopoiesis

1.2.1 Origins of fetal haematopoiesis

Mammalian haematopoiesis consists of three major waves (Ivanovs, 2017). However there are key differences in haematopoietic development between the species (Ernst and Carvunis, 2018). Human developmental stages are described in post-conception weeks (pcw) and embryonic day (E) is used to describe murine stages.

Briefly, within mice haematopoiesis begins in the yolk sac, where primitive erythro-myelopoiesis occurs (Huyhn et al, 1995; Dzierzak and Bigas, 2018). Subsequently, around E10-11, definitive HSCs emerge from the ventral wall of the intra-embryonic aorto-gonado-mesonephros (AGM) (Tavian et al, 1999; Ivanovs et al, 2011). After definitive HSCs have emerged (E10.5) and prior to their subsequent migration to and expansion within the FL, which becomes a key fetal haematopoietic site, the placenta also serves as a niche for HSC expansion (Gekas et al, 2005). During perinatal stages, the BM becomes the major haematopoietic site for the remainder of life (Dzierzak and Bigas, 2018).
Reports have also shown that the spleen acts as a supportive haematopoietic site around the same time the BM becomes colonized (Christensen et al, 2004).

Human primitive haematopoiesis also originates with erythro-myelopoiesis in the yolk-sac and by 4 pcw, definitive HSCs emerge from the AGM and vitelline arteries (McGrath et al, 2015). Similarly to mice, human HSCs then infiltrate and seed the FL which becomes the primary haematopoietic site (Tavian et al, 1999). From 10-12pcw when haematopoietic cells

are found in the FBM, the BM remains the major haematopoietic site throughout post-natal life (Ivanovs et al, 2017; O'Byrne et al, 2019).

1.2.2 Primitive versus definitive haematopoiesis

The spatiotemporally distinct waves of mammalian haematopoiesis represent differences in the maturity and capacities of the haematopoietic cells they produce; namely the products of 'primitive' or 'definitive' haematopoiesis, depicted in Figure 1.5 (new). Primitive and definitive haematopoiesis serve distinct, important functions in embryonic life and can be distinguished based on several characteristics (McGrath et al, 2015).

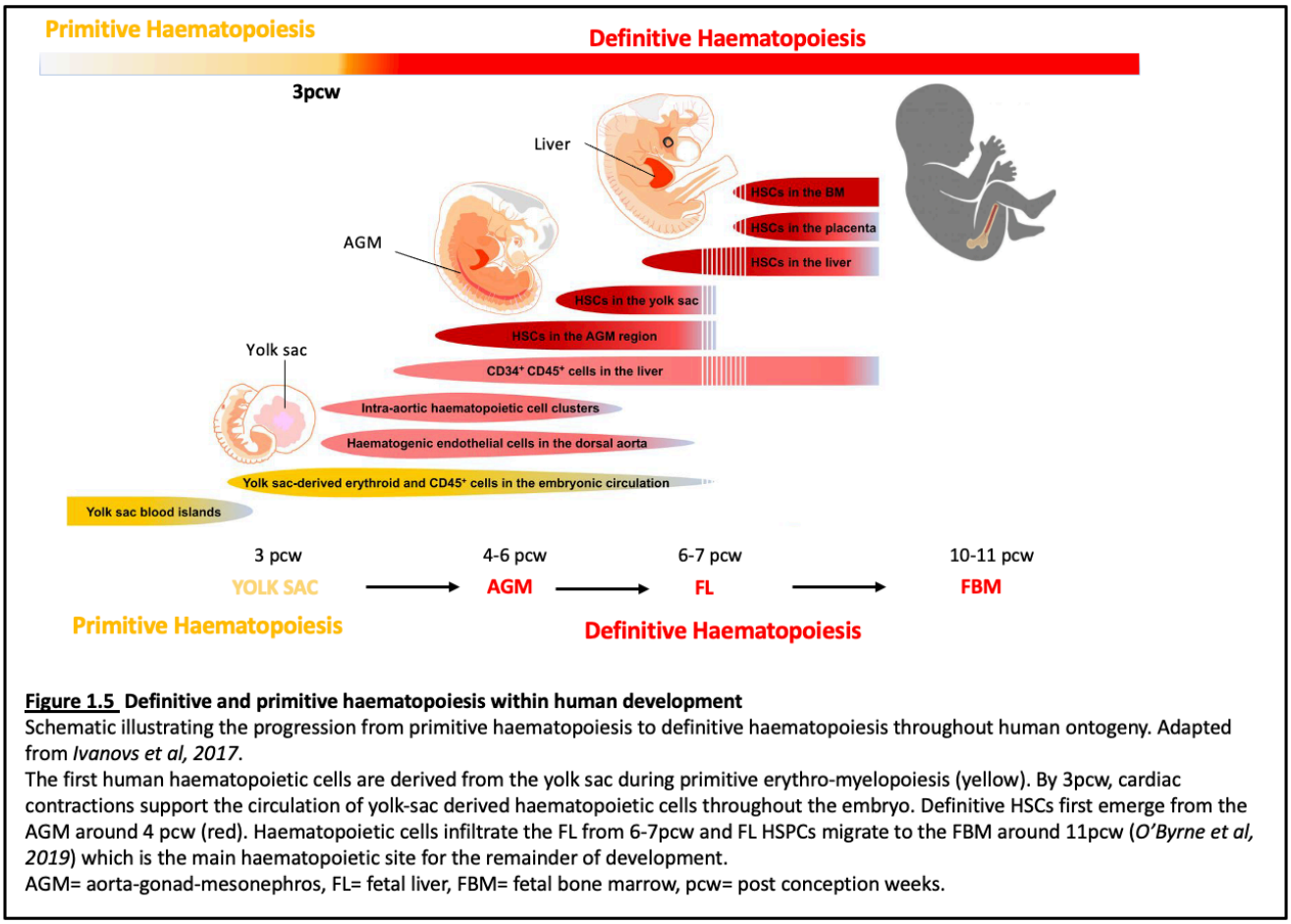


Figure 1.5 Definitive and primitive haematopoiesis within human development
Schematic illustrating the progression from primitive haematopoiesis to definitive haematopoiesis throughout human ontogeny. Adapted from *Ivanovs et al, 2017*.
The first human haematopoietic cells are derived from the yolk sac during primitive erythro-myelopoiesis (yellow). By 3pcw, cardiac contractions support the circulation of yolk-sac derived haematopoietic cells throughout the embryo. Definitive HSCs first emerge from the AGM around 4 pcw (red). Haematopoietic cells infiltrate the FL from 6-7pcw and FL HSPCs migrate to the FBM around 11pcw (*O'Byrne et al, 2019*) which is the main haematopoietic site for the remainder of development.
AGM= aorta-gonad-mesonephros, FL= fetal liver, FBM= fetal bone marrow, pcw= post conception weeks.

Primitive haematopoiesis

Primitive haematopoiesis is extra-embryonic and gives rise to nucleated erythrocytes (Frame et al, 2013) which are necessary to support the developing embryo until definitive haematopoiesis can be established. In contrast, definitive haematopoiesis generates all haematopoietic lineages, including definitive HSCs, which have high regenerative capacities, supporting multi-lineage long-term reconstitution throughout life (McGrath et al, 2015; Ivanovs et al 2017).

Within mice, the pre-HSC haematopoietic waves of primitive haematopoiesis are vital to ensure a steady supply of red cells throughout gestation to support the immediate needs and survival of the growing embryo before definitive fetal haematopoiesis is established in a seamless transition (Frame et al, 2013; McGrath et al, 2015). During this primitive wave, Erythro-Myeloid Progenitors (EMP) emerge from the yolk sac and give rise to erythroid, megakaryocytic, and myeloid progeny (Chen et al, 2011; Iturri et al, 2021; Soares-da-Silva et al, 2021). Indeed, loss of EMPs leads to embryonic lethality by E13.5 in mice, even if long term repopulating HSCs are present, reaffirming their importance in transiently supporting survival (Chen et al, 2011; Palis, 2016; Soares-da-Silva et al, 2021). For the most part, these earlier waves of haematopoiesis lack significant lymphoid progeny, which emerge during the subsequent waves of haematopoiesis that give rise to lympho-myeloid progenitors (LMPs), multipotent progenitors (MPPs), and HSCs (Böiers et al., 2013; Hadland and Yoshimoto, 2018; Inlay et al., 2014). Interestingly, however recent reports from mice reveal that some degree of lymphoid lineage commitment occurs earlier than previously thought and before the emergence of definitive HSCs (Böiers et al., 2013; Elsaid et al 2019). Boiers et al identified

a lymphoid-primed and immune-restricted progenitor which emerge in the yolk sac to give rise to both the lymphoid and some myeloid compartments of the immune system (Boiers et al 2013). Currently, however, there is no conclusive evidence yolk-sac derived lymphopoeisis in humans (Elsaid et al 2019).

Primitive haematopoiesis has not been so clearly defined within humans, but is known to involve yolk-sac derived primitive erythroid cells and monocytes/macrophages between 2-3pcw (Tavian et al, 1999; Ivanovs et al, 2017). After cardiac stimulation and contraction at 3pcw, these CD45+ cells are circulated throughout the embryo (Ivanovs et al, 2017). At present, there has been no conclusive evidence of the yolk sac EMP-wave observed in mice, but one early study hinted toward its existence between 4-5pcw (Migliaccio et al, 1986).

Definitive haematopoiesis

Definitive HSCs show self-renewal and long-term repopulating capacity and are found within the same immunophenotypic compartment as those in post-natal bone marrow, and functionally give rise to all of the major haematopoietic lineages (Muller et al, 1994; Medvinksy and Dzierzak 1996, de Bruijn et al 2002; Oberlin et al, 2010; Ivanovs et al, 2011; Dzierzak and Bigas, 2018; Ulloa et al 2021).

Several murine studies have highlighted the importance of definitive haematopoiesis. For example, EMP have no long-term repopulating capacity when transplanted into immunocompromised mice (McGrath et al, 2015) and whilst murine EMP and early progenitors can support the fetus to birth in the absence of transplantable HSCs, there are notable defects in lymphoid development (Chen et al, 2011; Dzierzak and Bigas, 2018), until the onset of definitive embryonic haematopoiesis. Similarly, recent reports that primitive and

definitive HSPCs show strikingly different transcriptomic signatures, reflect their distinct functions in embryonic development (Zhu et al, 2020).

Interestingly, however, recent lineage tracing studies in mice suggest that fetal HSCs make a relatively minimal contribution to haematopoiesis before birth (Soares-da-Silva et al, 2021; Yokomizo et al, 2022). Instead, the differentiation of non-HSC-derived progenitors transiently supports the haematopoietic homeostasis and growth of the embryo, which facilitates the preservation and expansion of HSC pools (Soares-da-Silva et al, 2021; Yokomizo et al, 2022).

Within mice, the first definitive HSCs in the mouse emerge at E10.5 from a specialised group of endothelial cells known as haemogenic endothelium, which is localised to the ventral wall of the dorsal aorta in a region known as the Aorto-Gonado-Mesonephros (AGM) (Muller et al, 1994; Medvinksy and Dzierzak 1996, de Bruijn et al 2002).

Within humans, definitive haematopoiesis also occurs within the AGM and this process of HSC emergence is known as the endothelial-to-hematopoietic transition (EHT) (Marshall and Thrasher, 2001; Ivanovs et al, 2011; Ivanovs et al, 2014). Whilst the AGM and yolk sac are structured and developed differently within mouse and human, the process of transitioning from primitive to definitive haematopoiesis in humans is broadly similar (Ivanovs et al, 2017; Dzierzak and Bigas, 2018). Definitive HSCs bud from the dosal aortal floor around 4pcw, after which they develop within intra-aortic haematopoietic clusters (IAHCs) of the AGM (Tavian et al, 1996; Easterbrook et al, 2019). Shortly after this, these definitive HSCs migrate to the FL (Tavian et al, 1999), which is an important haematopoietic niche for the expansion, differentiation and maintenance of HSCs throughout gestation. The onset of haematopoiesis

in the FBM occurs at 11 pcw and it is the predominant site for fetal B lymphopoiesis (Charbord et al, 1996; O'Byrne et al, 2019; Jardine et al, 2021; Ranzoni et al, 2021; Roy et al, 2021).

1.2.3 Human fetal B-lymphopoiesis

The FL and FBM are the two main sites of B-lymphopoiesis during fetal development (O'Byrne et al, 2019; Popescu et al, 2019; Roy et al, 2021; Jardine et al, 2021), and previous investigations into lineage differentiation hierarchies of human haematopoiesis have focused on delineating the process within adult cells and CB. However, recently extensive work within both mice and humans has revealed important distinctions between fetal and adult HSPCs (Boiers et al, 2013; Jassinskaja et al 2017, Chen et al, 2019; Jassinskaja et al, 2019; Bunis et al, 2021; Suo et al, 2022) and it is believed that distinct patterns of lineage biasing exist between fetal and adult HSPCs which reflect their different roles during ontogeny and exposure to vastly different environments (Copley et al, 2013).

Whilst B-lymphopoiesis originates in the FL, the BM is the primary site of B-cell expansion before birth (O'Byrne et al, 2019; Jardine et al, 2021; Roy et al, 2021). HSCs, MPPs and LMPPs can be detected in FL from 6 pcw and both immature B-progenitors and mature B-cells can be observed just one week later.

The current fetal B-lymphopoiesis differentiation pathway is depicted in Figure 1.6.

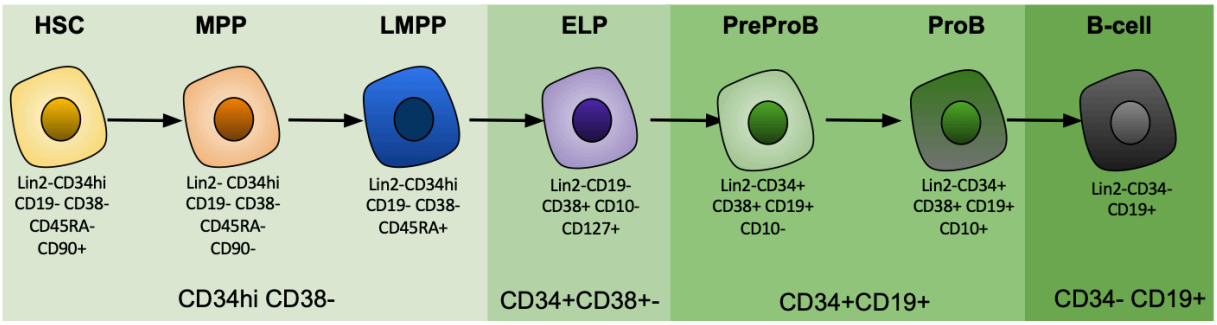


Figure 1.6 Human fetal B-lymphopoiesis pathway
Schematic illustrating the human B-differentiation pathway within fetal life, as resolved by *O'Byrne et al, 2019*.

HSC, haematopoietic stem cell; **MPP**, multipotent progenitor; **LMPP**, lymphoid-primed multipotent progenitor **ELP**, early lymphoid progenitor.
Lin2= CD2/3/14/16/56/235a

During our lab's characterisation of fetal lymphopoiesis, we showed the existence of a fetal-specific CD10-CD19- IL-7R+ progenitor named ELP (CD34+CD38+ CD127+CD10- CD19-) in FL and subsequently FBM (Roy et al, 2012; O'Byrne et al, 2019), which has also been described by others (Hussen et al, 2017; Boiers et al, 2018). Recent functional characterisation demonstrated that ELPs, which lie downstream of LMPPs, possess the ability to produce B-, NK- and T-cells but show minimal residual myeloid potential (O'Byrne et al, 2019). In addition, we recently demonstrated that PreProB progenitors (CD34+CD38+CD19+CD10-) are the earliest B-lineage restricted progenitor in the fetal B-lymphopoiesis pathway and that they are specific to fetal life (O'Byrne et al, 2019).

Although the B-progenitors within adults (CLP, ProB), and fetal life (ELP, PreProB, ProB), are functionally comparable, they are distinct at the molecular level, suggesting ontogeny-related differences. Whilst the expression of most B-cell genes was similar, fetal B-progenitors were shown to express higher levels of myeloid genes, fetal specific genes, including *LIN28B*, and genes associated with early B-lymphoid priming e.g. *DNTT, TCF3,*

LEF1, whilst ABM counterparts showed higher expression of mature B-cell genes including *CD72, CD79A* and *CD20* (Yuan et al, 2012; O'Byrne et al, 2019)

Finally, as of yet evidence for human fetal CLPs is lacking despite observations in human ABM and CB (discussed in 1.1.3 and 1.1.5). The presence of CD10- B-progenitors in FL and FBM but not ABM (Roy et al, 2012; O'Byrne et al, 2019) raises the question of whether adult B-lymphopoiesisis exhibits a more CD10+ phenotype and if so, what biological significance this may have.

One of the main reasons for gaining a fuller understanding of fetal B-lymphopoiesis and the HSPCs involved, is that B-ALL, one of the most common cancers in children, is believed to initiate in utero, with studies of fetal tissues (including liver and bone marrow) showing presence of ALL-causing oncogenic fusions as well as Guthrie cards showing the presence of leukaemic markers in neonatal bloodspots (Gale et al, 1997; Ford et al, 1998; Uckun et al, 1998; Wiemels et al, 1999; Greaves, 1999; Mori et al, 2002; Greaves et al, 2003; Zuna et al, 2003; McHale and Smith, 2004; Burjanivova et al, 2005; Gruhn et al, 2008; Hein et al, 2020; Jackson et al 2021). Indeed, some of the key genes involved in regulating fetal haematopoiesis have been linked to oncogenesis. For example, *LIN28B* (covered in chapters 1.1.1 and 1.1.2), a regulator of stemness, fetal-specific lineage priming and B-lymphopoiesis (Copley et al, 2013; Wang et al, 2022), has also been linked to oncogenic transformation (Viswanathan et al, 2009; Zhou et al, 2013; Oliveira-Mateos et al, 2019; Elcheva et al, 2020). Moreover, the unique existence of ELPs and PreProBs within fetal life has led to speculation these may act as the cell of origin for infant and/or childhood ALL (Jackson et al, 2021).

1.2.4 The FBM and FL as distinct haematopoietic sites

Emerging work has begun to characterise the microenvironment within the FL and FBM, which reflect the distinct roles played by these sites during haematopoietic development.

Fetal liver

Briefly, the FL microenvironment is composed of Hepatocytes, endothelial cells and other stromal cells which supply local growth factors to HSPCs (Popescu et al, 2019). Early work identified a higher density of N-cadherin- and osteopontin-expressing cells in FL stroma relative to adult BM as well as a relative enrichment for regulators of the Wnt signalling pathway (Martin and Bhatia, 2005). Furthermore, in both mouse and human FL (Lewis et al, 2021; Suo et al, 2022), early macrophages and mast cells were found to play a role in supporting the development of the niche, whereas this was not observed for FBM (Suo et al, 2022).

Briefly, recent comprehensive investigations of both first and second trimester FL reveal that FL haematopoiesis transitions from being largely erythroid-biased to predominantly supporting lympho-myeloid fates in later gestational stages (Popescu et al, 2019; Roy et al, 2021) with an enrichment for erythroid lineage genes in FL compared with FBM, especially during early gestation FL samples (Roy et al, 2021).

Interestingly, a recent study highlighted segregation of the early and late erythrocytes within FL, which suggests some kind of spatial compartmentalisation into distinct zones (Suo et al, 2022).

As well as the shift away from erythropoiesis, HSPCs found in FL were shown to be less proliferative as gestation progressed (Popescu et al, 2019).

Migration to the FBM

A recent study of the FBM revealed 19 stromal cell types and significant heterogeneity, with endothelial cells aggregating into 2 main types based on their gene expression profiles: sinusoidal and non-sinusoidal tip cells (Jardine et al, 2021). Endothelial cell sub-groups showed regional partition proximal to the diaphysis and metaphysis structures and there was also evidence of interplay with CXCL12+ cells (Jardine et al, 2021).

Moreover, these investigations, alongside other work, have shown that the migration of haematopoietic cells from the FL to FBM at the beginning of the second trimester is strongly associated with a transition toward a more quiescent state (Roy et al, 2021; Ranzoni et al, 2021). In line with the migration from FL to FBM around 11pcw, a recent analysis of FBM and FL showed an upregulation of genes associated with actin cytoskeleton remodellers, cellular adhesion and migration in the FL relative to FBM (Ranzoni et al, 2021). Moreover, *IFITM1*, a gene linked to adhesion and proliferation, was shown to be significantly upregulated in FL (Ranzoni et al, 2021). This in turn, is accompanied by a reduction in non-lineage-committed HSPCs in FBM, which implies a special role for the FBM microenvironment in promoting lympho-myeloid expansion and more broadly, haematopoietic maturation (Roy et al, 2021; Ranzoni et al, 2021).

Comparison of the FL and FBM microenvironments has thus far been limited. However, the distinct lineage skewing observed in HSPCs at each site is a compelling case for further comparative evaluation of their cellular composition and molecular profiles.

1.3 Down syndrome and haematopoiesis

1.3.1 Trisomy 21, aneuploidy and disease

Trisomy 21 (T21), characterised by an extra copy of chromosome 21 (Hsa21), is the most common constitutional aneuploidy in humans (1 in every 750 births) and manifests in humans as Down syndrome (DS) (Antonarakis, 2017). DS is a broad syndrome associated with several conditions including haematological and autoimmune abnormalities, cardiac complications and neurodevelopmental disorders (Bull, 2020).

The causal role of T21 in DS, the small size of Hsa21 and the fact it is one of the few viable aneuploidies, makes it a paradigm for the study of these disorders (Antonakaris et al, 2020). Since the successful sequencing of Hsa21 twenty years ago, it has become the most studied human chromosome (Antonakaris, 2017). Individuals harbouring T21 also display considerable genetic variability (Korbel et al, 2009; Antonakaris, 2017). This variability can come in the form of single nucleotide variants (SNVs) which may impact the function of the protein they encode and associated biochemical pathways or alternatively, SNVs can alter interaction sites within the mutated DNA sequence itself thereby impacting gene expression (Lappalainen, et al 2013). Additionally, Down syndrome patients may show copy number variation (CNV) of a wide and often unpredictable array of genes leading to a unique mosaic phenotype that varies on an individual basis (Korbel et al, 2009; Antonakaris, 2017).

The vast majority of cases, over 95%, are caused by meiotic non-disjunction, resulting in a full trisomy of Hsa21, the risk of which increases with maternal age (Bull, 2020). However, in 3-4% of DS patients there are translocations between Chr21 and Chr 14, 21 or 22, the risks of

which are typically increased by the presence of a parental carrier (Bull, 2020). Approximately 2 % of patients present a mosaic phenotype due to variation in the number of affected cells in patients and these patients often lack the typical phenotypic features of DS (Papavassiliou et al, 2015). Finally, up to 1% of patients show partial trisomy, meaning a duplication of a limited portion of Hsa21, rather than the full chromosome (Pelleri et al, 2016). The resulting phenotype will depend on the duplicated region, the direct functions in the genes in this locus, their potential downstream targets or neighbouring co-regulated genes (Pelleri et al, 2016).

Partial T21 has been a tantalising model for researchers hoping to link defined genomic loci to the complex phenotypes presented in DS. Efforts to delineate specific triplicated genetic regions of Hsa21 responsible for distinct clinical phenotypes of DS started in the 1970s which led to the identification of the Down syndrome critical region or DSCR twenty years later - see Figure 1.5 (Delabar et al, 1993; Rahmani et al, 1989). This work has relied heavily on mouse models (Gardiner et al, 2003, see Figure 1.7), most notably Ts65Dn which carries an approximately 55% triplication of the Mmu16 syntegenic region for Hsa21 (Davisson et al, 1990; Reeves et al, 1995). Current mouse models, their uses and limitations is reviewed in detail by Gupta et al and has been discussed more broadly by Antonakaris, 2017.

Since this early work, several studies have suggested an association between the 21q22 region and the most severe phenotypes associated with DS, whilst triplication of the short arm (21p) and distal segment of the long arm (21q21) do not seem to induce the same severe phenotype (Shapiro, 1999; Antonaros et al 2021). However, the notion of a DSCR has been debated due to the unlikelihood that a single duplicated region is able to manifest the full disease phenotype (Korenberg et al, 1994; Korbel et al, 2009; Lyle et al, 2009) as recent

studies have failed to definitively link smaller sub-regions of the DSCR to distinct phenotypic features (Antonaros et al 2021).

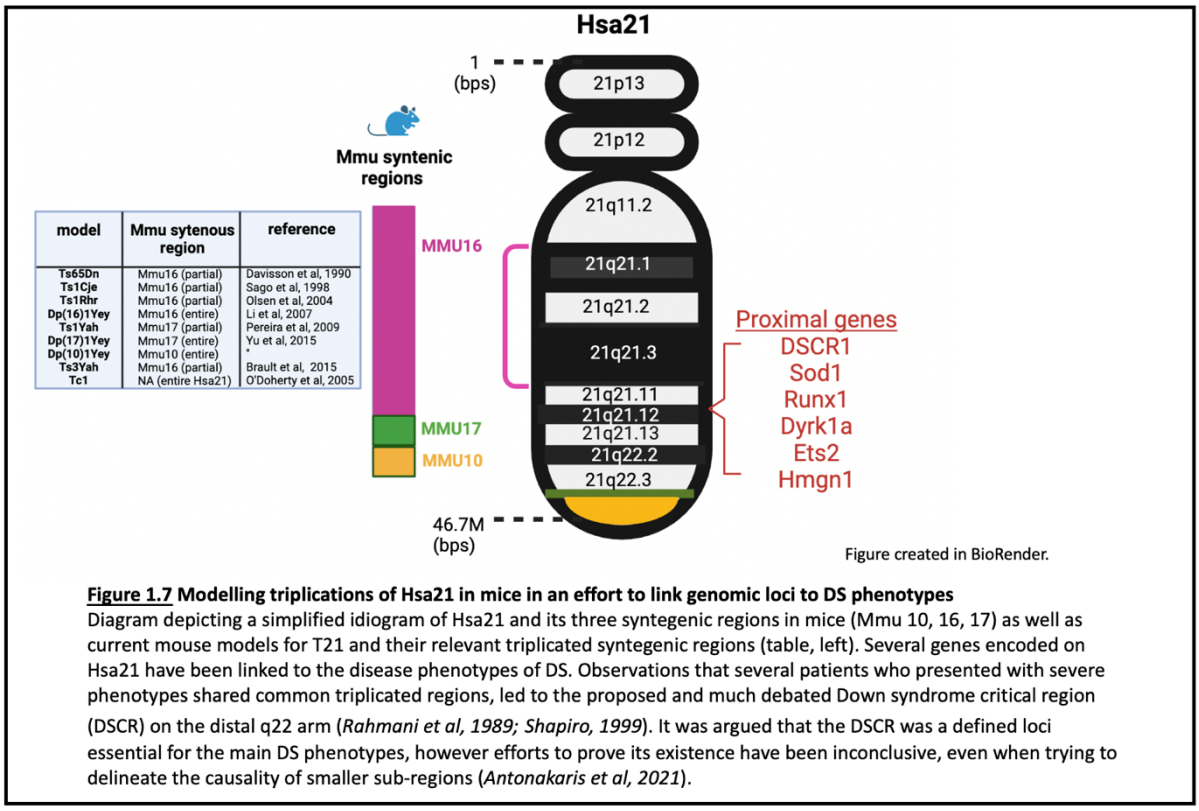


Figure 1.7 Modelling triplications of Hsa21 in mice in an effort to link genomic loci to DS phenotypes
Diagram depicting a simplified idiogram of Hsa21 and its three syntegenic regions in mice (Mmu 10, 16, 17) as well as current mouse models for T21 and their relevant triplicated syntegenic regions (table, left). Several genes encoded on Hsa21 have been linked to the disease phenotypes of DS. Observations that several patients who presented with severe phenotypes shared common triplicated regions, led to the proposed and much debated Down syndrome critical region (DSCR) on the distal q22 arm (*Rahmani et al, 1989; Shapiro, 1999*). It was argued that the DSCR was a defined loci essential for the main DS phenotypes, however efforts to prove its existence have been inconclusive, even when trying to delineate the causality of smaller sub-regions (*Antonakaris et al, 2021*).

As well as alterations in gene dosage, aneuploidy is thought to induce aberrant phenotypes through indirect mechanisms (Antonakaris et al, 2020). These indirect mechanisms include modulation of epigenetic modifiers on the affected chromosome which can lead to downstream mis-regulation of distal target genes on other chromosomes, the consequences of which will depend on the cell and tissue specific context. For example, individuals with Down syndrome are predisposed to Early Onset Alzheimers disease (EOAD) (Bull, 2020). Whilst Hsa21 encodes a high density of cytoskeletal proteins implicated in neurodegenerative disorders, the majority of the dysregulated proteins related to this phenotype are in fact TFs, whose increased dosage alters neural gene expression more diffusely throughout the genome (Bamburg and Bloom, 2009; Antonakaris, 2017).

In addition, topological changes induced by increased physical genetic material within the nucleus may impact the configuration of adjacent chromatin and thereby gene expression. If chromosome copies have been entirely or even partially gained, the ensuing increase in mRNA and protein levels may disturb the stoichiometric balance of proteins in the cytoplasm which can saturate protein folding machinery and degradation pathways, in some cases leading to the formation of protein aggregates (Chunduri and Storchova, 2019).

1.3.2 Abnormal haematopoiesis in DS

Individuals with DS display a distinct and abnormal haematopoietic profile although clinical presentations of this disruption in DS varies according to age and individual variation (summarised in Table 1.2).

Table 1.2 Clinical phenotypes of abnormal haematopoiesis in DS patients

	Phenotype	Reference
Fetal life (pre-birth)	HSC expansion in T21 FL	Roy et al, 2012
	MEP and mature Megakaryocyte expansion in T21 FL	Tunstall-Pedoe et al, 2008 Roy et al, 2012
	Reduction in B-lineage populations in T21 FL	Roy et al, 2012
	Enhanced myeloid lineage clonogenicity in T21 FL	Roy et al, 2012
	Erythroid bias in T21 FBM HSCs and MPPs	Jardine et al, 2021
Neonatal*- childhood life** (* Day 0 – 28 post birth) (** 1 - 15 years)	Significant abrogation of normal B/T lymphocyte expansion seen in healthy children, with counts severely decreased until adulthood (16 years and above),	deHingh et al, 2005
	Relative % of NK cells in the overall lymphocyte population is significantly increased in whole blood of neonates and children with DS, whilst the relative proportion of B-cells is significantly reduced	Bloemers et al 2010; Schoch et al, 2017
	Neonatal immune-deficiency believed to be caused by B-cell population shrinkage	Bloemers et al 2010; Schoch et al, 2017
	Neonatal TAM (~10% neonates), followed by GATA1 mutation driven AMKL in 20-30% of cases. Increased freq of infant DS-AMKL and MLDS within the first 4 years of life.	Groet et al, 2003 Roberts and Izraeli, 2014
	Increased incidence of childhood B-ALL	Roberts and Izraeli, 2014
Adult life	Non-specific haematological abnormalities are common, including; leukopenia, macrocytosis, erythrocytosis and elevated MCV.	Prasher 1994; McLean et al, 2009;
	Relative % of NK cells in the overall lymphocyte population is significantly increased in whole blood of adolescents with DS, whilst relative proportion of B-cells is significantly reduced	Schoch et al, 2017
	Reduced leukaemia presentation in adult patients – SIR for ALL drops from 27 in children up to 5 years old to 2 in adults >30 years old.	Hasle et al, 2016

Emerging research has revealed that perturbations of haematopoiesis in individuals with DS are present before birth (Tunstall-Pedoe et al, 2008; Roy et al, 2012; Jardine et al, 2021). Within children and neonates, there is a significantly higher risk of developing acute leukaemia, particularly in early life (Hasle et al, 2000; Roberts et al, 2013; Hasle et al, 2016; Lee et al, 2016; Wiemels et al, 2019), discussed further in DS- associated leukaemias (1.3.3).

The most notable of the non-malignant haematopoietic aberrations presented in DS children and young adults are various defects of the immune system, an association made as early as the 1970s (Yang et al, 2002). Several studies have demonstrated that trisomic individuals exhibit immune-deficiencies due to lymphopenias, namely both qualitative and quantitative aberrations of B and T-lymphocytes, which seem to hinder the functionality of these cells in the adaptive immune response (de Hingh et al 2005; Kusters et al 2009; Schoch et al, 2017). In addition, poor responses to vaccination have been documented in DS individuals, which has been hypothesised to be due to poor memory B responses (Valentini et al, 2015). As a result, many children suffer from infections, most commonly pneumonia and infections of the respiratory tract (Yang et al 2002; Hilton et al, 1999; Bloemers et al, 2010).

Alongside an increased risk of developing infections, children with DS often present with a more severe disease once infected due to an over-compensatory, enhanced pro-inflammatory cytokine release, in comparison with healthy peers (Broers et al, 2012). Similarly, individuals with DS present more frequently with autoimmune disorders such as diabetes mellitus, thyroid disease and coeliac disease (Anwar et al, 1998; Karlsson et al, 1998; Sanchez-Albisua et al, 2002; Kusters et al, 2009; Ram and Chinen et al, 2011; Pellegrini et al, 2012). These observations have led some in the field to consider DS as a primary immunodeficiency (Kusters et al, 2009; Carsetti et al, 2015), although it is probably more

accurate to say that T21 clearly disrupts the normal functioning of several aspects of the immune system.

1.3.2.1 Abnormal adult haematopoiesis in DS

Clinical records of the haematological and immune defects observed in adults with DS is less well documented than those of children (Prasher, 1994; McLean et al, 2009). Population-based studies assessing mortality and morbidity in DS indicates the Standardised Mortality Odds Ratio for aspiration pneumonia or Influenza peaked at 50-59 years of age (Yang et al, 2002), however recent studies suggest that the number of older DS adults experiencing infections is considerably lower than previously thought (Lott et al, 2010; Guffroy et al, 2019), though infection remains the most common cause of death in adults with DS (Englund et al, 2013).

1.3.2.2 Abnormal fetal haematopoiesis in DS

Most of our limited current understanding of fetal and perinatal haematopoiesis in DS have involved work done in FL (Tunstall-Pedoe et al, 2008; Roy et al, 2012; Wagenblast et al, 2020). Early studies sampling fetal blood using cordocentesis of second trimester DS, indicated significantly lower numbers of CD19+ B cells and a significantly lower ratio of CD4:CD8 helper and effector T-cells in DS fetuses, although absolute numbers of these were not significantly reduced (Zizka et al, 2006). Interestingly, B-lymphocytopenia was not observed in Edwards syndrome (the clinical manifestation of trisomy 18), therefore this deficiency was specific to T21 karyotypes rather than aneuploidy in general (Zizka et al, 2006).

Within the FL, our own lab and others have documented an expansion of FL HSCs, Megakaryocyte-Erythroid Progenitors (MEPs) and megakaryocytes with a concurrent block in

B-cell differentiation leading to a reduction in PreProB and ProB progenitors (Tunstall-Pedoe et al, 2008; Roy et al, 2012; Wagenblast et al, 2020). Human hESC and iPSCs harboring T21 also show megakaryocyte-erythroid skewed differentiation when grown under conditions designed to recapitulate fetal-liver or yolk sac-like conditions (Maclean et al, 2012; Chou et al, 2012). Primary DS FL HSPCs also show enhanced megakaryocyte-erythroid lineage output in colony forming assays and greater overall clonogenicity (Tunstall-Pedoe et al, 2008; Roy et al 2012; Wagenblast et al, 2020) underpinned by changes in megakaryocyte/erythroid gene expression programmes (Roy et al 2012).

1.3.3 DS-associated leukaemias

Children with DS have a much higher risk of developing acute leukaemia, particularly in early life (Hasle et al, 2000; Hasle et al, 2016; Lee et al, 2016). There is an increased risk of both myeloid leukaemia of DS (ML-DS) and of acute lymphoblastic leukaemia (DS-ALL), which collectively affect 3% of all children diagnosed with DS (an associated increased risk of 150-fold and 33-fold, for ML-DS and DS-ALL respectively) (Roberts and Izraeli, 2014; Lee et al, 2016). DS-associated leukaemias present predominantly in the first 4 years of life (Hasle et al, 2000). Interestingly however, children with DS are not cancer prone in general (Hasle et al, 2016); a decreased Standardised Incidence Ratio (SIR) is observed for solid tumours in cohort analyses of people with DS. Therefore, the marked increased risk for childhood leukaemia is a striking feature, with leukaemia accounting for 97% of cancers observed in DS children under the age of 15 (Hasle et al, 2000). This suggests that trisomy 21 haematopoietic cells are particularly susceptible to malignant transformation.

1.3.3.1 Myeloid leukaemia of DS (ML-DS)

The myeloid leukaemias of DS (ML-DS) were given special classification from non-DS acute myeloid and megakaryoblastic leukaemias of childhood, due to its unique biological and clinical features (Vardiman et al, 2009). These erythroid-megakaryoblastic leukaemias are characterised by the presence of a *GATA1* mutation which is required to but not alone sufficient to initiate ML-DS (Roberts and Izraeli, 2014). The step-wise process of ML-DS initiation has been well-characterised and entails a neonatal pre-leukaemic phase known as Transient Abnormal Myelopoiesis (TAM), a myeloproliferative disorder unique to DS that often spontaneously resolves (Zipursky, 2003; Roberts et al, 2013), but in some cases, is accompanied by the acquisition of additional mutations in a range of genes including those encoding Cohesin proteins and proteins involved in the RAS and JAK-STAT signalling pathways, leading to transformation into ML-DS which is typically diagnosed before 4 years of age (Roberts and Izraeli, 2014).

Interestingly, despite their higher propensity to myeloid leukaemias, children with DS on average respond much better than non-DS peers suffering megakaryoblastic leukaemias, due to a sensitivity to chemotherapy (Tunstall et al, 2018; Czogala et al, 2020).
ML-DS has been shown to originate in utero and the aforementioned *GATA1* mutations result in a truncated GATA1 protein (GATA1s) which is impaired in its normal function as a master regulator of many erythroid, megakaryocytic and myeloid genes, leading to disrupted haematopoiesis during development and the early years of life (Wechsler et al, 2002; Mundschau et al, 2003; Byrska-Bishop et al, 2015; Ling et al, 2019). The dual presence of T21 alongside GATA1s was also shown to be necessary for the development of TAM and ML-DS (Labuhn et al, 2021), as this phenomenon was shown to be unique to haematopoietic

cells of neonates with both full or mosaic DS (Klussman et al, 2008; Gamis et al, 2011), whereas disomic individuals who have inherited the GATA1s mutation do not develop leukaemia (Hollanda et al, 2006).

1.3.3.2 DS-ALL

Unlike ML-DS, where the majority of children with DS are cured using chemotherapy (Roberts and Izraeli, 2014), the outcome and relapse-free survival for childhood DS-ALL is less favourable compared to non-DS ALL age-matched patients (Bohnstedt et al, 2013; Buitenkamp et al 2014; Lee et al, 2016). Treatment-related morbidity and toxicities in DS-ALL contributes to higher relapse rates compared to non DS-ALL (Bohnstedt et al, 2013; Buitenkamp et al 2014; Lee et al, 2016). DS-ALL is clinically and molecularly distinct from non-DS-ALL. Firstly, DS-ALL is almost always B-lineage in origin, compared with non-DS-ALL where 20% of cases are T-lineage; and DS-ALL is genetically distinct (Roberts and Izraeli, 2014). DS-ALL patients, whilst cytogenetically heterogeneous, have an increased rate of genomic aberrations causing dysregulation of the cytokine-receptor-like-factor protein, also known as CRFL2, and JAK2 mutations (Russell et al, 2009; Kearney et al, 2009; Hertzberg et al, 2010; Lee et al, 2016; Kubota et al, 2019). CRLF2 is the receptor for TSLP and under normal circumstances, dimerises with the IL-7R to initiate downstream JAK/STAT signalling (Park et al, 2000). DS-ALL leukemogenesis (depicted in Figure 1.8), entails a primary somatic event, commonly translocation of *CRLF2* followed by subsequent secondary driver mutations which support the progression of the disease, such as JAK2 or RAS which are generally mutually exclusive (Nikolaev et al, 2014).

Immunophenotypically, DS-ALL is a highly heterogeneous disease, which has made it challenging to gain clues as to the cell of origin. Broadly speaking, whilst the

immunophenotype and transcriptome of DS-ALL cases seem to be linked inherently to the cytogenetic sub-type (Kubota et al, 2019), DS-ALL is invariably B-cell precursor in origin (Hertzberg et al, 2010; Roberts and Izraeli, 2014). Moreover, the significant overrepresentation of clones expressing mutant CRLF2 and JAK2 genes (Russell et al, 2009; Kearney et al, 2009; Hertzberg et al, 2010; Lee et al, 2016; Kubota et al, 2019) allows us to build a better picture of what the cell of origin may look like. Further characterisation of the early stages of DS-ALL initiation, including pre-leukaemic stages of the disease, are needed to identify the cell of origin and be able to trace and resolve it's pathology to the level of which has been achieved for ML-DS.

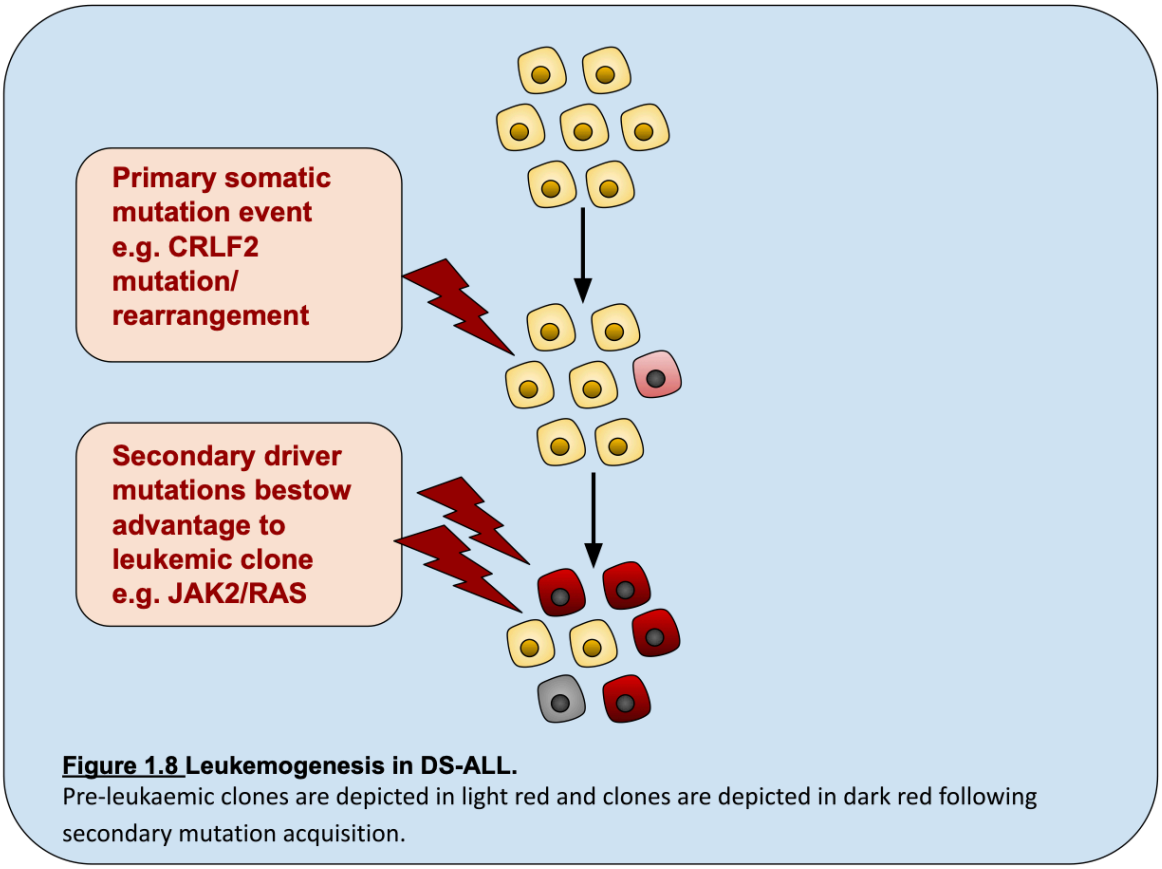


Figure 1.8 Leukemogenesis in DS-ALL.
Pre-leukaemic clones are depicted in light red and clones are depicted in dark red following secondary mutation acquisition.

Interestingly, although many childhood leukaemias originate in fetal life, evidence for a fetal origin or pre-natal stage of DS-ALL has never been shown, unlike ML-DS. Given the paucity of DS-ALL cases in infants under 1 year of age (Buitenkamp et al, 2014), one might argue that a pre-natal component of the disease is unlikely.

That being said, however, several observations, both in terms of intrinsic alterations in HSPCs from DS fetuses, and the DS fetal haematopoietic microenvironment, point toward T21 causing disruption of haematopoiesis during development, which predisposes ALL. Specifically, although infant DS-ALL is not seen in the clinic, DS-ALL does typically present in early childhood and does not present in adult life (Buitenkamp et al, 2014; Roberts and Izraeli, 2014). Moreover, both FL and FBM haematopoiesis is known to be abnormal in DS (Roy et al, 2012; Jardine et al, 2021), and recent work has shown genome-wide altered methylation of DS neonatal bloodspots (Muskens et al, 2021), which combined, supports the notion that T21-driven perturbation of lymphopoiesis in fetal life may underlie the increased risk of ALL in young children with DS (Roberts and Izraeli, 2014).

Further support for this hypothesis comes from several studies that show that T21 is the most common acquired chromosomal abnormality seen in childhood ALL (including non-DS cases) (Laurent et al, 2020) and by early observations that leukaemias in children harbouring mosaic trisomy 21 exclusively featured trisomic cells (Ferster et al, 1986; Simon et al, 1987). Moreover, recent single cell whole genome sequencing of fetal HSPCs has revealed a higher mutation rate than that of post-infancy and notably, this increase is even more marked in fetal T21 haematopoietic cells (Hasaart et al, 2020). Several theories have been presented to explain why fetal HSPCs display a higher mutation rate than post-natal cells (Kuijk et al, 2019; Hasaart et al, 2020). Single base substitution signature 1 (SBS1), which involves the

spontaneous deamination of methylated cytosines (Alexandrov et al, 2015; Blokzijl et al, 2016), is significantly enriched in fetal HSPCs and leads to a higher rate of somatic mutations as well as a greater variety in the mutations observed compared with post-natal cells (Kuijk et al, 2019; Hasaart et al, 2020). On a physiological level, it may be that the rapid proliferation that supports growth and expansion of the embryo comes at a biological cost, with the trade-off being reduced genome stability due to increased accumulation of mutations, as has been suggested (Kuijk et al, 2019). Recent work has shown that the tissue context, as well as ontogeny stage, determines cellular mutational rates, with fetal neural tissue showing the most elevated rates (Kuijk et al, 2019). This suggests an especially high demand for plasticity of the developing brain relative to other organs, which may reflect neural stem cells play comparatively minor roles in post-natal life relative to cells of the liver and intestine.

It was also found that the mutational frequency and pattern seen in T21 fetal HSPCs show similarities to those observed in DS-associated myeloid preleukaemia (Hasaart et al, 2020). Interestingly, the increased mutational burden was found pre-gastrulation, demonstrating that these changes initiate very early during development, with authors hypothesising that the aneuploidy itself may act as the first mutation initiating the cancer (Hasaart et al, 2020).

It seems likely that perturbation of fetal haematopoiesis and the dysregulation of haematopoietic genes by trisomy 21, presents a more permissible environment for oncogenic transformation (Malinge et al, 2012; Antonakaris, 2017). Therefore, supernumerary Hsa21 offers an opportunity to study the broader molecular and genetic mechanisms underpinning leukemogenesis and to expand upon the link between aneuploidy and cancer more broadly.

1.3.4. The molecular mechanism for T21-mediated perturbation of B-lymphopoieisis and DS-ALL

The molecular mechanism for abnormal B-lineage development and ALL susceptibility in DS remains elusive, but is likely to be a result of complex, genome-wide alterations induced by T21 at the both the transcriptional and epigenetic level (Antonakaris, 2020).

Transcriptional evidence

Current estimates indicate that there are 233 protein-coding genes on Hsa21 (ENSEMBLE; Antonakaris et al 2020). Of these, several have well known functions in haematopoiesis and in haematopoietic development and their increased expression has been proposed as one possible mechanism for the observed abnormalities. A summary of these genes in shown in Table 1.3. Amongst these genes, the most studied include *RUNX1*, *GABPA, ETS2 and ERG* (Toki et al, 2005; Ge et al, 2008; Stankiewicz and Crispino, 2009; Yu et al, 2011; Roberts et al, 2013; Roberts and Izraeli, 2014; Mowery et al, 2018). Work in T21-engineered ESCs/IPSCs and primary tissues, highlight the association of dysregulated of Hsa21 genes, including *RUNX1*, *DYRK1A* and *ERG* with the abnormal lineage skew observed and subsequent malignancy when co-opted with further mutations e.g. in *GATA1 (*Elagib et al, 2003; Xu et al, 2006; De Vita et al, 2010; Maclean et al, 2012; Chou et al, 2012; Roy et al, 2012; Jardine et al, 2021).

Rather than altered expression of a single gene, the majority of studies in T21 haemopoietic cells, including leukaemias, including recent work by our lab, have shown broad, but subtle genome wide perturbation of gene expression, including of Hsa21 genes, to varying degrees across multiple haematopoietic cell types (Liu et al 2015; Jardine et al, 2021). In support of

this, recent scRNAseq of fibroblasts from T21 discordant twins (Stamoulis et al, 2019) did not replicate the expected overexpression of trisomic genes that had been claimed previously in bulk RNAseq studies (Letourneau et al, 2014). Instead, several Hsa21 genes showed minimal dosage effect and the fold change observed for dosage-sensitive genes was significantly lower in the single cell analyses. The altered gene dosage was due to a higher proportion of trisomic cells simultaneously expressing Hsa21 genes (Stamoulis et al 2019) with the effect of the additional allele being more pronounced in genes that were originally lowly expressed according to two-burst transcription models. These models dictate that the majority of eukaryotic genes reside in either an ON or OFF state, with all present alleles being transcribed independently (Symmons et al, 2019). Within trisomic cells, this means that a greater proportion of cells are likely to exist in an active or ON state, even if the existing 2 allelic copies happens to be in the OFF state, because each allele is transcribed independently (Stamoulis et al 2019).

The authors suggested that, as genes encoding TFs are typically expressed at a lower level than non-TF genes, they may be more sensitive to the gene dosage imbalance and that a higher fraction of 'activated' cells expressing Hsa21-encoded TFs could lead to dysregulation of large gene expression networks in a cell-context dependent manner (Stamoulis et al 2019).

Table 1.3 Hsa21 genes with implications for haematopoiesis and haematopoietic development

Gene	Implications	Reference
AIRE	Transcription factor involved in quality control checks of T-cells, particularly during selection, to prevent the release of autoreactive T-cells. Altered activity of AIRE has been linked to increase autoimmunity.	Ferrari and Stagi, 2021
BACH1	Suppresses myeloid differentiation programs and promotes the activity of B-cell transcription factors such as EBF-1 to promote B-cell production.	Ito- Nakadai et al, 2014; Igarashi et al, 2017
DNMT3L	DNA methyl transferase that cannot act alone but can cooperate with and augment the methyltransferase activity of DNMT3A which itself has been linked to HSC self renewal and clonal haematopoiesis	Chedin et al, 2002; Challen et al, 2015; Scheller et al, 2021
DYRK1A	Altered expression of *DYRK1A* has been linked to impaired pluripotency of embryonic stem cells and acute megakaryocytic leukaemia of DS. Linked to cell cycle control within B and T-lymphocytes	Canzonetta et al, 2008; Malinge et al, 2012; Thomson et al, 2015
ERG	Forced expression of ERG drives an erythroid to megakaryocytic shift through induction of MK expression programmes. ERG is expressed in primary leukaemic cells from DS patients. Over expression of ERG in the hERG/Gata1s transgenic mouse, synergizes with Gata1s to cause transient TAM followed by full myeloid leukaemia.	Rainis et al, 2005; Korbel et al, 2009; Birger et al, 2013
ETS2	Plays a role in the erythroid to megakaryocytic shift by cooperating with *ERG*. *ETS2* transcripts are over expressed in DS-AMKL and non-DS-AMKL. Over expression of ETS2 lead to immortalization of GATA1-KO or Gata1s murine fetal liver haematopoietic progenitors.	Ge et al, 2007; Stankiewicz and Crispino, 2009 ; Korbel et al, 2009
GABPA	Master regulator of B-lymphoid and myeloid differentiation programmes by binding key lineage transcription factors	Xue et al, 2007; Yang et al, 2011; Yang et al, 2015
HMGN1	Over-expression of HMGN1 has been shown to be sufficient to reproduce several of the phenotypes in DS, including the impaired B-cell defect.	Lane et al, 2014; Mowery et al, 2018
IFNAR1/ IFNAR2 / IFNG2	These genes encode interferon receptors, which are involved in both pro/anti inflammatory signalling by binding type I and type II interferons produced in the local niche. Evidence of dysregulation of inflammatory signatures in DS which leads to a hyperinflammatory state with over-activated IFN signalling and that this state leads to cellular and tissue pathology.	Sullivan et al, 2016; Waugh et al, 2022
OLIG2	Appears to play a role in late stages of neutrophil differentiation and appears as a specific marker for monocytes in recent GRN analysis	Chung et al, 2016; Ranzoni et al, 2021
RCAN1 (DSCR1)	Regulates the calcineurin-NFAT pathway which has been linked to megakaryopoiesis and has been linked to megakaryocytic leukaemia of DS.	Kyttala et al, 2009; Zaslavsky et al, 2013; Grimm et al, 2021
RUNX1	Master haematopoietic regulator of many transcription factors involved in lineage specification, including early B-commitment Dysregulation of *RUNX1* has been linked to the abnormal haematopoietic lineage output in T21 patients and can precede and synergise with *GATA1* mutations in DS-associated malignancies.	Elagib et al, 2003; Xu et al, 2006; Korbel et al, 2009; Seo et al, 2012
SOD1	High SOD1 expression appears to be linked to a more pluripotent state within embryonic stem cells and has also been shown to impact proliferation and expansion of several haematopoietic lineages including lymphocytes and erythroid cells.	Hadjur et al, 2001; Solari et al, 2018
SON	DNA/RNA binding protein expressed in primitive HSPCs and leukaemic blasts. Has been shown to regulate GATA-2 which is itself a key haematopoietic transcription factor. SON mutations are have been identified in AML and recent work indicates that alterations in SON levels alter the composition of the HSPC compartment.	Ahn et al, 2013; Vukadin et al, 2019.
TIAM1	Guanine nucleotide exchange factor, which has been linked to the control of IL17a transcription and and Th-17 responses	Kurdi et al, 2016
USP16	Histone deubiquitinase linked to HSC function	Gu et al, 2016

Epigenetic evidence

Epigenetic studies suggest that trisomy of Hsa21genes may induce changes in histone methylation (including H3K4me3, H3K27me3, H3K27ac) and chromatin compaction, which in turn leads to subtle but not insignificant global gene expression changes (Letourneau et al, 2014; Mowery et al, 2018). Of note, recent work has shown that over expression of the epigenetic modulator HMGN1, which is encoded on Hsa21 and promotes an open chromatin state through H3K27ac, is sufficient to recapitulate the transcriptional and functional changes of impaired B-lymphopoiesis (Lane et al, 2014; Mowery et al, 2018). Although one study showed that genome-wide chromatin changes observed in T21 individuals could be mapped into defined gene expression dysregulation domains (GEDDs) (Letourneau et al, 2014), this has not been validated in other studies (Antonakaris, 2017).

Recent work, derived in part, from a collaboration between our lab and Adam de Smith's group (USC, USA) has shown global changes in DNA methylation within haematopoietic cells from DS neonatal bloodspots (Wiemels et al, 2019; Muskens et al, 2021). Differentially methylated regions (DMRs) were identified between normal and DS genomes on all chromosomes- but the highest proportion were on Hsa21- encoded genes. These DMRs overlapped with genes with known functions in haematopoiesis and associations with leukaemia, including hypermethylation of key regulators of haematopoietic development such as *FLI1* and the Hsa21 gene *RUNX1* (Wiemels et al, 2019; Muskens et al, 2021). Moreover, assessment of the T21 methylome using T21 fibroblasts from discordant monozygotic twins has revealed enhanced DNA methylation and expression of the DNA

methyltransferases DNMTL3 and DNMT3B (Sailani et al, 2015). These findings in trisomic cells mirror recent data which has shown hypermethylation of the Hsa21 haematopoietic TF *RUNX1* specifically in DS-ALL but not non-DS ALL (Kubota et al, 2019). These striking changes in methylation might represent a protective mechanism initiated to compensate for the broad elevation of gene expression in trisomic cells, to tolerate the impact of the aneuploidy and maintain embryonic viability. Paradoxically, however, these changes in DNA methylation in HSPCs may, in turn, drive some of the aberrant haematopoietic phenotypes associated with DS.

To summarise, the current understanding is that trisomy 21 leads to global gene expression changes through a combination of direct increased dosage of Hsa21 genes and indirect downstream epigenetic dysregulation of many genes, ultimately manifesting as aberrant phenotypes.

1.3.5 An altered progenitor compartment in DS FBM underlies perturbed haematopoiesis of DS and may provide clues as to the unique characteristics of DS-ALL

An interesting paradox for children with DS is that they almost never develop ALL in the first year of life, known as infant ALL (iALL) (Buitenkamp 2014). For children without DS, iALL confers a poor prognosis and has certain characteristic features that may indirectly provide clues to the pathogenesis of DS-ALL. In particular, iALL has a characteristic CD10-CD19+ immunophenotype, implicating a CD10-CD19+ B progenitor such as the recently described PreProB progenitor (O'Byrne et al, 2019; Jackson et al, 2021) as a possible cell of origin.

Our own work in normal FBM has shown that PreProB progentors are absent in adult BM (O'Byrne et al, 2019) and preliminary data from our lab showed that the CD10- fetal-specific PreProB and ELP progenitors were significantly reduced in DS FBM (Anindita Roy, ASH Abstract, 2014; Sorcha O'Byrne, ASH Abstract, 2019). In contrast, we showed that the proportion of CD10+ ProB progenitors, which also comprise the majority of B-progenitors in ABM, was comparable between normal and DS FBM (Sorcha O'Byrne, ASH Abstract, 2019). This preliminary work also highlighted that early DS progenitors (HSC, MPP, LMPP) show impaired B-lymphopoiesis, suggesting some kind of block in differentiation upstream (Sorcha O'Byrne, ASH Abstract, 2019). Why some B-progenitor populations seem to be impacted in DS FBM (PreProB, ELP), while others are less affected (ProB) is not known but these preliminary investigations may point toward DS FBM exhibiting a more adult-like B-lymphopoiesis pathway.

Given that the FBM is thought to be the site of ALL initiation (Jackson et al 2021), alterations in the progenitor composition in DS FBM and the absence of the potential cell of origin responsible for iALL may explain why DS-ALL presents after 1 year of age (Buitenkamp 2014; Roberts and Izraeli, 2014), though this is yet to be validated.

A more detailed characterisation of the disturbed progenitor compartment within DS FBM is needed with systematic functional assays to characterise the specific populations that are impacted to allow us to pin point the stage at which B-cell differentiation becomes impaired. Accompanying molecular profiling of normal vs DS FBM HSPCs is also needed to understand the mechanisms underpinning their altered functional output which will also hopefully provide insight into why DS FBM HSPCs may be predisposed to ALL initiation.

1.4 Hypothesis and Aims

To address my hypothesis that T21 drives changes in fetal B-cell development through both transcriptional and epigenetic modulation of fetal differentiation programmes, I had two specific aims: firstly to identify the specific immunophenotypic and functional differences in B-progenitor differentiation between normal and DS FBM and secondly, to understand these changes at the molecular level.

To address these aims, I refined several research questions.

Research questions

1. ***Is there an intrinsic defect in lymphopoiesis, specific to the B-lineage within DS FBM?*** I addressed this question by:
    a. Characterising normal and DS FBM HSPCs via immunophenotyping and MS-5 co-cultures to assess B-cell differentiation.
    b. Assessing non-B-lineage differentiation using specialised culture systems for distinct lineages: methylcellulose (megakaryocyte/ erythroid/ myeloid), MS-5 (NK), OP9-DL1 (T-cell/NK).

2. ***At what stage(s) does the defect in B-lymphopoiesis originate and are alternative pathways of B-cell differentiation being utilized differently in normal vs DS FBM?*** I addressed these questions by:
    a. Refining the existing B-differentiation hierarchy in normal FBM by characterising new CD10- and CD10+ intermediate progenitors identified during immunophenotyping using functional assays.

b. Functionally characterising the newly defined progenitors in DS FBM.

3. ***What is the molecular mechanism for impaired B-lymphopoiesis and differentiation biases in DS FBM?*** I addressed this question by:

    a. Performing whole genome transcriptomic analysis of normal vs DS FBM HSPCs.

    b. Performing whole genome ATAC sequencing to compare chromatin accessibility of normal vs DS FBM HSPCs.

Chapter 2

Methods

2.1 Samples

Fetal bone marrow

Fetal bone marrow (FBM) was extracted from tissue collected by the Human Developmental Biology Resource and under their National Research Ethics consent procedures (HDBR, www.hdbr.org; details of staging in table 2.1; REC: 18/LO/0822 and 18/NE/0290). Both the HDBR and MRC Weatherall Institute of Molecular Medicine, where processed samples are stored comply with the Human Tissue Act (HTA; 2004).

The HDBR analyses samples for chromosomal abnormalities which allows them to determine the presence or absence of T21 in samples (DS or normal, respectively) using SNP array or exome sequencing. Following sequencing, reads are aligned to the reference genome (hg38) and following downstream, abnormal duplications of loci can be determined and mapped to specific regions e.g. Hsa21.

Cord blood

Cord blood (CB) was obtained after elective caesarean section and after written informed consent (REC Ref. no. 15/SC/0027).

2.2 Sample processing and cryopreservation

Fetal tissue was preserved at 4 degrees during transit and processed immediately in line with previous lab protocols (Roy et al, 2012; O'Byrne et al, 2019). All processing was undertaken within sterile tissue-culture conditions with sterile TC reagents and dissection tools.

Long bones were flushed with sterile filtered Dulbecco's Modified Eagle Medium (DMEM) using a narrow-gauge needle to infiltrate bone cavities. The suspension was passed through at 70µm filter to obtain a single cell suspension.

Single cell suspensions were then red cell and granulocyte depleted by density gradient separation using Ficoll-Paque PLUS (GE Healthcare). Mononuclear cells (MNCs) were carefully isolated from the segregated interface using a sterile pipette. CD34 enrichment was carried out on freshly isolated MNC using a Miltenyi CD34 MicroBead kit (supplier).

Before and after CD34 enrichment, manual cell counts were performed to monitor efficiency of selection and for subsequent aliquoting. All cell counts were performed using a haematocytometer and cover slide, on cell suspensions which had been diluted 1:1 in the Trypan Blue viability dye (0.4%, Gibco). Trypan Blue works according to the dye exclusion test, whereby viable cells do not absorb impermeable dyes, such as Trypan Blue, but dead cells are permeable and therefore do stain blue. Following counting, samples were aliquoted and cryopreserved in heat-inactivated (HI) FBS with 10% DMSO as CD34- or CD34+ samples. Samples were maintained in liquid nitrogen storage until thawing.

2.3 Sample thawing

Samples were transported to the sterile tissue culture facility on dry ice and thawed at 37°C in a sterile water bath for approximately 1-2 minutes until just thawed (when the ice within had visibly disappeared). Samples were then immediately transferred from cryovials to a 15ml falcon containing 1ml of pre-warmed HI-FBS (Sigma-Aldrich), using a p1000 filtered pipette in a slow, drop wise fashion to minimise cell stress and improve recovery. Cells were further diluted in an excess (approximately 5ml) of pre-warmed HI-FBS (Sigma-Aldrich) and were centrifuged at 300xg for 5 minutes. Cell pellets were resuspended in a suitable volume of FBS-supplemented media or PBS+2%FBS+1mM EDTA to allow for counting using Trypan Blue. Post-thaw viability varied but was typically within a range of 65-85% recovered viable cells.

2.4 Fluorescently-activated-cell-sorting (FACS) of HSPCs by immunophenotype and flow cytometry

Once thawed and counted, suspensions were filtered through a 35 µm filter in excess FACS buffer (PBS+2%FBS+1mM EDTA) to remove any residual clumps and suspensions were centrifuged at 300xg for 5 minutes. After removing the supernatant, cells were resuspended in cocktails of fluorophore-conjugated monoclonal antibodies allowing identification of HSPC populations by presence of antigens. Antibody lists are described in Table 2.1. Gating strategies for functional readouts (MS-5 / OP9-DL1 / methocult readout panels) are featured in results sections 3 and 4 for and the gating strategy used to sort human HSPCs is shown in Figure 2.1.

Cells were stained for 30 minutes at 4°C in the dark, after which suspensions were washed twice in 1ml FACS buffer at 300xg /5minutes and resuspended in approximately 200ul FACS buffer. To allow identification of viable populations, fixed viability dye was either included in the antibody staining cocktails and stained as described above, or cells were resuspended into FACS buffer spiked with viability dyes depending on the appropriate staining panel. During panel set up, optimal laser voltages were determined using single stain controls. Compensation values were calculated to mitigate fluorescence overlap using unstained and Fluorescence Minus One (FMO) controls based on MNCs (Figure 2.2). FMO controls were generated using antibody cocktails that include every antibody in the relevant panel except the appropriate FMO colour and these were used to set fluorescent gates for panels (Figure 2.2). Optimal staining volumes of new antibodies were determined through titrations on MNCs (Figure 2.3). Samples were analysed using BD Fortessa X50 and BD Fortessa X-20-2 and sorted using BD Fusion instruments. Data was analysed using FlowJo Version 10.8.1

Table 2.1 Antibodies used for Fluorescently-activated-cell-sorting (FACS) and flow cytometry

Antibody	Fluorophore	Clone	Company	Cat no.
CD2	PerCP cy5.5	RPA-2.10	Biolegend	300215
CD2	APC			
CD2	FITC	RPA-2.10	Life Tech	11-0029-42
CD3	PerCP cy5.5	okt3	Biolegend	317336
CD3	AF700			
CD3	FITC	okt3	Life Tech	11-0037-42
CD4	PE	L200	BD Bioscience	550630
CD5	PE	L17F12	Biolegend	364013
CD7	BV421	MT701	BD Bioscience	562635
CD8	Pecy7	RPA-T8	Life Tech	
CD10	PEcy7	ebioCB-CALLA	eBioscience	25-0106-42
CD10	FITC	ebioCB-CALLA	Life Tech	11-0106-42
CD11b	PerCP cy5.5	ICRF44	Biolegend	301328
CD11b	AF700	ICRF44	Biolegend	301356
CD11b	PEcy7	ICRF44	Biolegend	301322
CD11b	FITC	ICRF44	eBioscience	11-0118-41
CD14	PerCP cy5.5	M5E2	Biolegend	301824
CD14	AF700	63D3	Biolegend	367114
CD14	PEcy7	HCD14	Biolegend	325618
CD14	FITC	61D3	eBioscience	11-0149-41
CD16	FITC	eBioCB16	Life Tech	11-0168-42
CD16	PerCP cy5.5.	3G8	Biolegend	302028
CD19	APC	HIB19	Biolegend	302212
CD19	PerCP cy5.5.	HIB19	Biolegend	302230
CD27	PerCP cy5.5	M-T271	Biolegend	356407
CD33	PerCP cy5.5	WM53	Biolegend	303414
CD33	FITC	p67.6	Biolegend	366620
CD34	Pecy7	4H11aka8G12	Thermofisher	25034942
CD34	APCef780	4H11aka8G12	Thermofisher	47034942
CD34	PerCP cy5.5	581	Biolegend	343522
CD34	BV421	561	Biolegend	343610
CD36	ef660	NL07	Life Tech	50-0369-42
CD38	AF700	HIT2	Life Tech	56-0389-42
CD41a	APCcy7	HIP8	Biolegend	303716
CD42b	PE		eBioscience	12-0429
CD43	BV421	1G10	BD Bioscience	562916
CD45	BUV395	HI30	BD Bioscience	563791
CD45	AF700	2D1	eBioscience	56-9459-42
CD45	FITC	2D1	BD Bioscience	345808
CD45RA	APC ef780	HI100	Life Tech	47-0458-42

Antibody	Fluorophore	Clone	Company	Cat no.
CD45RA	APC ef780	HI100	Life Tech	47-0458-42
CD56	BV605	HCD56	Biolegend	318344
CD56	BUV805	NCAM16.2	BD Bioscience	749086
CD56	PE	CMSSB	eBioscience	12-0567-41
CD56	PerCP cy5.5	HCD56	Biolegend	318322
CD71	BV711	M-A712	BD Bioscience	563767
CD90	BV421	5E10	Biolegend	328122
CD117	BV650	I04D2	Biolegend	313222
CD123	BV650	7G3	BD Bioscience	563405
CD127	PE	eBioRDR5	Life Tech	12-1278-42
CD235	PerCP cy5.5	HIR2	Biolegend	306614
CD235a	FITC	HIR2akaGA-R2	Life Tech	11-9987-82
IgD	BUV805	--	BD Bioscience	Custom
IgM	BUV805	--	BD Bioscience	Custom
Lineage	APC	--	Thermofisher	22777672
Viability	ef506	--	Thermofisher	65086618
Viability	7AAD	--	Cayman	11397
Viability	Hoechst 33258	--	Life Tech	H3569

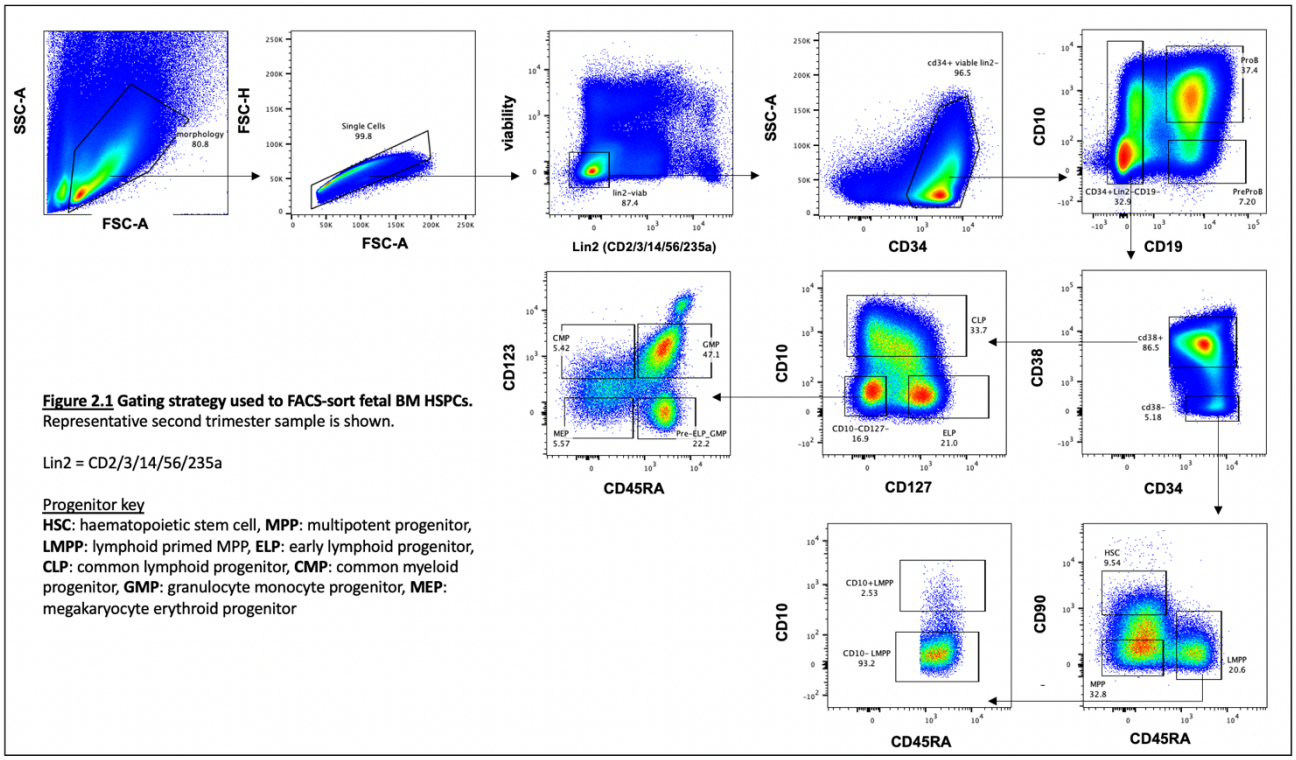


Figure 2.1 Gating strategy used to FACS-sort fetal BM HSPCs.
Representative second trimester sample is shown.

Lin2 = CD2/3/14/56/235a

Progenitor key
HSC: haematopoietic stem cell, **MPP**: multipotent progenitor, **LMPP**: lymphoid primed MPP, **ELP**: early lymphoid progenitor, **CLP**: common lymphoid progenitor, **CMP**: common myeloid progenitor, **GMP**: granulocyte monocyte progenitor, **MEP**: megakaryocyte erythroid progenitor

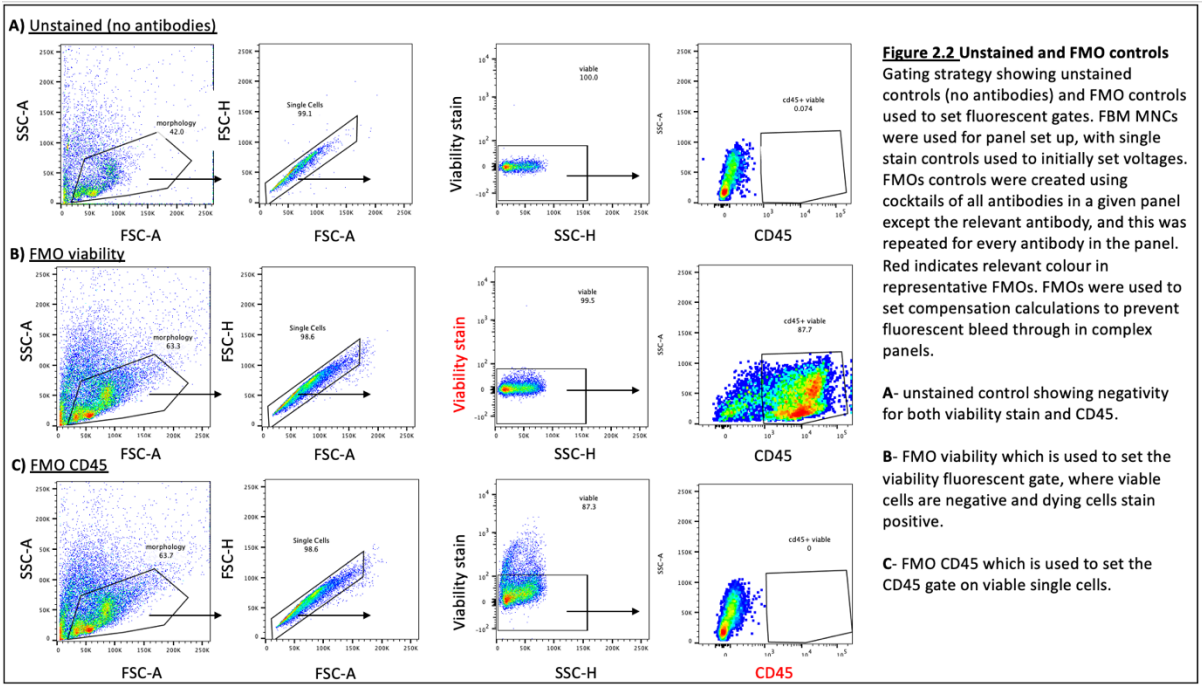


Figure 2.2 Unstained and FMO controls
Gating strategy showing unstained controls (no antibodies) and FMO controls used to set fluorescent gates. FBM MNCs were used for panel set up, with single stain controls used to initially set voltages. FMOs controls were created using cocktails of all antibodies in a given panel except the relevant antibody, and this was repeated for every antibody in the panel. Red indicates relevant colour in representative FMOs. FMOs were used to set compensation calculations to prevent fluorescent bleed through in complex panels.

A- unstained control showing negativity for both viability stain and CD45.

B- FMO viability which is used to set the viability fluorescent gate, where viable cells are negative and dying cells stain positive.

C- FMO CD45 which is used to set the CD45 gate on viable single cells.

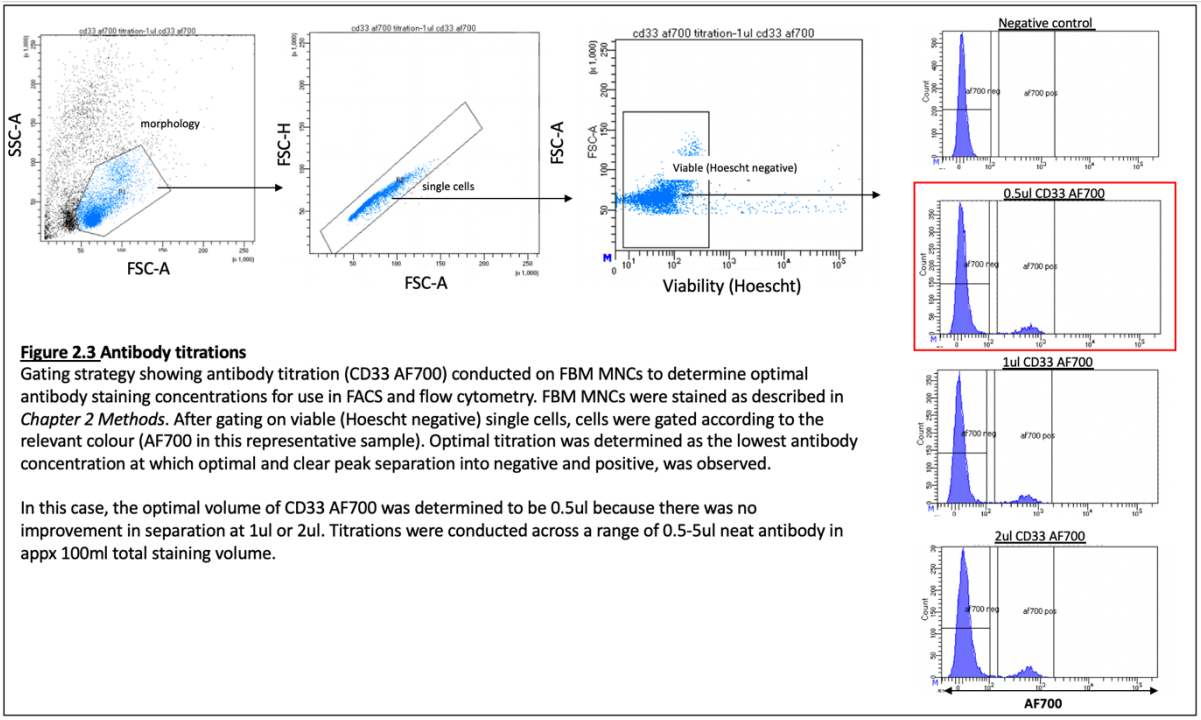


Figure 2.3 Antibody titrations
Gating strategy showing antibody titration (CD33 AF700) conducted on FBM MNCs to determine optimal antibody staining concentrations for use in FACS and flow cytometry. FBM MNCs were stained as described in *Chapter 2 Methods*. After gating on viable (Hoescht negative) single cells, cells were gated according to the relevant colour (AF700 in this representative sample). Optimal titration was determined as the lowest antibody concentration at which optimal and clear peak separation into negative and positive, was observed.

In this case, the optimal volume of CD33 AF700 was determined to be 0.5ul because there was no improvement in separation at 1ul or 2ul. Titrations were conducted across a range of 0.5-5ul neat antibody in appx 100ml total staining volume.

2.5 MS-5 co-cultures to assess multi lineage output potential

Murine MS-5 stromal cells (Itoh et al, 1989) were grown to confluency and passaged as described previously (O'Byrne et al, 2019). Briefly, MS-5 cells were thawed according to the cell thawing protocol described above and grown in specialised maintenance media (α-MEM supplemented with 10% HI FBS, 100U/mL Penicillin, 100ug/mL Streptomycin, 2mM L-glutamine, 50µM 2-Mercaptoethanol, 10mM HEPES) within a tissue-culture conditioned 75 cm^2 flask. Approximately 2 days post-thaw (depending on the number of cells thawed) once cells had reached 70% confluency, cells were passaged. Passaging entailed carefully removing media using a sterile aspirator without disrupting the monolayer below, after which monolayers were gently washed with PBS, and then incubated with sufficient 0.05% trypsin (Gibco) to coat the flask for 5 minutes at 37°C within a sterile incubator. To improve cell detachment, flasks were gently agitated before incubation. Trypsinisation was neutralised in excess FBS- supplemented base media (α-MEM supplemented with 10% HI FBS).

During and between co-culture experiments, stocks of MS-5 cells were maintained and expanded at <18 passage numbers to optimally support haematopoietic differentiation in 75 cm^2 or 175 cm^2 tissue culture flasks. For co-culture of human HSPCs, 3 $x10^4$ MS-5 cells were plated per well in a 24 well plate 24-48 hours prior to co-culture initiation, in maintenance media. 30-100 fetal BM CD34+ HSC or progenitors were FACS sorted and plated on confluent MS-5 stroma in cytokine supplemented α -MEM (Gibco) (10% HI FBS, 100U/mL Penicillin, 100µg/mL Streptomycin, 2mM L-glutatmine,50µM 2- mercaptoethanol, 10mM HEPES, SCF (20ng/mL), Flt3L (10ng/mL), IL-2 (10ng/mL) and IL-7 (5ng/mL)) in 24 well plates. All cytokines were purchased from Peprotech, Rocky Hill, USA.

Co-cultures were replenished with biweekly half (cytokine-supplemented) media changes. At weekly time-points, wells were harvested for assessment of myeloid, B and NK-lymphoid differentiation. Briefly, wells were harvested by dispersing media across the well using firm up and down pipetting using a filtered P1000 pipette to manually dislodge cells. Wells were washed with 1ml media approximately 4-5 times and filtered through a 70µm into a 50ml falcon tube to generate a final suspension of approximately 6-7ml. Before further steps, empty wells were inspected under a microscope to clarify that the monolayer had been completely removed.

Suspensions were then centrifuged at 300xg for 5 minutes, washed and filtered a second time through a 30µm filter to isolate a haematopoietic cell suspension from the MS-5 stromal cells by cell size exclusion and to minimise clumping for subsequent flow cytometry. From this point, the entire haematopoietic suspensions from wells were either stained for flow cytometry if sorted cell numbers permitted, or in cases of limited cell numbers, a fraction of the filtered cell suspension was reserved for flow cytometry readout before the remaining cells were re-plated on fresh stromal layers in cytokine supplemented α -MEM (Gibco). Where absolute cell numbers are given from MS-5 differentiation assays, CountBright beads (Invitrogen) were used to calculate the number of cells present in each well at each time point.

2.6 Single cell methocult assays to assess myeloid/erythroid/MK output

Methocult (Stem Cell Technologies, H4230) was supplemented with 20% IMDM (Gibco) including 1ng/ml Pen/Strep (Gibco), and human cytokines 10ng/mL for the following IL-6, IL-11, SCF, Flt3L, 50ng/mL GM-CSF and TPO, 20ng/mL IL-3 (all PeproTech), and 4 U/ml EPO (EPREX/Janssen) as described in (Roy et al, 2012; Jardine et al, 2021). Supplemented methocult was vigorously vortexed and bubbles were allowed to settle before aliquoting 50ul of supplemented methocult into 96 well TC plates (Sigma).

Methocult plates were wrapped in parafilm to prevent contamination and dry-out and were stored at 4°C the night before sorting. 30 mins prior to sorting, plates were pre-warmed at 37°C in a sterile incubator. FBM samples were thawed and stained as described above in preparation for FACS-sorting. Human FBM HSPC subpopulations were index-sorted as viable single cells via FACS directly into 96 well TC plates (Sigma) of supplemented methocult (50ul/well). Sorting was performed on a BD FACSAria Fusion Cell Sorter (BD Biosciences). Plates were incubated at 37°C and 5% CO_2 for 14 days.

At day 14, colonies were counted and imaged for morphological characterisation using an EVOS XL Core Imaging System microscope. Selected colonies were picked for flow cytometry readout and cytospin. Representative images can be found in chapters 3 and 4. Colonies were carefully plucked from wells using a p10 pipette tip to minimise methocult carry over, with the EVOS XL Core Imaging System used to guide the retrieval process. Plucked colonies were dispensed into non-filtered FACS tubes containing 50ul FACS buffer (PBS+2%FBS+1mM EDTA) and were centrifuged at 300xg for 5 minutes. After this, cells were resuspended in antibody staining cocktails and were stained as described above. Samples were analysed using BD Fortessa X50 or the BD Fortessa X-20-2.

2.7 OP9-DL1 stromal co-cultures to assess T-cell output

OP9 stromal cells ectopically expressing Notch ligand, Delta-like 1 (OP9-DL1) and GFP (Awong et al, 2008; Holmes and Zuniga-Pflucker, 2009) were grown to 60% confluency and passaged every 2-3 days as described previously (O'Byrne et al, 2019). Briefly, OP9-DL1 cells were thawed and counted and stocks were maintained up to 70% confluency in 75-175cm^2 flasks using supplemented maintenance media comprising: α-MEM (no deoxy/ribonucleosides, Gibco) supplemented with 20% HI FBS, 100U/mL Penicillin, 100µg/mL Streptomycin, 2mM L-glutamine, 1:1000 of 97% pure 1-Thioglycerol (Merck).

Before stromal layer preparation, 24-well tissue-culture plates were conditioned by coating with sterile-filtered 0.1% gelatin (Merck) for 1 hour, after which gelatin was removed using a P1000 filtered pipette, and plates were left to airdry in a sterile TC flow hood.

OP9-DL1 stocks, maintained within 75-175cm^2 flasks, were passaged and prepared for seeding by removing maintenance media and incubating with sufficient 0.05% trypsin (Gibco) to coat the flask for 15 minutes at 37°C within a sterile incubator. Due to OP9-DL1s adhering particularly strongly, flasks were inspected down the microscope to ensure that cells had detached. Trypsinisation was neutralised in excess FBS- supplemented base media (α-MEM supplemented with 20% HI FBS) and having washed the flasks thoroughly to retrieve all cells, suspensions were centrifuged 300xg for 5 minutes, after which cells were counted.

Stromal layers were then prepared by plating 2x10^4 OP9-DL1 cells per well. After 24-48 hours, 50-100 sorted HSPCs were seeded onto the stromal layers and co- cultured with maintenance α-MEM supplemented with Flt3L (5ng/mL), human SCF (10ng/mL) and IL-7

(5ng/mL). All cytokines were purchased from Peprotech, Rocky Hill, USA. Co-cultures were replenished with biweekly half media changes.

T-lymphoid differentiation was assessed at weekly time points during the re-plating of co-cultures where one fourth of the cell suspension was reserved for flow cytometry before the cells were re-plated on fresh stromal layers. Briefly, co-cultures were firmly scraped using individually wrapped sterile cell scrapers to remove monolayers. Scraping was minimised as much as possible to minimise cellular destruction. Wells and scrapers were washed thoroughly with excess FBS- supplemented base media (α-MEM supplemented with 20% HI FBS) to collect cells into a 50ml falcon tube through a 70µm filter. Suspensions were then centrifuged and filtered again (30µm) to separate haematopoietic cells from OP9-DL1 stromal cells. On occasions where the entire well was to be used for readout, suspensions were resuspended in antibody cocktails for staining as described above. For replating, suspensions were split with ¼ being used for readout and the remaining ¾ being plated onto new OP9-DL1 monolayers.

During flow cytometry, murine OP9 stromal cells were gated out of analysis according to their expression of GFP. Where absolute cell numbers are given from OP9-DL1 differentiation assays, CountBright beads (Invitrogen) were used to calculate the number of cells present in each well at each time point.

2.8 Small bulk RNA sequencing of FBM HSPCs

Fetal BM bulk RNA sequencing was performed following the library preparation protocols using SMARTseq3 (Rodriguez-Meira et al, 2020). Prior to sorting, lysis buffer (Triton 0.4%, RNAse Inhibitor, dNTPs 10mM, Oligo dT 10uM, ERCC E6 spike in standard) was prepared in clean room (no post PCR product) conditions and 4ul was aliquoted into clean PCR tubes which were kept on ice until sorting commenced. 50-100 cells of each HSPC population were FACS sorted (over 3 sort experiments) directly into lysis buffer and snap frozen by transfer onto dry ice and subsequently to -80°C. Details of samples and replicates are shown in chapter *5.2*.

cDNA synthesis was performed in the clean room to prevent potential genomic contamination. For reverse transcription, RNA samples were split in to 3 batches of 25 tubes to minimise potential time delays. Plates were transported from -80°C on dry ice, and left to thaw on a clean cold rack. During thawing, basic SMARTScribe RT master mix (Takara Clontech) was generated (Buffer 5X, RNAse inhibitor, TSO 100uM, clean water, SMARTScribe enzyme). At this point thawed racks were heat-shocked at 72°C for 3 minutes in a PCR-clean thermocycler and during this step, the RNAse inhibitor, TSO and SMARTScribe were added to the RT mix which was aliquoted into clean PCR strips. After heat shock, RT master mix was rapidly transferred to the cell lysates before an RT programme was run in a second PCR-clean thermocycler (Table 2.2).

Table 2.2 Reverse Transcription (RT) programme (adapted from Rodriguez-Meira et al, 2020)			
Temperature	Time	Cycles	Details
42°C	90 min		RT
50°C	2 min	10 cycles	Unfolding of secondary structures
42°C	2 min		RT
70°C	15 min		RT inactivation
4°C	HOLD		

PCR mastermixes for the subsequent amplification step were prepared during RT (2X buffer, ISPCR Primers 10uM, clean water, SeqAMP enzyme), with the SeqAMP enzyme added to mastermix immediately before RT step completes. cDNA was immediately PCR amplified to generate libraries outside of the clean room (Table 2.3).

Subsequently, libraries were bead-cleaned using AMPure XP magnetic beads (Beckman Coulter) to size exclude undesired DNA fragments, quantified using the Qubit system (Thermofisher) and quality control (QC) was performed using the Agilent High Sensitivity DNA Bioanalyzer Kit (Figure 2.4). Where possible two technical replicates for cDNA synthesis were generated and the best quality sample was taken forward used.

Finally, libraries were tagmented and indexed to allow samples to be deconvoluted after pooling and sequencing. Libraries were QC'd again to confirm successful tagmentation and indexing using the Agilent High Sensitivity DNA Bioanalyzer Kit (Figure 2.4), before libraries were pooled and single lane sequenced using the PE150-NovaSeq system (Novogene, UK, Cambridge).

Table 2.3 PCR amplification of RNA seq cDNA libraries (adapted from Rodriguez-Meira et al, 2020)			
Temperature	Time	Cycles	Details
42°C	90 min		RT
50°C	2 min	10 cycles	Unfolding of secondary structures
42°C	2 min		RT
70°C	15 min		RT inactivation
4°C	HOLD		

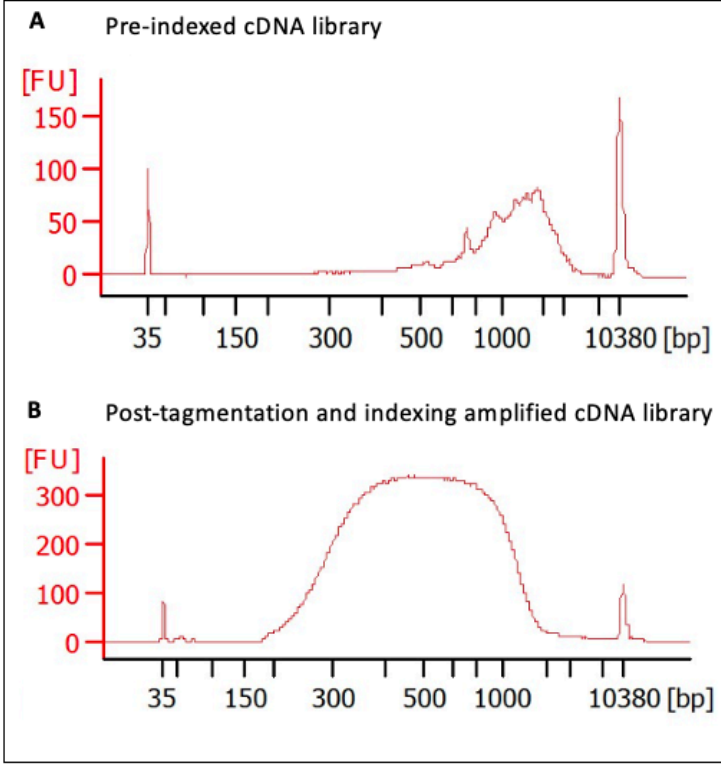


Figure 2.4 RNA sequencing - quality control of cDNA libraries
High sensitivity Bioanalyzer traces (Agilent) of cDNA libraries generated through RNA sequencing using Target-seq protocol (Rodriguez-Meira et al, 2020), showing peaks in the expected base pair ranges with minimal degradation. Representative traces are shown.

A. Traces of PCR-amplified and bead-cleaned (Ampure XP, Beckman Coulter), pre-indexed cDNA libraries.

B. Traces of cDNA libraries post tagmentation and indexing.

2.9 RNA sequencing analysis

A detailed summary of the RNA sequencing workflow and analysis performed is shown in Figure 2.5. First, pre-mapping QC was performed on sequenced reads using my own scripts written in the UNIX command line in BASH on the CCB server. Specifically, my BASH scripts installed the required packages, directed these packages to the correct filepath and also contained all the necessary commands in series for all of the pre-processing and mapping steps, which I ran as an automated for-loop on all samples in the raw data directory. Briefly, pre-processing QC and mapping first involved the using fastqc and trimgalore packages to prepared trimmed reads. High quality reads which passed QC were mapped to the genome using the STAR aligner, generating sorted and aligned BAM files. I then used the featureCounts function to generate an annotated raw counts matrix with all the necessary meta data (e.g. sample name and GeneID etc). To do this, I wrote my own BASH script to direct the featureCounts package to the BAM files.

I imported my annotated raw counts table into rstudio where all subsequent pre-processing and QC, tabular manipulation, visualisation and statistical comparisons were performed using R.

Details of the QC performed on the mapped RNA sequencing data, using EdgeR, is shown in Figures 2.6 and 2.7. Briefly, I first excluded samples of small library size (DSOX11 CMP and ICH14425 CMP 1), (Figure 2.5). I then compared 3 common normalisation techniques: TMM, UQ and RLE (unabbreviated) by doing a comparison of the number of DEGs between all normal and DS populations ($P < 0.05$), comparing by condition only (N vs DS) (Figure 2.7). Approximately 4000 genes were DEG ($P < 0.05$) between normal and DS, with UQ reporting the greatest number of unique DEGs (1618, Figure 2.7), followed by RLE (100, Figure 2.7). I

decided to use TMM normalisation as it was the most conservative of the 3 approaches, identifying only 52 DEGs (Figure 2.7), to minimise potential overrepresentation of not biologically meaningful significant results.

Following TMM normalisation, I calculated the Biological coefficient of variation (BCV) of the RNA sequencing libraries (Figure 2.7). As expected, genes with the lowest expression (Average logCPM), show the greatest variation, with a downward trend in the more highly expressed genes. Overall, despite a relatively small sample size (n=3 N FBM and n=2 DS FBM biological replicates), the common dispersion was low (1.87) (Figure 2.7).

After QC, data was analysed using a combination of DESEQ2 and EdgeR packages to normalise the data and generate large objects from which matrices could be exported and manipulated for downstream visualisation (see detailed work flow in Figure 2.5).

All statistical comparisons were performed in EdgeR and this entailed running ANOVA-like tests on all populations for hierarchical based analysis or pairwise comparisons of key HSPCs e.g. normal HSC vs DS HSC. Similar visualisation tools were used on outputs from both DESEQ2 and EdgeR and these included ggplot2, ggpubr, pheatmap.

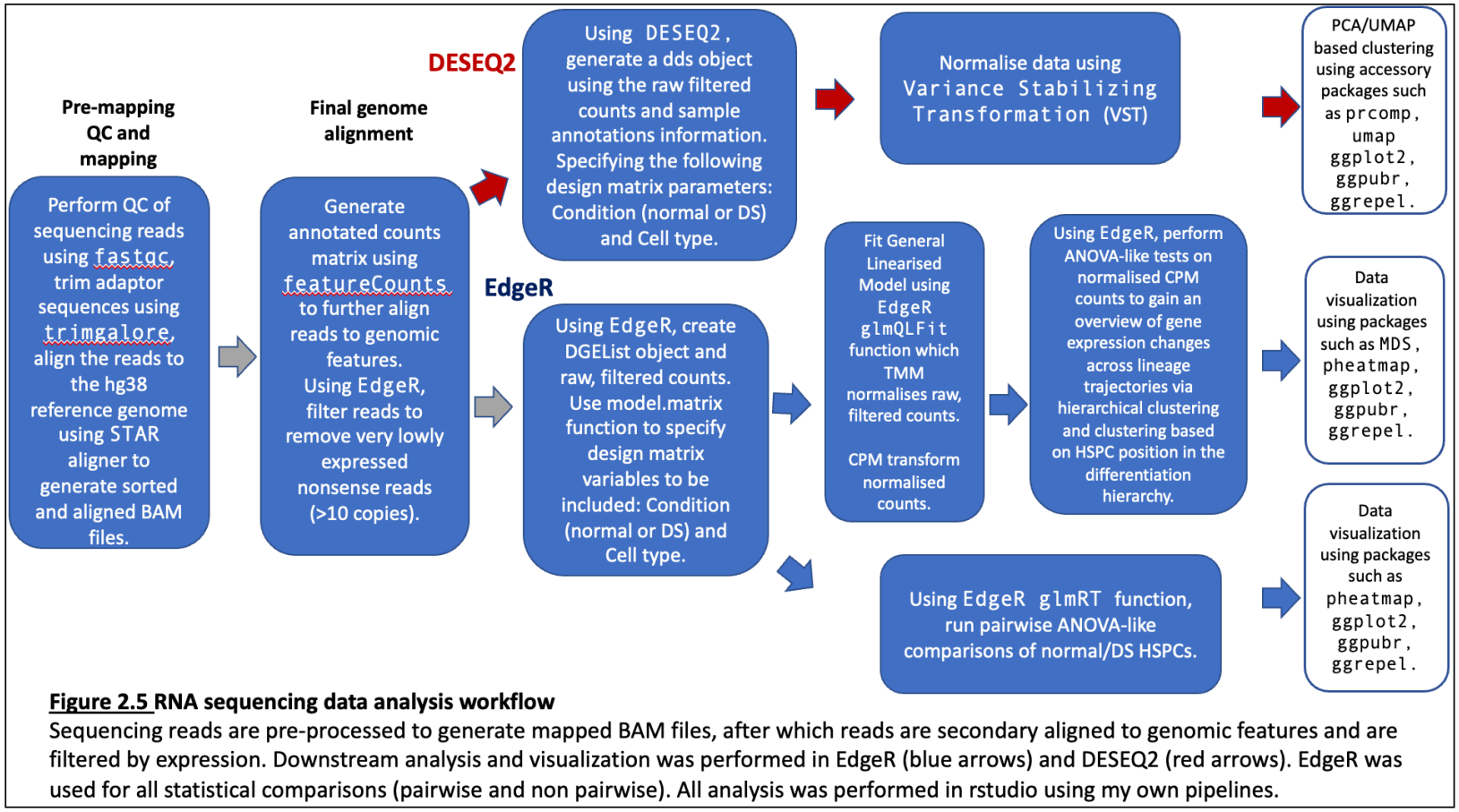
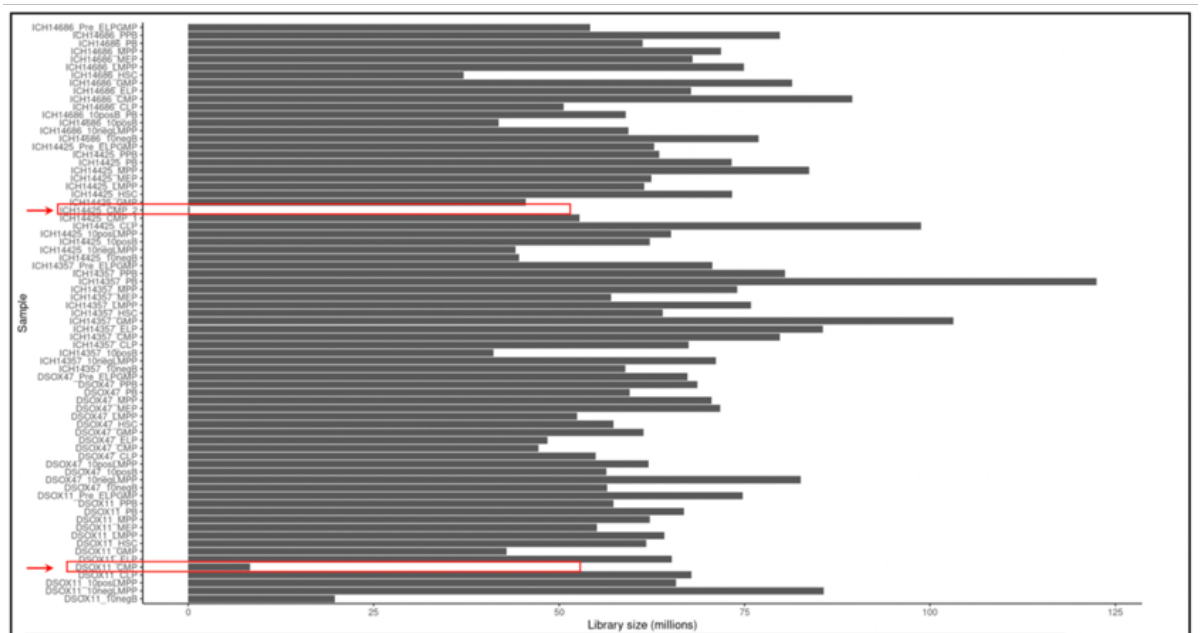


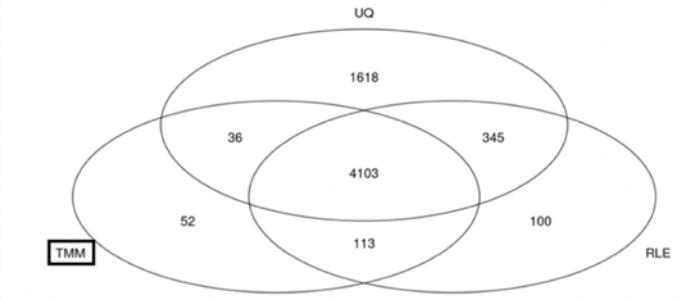
Figure 2.5 RNA sequencing data analysis workflow
Sequencing reads are pre-processed to generate mapped BAM files, after which reads are secondary aligned to genomic features and are filtered by expression. Downstream analysis and visualization was performed in EdgeR (blue arrows) and DESEQ2 (red arrows). EdgeR was used for all statistical comparisons (pairwise and non pairwise). All analysis was performed in rstudio using my own pipelines.



Number of replicates post- sample exclusion

HSPC pop	HSC	MPP	10-LMPP	10+LMPP	Pre-ELP/GMP	ELP	CLP	PPB	PB	10negB	10posB	CMP	GMP	MEP
Normal	3	3	3	1	3	2	3	3	3	3	3	3	3	3
DS	2	2	2	2	2	2	2	2	2	2	1	1	2	2

Figure 2.6 Normal and DS FBM RNASeq libraries - pre analysis sample exclusion
A) Library size (millions of reads) of sequenced small bulk RNA-Seq libraries. Red arrows indicate samples excluded due to low library size
B) Summary table of HSPC population type and number of replicates for normal and DS



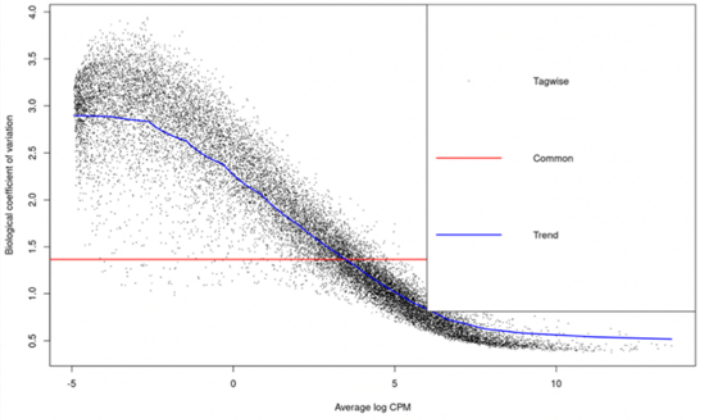


Figure 2.7 Normal and DS FBM RNASeq libraries - pre analysis QC
A. Evaluation of RNASeq normalisation methods using EdgeR and selection of Trimmed Mean of M-values (TMM) normalisation. Compartments indicate the number of differentially expressed genes (DEGs) between Normal (n=3) and DS- FBM (n=2) RNASeq libraries,detected after normalisation using TMM, Upper Quartile (UQ) and Relative Log Expression (RLE). TMM was selected as a conservative approach with the fewest unique DEGs (52).

B. Biological Coefficient of Variation plot indicating the common dispersion (red line) of N and DS FBM RNASeq libraries = 1.87, following TMM normalisation.

2.10 Small bulk ATAC-sequencing of FBM HSPCs

Fetal BM bulk ATAC-Sequencing protocols were performed as described in O'Byrne et al, 2019. Briefly, cells were sorted (800-2000 depending on population scarcity), directly into Tn5 lysis buffer (2X Tagment DNA buffer - Illumina, 1% Digitonin - Promega, PCR clean water) and were kept on ice and transported for transposition in batches of 8-12. Details of samples and replicates are shown in chapter 5.2.

Transposition was conducted by incubating cells with Tn5 enzyme (Illumina) at 37°C for 30mins with agitation at 300rpm. Transposed DNA was then isolated in a reaction clean up (Qiagen) and was subsequently indexed and amplified via PCR (indexes from the NEBNext Library Prep kit) overnight (Table 2.4). Amplified libraries were purified using AMPure XP bead clean up (Beckmann Coulter), to select out smaller size non desired primer DNA.

Table 2.4 PCR amplification of ATAC seq cDNA libraries (adapted from Corces et al, 2016)

Temperature	Time	Cycles
72°C	5 min	
98°C	30 seconds	
98°C 63°C 72°C	10 seconds 30 seconds 1 min	13 cycles
4°C	HOLD	

Quality control of cleaned libraries was performed using the Agilent Technologies High Sensitivity Tapestation, to check for characteristic ATAC peaks at expected base pairs (Figure 2.8). Libraries were quantified using Qubit (Thermofisher) and Kapa (Roche) before being sequenced on an Illumina NextSeq instrument using 150 cycles for paired end sequencing.

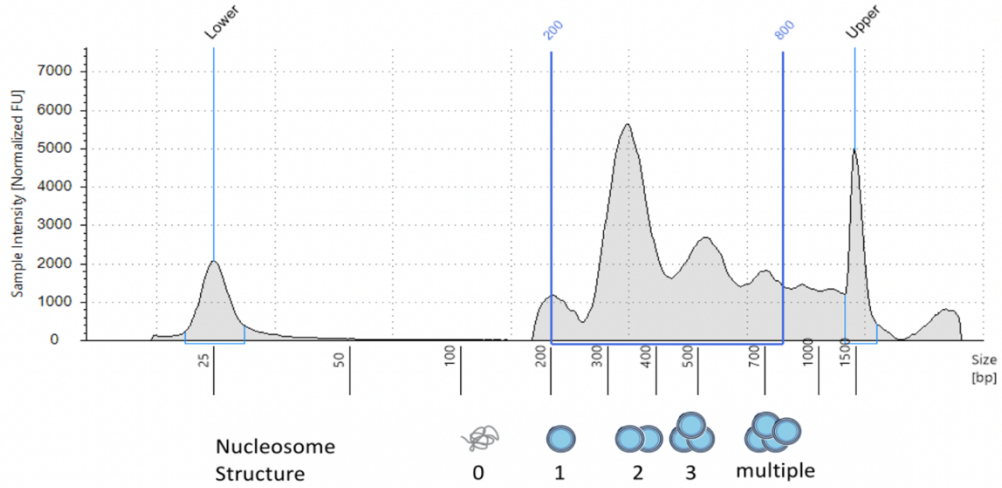


Figure 2.8 ATAC sequencing - quality control of cDNA libraries
High sensitivity Bioanalyzer traces (Agilent) of cDNA libraries generated through ATAC sequencing using an optimized protocol for small numbers of haematopoietic cells (Corces et al, 2016). Libraries were run on D1000 High sensitivity TapeStation tapes (Agilent) to verify that tagmentation was successful. Representative successful trace shows characteristic mononucleosome, dinucleosome and multinucleated fragments, with a periodicity of 150-180bp – the approximate length of DNA wrapped around each nucleosome.

2.11 ATAC-sequencing analysis

A summary of the ATAC-Sequencing workflow and analysis performed is detailed in Figure 2.9.

Following sequencing, reads were prepared for downstream analysis. First, reads were concatenated to link read 1 and read 2 for each sample e.g. normal #1 HSC. Following this, QC was performed on the concatenated reads using fastqc and trimgalore as was done for the RNA sequencing data. Following this, reads were aligned to the genome using Bowtie2, after which post-alignment QC was performed with Samtools. Peak calling was performed using the peak caller MACS2 (Zhang et al, 2008) to identify genomic loci which have been enriched for peaks.

Like the RNA sequencing data, all QC, mapping and alignment of ATAC reads was performed using the UNIX command line in BASH. In addition, bigWig files were generated for visualisation of merged chromatin accessibility traces using the UCSC Genome browser (http://genome.ucsc.edu). All subsequent data pre-processing, tabular manipulation, visualisation and statistical comparisons have been performed in R using rstudio.

Briefly, peak annotation was performed using nearest gene linkage in 401 base pair tiles using GenomicRanges, providing useful contextual information, such as their chromosome, geneID, location within the gene. Annotations were validated against an annotation reference using the annotables package.

Following this, the annotated peaks were analysed downstream using DiffBind, DESEQ2 and EdgeR which were used to generate giant meta objects from which information e.g. binding matrices and counts values, could be exported. All of the dimensionality reduction e.g. PCA and UMAP-based clustering was performed using DESEQ2 whilst the ANOVA-like statistical

tests used as input for heatmaps were performed in EdgeR. Several visualisation packages were used to plot the output of both DESEQ2 and EdgeR and these included ggplot2, umap, ggrepel, ggpubr, pheatmap. Accessibility traces on the UCSC browser were surveyed for regions which visually appeared differentially accessible. These regions were then cross referenced to ensemble gene assemblies and the Eukaryotic Promoter Database (epd.epfl.ch).

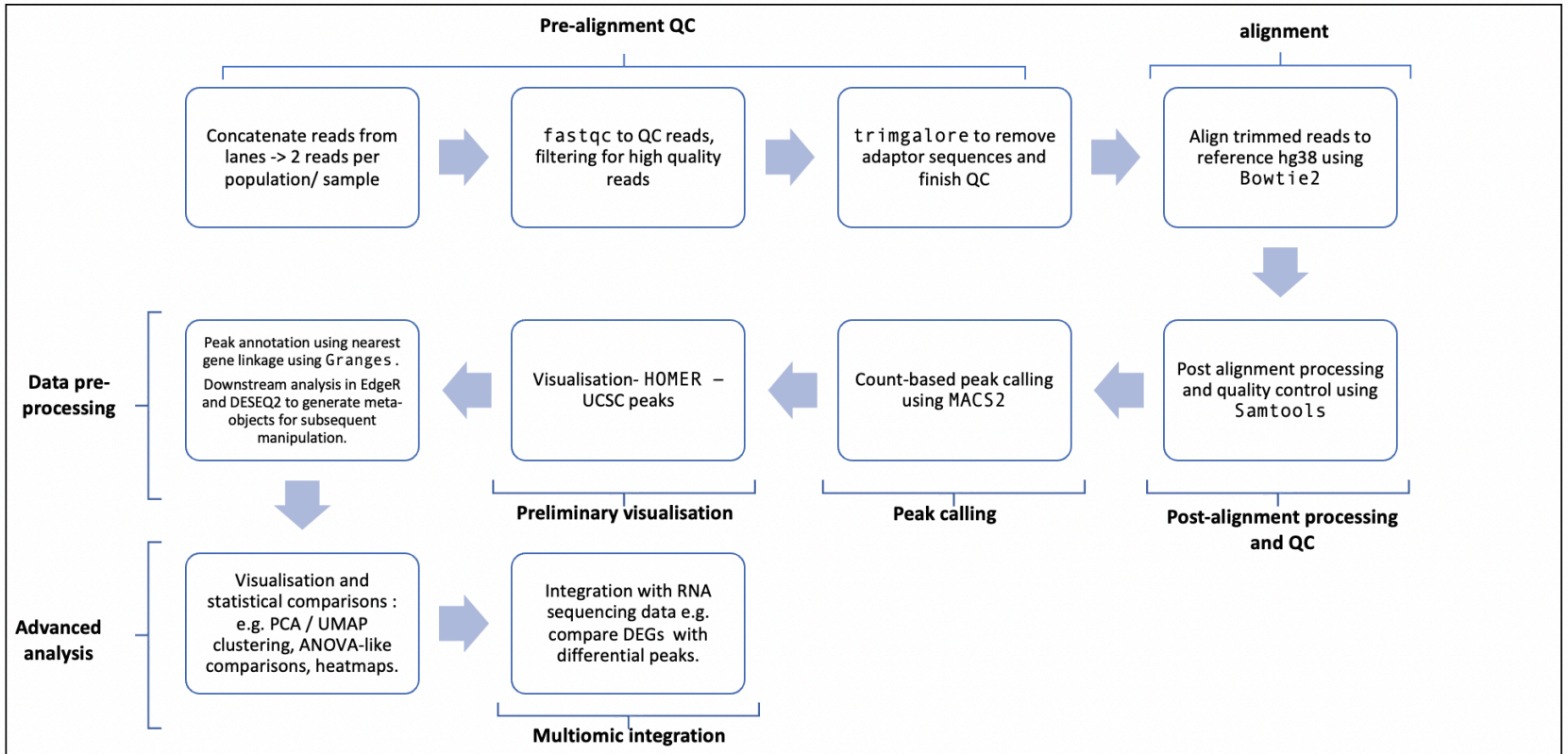


Figure 2.9 ATAC sequencing data analysis workflow

Sequencing reads are first concatenated to group reads by sample e.g. *normal #1 HSC* before they are pre-processed including QC, after which reads are aligned to hg38 genomic features. After post-alignment QC, peak calling is performed using MACS2. Peak calling is used to identify genomic loci at which aligned reads have been enriched. Following peak calling, the data are further processed (including nearest gene linkage) and visualised in rstudio and the UCSC browser. Downstream analysis and visualization was performed in EdgeR (blue arrows) and DESEQ2 (red arrows). EdgeR was used for statistical comparisons. All analysis was performed in rstudio using my own pipelines.

2.12 Statistics

Statistical comparisons of molecular data were performed in rstudio using EdgeR. Briefly, these comparisons included broader ANOVA-like tests to compare variance across several cell types and for direct cell-type comparisons, e.g. DS HSC vs N HSC, pairwise statistical comparisons were performed. Unless otherwise stated, significantly differentially expressed genes (DEGs) were determined through a P-value-adjusted false discovery rates (FDR), with the threshold as stated in the respective figure e.g. FDR < 0.1. Where stated, some DEG were determined by a combination of Log_2FC and P-value adjusted FDR thresholds.

For the functional data featured in chapters 3 and 4, all error bars on bar charts and absolute count graphs are expressed as the mean ± standard error of mean (SEM). To determine the correct statistical test for a given data set, I first assessed whether data were normally distributed, by performing normality testing in GraphPad prism. Normally distributed data were assessed using parametric tests, such as paired or unpaired t-tests, depending on whether the sample being analysed were from within biological replicates or between biological replicates.

Non-normally distributed data was assessed through non-parametric tests including single or multi-way ANOVA and Mixed Effects analyses. Depending on the nature of the comparisons, if necessary, corrections for multiple comparisons were applied, such as the Bonferroni correction, such as the methylcellulose datasets which involved comparing colony type (e.g. BFU-E vs GM) and condition (normal vs DS).

Due to the inherently high variability of the data, I made no assumptions regarding consistent standard deviations or variances across datasets to ensure any statistical comparison was as conservative as possible.

Unless otherwise stated, * $P<0.05$, ** $P<0.01$, *** $P<0.001$, **** $P<0.0001$.

Chapter 3

Immunophenotypic and functional characterisation of fetal bone marrow haematopoiesis to understand alternative pathways of human fetal B-lymphopoiesis

3.1 Background and aim

B-cell production before birth is a highly important process for subsequent childhood development as it ensures the adaptive immune system is ready and primed to respond and develop immune memory once the fetus becomes exposed to extraneous pathogens after birth.

Until the last decade, detailed understanding of B-lymphopoiesis within the FBM was limited, with the majority of information coming from mouse work. More recently, within the FL, our group first identified the ELP, a CD34+CD19-CD10-CD127+ progenitor with B, NK and T-lymphoid potential (Roy et al, 2012), which has since been characterised in detail (Hussen et al, 2017; Boiers et al, 2018; O'Byrne et al, 2019). In addition, studies in both FL and FBM revealed the presence of more than one CD34+CD19+ B-restricted progenitor, distinguishable by the expression of CD10 (O'Byrne et al, 2019). This showed that CD10-CD19+ B progenitors in FBM lay upstream of CD10+CD19+ BProB progenitors and therefore these CD10- B progenitors were designated PreProB- progenitors (O'Byrne et al, 2019).

Interestingly, previous work on cord blood (CB) cells, had also identified CD34+CD19+CD10- progenitors that were hypothesised to immediately precede CD34+CD19+CD10+ ProB progenitors (Sanz et al, 2003 and 2010).

Subsequently, our lab demonstrated that fetal B-lymphopoiesis begins in the FL (Roy et al, 2012), after which, the FBM becomes the main site of B-lymphopoiesis (O'Byrne et al, 2019) and remains so throughout postnatal life. The existence of fetal-specific ELP and PreProB-progenitors suggests fetal B-lymphopoesis is distinct from the process within adults and involves progenitors which possess ontogeny-specific molecular and functional developmental programmes.

The identification of CD10- and CD10+ B progenitors in fetal tissues raises the possibility that there could be two alternative pathways of B cell development in fetal life. The aim of the experiments discussed in this chapter, was to systematically identify and immunophenotypically and functionally characterise haematopoiesis in normal FBM, with a focus on lymphopoiesis. Specifically, I aimed to better define the early and intermediate HSPCs that lie upstream of ELP and resolve the molecular basis of the B-differentiation trajectory. In doing so, these experiments aimed to provide a reference point for subsequent comparison to understand how alterations to these programmes in Down syndrome, drive distinct lineage fates and functional phenotypes, especially for B -lymphopoiesis.

3.2 Discovery of novel fetal lympho-myeloid progenitors in normal FBM through immunophenotypic characterisation of FBM HSPC

To identify early progenitors and those of the B-, myeloid, and erythroid lineages present in FBM, I designed and optimised extensive flow cytometry panels to facilitate analysis of second trimester FBM (immunophenotypes can be found in Table 3.1 and gating strategies in Figure 3.1). Extension of established flow panels with additional markers enabled me to better define intermediate progenitor populations in the FBM. This facilitated the discovery of three novel FBM HSPC populations: Pre-ELP/GMP as well CD10- and CD10+ LMPPs which were previously incompletely defined in fetal tissues (Table 3.1). Analysis was performed on several biological replicates of second trimester normal FBM, n=13. Gestational ages of normal FBM samples used for immunophenotypic characterisation and subsequent vitro experiments are summarised in Table 3.2.

Table 3.1 Immunophenotypes

HSPC population	Immunophenotype
HSC	Lin2-CD19-CD34hiCD38-CD45RA-CD90+
MPP	Lin2-CD19-CD34hiCD38-CD45RA-CD90-
LMPP	Lin2-CD19-CD34hiCD38-CD45RA+
CD10-LMPP	Lin2-CD19-CD34hiCD38-CD45RA+CD10-
CD10+LMPP	Lin2-CD19-CD34hiCD38-CD45RA+CD10+
MEP	Lin2-CD34+CD38+CD19-CD10-CD127-CD45RA-CD123-
CMP	Lin2-CD34+CD38+CD19-CD10-CD127-CD45RA-CD123+
Pre-ELP/GMP	Lin2-CD34+CD38+CD19-CD10-CD127-CD45RA+CD123-
GMP	Lin2-CD34+CD38+CD19-CD10-CD127-CD45RA+CD123+
ELP	Lin2-CD34+CD38+CD19-CD10-CD127+
CLP	Lin2-CD34+CD38+CD19-CD10+
PreProB	Lin2-CD34+CD38+CD19+CD10-
ProB	Lin2-CD34+CD38+CD19+CD10+
Lin2 cocktail	CD2/3/14/56/235a

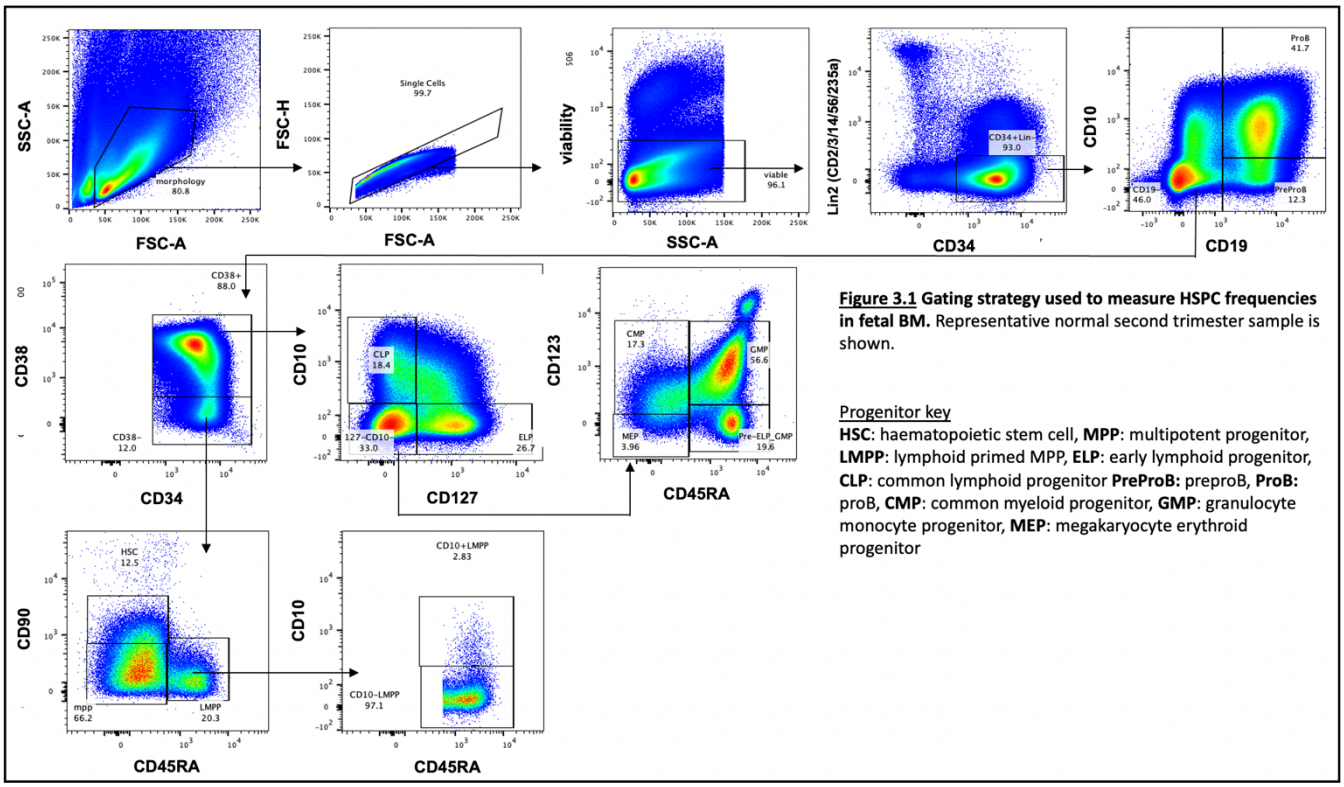


Figure 3.1 Gating strategy used to measure HSPC frequencies in fetal BM. Representative normal second trimester sample is shown.

Progenitor key

HSC: haematopoietic stem cell, **MPP**: multipotent progenitor, **LMPP**: lymphoid primed MPP, **ELP**: early lymphoid progenitor, **CLP**: common lymphoid progenitor **PreProB:** preproB, **ProB:** proB, **CMP**: common myeloid progenitor, **GMP**: granulocyte monocyte progenitor, **MEP**: megakaryocyte erythroid progenitor

Table 3.2 Gestational ages (GA) of samples used for normal FBM experiments

Assay	GA, in post conception weeks (pcw)	Purpose
Measuring immunophenotypic progenitor frequencies by flow cytometry	17, 19, 20, 20, 14, 14, 19, 19, 17, 19, 19, 21, 17.	Assess progenitor composition of normal FBM
MS5 co-culture (bulk)	17, 19, 20, 20.	Assess B/NK/myeloid output of HSPCs
Methylcellulose (single cell)	19, 21, 17, 14, 14.	Assess myeloid/megakaryocyte/ erythroid output of HSPCs
OP9-DL1 co-culture (bulk)	17, 15, 19, mixed well (17, 19, 19)	Assess T/NK output of HSPCs

In keeping with the FBM being the main site of B-cell production from before the second trimester (O'Byrne et al, 2019), approximately 50% of the Lin2-CD34+ progenitors in normal FBM are positive for CD19, a key marker of B-cells, (11.38± 1.55% PreProB + 35.83 ±4.196% ProB, Figure 3.2), with a further 12% comprised of ELPs and CLPs (5.56% ELP± 1.31% + 6.69± 1.2% CLP, Figure 3.2).

The majority of the FBM progenitors I detected are negative for CD10 (~60%, excluding CD10+ CLP, 6.69% ±1.2% and ProB, 35.83% ±4.196%), which is a known marker of B-lineage commitment (Ichii et al, 2010). Given that the FBM is key developmental site of B-lymphopoiesis (O'Byrne et al, 2019), I reasoned that these CD10- cells may be upstream, not yet B-restricted progenitors, which possess sufficient potential to eventually give rise to B-cells.

When evaluating the CD10- compartment, during these early immunophenotyping experiments, I observed a previously undefined and uncharacterised population with the immunophenotype: Lin-CD34+CD19-CD38+CD127-CD10-CD123-CD45RA+. These progenitors were subsequently described by me as Pre-ELP/GMP based on their functional output (see chapter 3.3). Based on their immunophenotype, Pre-ELP/GMP resemble a mature (CD38+) LMPP (Table 3.1) and they comprise 4.5 ±0.8% of the Lin2-CD34+ compartment (Figure 3.2), suggesting these are a substantial progenitor sub-type in normal FBM.

During these preliminary analyses, I observed distinct populations of LMPPs, distinguishable based on the expression of CD10, as described recently in cord blood (CB) (Karamitros et al,

2018). In addition, a population with a similar immunophenotype ($CD34^{+}CD38^{-}Thy\text{-}1^{neg-lo}CD45RA^{+}Flt3^{+}CD7^{-/+}CD10^{+}$), named multi-lymphoid progenitors, MLPs, had previously been revealed in CB and adult BM (Doulatov et al, 2010). To date, however, there has been no functional data describing CD10+ and CD10- LMPP in fetal tissue. Within normal FBM, the overwhelming majority of LMPPs are CD10-, whilst less than 5% are CD10-high-expressing (95.58± 1.102% CD10-LMPP vs 4.424 ± 1.102% CD10+LMPP of total LMPPs, Figure 3.3) and a paired t-test showed this difference in 10-/+LMPP frequencies in normal FBM to be highly significantly (**** P< 0.0001).

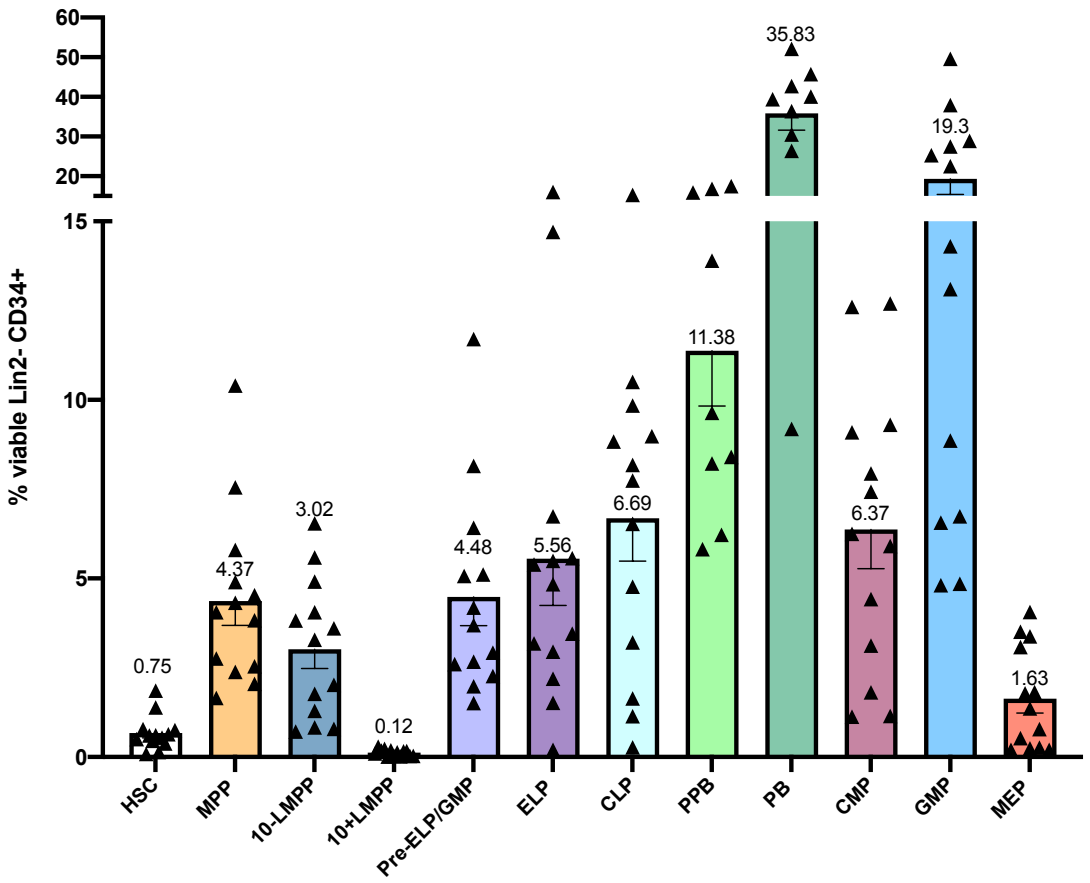


Figure 3.2 Frequency of Haematopoietic Stem and Progenitors (HSPCs) in normal FBM
Analysed by flow cytometry, (n= 13). Individual HSPC frequencies are shown as % viable CD34+ Lin2- cells, with mean values as indicated.
Lin2 cocktail: CD2/3/14/56/235+. Error bars show SEM.

Progenitor key
HSC: haematopoietic stem cell, **MPP**: multipotent progenitor, **LMPP**: lymphoid primed MPP, **ELP**: early lymphoid progenitor, **PPB:** preproB progenitor, **PB:** proB progenitor, **CMP**: common myeloid progenitor, **GMP**: granulocyte monocyte progenitor, **MEP**: megakaryocyte erythroid progenitor

In contrast to the high frequency of progenitors with lymphoid potential, MEPs represent only a small percentage of normal FBM HSPCs, approximately 30-fold less than the combined frequency of PreProB and ProB progenitors (1.63% MEP± 0.4% and 47.21% combined PreProB and ProB respectively, Figure 3.2), suggesting that the FBM is not primarily a site of mega-erythropoiesis, unlike second trimester normal FL, where the frequency of MEP exceeds that of committed B-progenitors (CD34+CD19+, CBP) (Roy et al, 2012) with CBPs corresponding to the PreProB and ProB progenitors within this study. The

relative frequency of myeloid progenitors, CMP and GMP make up approximately 25% of the Lin2-CD34+ compartment in FBM, highlighting that the FBM is an important site for myelopoiesis (6.37± 1.099% CMP and 19.3± 3.907% GMP, Figure 3.2).

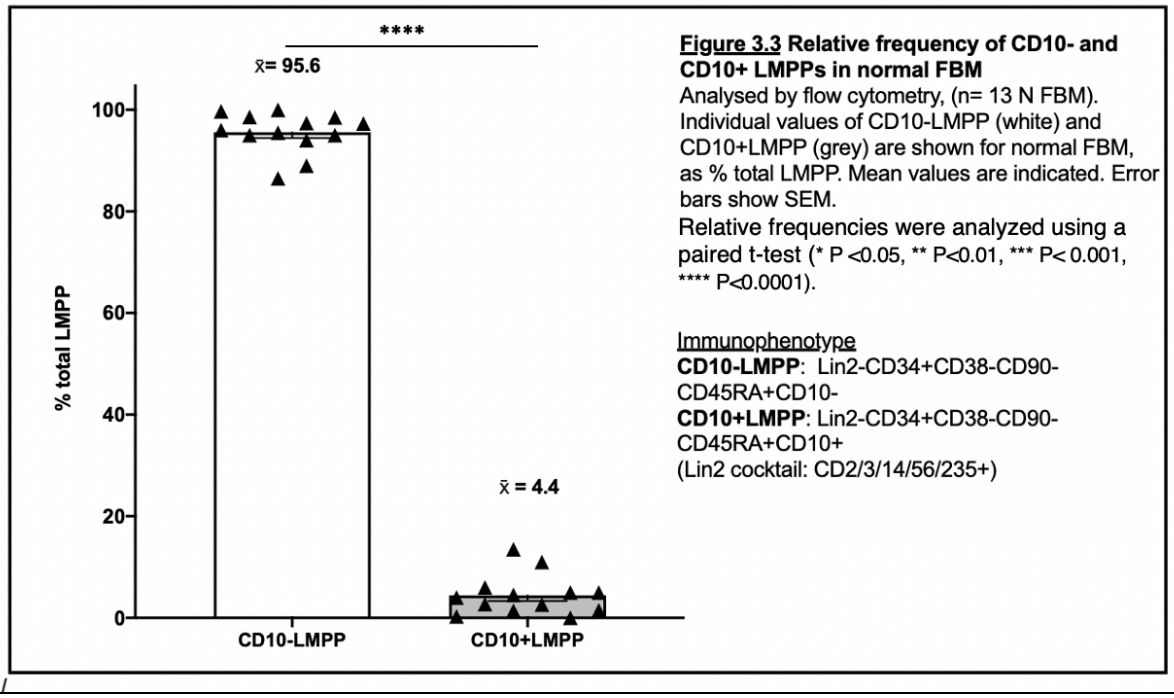


Figure 3.3 Relative frequency of CD10- and CD10+ LMPPs in normal FBM
Analysed by flow cytometry, (n= 13 N FBM). Individual values of CD10-LMPP (white) and CD10+LMPP (grey) are shown for normal FBM, as % total LMPP. Mean values are indicated. Error bars show SEM.
Relative frequencies were analyzed using a paired t-test (* P <0.05, ** P<0.01, *** P< 0.001, **** P<0.0001).

Immunophenotype
CD10-LMPP: Lin2-CD34+CD38-CD90-CD45RA+CD10-
CD10+LMPP: Lin2-CD34+CD38-CD90-CD45RA+CD10+
(Lin2 cocktail: CD2/3/14/56/235+)

To gain clues as to whether the provisionally designated "Pre-ELP/GMP" population observed during HSPC immunophenotypic profiling was unique to fetal life, HSPC frequencies were compared between human CB and FBM. Frequencies of HSPC populations were statistically compared using multiple unpaired Kolmorgorov Smirnov tests with an adjusted FDR to determine significance.

To my knowledge, this is the first comprehensive comparison of CD34+ HSPC frequencies between CB and FBM, although a previous DPhil student in the lab did compare the frequency of B progenitors in CB and FBM (Sorcha O'Byrne DPhil thesis, 2019). Ideally, progenitor frequencies would be compared across fetal, paediatric (PBM) and adult BM as, firstly, residual fetal cells perfuse CB and secondly, CB is not considered a true haematopoietic site in its own right. Unfortunately, working with PBM and ABM was not

within the scope of this project, hence I used CB as a later developmental stage tissue to compare to. I discuss these limitations further in chapter 3.5 and chapter 6.

Within CB, B-progenitors were either undetectable or significantly reduced when compared to FBM (ELP 0, P= 0.004, PPB 0.7 ±0.336%, P= 0.009 PB 1.543 ±0.722%, P = 0.009), in line with previous observations that lymphoid populations make up a small minority in CB (Mantri et al, 2020). Whilst Pre-ELP/GMP were detectable, they were significantly reduced in CB, (approximately 5-fold: 0.86%± 0.324 in CB vs 4.5%± 0.8% in FBM, P = 0.0036). These findings suggest that Pre-ELP/GMP are enriched in fetal life, however given that CB contains residual fetal HSPCs, confirmation that Pre-ELP/GMP are fetal-specific would also require evaluation of adult and paediatric BM.

Interestingly, whilst the overall LMPP compartment was comparable in CB compared with FBM (3.203± 0.738% CB vs 3.136± 0.553% FBM), the proportion of CD10+LMPP was significantly higher (P=0.0036), comprising 30% total LMPP (Figure 3.4), versus 4.4% in FBM (Figure 3.3).

Given that a CD10+ LMPP equivalent have been previously identified in CB (Karamitros et al, 2018) and that ELP and PPB, both CD10-, are respectively absent and markedly reduced, may indicate that progenitors involved in B-lymphopoiesis exhibit a more CD10+ phenotype in post-natal life, while the FBM is enriched for CD10- progenitors, possibly including Pre-ELP/GMP.

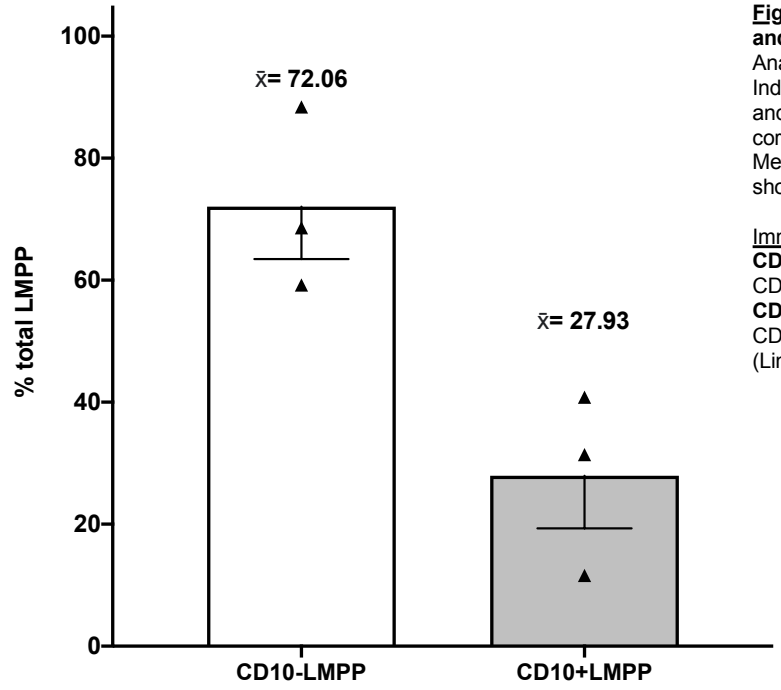


Figure 3.4 Relative frequency of CD10- and CD10+ LMPPs in normal CB. Analysed by flow cytometry, (n= 3). Individual values of CD10-LMPP (white) and CD10+LMPP (grey) in normal human cord blood are shown as % total LMPP. Mean values are indicated. Error bars show SEM.

Immunophenotype
CD10-LMPP: Lin2-CD34+CD38-CD90-CD45RA+CD10-
CD10+LMPP: Lin2-CD34+CD38-CD90-CD45RA+CD10+
(Lin2 cocktail: CD2/3/14/56/235+)

3.3 Functional characterisation of novel fetal lympho-myeloid progenitors in normal FBM

To systematically determine the lineage output of normal FBM HSPCs, I FACS-sorted each FBM HSPC population based on their immunophenotype and performed in vitro assays primed toward NK/B-lymphoid differentiation (MS-5 co-cultures), myelo/erythroid clonogenic assays (methylcellulose) and NK/T-lymphoid differentiation (OP9-DL1 co-cultures). During these investigations, I particularly focused on describing CD10- vs CD10+ LMPPs for the first time, as well as the putative "Pre-ELP/GMP" progenitor, in order to characterise their lineage potential and establish their position in the B-cell differentiation hierarchy, allowing me to develop and refine the established fetal B-lymphopoiesis pathway (O'Byrne et al, 2019). Characterisation of the T- and myeloid/mega/erythroid lineage potential of the novel progenitors (from the OP9-DL1 and methylcellulose assays, respectively) is discussed alongside the established HSPC FBM populations in chapter 3.4.

MS-5 co-culture assays: CD10+ and CD10-LMPP and Pre ELP/GMP

To determine the myeloid, B-cell and NK cell potential of "Pre-ELP/GMPs", CD10-LMPPs and CD10+LMPPs, I co-cultured FACS-sorted HSPC populations from normal FBM on MS-5 stroma and measured their lineage output over time. Samples spanned 14-20 pcw and for all experiments n=3, except for whole LMPP where n=2 and 10+LMPP where n=1 due to population rarity.

Previous work within the lab using the MS-5 system has enabled the establishment of the fetal B-lymphopoiesis pathway. Namely, HSCs, MPPs and LMPPs give rise initially to predominantly myeloid output, after which B-cells emerge at day 14 (O' Byrne et al, 2019).

By contrast, myeloid output is minimal for ELP and absent for PreProB/ProB progenitors respectively, with robust B-cell output throughout the duration of the time course (d3-21). Moreover, these experiments gave us clues as to the order of B-progenitors in the B-differentiation pathway, namely CD10- ELP can give rise to CD10- PreProB and subsequently CD10+ ProB through the stepwise acquisition of CD19 and CD10.

In order to resolve both the immature (CD34+) and mature (CD34-) output of normal FBM HSPCs, I optimised several flow cytometry panels by combining HSPC markers e.g. CD90, CD45RA, CD127, and more mature lineage markers e.g. CD19. Altogether these panels enabled refinement of the established readout for the co-culture assays including the identification of progenitor stages at different timepoints. Analysis was performed on days 3 and 7 of the co-culture to capture the earliest differentiation transitions.

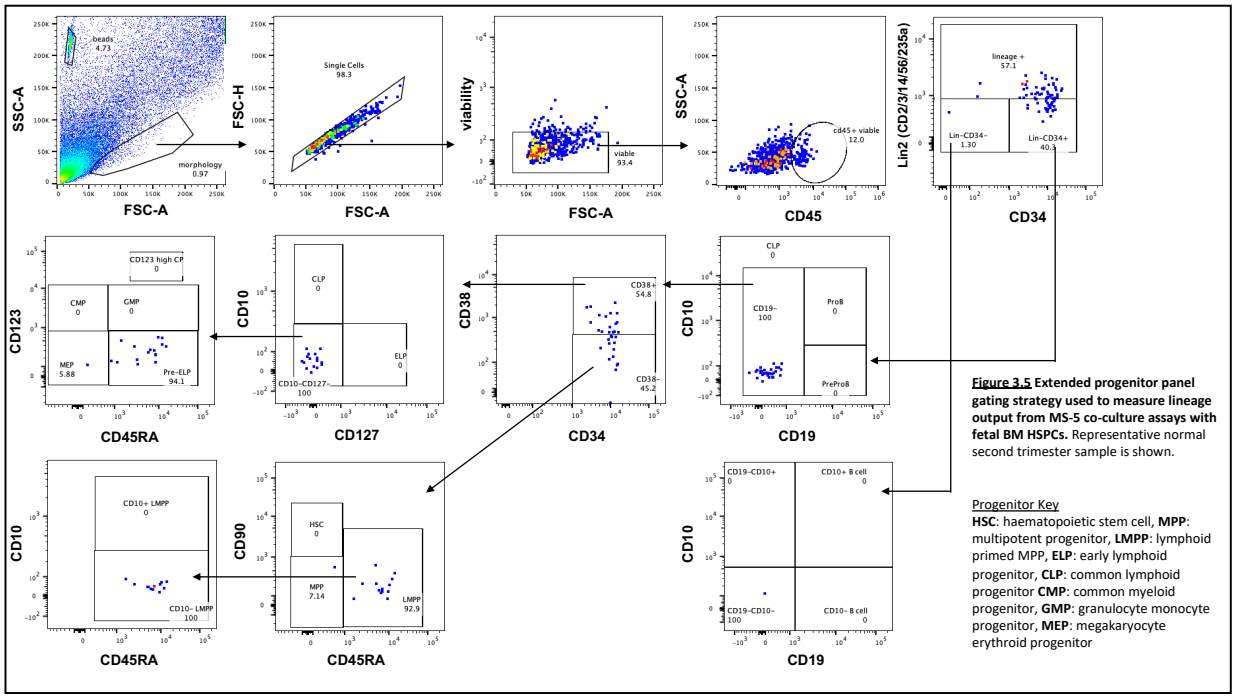


Figure 3.5 Extended progenitor panel gating strategy used to measure lineage output from MS-5 co-culture assays with fetal BM HSPCs. Representative normal second trimester sample is shown.

Progenitor Key
HSC: haematopoietic stem cell, **MPP**: multipotent progenitor, **LMPP**: lymphoid primed MPP, **ELP**: early lymphoid progenitor, **CLP**: common lymphoid progenitor **CMP**: common myeloid progenitor, **GMP**: granulocyte monocyte progenitor, **MEP**: megakaryocyte erythroid progenitor

First, using the extended immature output panel (for gating strategy see Figure 3.5), I showed that CD10-LMPPs (and whole LMPPs) exhibit lympho-myeloid potential and give rise to immunophenotypically-defined "Pre-ELP/GMPs" and ELPs (Figure 3.6 A), which comprise 38± 16.12% and 10± 6.41% of the CD34+ output on day 3 for CD10-LMPPs respectively (Figure 3.6 B). These findings place CD10-LMPPs upstream of both populations.

In addition, CD10- LMPP cultures also produced small numbers of CD10+LMPPs, placing CD10+LMPPs downstream of CD10-LMPPs (Figure 3.6 B).

The observation that CD10- LMPPs can give rise to progressively differentiated CD10- progenitor output (Pre-ELP/GMP -> GMP or Pre-ELP/GMP -> ELP-> PPB) as well as CD10+LMPPs, may suggest that CD10- LMPPs represent a bifurcation point after which two pathways can be taken, distinguished by CD10 expression.

Current data from our group and others (Ichii et al, 2010; Roy et al, 2012; O'Byrne et al, 2019) suggest that CD10 is upregulated throughout B-lymphopoiesis and is positively correlated with B-lineage progression (Ichii et al, 2010). That CD10 expression is lost during the later stages of B-cell maturation (Béné, 2005), indicates it may play a stage-specific role in lineage priming and commitment up to the Pre-B stage (Mishra et al, 2016).

"Pre-ELP/GMPs" gave rise to immunophenotypic ELPs, B-progenitors (PreProB and ProB) as well as GMPs, allowing me to name them with confidence, based on their functional output. Crucially, Pre-ELP/GMPs failed to produce any LMPPs confirming that they lie downstream of LMPPs (Figure 3.6 A/B).

Compared to total LMPPs and CD10-LMPPs, Pre-ELP/GMP output is more B-lymphoid biased (Figure 3.6 B). However, the GMPs make up a similar proportion of the CD34+ output of Pre-ELP/GMPs and CD10-LMPPs at day 3 (16.6 ± 16.6% vs 17.2 ± 16.38% viable CD34+, respectively), suggesting that Pre-ELP/GMPs retain residual myeloid potential.

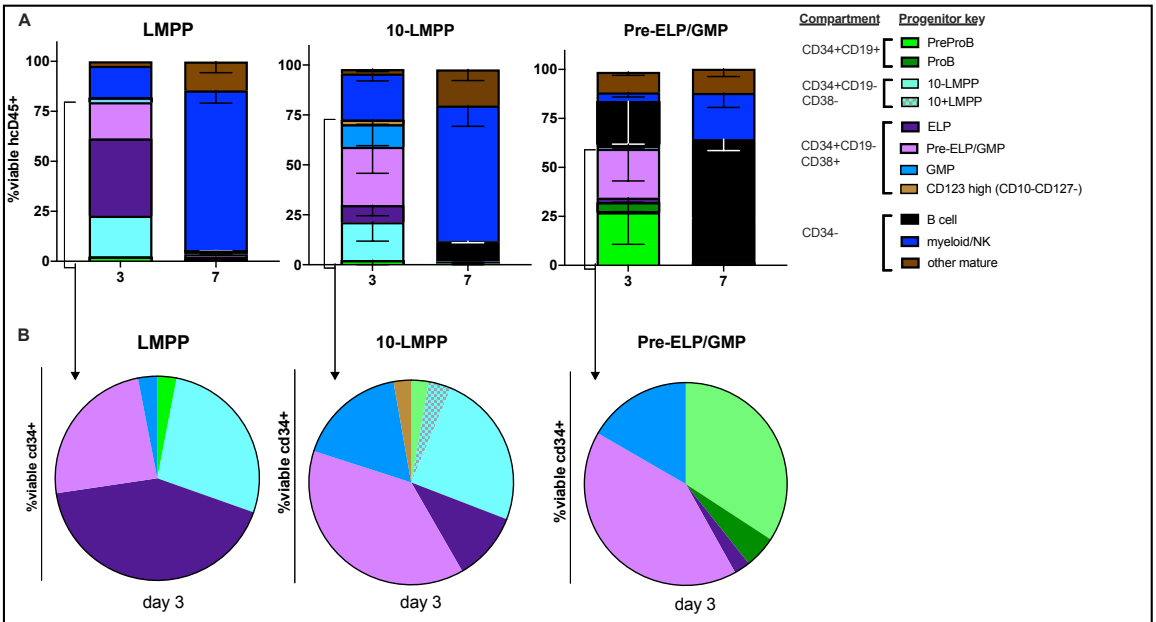


Figure 3.6 Normal FBM LMPPs and CD10-LMPPs show lymphomyeloid potential and both give rise to Pre-ELP/GMPs. Downstream Pre-ELP/GMPs are comparatively B-cell restricted; giving rise to predominantly ELP, PPB and PB B-progenitors, as well as GMPs.
Differentiation assay of flow-sorted normal fetal BM HSPCs co-cultured on MS-5 stromal cells with cytokines (FLT3L, SCF, IL-7, IL-2).
A) Total lineage output is shown as % viable hCD45+ cells at day 3 and day 7 or **B)** CD34+ progenitor output is shown as % viable hCD45+ CD34+ cells at day 3.
N=2 for total LMPP and N=3 for Pre-ELPGMP. Data was not analysed where hCD45+ events <10, leading to sample exclusion.
myeloid/NK = Lineage +, Lin cocktail = CD2,3,11b,14,56,235a
other mature= Lin-CD34-CD19-.

Given that the mature output of Pre-ELP/GMPs at days 3 and 7 is predominantly B-lineage compared with both total LMPPs and CD10-LMPPs (Figure 3.6 A), this suggests that whilst residual myeloid potential exists, it does not appear to translate into substantial mature myeloid output, possibly due to greater intrinsic B-lineage priming, which future single cell studies will hopefully shed light on.

Having profiled the early progenitor decisions of Pre-ELP/GMPs, CD10-LMPPs and CD10+LMPPs, I next performed MS-5 co-culture assays using a mature output panel (gating strategy shown in Figure 3.7) to characterise their output over longer time course (21/28 days).

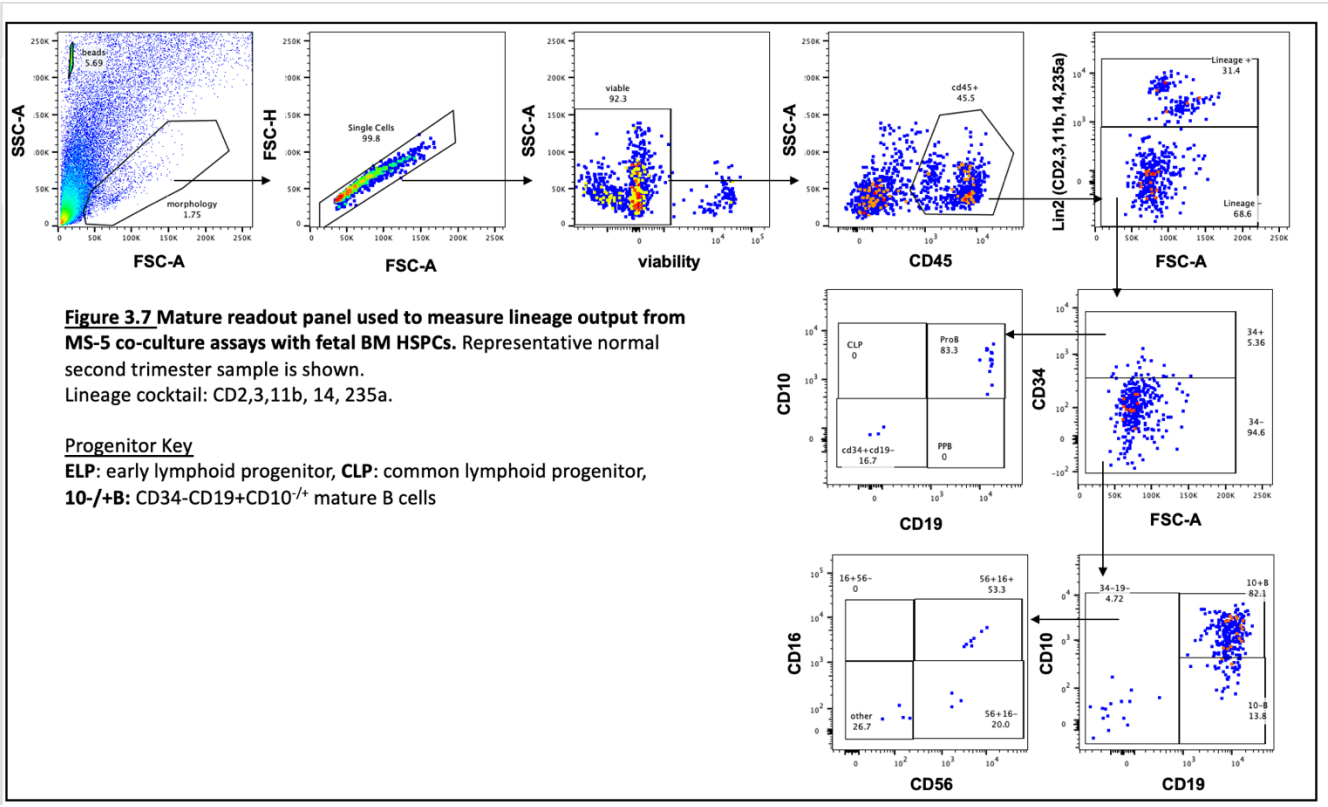


Figure 3.7 Mature readout panel used to measure lineage output from MS-5 co-culture assays with fetal BM HSPCs. Representative normal second trimester sample is shown.
Lineage cocktail: CD2,3,11b, 14, 235a.

Progenitor Key
ELP: early lymphoid progenitor, **CLP**: common lymphoid progenitor, **10-/+B:** CD34-CD19+CD10$^{-/+}$ mature B cells

After predominantly producing myeloid cells between days 3-7, CD10-LMPP gave rise to robust B-cell output on day 14 and by day 21, I demonstrated that CD10-LMPPs also give rise to NK cells, which make up appx 25% of the output at day 21 (Figure 3.8 A).

CD10+LMPPs are notably lymphoid-primed compared to CD10-LMPPs, and show initially B-cell, followed by mainly NK output by day 21 (Figure 3.8 A). The proportion of B-cells in the overall output of both LMPPs is similar (Figure 3.8 A), so CD10+LMPPs appear to be more restricted in what they can produce (minimal myeloid), rather than they actively produce a greater proportion of B-cells, which is validated by the absolute counts data (Figure 3.8 B). By contrast, at day 21, the proportional NK output for CD10+LMPPs is approximately double that of CD10-

LMPP (Figure 3.8 A), which may suggest CD10+LMPP are specifically primed to produce these, although this difference in NK frequency is not statistically significant. In contrast, the delayed NK output within CD10-LMPP compared with 10+LMPP may indicate an initial strong bias toward myeloid/B-cells. Despite clear differences in the proportional myeloid output of CD10-/+ LMPPs, most notably at day 7 (63.2± 12.6% 10-LMPP vs 24.7± 17.5% 10+LMPP), this difference is not statistically significant (P= 0.016, day 7).

Of the three novel progenitor populations, Pre-ELP/GMP are clearly the most lineage restricted, with B-cells being the dominant output from day 3 onwards (Figure 3.8 A), though their greater proportional B-lineage output was not statistically significant when compared to the other populations. Supporting observations of GMPs in the progenitor panel data (Figure 3.6 B), Pre-ELP/GMPs do give rise to mature myeloid output (Figure 3.8 A), however this is reduced compared to upstream CD10-LMPP (Figure 3.8 A/B), though this is not statistically significant. Likewise, the proportion of NK cells in Pre-ELP/GMP cultures is greatly reduced compared to both the LMPP populations (Figure 3.8 A), though not significantly, which may suggest less multi-lymphoid priming in these downstream progenitors in favour of a B-lineage primed state.

Corresponding absolute counts demonstrate that CD10-LMPPs produce higher absolute numbers of both B and myeloid lineages than CD10+LMPPs (Figure 3.8 B), with the increased myeloid output determined to be statistically significant (day 7, P= 0.0025). Specifically, the B-cell output (green, Figure 3.8 B) for both CD10-/+ LMPP peaks at day 14, with the B-cell output for CD10+LMPPs was 6-fold lower than CD10-LMPPs (4393± 2500 10-LMPP vs 744± 308 10+LMPP).

The most marked and only significant difference in absolute myeloid output (blue, Figure 3.8 B) was observed at day 7 (1837 10-LMPP vs 73± 61 10+LMPP, P= 0.0025). Altogether, this may suggest enhanced regenerative potential of CD10-LMPPs which would support greater expansion. Interestingly, whilst the NK output (orange, Figure 3.8 B) for CD10+LMPP was lower than CD10-LMPP at day 14 (179± 57 10-LMPP vs 149± 132 10+LMPP), it exceeded the CD10+LMPP output at both day 7 (23 10-LMPP vs 158± 128 10+LMPP) and 21 (447± 144 10-LMPP vs 495± 339 10+LMPP).

Despite their lineage bias, the reduced absolute mature cell counts from CD10+LMPPs combined with observation that CD10-LMPPs give rise to CD10+ LMPPs (Figure 3.6 B) may suggest that CD10+LMPPs are more differentiated than CD10-LMPPs.

Moreover, Pre-ELP/GMPs show reduced absolute B/NK/myeloid output compared with 10-LMPPs (day 14: B-cells 4393± 2500 10-LMPP vs 183± 23 Pre-ELP/GMP, Myeloid 724± 491 10-LMPP vs 75± 68 Pre-ELP/GMP, NK 179± 57 10-LMPP vs 134± 123 Pre-ELP/GMP) supporting their place downstream within the differentiation trajectory, although none of these differences were significant (p= 0.23, 0.40, 0.78, respectively).

10+LMPPs generated greater (though not significantly) absolute numbers of B-cells than Pre-ELP/GMP, with exception of day 7 where the output was comparable (B-cells 181 10+LMPP vs 207± 126 Pre-ELP/GMP). Pre-ELP/GMPs generated comparable or slightly higher myeloid counts than 10+LMPPs, whilst 10+LMPPs NK output was consistently higher, though none of these differences were significant.

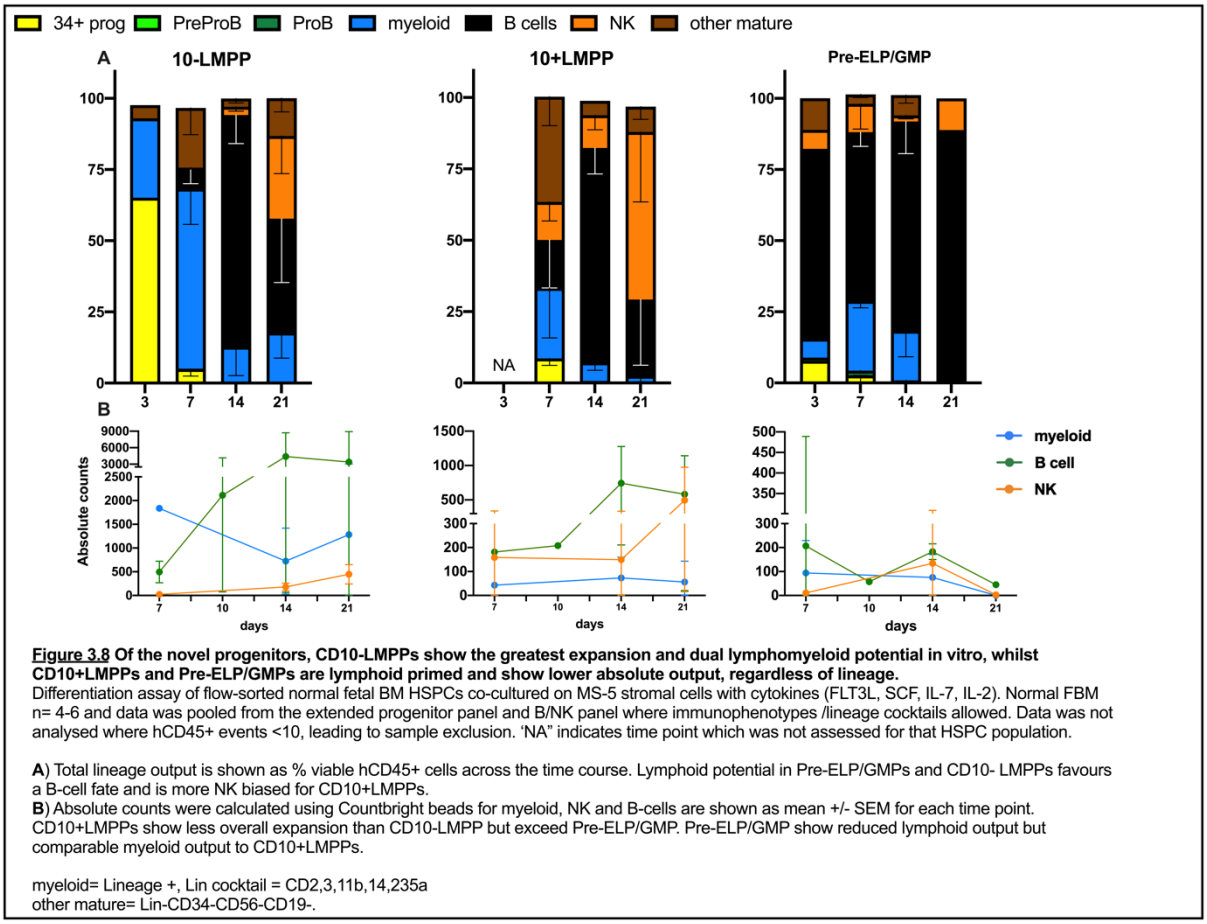


Figure 3.8 Of the novel progenitors, CD10-LMPPs show the greatest expansion and dual lymphomyeloid potential in vitro, whilst CD10+LMPPs and Pre-ELP/GMPs are lymphoid primed and show lower absolute output, regardless of lineage.
Differentiation assay of flow-sorted normal fetal BM HSPCs co-cultured on MS-5 stromal cells with cytokines (FLT3L, SCF, IL-7, IL-2). Normal FBM n= 4-6 and data was pooled from the extended progenitor panel and B/NK panel where immunophenotypes /lineage cocktails allowed. Data was not analysed where hCD45+ events <10, leading to sample exclusion. 'NA" indicates time point which was not assessed for that HSPC population.

A) Total lineage output is shown as % viable hCD45+ cells across the time course. Lymphoid potential in Pre-ELP/GMPs and CD10- LMPPs favours a B-cell fate and is more NK biased for CD10+LMPPs.
B) Absolute counts were calculated using Countbright beads for myeloid, NK and B-cells are shown as mean +/- SEM for each time point. CD10+LMPPs show less overall expansion than CD10-LMPP but exceed Pre-ELP/GMP. Pre-ELP/GMP show reduced lymphoid output but comparable myeloid output to CD10+LMPPs.

myeloid= Lineage +, Lin cocktail = CD2,3,11b,14,235a
other mature= Lin-CD34-CD56-CD19-.

Overall, the extent to which lineage potential translates to increased absolute output appears to depend on differentiation stage.

In summary, these data indicate that CD10- progenitors retain greater myeloid potential than CD10+LMPP, and their lymphoid potential is B-cell biased, whilst CD10+LMPPs lymphopoiesis is more evenly distributed between B and NK lineages. Discrepancies between lineage representation in the proportional frequency and the absolute counts data (Figure 3.8 A/B) indicate a fine balance exists between lineage restriction and self-renewal/ expansion capacity. Many of the functional differences observed in FBM HSPC populations (both of novel and established HSPCs, chapter 3.3 and 3.4, respectively) were not statistically significant due to a combination of highly variable primary human data and low replicate numbers.

3.4 Functional characterisation of normal FBM HSPCs to refine the fetal B cell developmental hierarchy

Having established their hierarchy and functional differences on MS-5 stroma, I wanted to explore the T- and myeloid/mega/erythroid potential of 10- and 10+LMPP, and Pre-ELP/GMP using other specialised systems. All functional assays of the novel progenitors, were performed alongside other upstream and downstream progenitors FBM HSPCs, to contextualise the new findings in terms of the established FBM lineage hierarchies.

MS-5 co-culture assays: established HSPCs of the FBM differentiation hierarchy

Co-culture of normal FBM HSPCs yielded the expected lineage output over time (Figure 3.9 A). Specifically, normal HSCs and MPPs first give rise to myeloid cells, peaking between day 7-14, after which time B cells emerge by day 21 in HSCs and day 14 in MPPs and finally, NK cells are detectable from day 21 (Figure 3.9 A). Downstream ELPs give rise to almost exclusively lymphoid output which is, for the most part B-lineage, starting with PreProB and ProB progenitors on day 3, followed by maturation into mature CD34- B cells from day 7 (Figure 3.9 A). When compared to HSCs and MPPs, the increase in the frequencies of B-cells in Pre-ELP/GMP and ELP cultures was statistically significant (P= 0.0002 and P= 0.003 for HSC vs Pre-ELP/GMP d7/d14 respectively, P= 0.007 for MPP vs Pre-ELP/GMP at d14, and P= 0.0003 and P= 0.00015 for HSC vs ELP d7 and d14), indicating that these progenitors are more B-cell primed than their upstream precursors. The proportional B-cell output was significantly higher for CD10-LMPPs relative to HSCs at day 14 (P=0.002), however there was no statistical difference at any other time point or between CD10-LMPP and MPP, which

may indicate that CD10-LMPP are less significantly B-cell primed when compared to Pre-ELP/GMP and ELP.

NK output from normal FBM ELPs can be detected by the end of the time course, but is limited (Figure 3.9 A). Finally, PreProB progenitors give rise to ProB progenitors, and aside from this, the output of both is exclusively mature B cells (Figure 3.9 A).

The corresponding absolute counts data for each HSPC population mirrors their degree of differentiation; namely, earlier progenitors give rise to higher numbers of B/NK/myeloid cells than the more terminally differentiated progenitors (Figure 3.9 B). For example, the maximum absolute myeloid count at any time point for the upstream progenitor populations was as follows: HSC 5132± 2807 (d14), MPP 13304± 7170 (d14), 10-LMPP 1837 (d7), 10+LMPP 73± 61 (d14), Pre-ELP/GMP 94± 78 (d7) (Figure 3.9 B). Interestingly, however, the maximum B cell counts observed for LMPPs, specifically CD10- LMPPs (4393± 2500, d14), exceed that of both upstream HSCs (1543± 504, d21) and MPPs (1159± 460, d21) (Figure 3.9 B) and the downstream comparatively B-lineage restricted Pre-ELP/GMPs (207± 126, d7), demonstrating that LMPPs serve as a driver of B cell expansion.

Interestingly, despite strong B-lineage priming, the maximum absolute B-cell output of Pre-ELP/GMPs (207± 126, d7) is lower than that of ELPs (1098± 450, d7) and PreProBs (361± 156, d14), but exceeds that of ProBs (96± 50, d7). This may indicate that there is a potential trade-off between the relative multi-potency of Pre-ELP/GMPs, which produce greater myeloid and NK output, and the extent to which their apparent B-lineage priming translates

into absolute output. In contrast, the more B-committed ELPs and the B-progenitors are able to generate comparatively greater numbers of B-cells within this system.

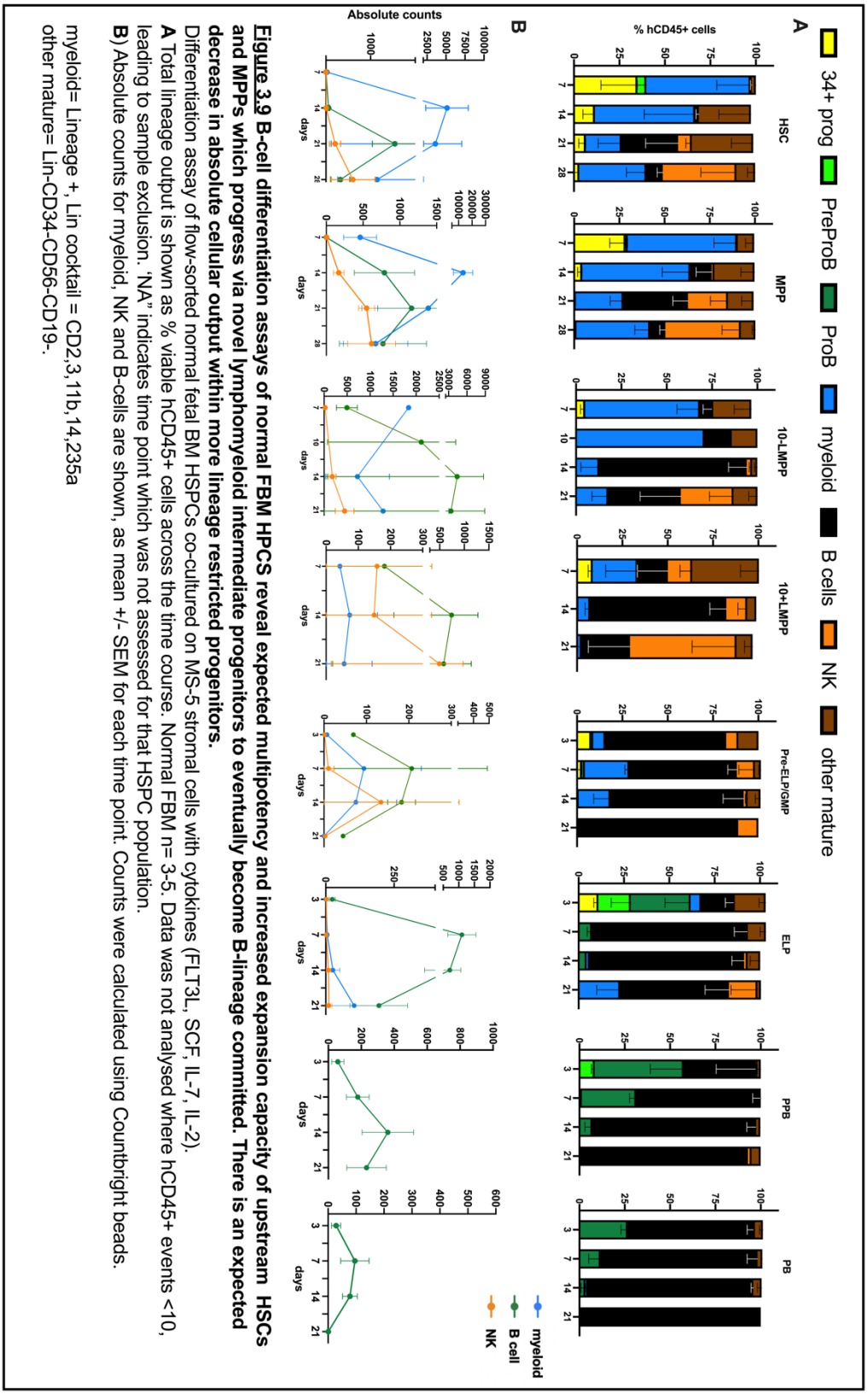


Figure 3.9 B-cell differentiation assays of normal FBM HPCS reveal expected multipotency and increased expansion capacity of upstream HSCs and MPPs which progress via novel lymphomyeloid intermediate progenitors to eventually become B-lineage committed. There is an expected decrease in absolute cellular output within more lineage restricted progenitors.

Differentiation assay of flow-sorted normal fetal BM HSPCs co-cultured on MS-5 stromal cells with cytokines (FLT3L, SCF, IL-7, IL-2).

A Total lineage output is shown as % viable hCD45+ cells across the time course. Normal FBM n= 3-5. Data was not analysed where hCD45+ events <10, leading to sample exclusion. 'NA" indicates time point which was not assessed for that HSPC population.

B) Absolute counts for myeloid, NK and B-cells are shown, as mean +/- SEM for each time point. Counts were calculated using Countbright beads.

myeloid= Lineage +, Lin cocktail = CD2,3,11b,14,235a

other mature= Lin-CD34-CD56-CD19-.

OP9-DL1 co-culture assays

In order to assess T-lymphoid output of both the known HSPCs of the established fetal B-differentiation hierarchy (O'Byrne et al, 2019), and the newly described progenitors, HSPCs were sorted and cultured on OP9-DL1 stromal cells. OP9-DL1 have been engineered to express Notch ligand Delta-like 1 and are commonly used for the efficient differentiation and proliferation of T-cells and NK-cells from human HSPCs (Holmes and Zúñiga-Pflucker, 2009). HSPCs and OP9-DL1 were co-cultured in cytokine-supplemented medium containing Flt3L, SCF and IL-7 which support myeloid and pan-lymphoid differentiation. To comprehensively characterise the output from these assays, I developed an extended readout panel comprising both immature and mature T-cell, NK, B and myeloid markers (gating strategy shown in Figure 3.10).

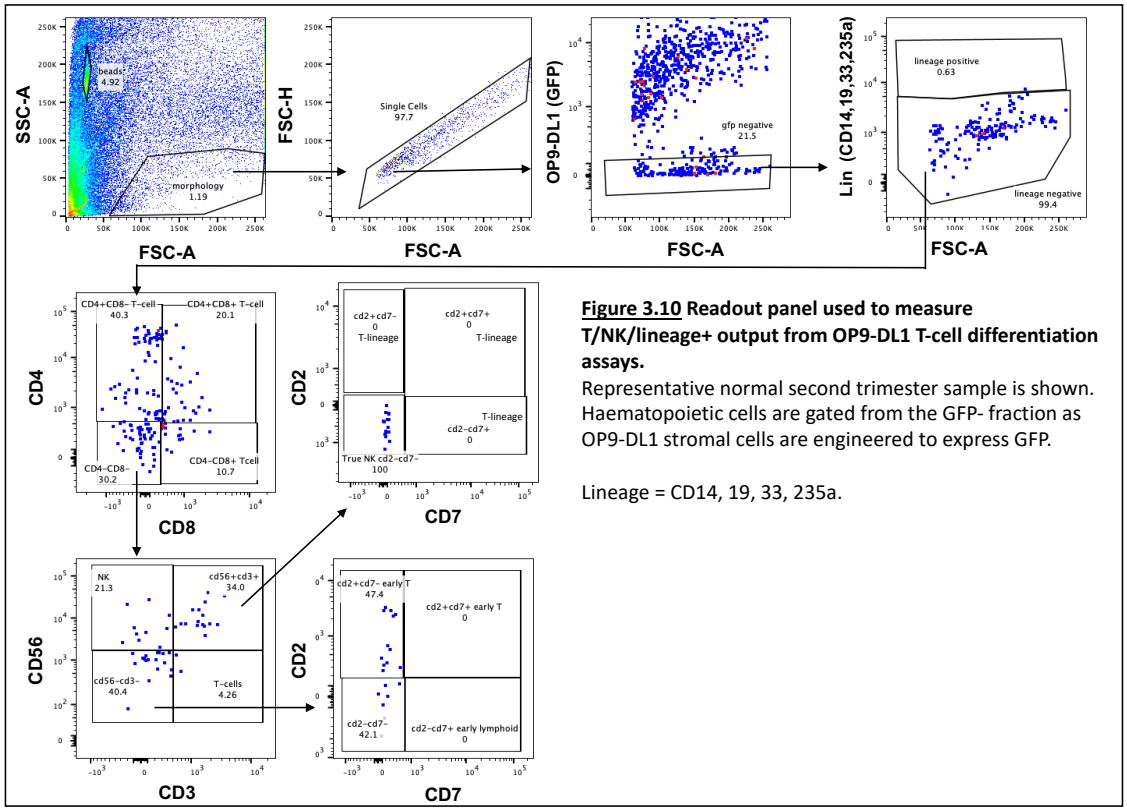


Figure 3.10 Readout panel used to measure T/NK/lineage+ output from OP9-DL1 T-cell differentiation assays.
Representative normal second trimester sample is shown. Haematopoietic cells are gated from the GFP- fraction as OP9-DL1 stromal cells are engineered to express GFP.

Lineage = CD14, 19, 33, 235a.

OP9DL1 assays: CD10-/+ LMPP and Pre-ELP/GMP

Focusing first on the newly described progenitors, on OP9-DL1 CD10-LMPPs show robust T-cell potential with greater than 65% of the output being T-lineage at assessed time points (d14 77± 6%, d21 67± 10%, Figure 3.11 A) compared to CD10+LMPPs and downstream Pre-ELP/GMPs cultures, in which T-lineage output did not exceed 25% or 60%, respectively (Figure 3.11 A). This translates into higher absolute T-cell counts in CD10-LMPP cultures (Figure 3.11 B) (maximum absolute T-cell count: 10-LMPP 813± 326, day 14, 10+LMPP 186 day 21, Pre-ELP/GMP 168 ±49, day 14).

As was the case in MS-5 B-cell differentiation assays (see Figure 3.8 A/B), CD10+LMPPs display efficient NK-cell production (Figure 3.11 A). Due to the scarcity of CD10+LMPPs present in normal FBM, I was able to be analyse this population only in one experiment, (using pooled biological samples, n=3), making it difficult to draw firm conclusions. Validating observations of increased absolute NK output for CD10+LMPP vs CD10- counterparts and Pre-ELP/GMP (Figure 3.8 B), CD10+LMPPs also produced more NK cells on OP9-DL1 stroma (maximum absolute NK-cell count: 10+LMPP 811, day 21 vs 10-LMPP 124 ±104, day 14 and Pre-ELP/GMP 111± 83 day 21). These preliminary findings may indicate that whilst CD10+LMPPs produce lower numbers of both B- and myeloid- lineages, they are able to translate their intrinsic priming using what expansion capacity they have left, into increased NK output.

Downstream, Pre-ELP/GMP show multi-lineage output, producing T-, NK and >15% Lin+ output at all given time points (Lin cocktail= CD14/19/33/235a (Figure 3.11 A).

Interestingly, although the frequency of T-cells in Pre-ELP/GMP cultures exceeds that of CD10+LMPP (day 14= 56.9 ±18% vs 25% and day 21= 34.5± 5.8% vs 19.6 %, respectively) these populations produced similar maximum absolute numbers of T-cells (168± 49 Pre-ELP/GMP day 14 vs 186 CD10+LMPP day 21, Figure 3.11 B), which could reflect potentially reduced expansion capacity of Pre-ELP/GMP relative to CD10+LMPPs. This must be further validated due to n=1 for 10+LMPP, but would support the data generated from MS-5 differentiation assays, in which 10+LMPPs produced greater numbers of B and NK-cells than Pre-ELP/GMP across most time points (Figure 3.8 B).

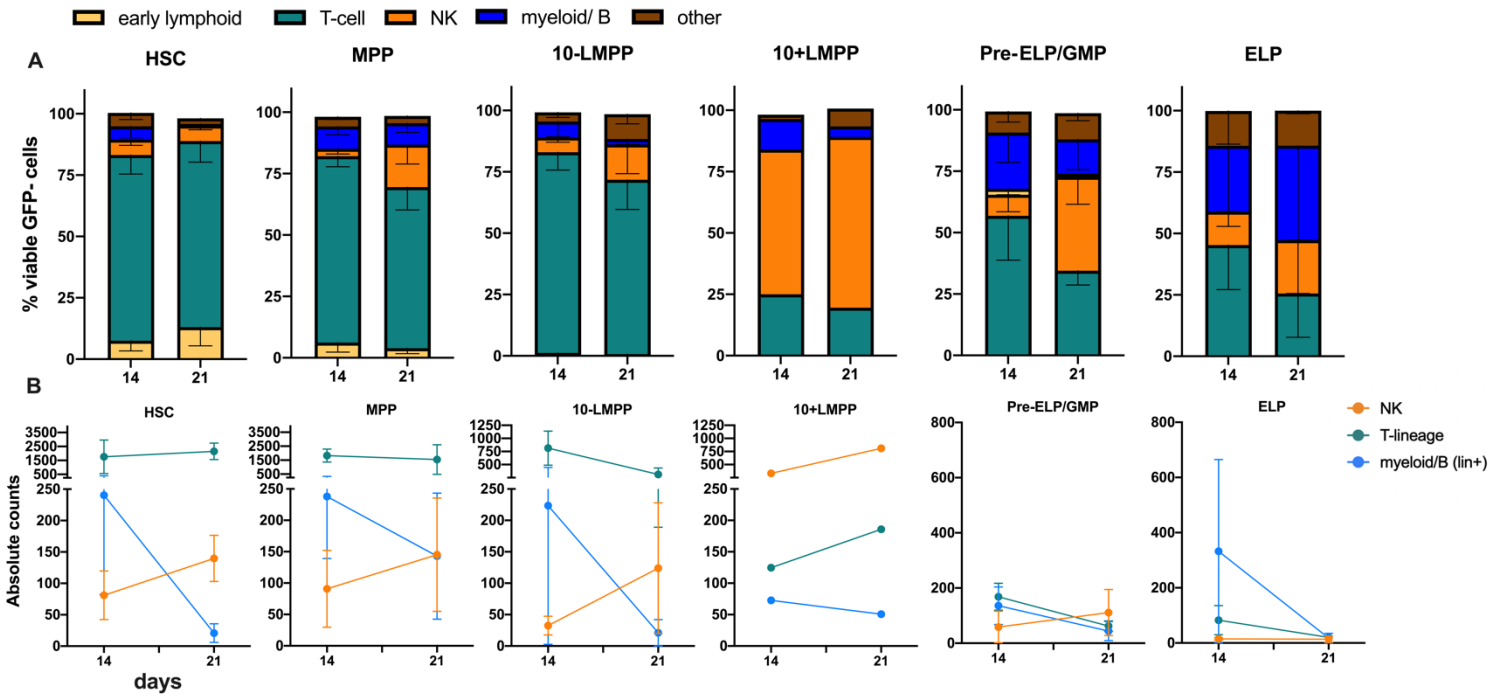


Figure 3.11 Normal FBM HSCs, MPPs and CD10-LMPPs show the greatest proportional T-cell frequencies and absolute output in OP9-DL1 differentiation assays. CD10+LMPP produce minimal T-cell output and are biased toward NK production. Within the CD10- progenitors, absolute T and NK output diminishes down the differentiation trajectory.
Differentiation assay of flow-sorted normal fetal BM HSPCs co-cultured on OP9-DL1 stromal cells with cytokines (FLT3L, SCF, IL-7). Normal FBM n= 3-5 except 10+LMPP (n=1).

A Total lineage output is shown as % viable gfp- cells across the time course.
B Absolute counts T-cell counts, calculated using Countbright beads (Thermofisher).

early lymphoid= Lin-CD4-8-CD56-CD3-CD7+.
myeloid/ B= Lineage +, Lin cocktail = CD19,14,33,235a.
other = Lin-CD4-8-56-3-2-7-.

OP9DL1 assays: established HSPCs of the FBM differentiation hierarchy

On OP9-DL1 stroma the upstream progenitors: HSCs, MPPs and CD10-LMPPs yielded the greatest T-cell output over 4 weeks, both in terms of relative frequency and absolute number (Figure 3.11 A, B), with the absolute frequency of T-cells exceeding 70% for all three populations at both day 14 and 21 (Figure 3.11 A). As expected, the maximum absolute T-cell output of the HSPC populations (Figure 3.11 B) decreased down the lineage trajectory (2150 ± 588 HSC day 21, 1829 ± 463 MPP day 14, 813 ± 325 10-LMPP day 14, Pre-ELP/GMP 168 ±49, day 14), which likely reflects the progressive decline in self-renewal and expansion capacity, although none of these decreases were statistically significant.

Briefly, ELPs showed reduced proportional and absolute T-cell output compared to all of the upstream CD10- progenitors, which may indicate that the strong B-cell priming in these progenitors limits their functional T-cell potential. By contrast, ELPs did produce the greatest proportion of Lin+ output throughout the time course, (Lin cocktail = CD14/19/33/235a). Mature cell output from ELPs was minimal by d21, whilst output from the earlier CD10- progenitors showed increased longevity in culture, supporting their place upstream in the differentiation hierarchy. PPB and PB were not analysed as our lab have previously shown these have no T cell output (O'Byrne et al, 2019).

To summarise, all of the assessed normal FBM populations assessed possess, to differing degrees, T-cell potential. The frequency and absolute output of the newly described progenitors reflects their proposed position in the established progenitor hierarchy. Unlike CD10-LMPP, the strong B-cell priming of Pre-ELP/GMPs (Figure 3.8), appears to limit their

functional T-cell potential, similarly to ELPs. Further study of CD10+LMPPs is needed to confirm their apparent NK biasing.

Single cell methylcellulose assays

In order to assess the myeloid, erythroid and megakaryocytic potential of normal FBM HSPCs, I FACS-sorted single HSPCs for clonogenic analysis. Colonies generated were analysed on day 14, in accordance with previous lab protocols for human fetal cells (Roy et al, 2012; O'Byrne et al 2019; Jardine et al, 2021). The overall percentage clonogenicity (number of colonies/ number of single cells plated) was calculated for each HSPC population across four biological replicates for CD10-LMPP and Pre-ELP/GMP and three biological replicates for CD10+LMPP.

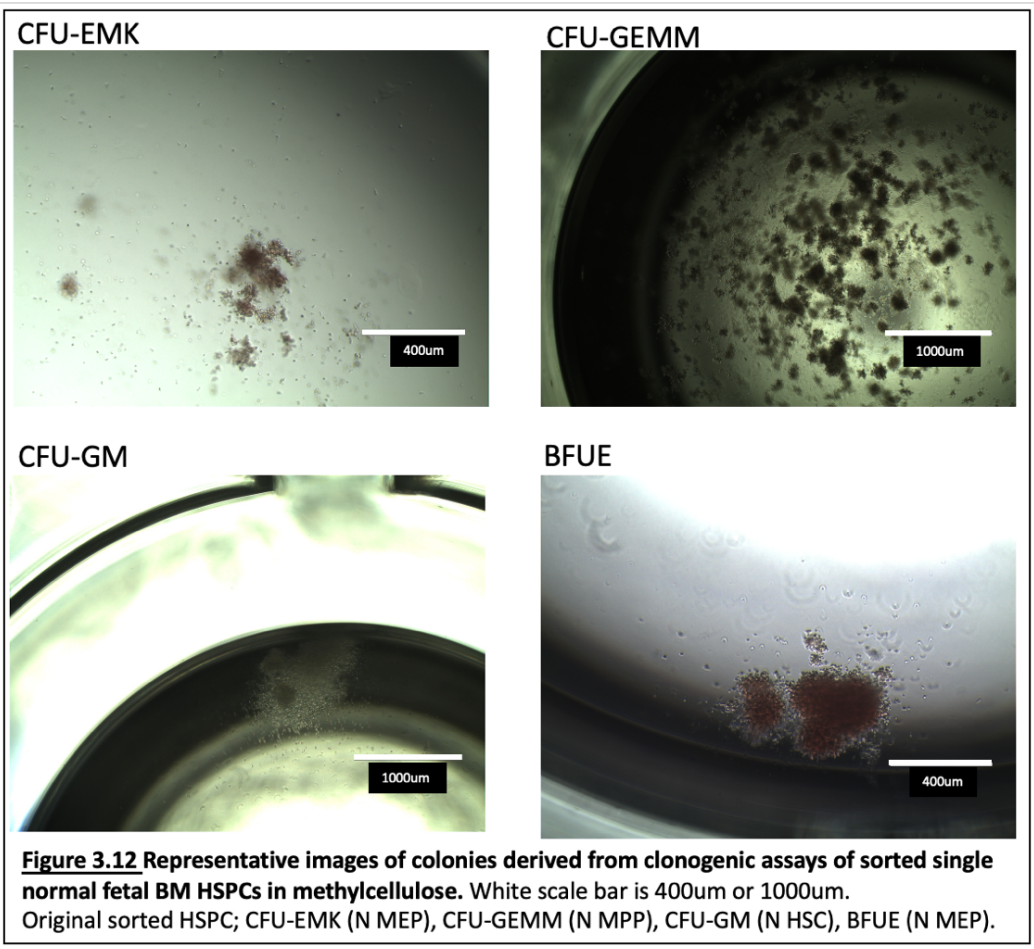


Figure 3.12 Representative images of colonies derived from clonogenic assays of sorted single normal fetal BM HSPCs in methylcellulose. White scale bar is 400um or 1000um.
Original sorted HSPC; CFU-EMK (N MEP), CFU-GEMM (N MPP), CFU-GM (N HSC), BFUE (N MEP).

Colony type was determined based on morphological classification (representative images shown in Figure 3.12) followed by confirmatory flow cytometry (gating strategy shown in Figure 3.13) and cytospin.

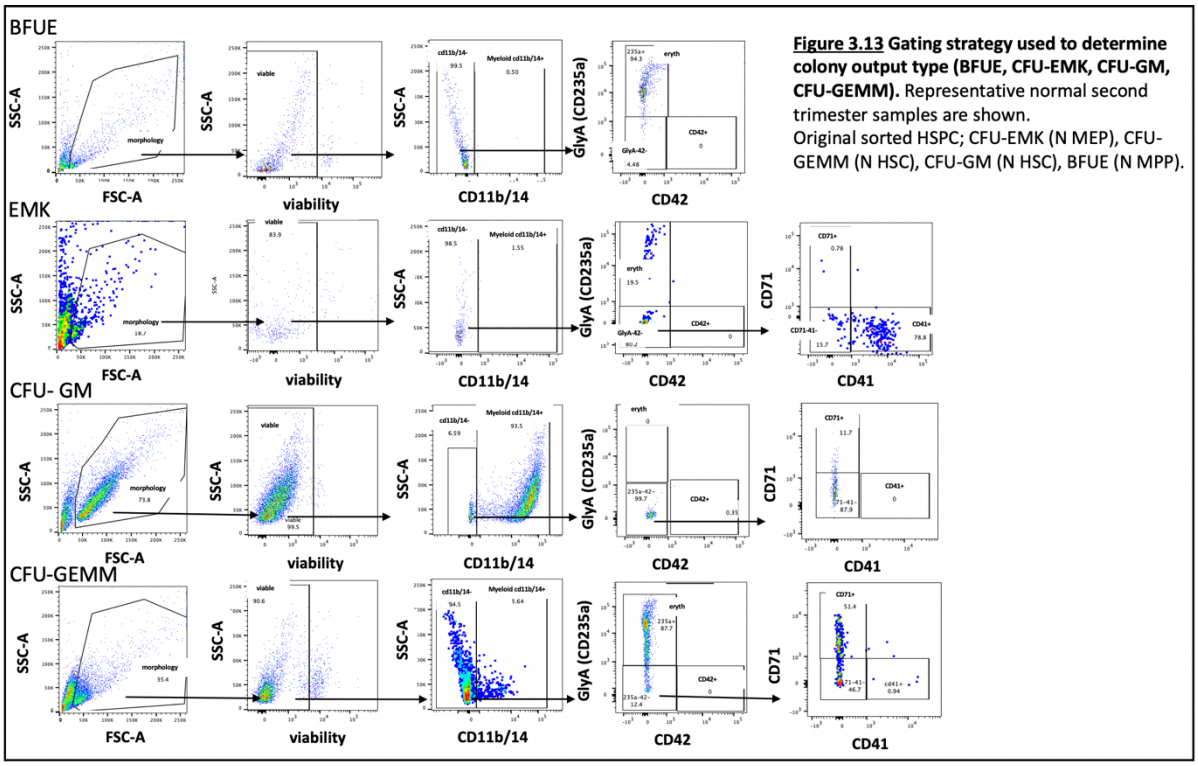


Figure 3.13 Gating strategy used to determine colony output type (BFUE, CFU-EMK, CFU-GM, CFU-GEMM). Representative normal second trimester samples are shown.
Original sorted HSPC; CFU-EMK (N MEP), CFU-GEMM (N HSC), CFU-GM (N HSC), BFUE (N MPP).

Methylcellulose assays: CD10-/+ LMPP and Pre-ELP/GMP

In concordance with the observations from MS-5 co-culture assays, both Pre-ELP/GMP and CD10-LMPP produced myeloid colonies (GM), with the clonogenicity for CD10-LMPP exceeding that of downstream Pre-ELP/GMP (15.8± 6% and 1.9± 0.9% respectively), Figure 3.14 A), though not significantly (P= 0.0757). By contrast, CD10+LMPP did not produce any colonies within this system and the clonogenicity of CD10+LMPP was significantly reduced compared to CD10-LMPP (*, P=0.0392), mirroring previous observations of their lymphoid restriction in MS-5 co-cultures compared with the CD10- progenitors (Figure 3.8 A, B).

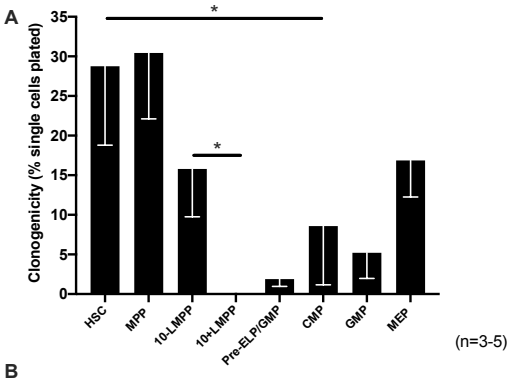


Figure 3.14 Normal FBM HSPCs generate myeloid colonies within clonogenic assays and limited erythroid output, with exception of MEP. Of the newly described progenitors, CD10-LMPP and Pre-ELP/ GMP both produce colonies, unlike CD10+LMPP.

Clonogenic assay of index flow-sorted single normal fetal BM HSPCs cultured in methocult with cytokines (IL-3, IL-6, IL-11, SCF, FLT3L, GM-CSF, TPO, EPO), to assess myeloid/ megakaryocyte/ erythroid differentiation, assessed at day 14. n=3-5 biological replicates, number of single cells plated is represented by k. Error bars show SEM and statistical analyses were performed using multiple paired t-tests where * indicates $p< 0.05$.

A Clonogenicity is shown as % single cells plated ((no. of colonies / no. of single cells plated) x 100). Early progenitors show greater clonogenicity than lineage restricted progenitors. CD10-LMPPs show increased clonogenicity compared with Pre-ELP/GMP.

B Frequency of different colony types generated from normal FBM HSPCs, determined by morphology-based scoring and confirmatory flow cytometry/ cytospin. The majority of colonies generated are GM (myeloid), with MEP showing the greatest proportional erythroid output of all HSPCs.

GM= granulocyte-monocyte. GEMM= granulocyte, erythrocyte, macrophage, megakaryocyte. EMK= erythroid, megakaryocyte. MK= megakaryocyte.

Methylcellulose assays: normal FBM HSPCs

Of the other HSPC populations assessed, HSCs and MPPs displayed the highest clonogenicity (28.7± 10% and 30.4± 8.3%, respectively), followed by MEPs (16.9± 4.6%) (Figure 3.14 A). Whilst CD10-LMPPs showed reduced clonogenicity compared with both upstream populations (Figure 3.14 A), these differences were not statistically significant (HSC vs 10-LMPP, P= 0.2553; MPP vs 10-LMPP, P= 0.1814).

Interestingly, the clonogenicity of CMPs and GMPs (8.6± 7.4% and 5.2± 3.2%, respectively), was lower than HSCs and MPPs (Figure 3.14 A), although these differences were not significant, except for between HSC and CMP (*, P= 0.0477). This may be a unique property of FBM HSPCs and may be explained by these more myeloid-primed populations exhibiting

less expansion and/or renewal potential compared to earlier progenitors which possess enhanced colony-forming capacity (Figure 3.14 A).

In terms of output type, HSCs and MPPs displayed both myeloid and erythroid potential (Figure 3.14 B), with the frequency of GEMM colonies higher in HSC and the frequency of erythroid colonies higher in MPP, though neither of these differences were significant (P= 0.0918 and P= 0.2734, respectively).

As expected, MEPs produce predominantly erythroid colonies (70± 18.4%), as well as myeloid and a minority of MK colonies (28.3± 18.5% and 2.0± 2%, respectively) (Figure 3.14 B). The proportion of erythroid colonies in MEP cultures was significantly higher than those of HSC (70± 18.4% vs 12± 7.9%, * P= 0.029), but not MPP (70± 18.4% vs 21.7 ± 6.8%, P=0.0615). CMPs produced almost exclusively myeloid colonies and a minority of erythroid, whilst GMP output was exclusively GM (Figure 3.14 B).

3.5 Summary and discussion

Within this results chapter, I have functionally characterised 3 newly described progenitors within FBM: CD10- LMPP, CD10+LMPP and Pre-ELP/GMP. Whilst CD10-/+ LMPPs have been explored previously within CB (Karamitros et al, 2018), this is the first presentation of these within fetal tissue and to my knowledge this is the first discussion of Pre-ELP/GMP in any haematopoietic site.

The discovery of new progenitors in FBM and the observation that CD10- progenitors are enriched within fetal life

Given the recent identification of fetal-specific PreProB and ELP progenitors within FBM that serve ontogeny-related functions (O'Byrne et al, 2019), I set out to further characterise the progenitor composition of FBM to identify other populations which may be important for the considerable B-lymphoid expansion that occurs in FBM before birth (O'Byrne et al, 2019). I also hoped in doing this, that I could provide reference data for subsequent comparisons with DS FBM to build on preliminary data indicating disrupted B-lymphopoiesis in DS FBM (O'Byrne ASH Abstract, 2019), as was already shown for FL (Roy et al, 2012). Specifically, I hoped that by refining models of normal FBM B-lymphopoiesis, I could identify the stage at which B-lymphopoiesis is disrupted in DS (see chapter 4).

Using an optimised and extended progenitor panel to immunophenotype second trimester normal FBM, I confirmed the presence of 3 newly described progenitors and characterised their functional output in detail: CD10-LMPP, CD10+LMPP and Pre-ELP/GMP. Immunophenotypically, Pre-ELP/GMP resemble a CD38+ more mature CD10-LMPP (Lin-

CD34+CD38+CD127-CD10-CD123-CD45RA+). Within these experiments, I observed that CD10+LMPP, whilst a distinct population, were very rare in normal FBM, with the majority of LMPPs being CD10-.

Given that post-natal B-lymphopoiesis is known to involve a CD10+ CLP (Pang et al, 2011; Saxena et al, ASH Abstract, 2016) whilst CD10- PreProB and ELP are specific to fetal life (Roy et al, 2012; O'Byrne et al, 2019), I also compared the relative frequencies of the new CD10-/+ progenitors in CB, where the frequencies of Pre-ELP/GMP and 10+LMPP were respectively significantly reduced and increased compared to FBM. Whilst CD10-LMPP did not show a significant shift in frequency, the proportion of CD10-LMPP in the total LMPP pool was much lower in CB than FBM consistent with previous characterisation of these populations in CB (Karamitros et al, 2018).

Altogether, these findings may indicate that Pre-ELP/GMP and CD10-LMPP are enriched in fetal life, and that both lymphoid and B-lymphoid progenitors in FBM seem to be predominantly more CD10- compared to tissues from later in ontogeny.

Refining the fetal B-lymphopoiesis hierarchy using functional assays

To place these new progenitors within the existing fetal B-differentiation hierarchy (O'Byrne et al, 2019) and capture their earliest differentiation transitions, I performed MS-5 co-culture assays over a short time course using the extended progenitor panel to focus on the CD34+ immature output.

These experiments revealed that CD10-LMPP can give rise to both CD10+LMPP and Pre-ELP/GMP (as well as the downstream B-progenitors and GMP), placing them upstream of both of these populations. By contrast Pre-ELP/GMP did not produce any LMPPs but did self-renew to produce further Pre-ELP/GMP, as well as ELP, PreProB and to a lesser extent,

GMP, consistent with the designation Pre-ELP/GMP based on their functional output. Given that ELPs are rare even in normal FBM, it is feasible that Pre-ELP/GMP could also give rise to CLP and PreProB directly by acquiring CD10 or CD19 respectively without passing through an CD127+ ELP intermediary. This direct transition would explain the rapid PreProB production from Pre-ELP/GMP from day 3 on MS-5 co-culture.

Along with Pre-ELP/GMP, these studies revealed that CD10-LMPP exhibit lympho-myeloid potential which mirrors previous observations in CB that CD10-LMPP^{mix} show both lymphoid and myeloid output (Karamitros et al, 2018). By contrast, CD10+LMPP showed did not produce any colonies on methylcellulose, a significant reduction when compared to their CD10- counterparts, supporting previous observations that CB LMPPs positive for CD10, LMPP^{Ly}, showed minimal myeloid potential (Karamitros et al, 2018).

CD10-LMPPs drive fetal B-cell expansion, with support from B-restricted Pre-ELP/GMP

Through comprehensive in vitro differentiation assays designed to support T- (OP9-DL1), B/NK- (MS-5) and myeloid/ erythroid/ megakaryocytic (methylcellulose) development, I found that FBM CD10-LMPPs robustly produce B-cells and also to a lesser degree, myeloid and NK cells. Pre-ELP/GMP, whilst less productive than CD10-LMPP in terms of absolute output (though not significantly), are almost entirely B-lymphoid restricted, further supporting the idea that these are a downstream, more lineage committed CD10-LMPP.

Although I was only able to study one CD10+LMPP sample for MS-5 and OP9-DL1 assays (n=3 biological replicates for methylcellulose), my data suggest that CD10+LMPP are lymphoid-restricted and show limited expansion capacity of all lineages when compared to CD10-LMPP, consistent with previous findings in CB (Karamitros et al, 2018). Altogether

these results, if validated, would suggest that CD10+LMPPs are more differentiated. Altogether, these results indicate that like CD10- ELP and PreProB, CD10-LMPP and Pre-ELP/GMP support the B-cell expansion in FBM and that disruption of these progenitors, such as in the DS context, may lead to impaired B-cell development as has been proposed for ELP and PreProB (O'Byrne DPhil thesis, 2019).

Future work

The findings from the experiments presented within this chapter have allowed me to refine the current B-lymphopoiesis pathway, described by O'Byrne et al, 2019. I present the refined model in Figure 3.15.

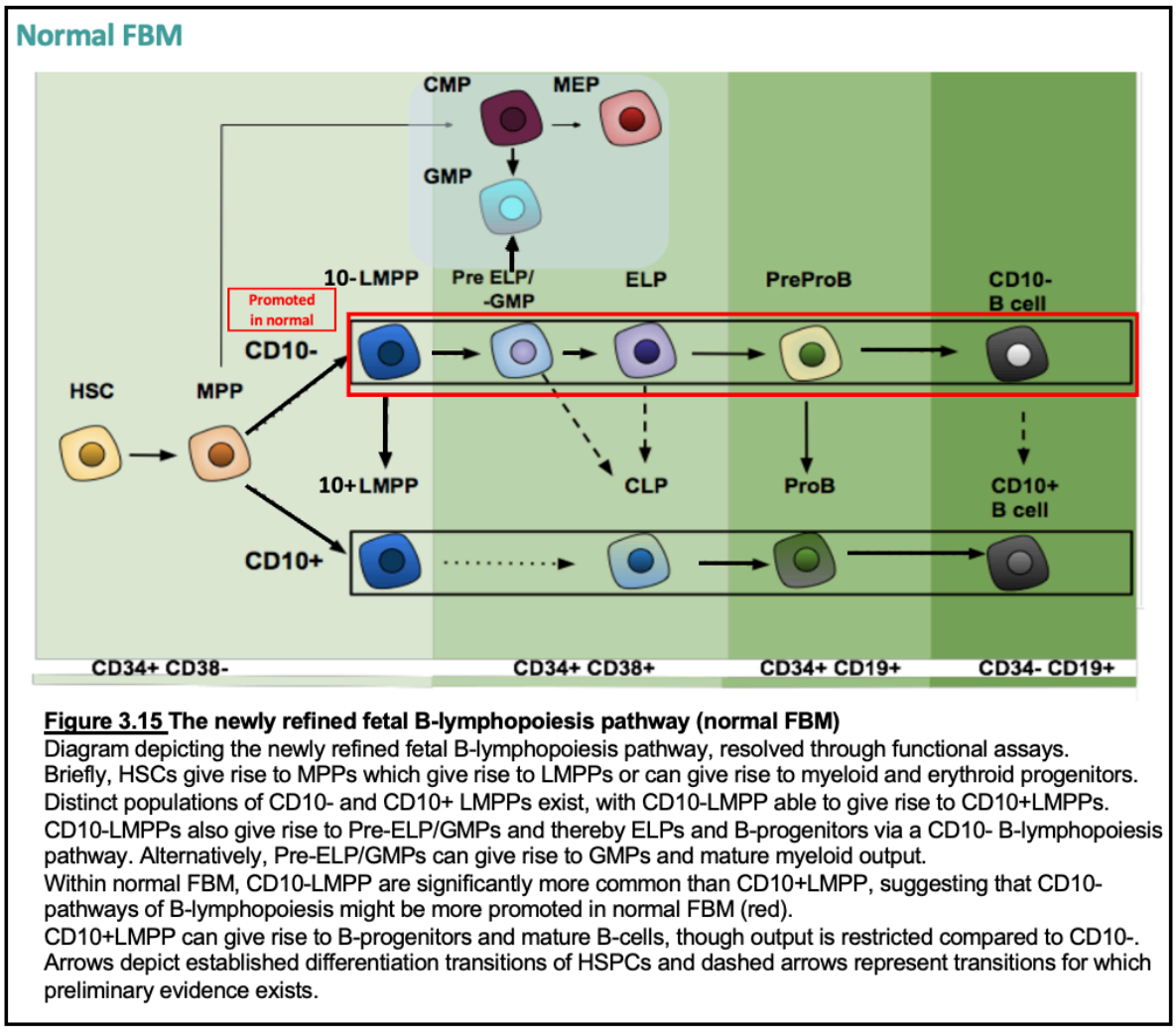


Figure 3.15 The newly refined fetal B-lymphopoiesis pathway (normal FBM)
Diagram depicting the newly refined fetal B-lymphopoiesis pathway, resolved through functional assays. Briefly, HSCs give rise to MPPs which give rise to LMPPs or can give rise to myeloid and erythroid progenitors. Distinct populations of CD10- and CD10+ LMPPs exist, with CD10-LMPP able to give rise to CD10+LMPPs. CD10-LMPPs also give rise to Pre-ELP/GMPs and thereby ELPs and B-progenitors via a CD10- B-lymphopoiesis pathway. Alternatively, Pre-ELP/GMPs can give rise to GMPs and mature myeloid output. Within normal FBM, CD10-LMPP are significantly more common than CD10+LMPP, suggesting that CD10- pathways of B-lymphopoiesis might be more promoted in normal FBM (red). CD10+LMPP can give rise to B-progenitors and mature B-cells, though output is restricted compared to CD10-. Arrows depict established differentiation transitions of HSPCs and dashed arrows represent transitions for which preliminary evidence exists.

The characterisation of the newly defined progenitors presented in this chapter is an exciting starting point for their further exploration.

Firstly, to compare the existence of these progenitors at different stages of ontogeny it would be interesting to measure their frequencies within adult bone marrow (ABM). Primary human samples are inherently variable therefore it is important that this work is performed across a suitable number of biological replicates to gain an accurate picture of these progenitor frequencies. If Pre-ELP/GMP are not present in ABM, it may indicate a unique role for them in fetal development, similar to ELP and PreProB. This work could have implications for understanding the cell of origin of infant B-ALL, for which fetal-specific CD10- ELP and PreProB have been proposed (O'Byrne et al, 2019; Jackson et al, 2021; Khabirova et al, 2022).

In addition, it would be particularly interesting to compare the lineage output and functional properties of CD10-/+LMPP and Pre-ELP/GMP from FBM, paediatric BM and ABM to gain an insight into whether there are intrinsic differences in how progenitors from developmentally distinct haematopoietic sites are programmed.

For instance, we know that a massive B-cell expansion occurs in second trimester FBM (O'Byrne et al, 2019) and that this process is probably important for neonatal immunity (Adkins et al, 2004), whilst in ABM there is a skew toward myelopoiesis (Pang et al, 2011; Mejia-Ramirez and Florian, 2020).

One of the major limitations of this work is the lack of single cell data for the MS-5 and OP9-DL1 assays in order to confirm the lineage output of these cells. Culture of single human

haematopoietic cells on MS-5s are performed in Long Term Cultures (LTCs) (Lee et al, 2015; Ranzoni et a, 2021; Anjos-Afonso et al, 2022), where analysis is performed several weeks after cells are seeded to allow sufficient cell numbers to be generated before readouts. It is unknown how the differentiation kinetics of single FBM HSPCs would differ from bulk in this system, however my observations that B-cells emerge from Pre-ELP/GMPs on day 3 and LMPPs on day 7, may mean that key differentiation transitions could be missed in LTCs of single FBM HSPCs.

Chapter 4

Immunophenotypic and functional characteristics of B-cell differentiation in DS FBM

4.1 Background and aims

Trisomy 21 (T21) is known to cause broad perturbations to haematopoiesis. Historically, the field has made the greatest progress understanding the myeloid and megakaryocytic hallmarks of T21- altered haematopoiesis (Laurent et al, 2020). This is perhaps because the step-wise aetiology of myeloid leukaemias of DS, designated ML-DS have been so effectively delineated, with clinical findings supported by research efforts to resolve the cellular and molecular changes in DS FL, where ML-DS initiates (Labuhn et al, 2019; Wagenblast et al, 2021). Work by our lab and others in DS FL has consistently shown increases in the frequency of HSCs, MEPs and mature megakaryocytes in DS FL when compared to normal counterparts, whilst in vitro B-cell output was reduced in T21 FL HSPCs (Roy et al, 2012). Lineage bias within DS FL appears to originate at the HSC level and is underpinned by a pro-erythro-megakaryocytic gene expression signature (Roy et al, 2012; Wagenblast et al, 2021). Moreover, profiling of DS neonatal peripheral blood MNCs also revealed erythroid, platelet and leukocyte abnormalities, further supporting the existing data that these alterations occur before birth (Roberts et al, 2013).

In contrast to ML-DS, DS-ALL has a relatively poor prognosis (Hunger and Mullighan, 2015). Evidence for an in-utero origin for non-DS infant and childhood ALL has been accumulating

over the last 40 years since first mooted by work in Mel Greaves' lab (Wiemels et al, 1999), though this remains to be shown for DS-ALL. Interestingly, DS-ALL is invariably B-lineage and T-ALL (which accounts for 20% of the cases in non-DS cohorts), almost never presents in DS (Buitenkamp et al, 2013), the reason for which is unknown. Aside from a significantly increased risk of ALL (Buitenkamp et al, 2013), a non-malignant haematopoietic hallmark observed throughout life in individuals with DS is functional and quantitative B- and T-lymphocyte immunodeficiencies (Kusters et al, 2009).

Despite these observations and the discrepancies between B- and T-ALL incidence in DS, work on the lymphoid defects observed in DS has been comparatively limited, especially in fetal tissue.

Our own group showed a reduction in B-progenitors and B cells in T21 FL, and that T21 FL HSCs, MPPs, LMPPs and ELPs have significantly reduced B-cell output in MS-5 co-culture assays, when compared to normal FL (Roy et al, 2012). Interestingly, in FL there were no differences in T progenitor frequency (Roy et al, 2012), which suggested that the lymphoid defects in FL may be specific to the B-lineage. Characterisation of DS FL lymphopoiesis by others revealed an in vitro NK differentiation defect (Wagenblast 2018, Abstract), which might suggest the disruption of pan-lymphoid regulatory pathways.

Since identifying the FBM as the main site of B-lineage expansion before birth (O'Byrne et al, 2019), our group found preliminary evidence of a reduction in B-progenitors and an expansion of HSC and MEP frequency in DS FBM (Roy at al, 2014 ASH abstract; O'Byrne et al, 2019 ASH abstract) similar to that observed in DS-FL (Roy at al, 2012). However, further

studies are required to identify whether the perturbations in FBM lymphopoiesis are B-lineage specific or pan-lymphoid.

Outside the FBM and FL, early work indicated a reduction in the number of B, NK and T-lymphocytes in fetal blood and the fetal thymus (Thilaganathan et al, 1993), mirroring findings from peripheral blood of children with DS (deHingh et al, 2005; Bloemers et al, 2010). Other studies of NK cells in DS have shown contradictory findings, in part due to outdated immunophenotypes used to distinguish NK and T-lymphocytes. The NK lineage is an evolutionarily older component of human immunity, onto which adaptive immune programmes (B/ T) were later layered (Sun and Lanier, 2009; Cichocki et al, 2019). The finding that B/T -lineage biased, or even restricted progenitors, show residual NK and myeloid potential has led to the hypothesis that if 'younger' B/T-cell programmes are not sufficiently activated, these retained ancestral NK/myeloid programmes may become the default (Cichocki et al, 2019).

Whilst several groups have shown reduced frequencies and absolute numbers of NK cells in fetuses and children with DS (Thilaganathan et al, 1993; deHingh et al, 2005; Bloemers et al, 2010), others have shown the converse (Cossarizza et al, 1991; Zizka et al, 2006; Cetiner et al, 2010; Schoch et al, 2017; Waugh et al, 2019; Lambert et al, 2021; Lambert et al, 2022). A recent study showed significantly increased frequencies of CD3+CD56+ NKT cells within the PMBCs of individuals with DS spanning 2-55 years of age (Lambert et al, 2021; Lambert et al, 2022), mirroring findings from a much larger recent study of adults with DS (Waugh et al, 2019). Hierarchal based clustering of DS and controls by B, NKT and T gene subsets revealed the oldest DS participants showed the greatest enrichment for NKT signatures, whilst the youngest individuals were more similar to typical controls, albeit older individuals (Lambert

et al, 2022). Whilst reports seem to be in agreement that the function of NK cells is abrogated at all stages of development (Montagna et al, 1988; Cossarizza et al, 1991), this work suggests indicates age may be a contributing factor in these immune changes. Increased levels of pro-inflammatory cytokines such as IL-6 and TNF- α, in the sera of individuals with DS and a pro-inflammatory gene expression signature (Sullivan et al, 2017; Waugh et al,2019; Lambert et al, 2022), combined with observed B/T lymphopenia and increases in NK cells in DS PMBCs has led some in the field to speculate that the DS immune system may exhibit inflammation-driven precocious ageing or 'inflammaging' (Cossarizza et al, 1991; Waugh et al,2019; Lambert et al, 2022; Waugh et al, 2022).

Altogether it is unclear whether disruptions in lymphopoiesis are observed in all lineages in DS fetal development, or whether there is specific perturbation of selected lymphoid lineages with re-direction of lymphoid potential.

Aims

1. To characterise the HSPC composition of DS FBM, including the novel intermediate progenitors for comparison with normal controls (see *Chapter 3.2*).

2. To systematically assess multiple lineage capacities of each HSPC population with a particular focus on the newly described lymphomyeloid progenitors, as I hypothesised these may act as a junction point through which lineage biases are propagated.

4.2 Immunophenotypic characterisation of DS FBM shows striking differences in HSPC frequencies, especially CD10- and CD10+ populations

To characterise the multi-lineage composition of the HSPC compartment of DS FBM, I performed flow cytometry analysis of second trimester DS FBM using the same extended progenitor flow panel used in chapter 3 which captures HSPC of the B-, myeloid and megakaryocytic-erythroid lineages. Gestation-matched DS and normal samples (Table 4.1) were compared where available, to minimise potential variability due to developmental stage.

Table 4.1 Gestational ages (GA) of samples used for N and DS FBM experiments

Normal		
Assay	GA, in post conception weeks (pcw)	Purpose
Measuring immunophenotypic progenitor frequencies by flow cytometry	17, 19, 20, 20, 14, 14, 19, 19, 17, 19, 19, 21, 17.	Assess progenitor composition of N FBM
MS5 co-culture (bulk)	17, 19, 20, 20.	Assess B/NK/myeloid output of HSPCs
Methylcellulose (single cell)	19, 21, 17, 14, 14.	Assess myeloid/megakaryocyte/ erythroid output of HSPCs
OP9-DL1 co-culture (bulk)	17, 15, 19, mixed well (17, 19, 19)	Assess T/NK output of HSPCs
DS		
Assay	GA, in post conception weeks (pcw)	Purpose
Measuring immunophenotypic progenitor frequencies by flow cytometry	17, 20, 14, 14, 19, 17, 15, 17	Assess progenitor composition of DS FBM
MS5 co-culture (bulk)	17, 20	Assess B/NK/myeloid output of HSPCs
Methylcellulose (single cell)	19, 17, 14, 14	Assess myeloid/megakaryocyte/ erythroid output of HSPCs
OP9-DL1 co-culture (bulk)	14, 15, 17	Assess T/NK output of HSPCs

Frequencies were measured over several biological replicates to minimise the size effect of sample-to-sample variation. The gating strategy used is the same as described in Ch 3 (Figure 3.1), representative data from a DS FBM sample is shown in Figure 4.1.

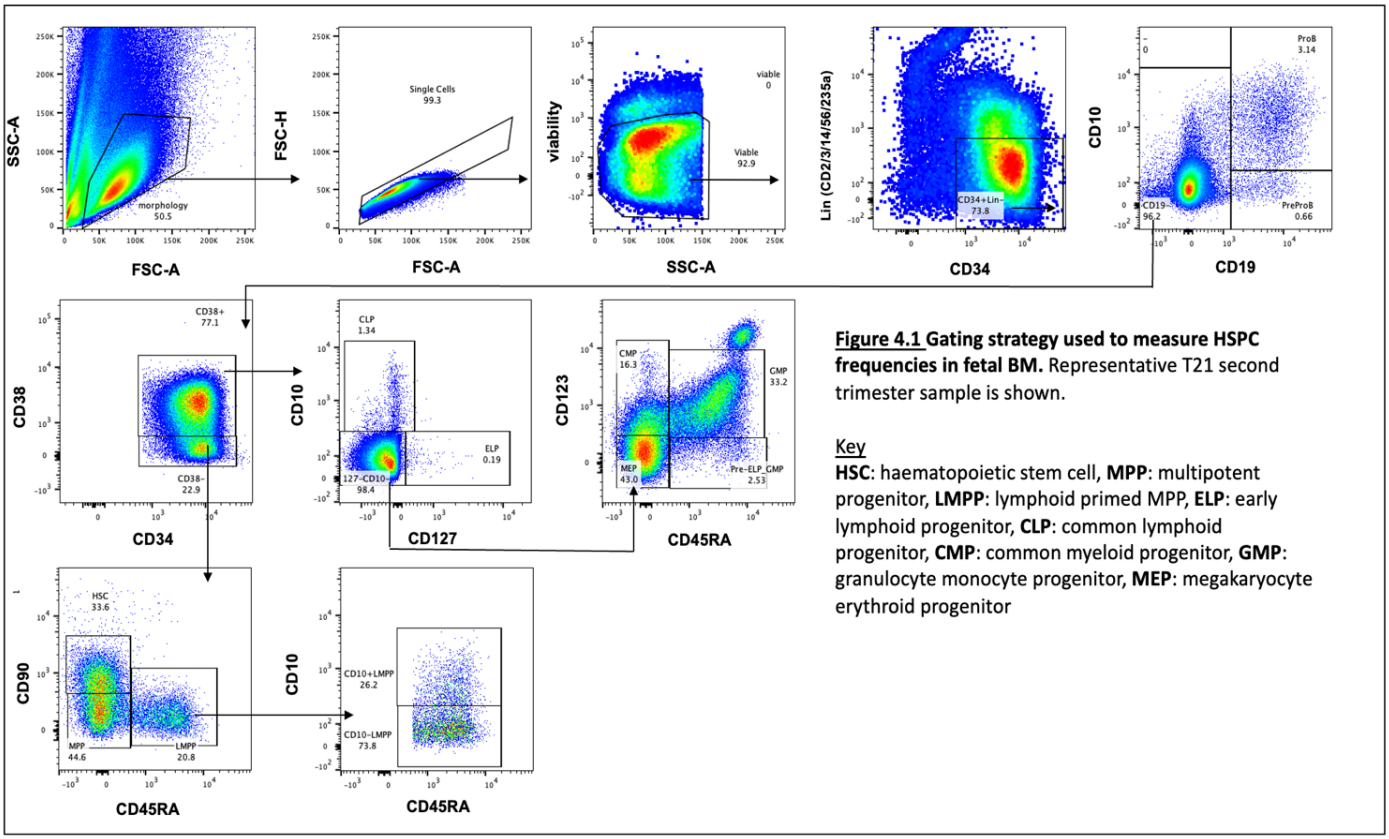


Figure 4.1 Gating strategy used to measure HSPC frequencies in fetal BM. Representative T21 second trimester sample is shown.

Key

HSC: haematopoietic stem cell, **MPP**: multipotent progenitor, **LMPP**: lymphoid primed MPP, **ELP**: early lymphoid progenitor, **CLP**: common lymphoid progenitor, **CMP**: common myeloid progenitor, **GMP**: granulocyte monocyte progenitor, **MEP**: megakaryocyte erythroid progenitor

Specifically, I hoped that measuring the frequencies of the novel lymphomyeloid progenitor Pre-ELP/GMP and poorly characterised CD10- and CD10+ LMPPs might offer clues to the stage of the B-differentiation hierarchy which was blocked in DS FBM.

In line with previous observations in FL, I observed a significant increase in the frequency of HSCs and MEPs in DS FBM (*** $p < 0.001$ and **** $p < 0.0001$ respectively), along with a significant decrease in the frequency of all of the downstream lymphoid-committed progenitors, namely ELP (*** $p < 0.001$), CLP (** $p < 0.01$), PreProB (*** $p < 0.001$) and ProB (* $p < 0.05$) (Figure 4.2)

Interestingly, however I observed the greatest reduction in the proportion of CD10- ELP and PreProB progenitors (14.3-fold and 11.5-fold reduction, respectively) in DS FBM compared to CD10+ CLP and ProB (6.2-fold and 3.94-fold reduced) (Figure 4.2).

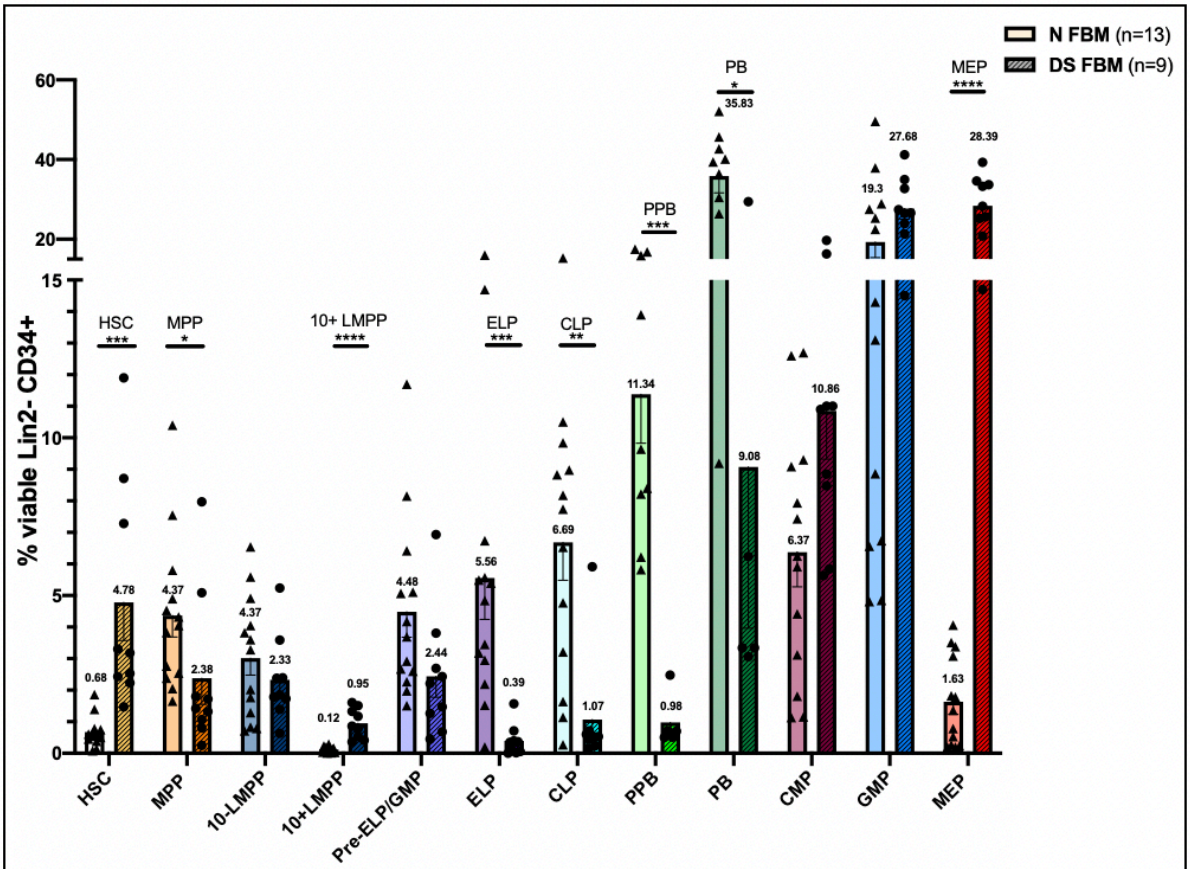
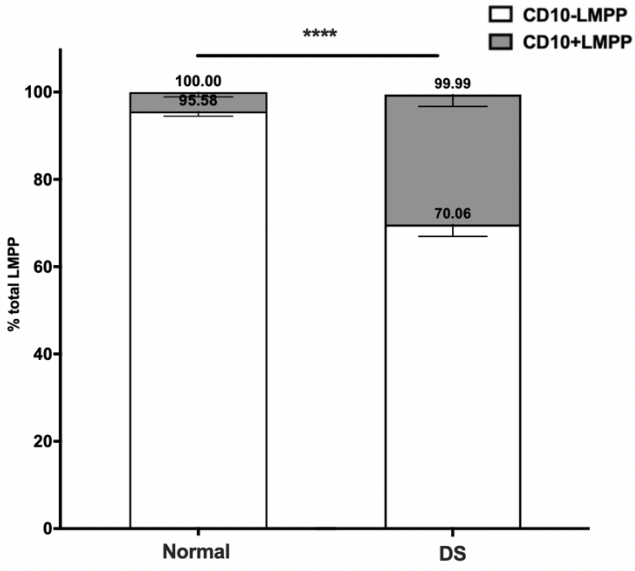


Figure 4.2 HSPC frequencies in normal and DS FBM
Analysed by flow cytometry, (n= 13 N FBM and n=9 DS FBM), shown as % viable CD34+ Lin2- cells. Lin2 cocktail: CD2/3/14/56/235+. Error bars show SEM. For statistical comparisons, multiple unpaired T-tests were performed, ns p>0.05, * p≤ 0.05; ** p ≤0.01, *** p≤ 0.001; **** p<0.0001. N FBM in plain bars (left), DS FBM in hashed bars (right).
Progenitor key
HSC: haematopoietic stem cell, **MPP**: multipotent progenitor, **LMPP**: lymphoid primed MPP, **ELP**: early lymphoid, **PPB:** preproB, **PB:** proB, **CMP**: common myeloid, **GMP**: granulocyte monocyte, **MEP**: megakaryocyte erythroid

Note: normal FBM frequency data is also featured in chapter *3.2 Immunophenotypic and functional characterisation of fetal bone marrow haematopoiesis to understand alternative pathways of human fetal B-lymphopoiesis.*

These trends might suggest that CD10- progenitors are especially impaired in DS FBM compared with CD10+ progenitors. Furthermore, the fact that PreProB showed a much more striking decrease when compared to downstream ProB could suggest that ProB progenitors may be developing through an alternative route independent of PreProB progenitors in DS FBM (Figure 4.2).

Perhaps most interesting, was the marked increase in CD10+LMPPs in DS FBM compared to normal, their frequency being approximately 8-fold higher: 0.95 vs 0.12of Lin2-CD34+ cells; **** p<0.0001 (Figure 4.2) even though the total frequency of LMPPs in normal vs DS FBM is very similar (3.14± vs 3.28± respectively). Within normal FBM, CD10+LMPPs comprise less than 5% of the total LMPP pool, whereas in DS FBM, this number rises to ~30% (Figure 4.3).



	CD10-LMPP	CD10+LMPP
Normal	95.6 ± 1.1%	4.4 ± 1.1%
DS	70.1 ± 2.8%	29.9 ± 2.8%

Figure 4.3. Relative frequency of CD10- and CD10+ LMPPs in normal and DS FBM
Analysed by flow cytometry, (n= 13 N FBM and n=9 DS FBM), shown as % total LMPP.
Composite bar graph showing mean frequency of CD10-LMPP (white) and CD10+LMPP (grey) as % total LMPP. Error bars show SEM and mean values are indicated.
For statistical comparisons, multiple unpaired T-tests were performed, ns p>0.05, * p≤ 0.05, ** p ≤0.01, *** p≤ 0.001, **** p<0.0001.

Immunophenotype
CD10-LMPP: Lin2-CD34+CD38-CD90-CD45RA+CD10-
CD10+LMPP: Lin2-CD34+CD38-CD90-CD45RA+CD10+
(Lin2 cocktail: CD2/3/14/56/235+)

Note: normal FBM frequency data is also featured in chapter *3.2*

Altogether, these findings indicate that, as in FL, T21 induces changes in the relative frequencies of progenitors in FBM. In particular, CD10- lymphoid-progenitors and B-

progenitors display the most severe reduction, whilst CD10+ HSPCs show a less severe defect, or are even significantly increased.

4.3 DS FBM HSPCs show altered lineage potential in vitro

In order to ascertain whether the alterations in HSPC frequency in DS FBM were accompanied by functional differences in lineage potential in DS FBM, HSPC populations were FACS sorted, in parallel with gestation-matched normal FBM (see chapter *3.3.*) for comparative in vitro differentiation assays. HSPCs were assessed within several culture systems conditioned to support the major lineages: B/NK (MS-5 stroma), megakaryocyte-erythroid/myeloid (methylcellulose) and T-cell output (OP9-DL1 stroma).

By systematically sorting populations at every stage of the differentiation trajectory, I hoped to identify the stage at which lineage biasing and the B-cell defect originates in DS HSPCs. I particularly focused on describing the output of the newly described CD10- / CD10+ LMPPs and Pre-ELP/GMP as I hypothesised these were an intermediate through which myeloid biasing may be propagated. I also hoped to better distinguish whether the previously described lymphoid defects were pan-lymphoid in nature or specific to the B-lineage.

4.3.1 DS FBM HSPCs show an intrinsic B-cell defect and a myeloid/ NK bias from the HSC-level

Novel intermediate lymphomyeloid progenitors are a junction point of lineage skewing in DS FBM

To first capture their CD34+ progenitor output, I co-cultured flow-sorted CD10-/+ LMPPs and Pre-ELP/GMPs on MS-5 stroma and used the extended progenitor readout panel to measure their output over a short time course. For all experiments using DS FBM novel populations, n=2-3. The gating strategy for the read outs is shown in Figure 4.4.

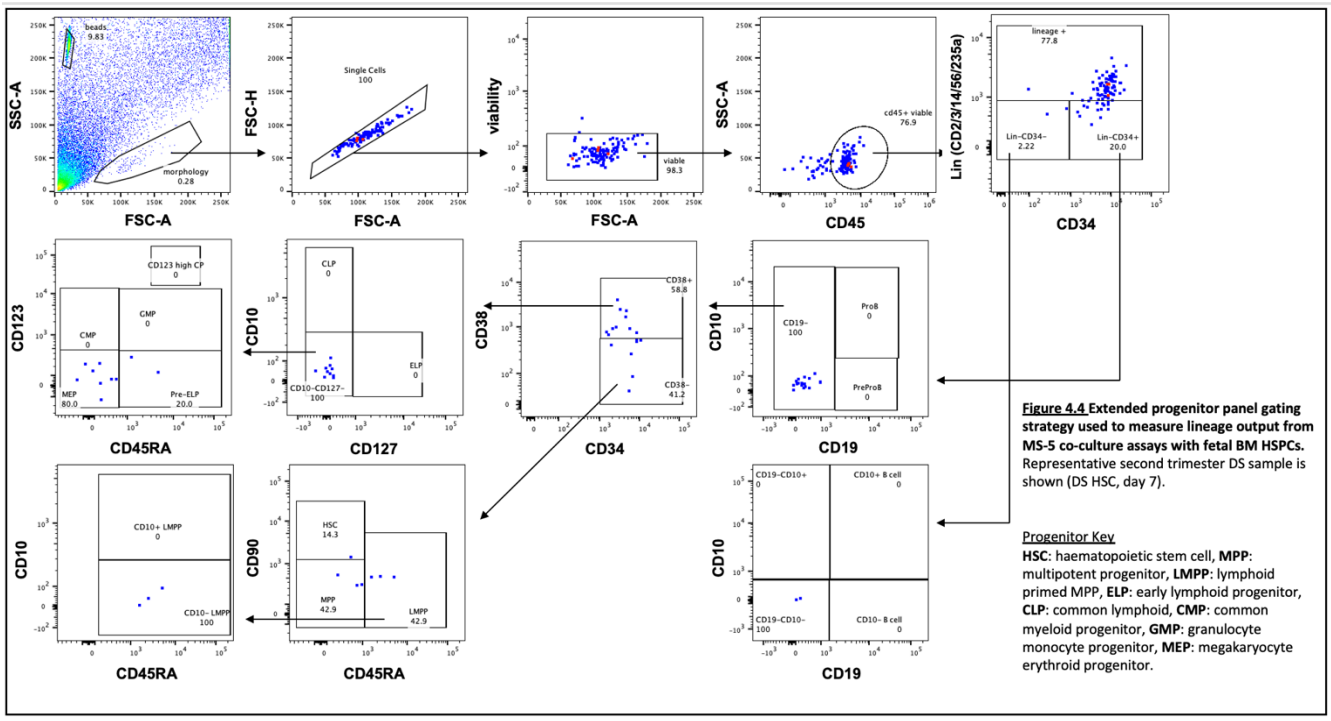


Figure 4.4 Extended progenitor panel gating strategy used to measure lineage output from MS-5 co-culture assays with fetal BM HSPCs. Representative second trimester DS sample is shown (DS HSC, day 7).

Progenitor Key
HSC: haematopoietic stem cell, **MPP**: multipotent progenitor, **LMPP**: lymphoid primed MPP, **ELP**: early lymphoid progenitor, **CLP**: common lymphoid, **CMP**: common myeloid progenitor, **GMP**: granulocyte monocyte progenitor, **MEP**: megakaryocyte erythroid progenitor.

One of the most striking observations during these cultures was that for all of the intermediate populations assessed, a far greater proportion of output in normal FBM co-cultures was CD34+ when compared with DS FBM (Figure 4.5). Almost 75% of the viable CD45+Lin2- output was still CD34+ on day 3, whilst for DS FBM this was less than 5% (Figure 4.5). Similarly, approximately 60% of the viable CD45+ output from normal Pre-ELP/GMP was Lin2-CD34+, whereas this was around 20% in DS FBM (Figure 4.5). In contrast, Lin2-

CD34+ output could not be detected for either normal or DS 10+ LMPP. The absence of Lin2-CD34+ output may reflect accelerated differentiation of HSPCs towards mature CD34- output, exclusively myeloid/NK for DS FBM, unlike in normal cultures where B-cells were detected (Figure 4.5). Alternatively, the absence of CD34+ output in DS cultures could point toward reduced survival of DS HSPC in vitro due to intrinsic abnormalities in these cells.

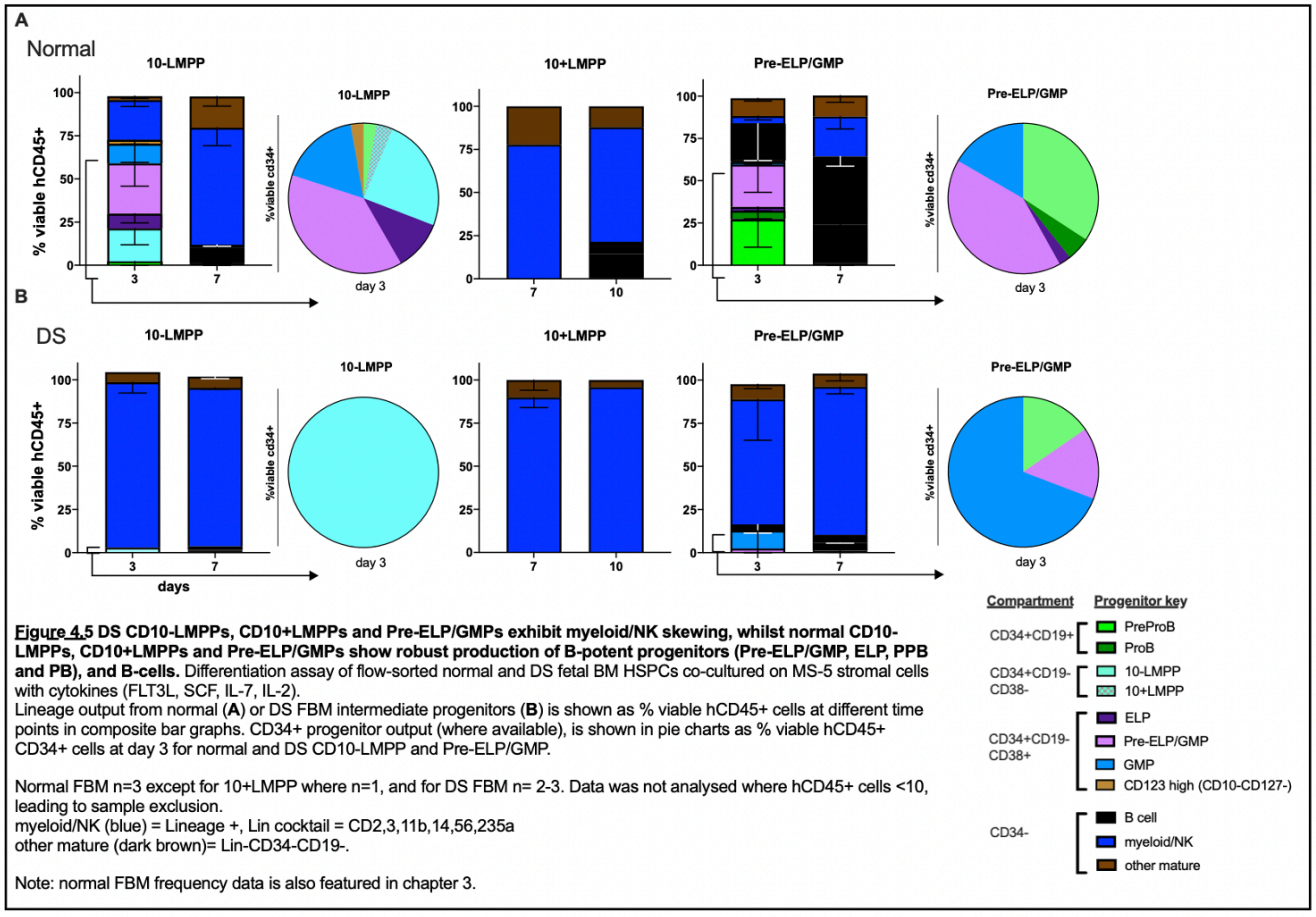


Figure 4.5 DS CD10-LMPPs, CD10+LMPPs and Pre-ELP/GMPs exhibit myeloid/NK skewing, whilst normal CD10-LMPPs, CD10+LMPPs and Pre-ELP/GMPs show robust production of B-potent progenitors (Pre-ELP/GMP, ELP, PPB and PB), and B-cells. Differentiation assay of flow-sorted normal and DS fetal BM HSPCs co-cultured on MS-5 stromal cells with cytokines (FLT3L, SCF, IL-7, IL-2).
Lineage output from normal (**A**) or DS FBM intermediate progenitors (**B**) is shown as % viable hCD45+ cells at different time points in composite bar graphs. CD34+ progenitor output (where available), is shown in pie charts as % viable hCD45+ CD34+ cells at day 3 for normal and DS CD10-LMPP and Pre-ELP/GMP.

Normal FBM n=3 except for 10+LMPP where n=1, and for DS FBM n= 2-3. Data was not analysed where hCD45+ cells <10, leading to sample exclusion.
myeloid/NK (blue) = Lineage +, Lin cocktail = CD2,3,11b,14,56,235a
other mature (dark brown)= Lin-CD34-CD19-.

Note: normal FBM frequency data is also featured in chapter 3.

The CD34+ output from DS FBM CD10-LMPP was exclusively CD10-LMPP. Despite observing exclusively myeloid/NK mature output (Figure 4.5), I did not manage to detect CD34+ GMP, which may be due to a very small proportion of Lin2-CD34+ cells remaining due either to cell death or to a rapid acceleration toward a mature myeloid cell fate. In comparison, normal CD10-LMPP give rise to CD10+LMPP, Pre-ELP/GMP, ELP and PreProB progenitors (Figure 4.5).

DS FBM Pre-ELP/GMP gave rise mainly to GMP (70%) but also to PreProB progenitors. The proportion of GMP produced by DS FBM Pre-ELP/GMP was 5-fold higher than that by normal FBM Pre-ELP/GMP cultures (16.6% vs 69.2%, Figure 4.5). DS FBM Pre-ELP/GMP failed to give rise to ELP or ProB progenitors in contrast to their normal counterparts (Figure 4.5).

In addition to the B-cell progenitors, I also observed marked reduction in the proportion of B-cells in DS FBM Pre-ELP/GMP on day 7 whilst the B-cell output from normal Pre-ELP/GMP is robust (Figure 4.5). Similarly, DS CD10-LMPPs also show reduced B-cell output in addition to an absence of B-cell progenitors and CD10+LMPPs also show reduced B-cell output. Overall, all three HSPC populations show a bias away from B-lymphopoiesis, toward myeloid/NK output and this was also seen at the progenitor level for DS FBM Pre-ELP/GMPs with an increased GMP output compared to normal.

CD34+ progenitor output from upstream DS FBM HSPCs is myeloid-biased in MS-5 assays

Since these data suggested that there was potential lineage skewing towards the myeloid lineage in CD10-LMPP and PreELP/GMP, I wanted to identify whether this bias was also seen in the upstream HSPCs, HSCs and MPPs. Output from DS FBM HSC, MPP and total LMPP co-cultured on MS-5 stroma was analysed using flow cytometry.

In contrast to normal HSC where the majority of hCD45+Lin2- cells remained CD34+ on day 3, the Lin2-CD34+ compartment in DS HSC co-cultures at day 3 was approximately half the size of normal HSCs (40% vs 75 % of viable CD45+ output, Figure 4.6). In addition, while

normal HSCs gave rise mainly to MPPs by day 3, the majority of these progenitors in DS FBM HSC cultures were GMPs, with a smaller population of CD10-LMPP and Pre-ELP/GMP (Figure 4.6).

By day 7, the proportion of MPPs produced by normal HSCs is reduced and the majority of output is Pre-ELP/GMP and CD10-LMPP, along with a minority of CMP, GMP, MEP and ELP, demonstrating that normal HSCs are able to differentiate into all of the major lineages in this culture system (Figure 4.6).

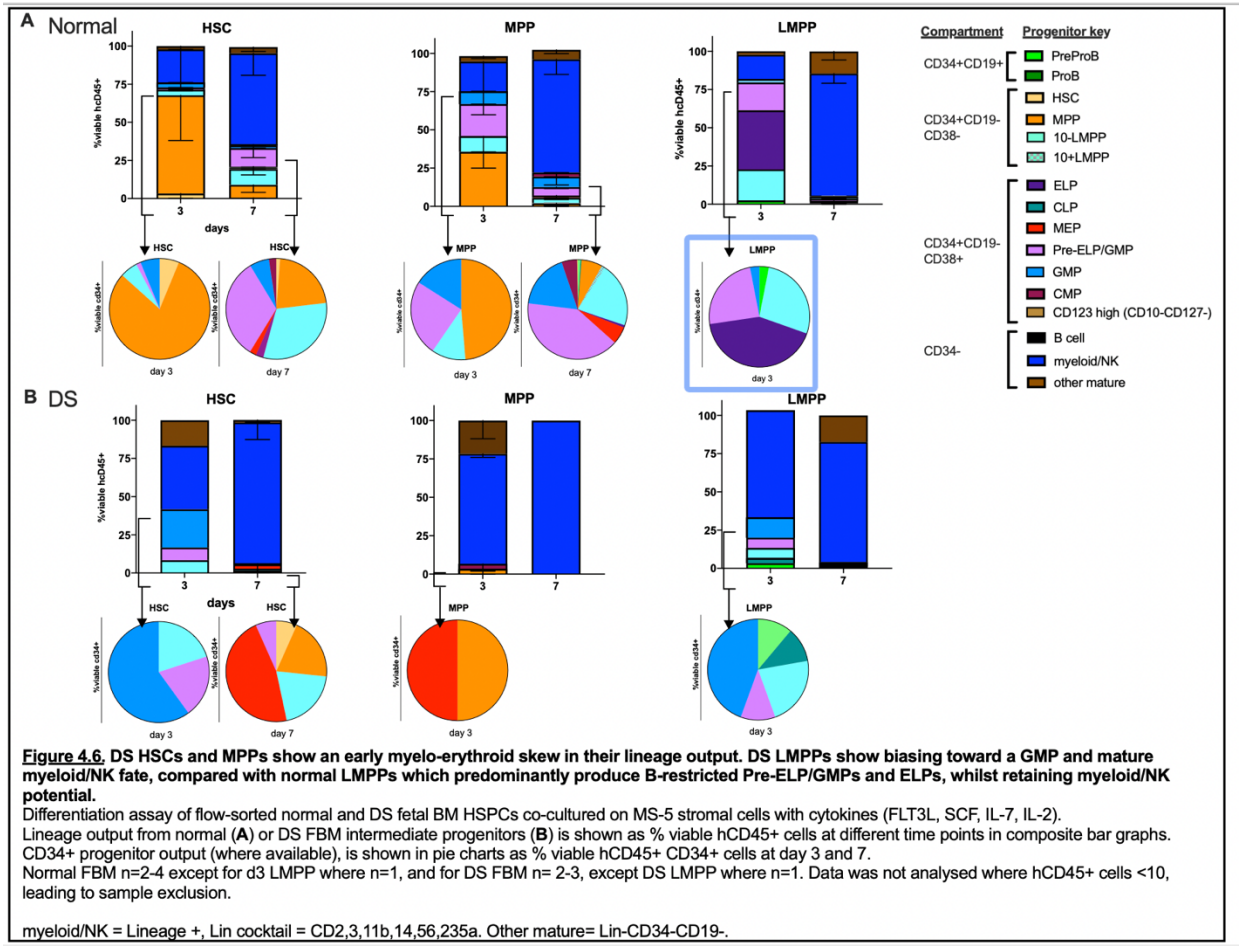


Figure 4.6. DS HSCs and MPPs show an early myelo-erythroid skew in their lineage output. DS LMPPs show biasing toward a GMP and mature myeloid/NK fate, compared with normal LMPPs which predominantly produce B-restricted Pre-ELP/GMPs and ELPs, whilst retaining myeloid/NK potential.
Differentiation assay of flow-sorted normal and DS fetal BM HSPCs co-cultured on MS-5 stromal cells with cytokines (FLT3L, SCF, IL-7, IL-2).
Lineage output from normal (**A**) or DS FBM intermediate progenitors (**B**) is shown as % viable hCD45+ cells at different time points in composite bar graphs.
CD34+ progenitor output (where available), is shown in pie charts as % viable hCD45+ CD34+ cells at day 3 and 7.
Normal FBM n=2-4 except for d3 LMPP where n=1, and for DS FBM n= 2-3, except DS LMPP where n=1. Data was not analysed where hCD45+ cells <10, leading to sample exclusion.

myeloid/NK = Lineage +, Lin cocktail = CD2,3,11b,14,56,235a. Other mature= Lin-CD34-CD19-.

In contrast, almost half of the Lin2-CD34+ output from DS HSCs at day 7 were immunophenotypic MEP (Figure 4.6), mirroring previous findings in DS FL and FBM which indicated a mega-erythroid bias (Roy at al, 2012; Jardine et al, 2021). Small populations of HSC, MPP and CD10-LMPP were detectable in DS HSC cultures on day 7 that were not

observed at day 3 which may suggest a small population of residual HSCs present at day 3 that have since differentiated (Figure 4.6).

By day 7 less than 5% of the total CD45+ output in DS HSC wells was CD34+ and the large population of GMPs observed on day 3 replaced by mature myeloid output (Figure 4.6).

DS MPPs show a striking MEP bias compared with normal MPP, the latter of which produced progenitors of multiple lineages, including a large population of Pre-ELP-GMPs and LMPPs (majority CD10-) (Figure 4.6), whilst CD34+ output in DS MPPs was transient and entirely MEP (Figure 4.6) within these assays. Like DS HSCs, DS MPP show a proportionately expanded mature myeloid/NK output at both time points (Figure 4.6).

Like both CD10-/+ LMPP, DS total LMPP showed an early myeloid bias, with almost half of their CD34+ output being GMP and the majority of total output being mature myeloid (Figure 4.6). Compared to normal LMPP, which produced mainly Pre-ELP/GMPs and ELPs, DS LMPP failed to produce ELP and the proportion of Pre-ELP/GMP was greatly reduced (18.2% vs 6.67 % viable hCD45+, day 3). However, DS LMPP did produce both PreProB progenitors and CLP which demonstrates lymphoid output is not completely abrogated (Figure 4.6).

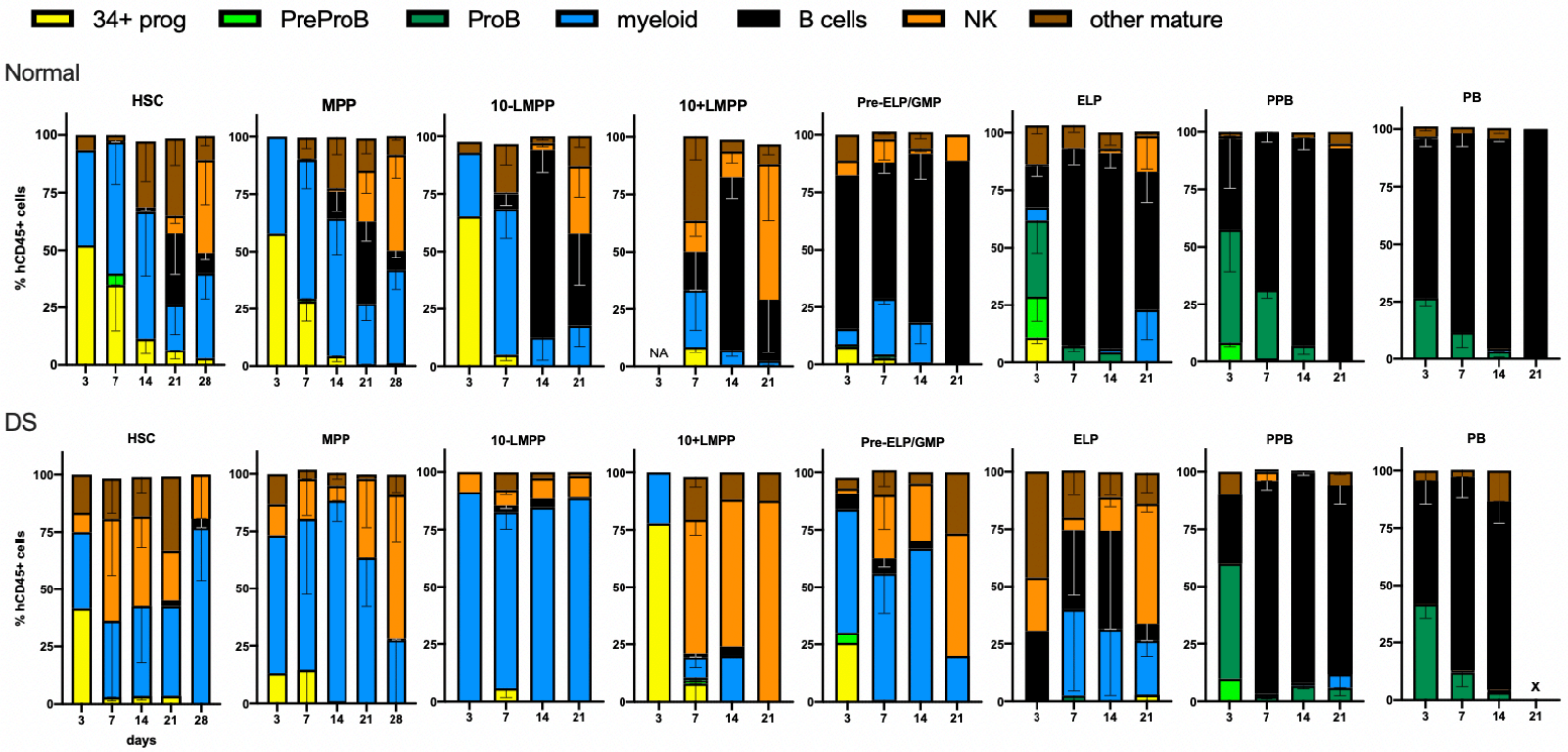
Overall, these results suggest that the myeloid skewing observed in DS FBM lympho-myeloid CD10-/+ LMPP and Pre-ELP-GMP populations is also present at the HSC and MPP level (Figure 4.6), which in addition, also present a mega-erythroid bias.

Impaired B-lymphopoiesis and lineage skewing is most severe in the earliest DS FBM HSPCs and becomes less marked in progressively B-restricted progenitors

Having observed a skewed lineage output over a shorter time course designed to assess the CD34+ progenitor output, I conducted time course experiments across 3-4 weeks, using the mature output panel to determine whether B-cell and NK cell differentiation was impaired or delayed in DS FBM HSPC, when compared to normal FBM (described in chapter 3).

These experiments revealed that early and intermediate DS FBM HSPCs display a striking B-cell defect which is most severe in the earliest stages of the differentiation hierarchy, in HSCs, MPPs and LMPPs; whereas B-lymphopoiesis appears to be relatively preserved in downstream B-cell committed PreProB and ProB progenitors.

During these experiments I observed two distinct trends. The first trend pertains to lineage biasing in CD10- vs CD10+ HSPCs in DS FBM. Compared to normal, CD10- HSPCs in DS FBM (HSCs, MPPs, CD10-LMPPs and Pre-ELP/GMPs) show a myeloid lineage bias, whereas DS CD10+LMPP show lymphoid restriction, like in normal FBM (*see chapter 3.3*), however this is almost exclusively NK cell output, rather than B and NK output. During later time points, DS CD10-HSPCs also show expanded NK potential compared with normal counterparts (where NK cells comprise a minority of the output).



<u>Figure 4.7.</u> In vitro differentiation assays of early and intermediate DS FBM HSPCs reveal a pronounced B-cell defect, with marked myeloid and NK lineage biasing, compared with normal counterparts. Downstream B-restricted progenitors show no defect in proportional B-cell output, suggesting the defect lies upstream in the differentiation hierarchy.

Differentiation assay of flow-sorted normal and DS fetal BM HSPCs co-cultured on MS-5 stromal cells with cytokines (FLT3L, SCF, IL-7, IL-2).
Total lineage output is shown as % viable hCD45+ cells across the time course. Normal FBM n= 3-5, DS FBM n= 3-4, except ELP, PPB, PB where n=2. Data was not analysed where hCD45+ events <10, leading to sample exclusion. 'NA" indicates time point which was not assessed for that HSPC population.

Note: normal FBM frequency data is also featured in chapter 3.4.
myeloid= Lineage +, Lin cocktail = CD2,3,11b,14,235a
other mature= Lin-CD34-CD56-CD19-.

The second observed trend was that the severity of the B-cell defect depends on the differentiation stage of the relevant HSPC population. Whilst DS ELP showed reduced B-cell output (though less drastic than that of upstream progenitors), downstream DS PPB and PB presented normal B-cell output. This suggests that the block in B-cell differentiation represents a failure of upstream HSPC to commit to B-cell progenitors, rather than an already B-lineage committed progenitor being unable to yield mature B-cells.

Early and intermediate DS FBM HSPCs show impaired expansion capacity in vitro

Several early and intermediate DS FBM HSPCs show lower absolute counts of B-, myeloid- and NK-cells generated in vitro (Figure 4.9). Given that the conditions of the co-culture system were kept identical in normal vs DS and experiments were conducted in parallel with, for the most part, gestation-matched controls (Table 4.1), these data indicate that intrinsic abnormalities exist within DS FBM HSPCs.

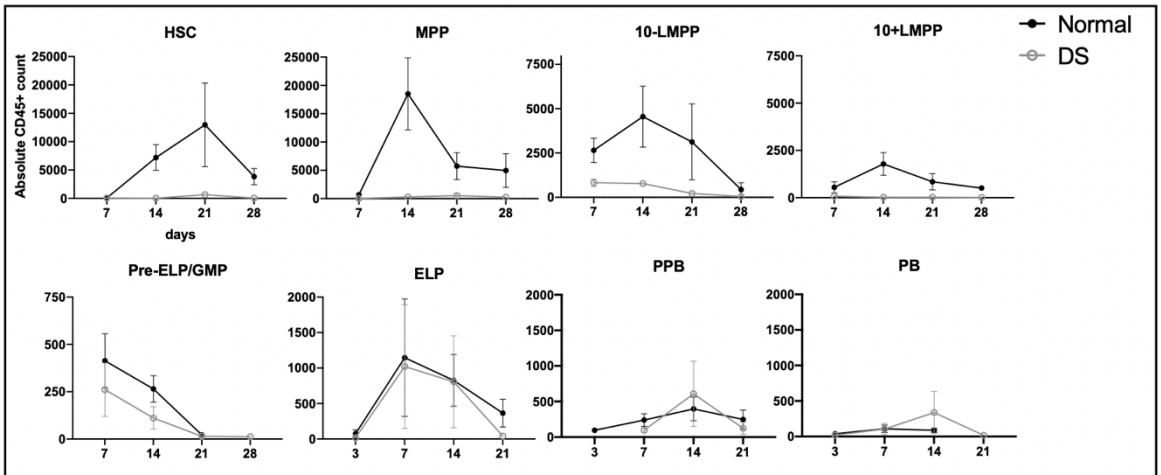


Figure 4.8 Absolute hCD45+ cell counts derived from DS FBM HSCs, MPPs, LMPPs and Pre-ELP/GMPs grown on MS-5 stroma are markedly lower when compared to normal FBM. Absolute counts of ELP co-cultures were comparable between normal and DS, while cd45+ counts of DS PPB and PB progenitors exceeded normal at day 14 and 21.

Differentiation assay of flow-sorted normal and DS fetal BM HSPCs co-cultured on MS-5 stromal cells with cytokines (FLT3L, SCF, IL-7, IL-2). Absolute CD45+ counts are shown, error bars =SEM. Normal FBM n= 4-6, DS FBM n= 2-5. Data was not analysed where CD45+ events <10, leading to sample exclusion. Absolute counts were calculated using CountBright beads (Thermofisher).

Potentially, intrinsic abnormalities in DS HSPCs could impact their expansion capacity compared with normal HSPCs of the same immunophenotype. This is supported by the absolute hCD45+ counts derived from upstream and intermediate DS HSPCs grown in these co-cultures, which are strikingly lower than normal (Figure 4.8), suggesting an intrinsic growth defect irrespective of the lineage output type. Although none of the reduced DS CD45+ counts were statistically significant, likely due to the high variability in primary human fetal samples combined with limited biological replicates for DS FBM, the most striking differences between normal and DS were observed in upstream HSPCs (N vs DS HSC day 14, 7206± 2268 vs 37± 17 P= 0.05, N vs DS MPP day 14, 18505± 6367 vs 308± 29 P= 0.06, N vs DS CD10-LMPP day 7, 2647±685 vs 821± 218 P= 0.05).

Downstream DS progenitors show comparable or even increased absolute hCD45+ counts (N vs DS ELP day 14, 826± 365 vs 805± 648 P= 0.98, N vs DS PPB day 14, 396± 164 vs 607± 458 P = 0.72, N vs DS PB day 14, 87± 28 vs 338± 297 P= 0.55), which might indicate a proliferative drive to compensate for reduced expansion capacity in upstream progenitors (Figure 4.8).

The upstream B-cell defect observed in DS FBM HSPCs is both a qualitative and quantitative one, however B-progenitors are as, or even more proliferative in DS

When comparing the reduced output of the of B-, myeloid- and NK-lineages, B-cell production is the most markedly reduced when compared to normal counterparts (Figure 4.9). These absolute counts data reveal that, as was the case for the frequency output, (Figure 4.7), the B-cell defect is most severe in the upstream and intermediate populations. DS HSCs, MPPs, CD10-LMPPs and CD10+LMPPs gave rise to very few or no B-cells (Figure 4.9). Comparing N vs DS HSC at day 14, DS HSC produce no B-cells across 3 biological replicates whilst normal HSC produce 61 ±22, however this difference was not statistically significant (P= 0.07), nor were any of the

differences between N and DS HSC, likely due to high variability across a small sample dataset. B-cell output is only detectable in DS HSC cultures from day 21- 28, when output is negligible. At day 21, DS HSCs produce almost 100-fold fewer B-cells than normal (N HSC vs DS HSC = 1543± 504 vs 16 respectively).

Overall DS MPPs, LMPPs and Pre-ELP/GMPs fail to produce substantial B-cell output at any time point (Figure 4.9). Despite the striking trends observed, these differences were not statistically significant when compared to normal FBM counterparts (N vs DS MPP day 14= 789± 410 vs 0± 0 P= 0.13, N vs DS 10-LMPP day 7 = 495± 131 and 20± 6 P= 0.068, N vs DS Pre-ELP/GMP day 7= 207± 126 and 10± 4 P= 0.19).

Whilst absolute numbers of cells of all lineages (Figure 4.9) and total hCD45+ counts (Figure 4.8) generated are severely reduced in upstream and intermediate DS HSPCs compared with normal, detectable myeloid and NK output reinforces that the B-cell impairment is especially severe.

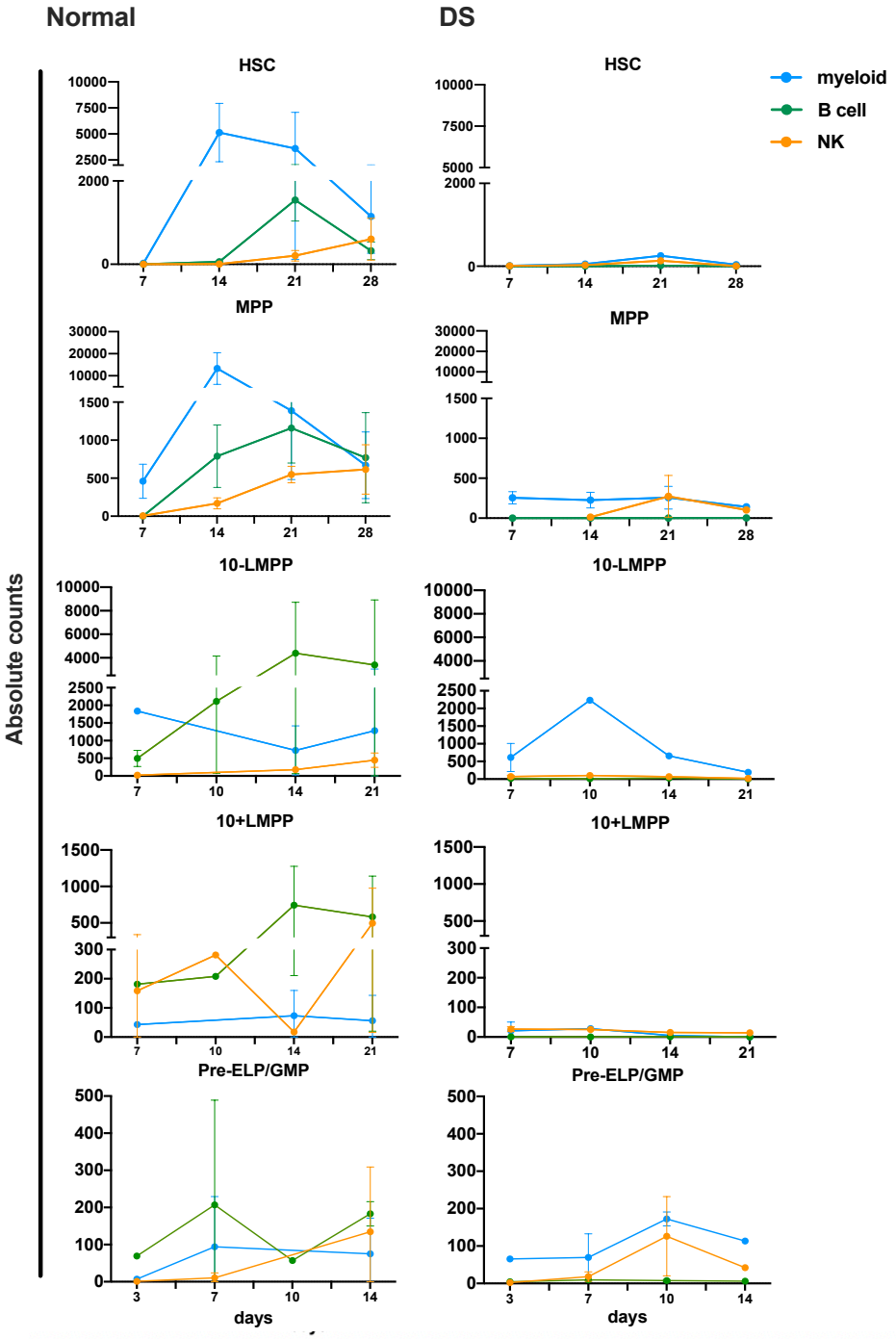


Figure 4.9 Upstream and intermediate DS FBM HSC, MPPs and LMPPs show severely reduced absolute counts of myeloid, NK and B-cells in MS-5 co-culture assays, suggesting intrinsic quantitative deficiences.

Differentiation assay of flow-sorted fetal BM HSPCs co-cultured on MS-5 stromal cells with cytokines (FLT3L, SCF, IL-7, IL-2). Absolute mean counts are shown for myeloid, B- and NK- lineages, with error bars showing +/- SEM for each time point. Normal FBM n= 4-6, DS FBM n= 3-5. Data was not analysed where hCD45+ events <10, leading to sample exclusion.
Note: normal FBM absolute counts data also features in *chapters 3.3-3.4*
myeloid= Lineage +, Lin cocktail = CD2,3,11b,14,235a
B-cell= Lin-CD34-CD19+
NK-cell=Lin-CD34-CD19-CD56+/CD16+

Like the trend observed in the frequency data (Figure 4.7), the absolute B-cell counts for the downstream progenitors are less severely impacted if at all (Figure 4.10).

Although the maximum absolute B-cell output for normal ELP exceeds that of DS ELP (1816 day 10 vs 623± 623 day 14, respectively), by day 14, the B-cell output for normal and DS ELP is comparable (713± 351 and 623 ± 623, respectively, Figure 4.10), directly mirroring the frequency data, though the DS ELP data shows high variability, exacerbated by there being n=2 for DS FBM. For DS PreProB and ProB progenitors the absolute B-cell output is generally comparable (Figure 4.10). Interestingly, however, B-cell output from DS B-progenitors exceeded that of normal at day 14 (78±27 vs 304 ±275, Figure 4.10). This may suggest a proliferative drive to compensate for the B-cell impairment in earlier precursors, however this finding was not statistically significant because of the relatively small numbers of samples (n=2) and their heterogeneity. In support of this finding, our lab has previously found higher B-cell counts derived from DS FBM ProB progenitors on MS-5 stroma (Sorcha O'Byrne DPhil thesis, 2019).

Overall, these data indicate that in DS FBM, myeloid-potent CD10- progenitors lean toward myeloid fates, whilst CD10+ LMPP retain lymphoid restriction, which appears to favour an NK fate in DS FBM. Despite clear biases in lineage fate, early and intermediate progenitors show quantitative defects across all lineages (B, mye and NK), which imply intrinsic abnormalities in the self-renewal and proliferative capacities of DS HSPCs. Interestingly, however, the absolute myeloid output of DS CD10-LMPP and Pre-ELP/GMP and NK output of Pre-ELP/GMP is preserved. This might suggest that due to sufficient myeloid/NK priming, all of the reduced self-renewal capacity of these progenitors in DS is being entirely directed towards these lineages to produce comparable output but at the complete expense of B-cell production.

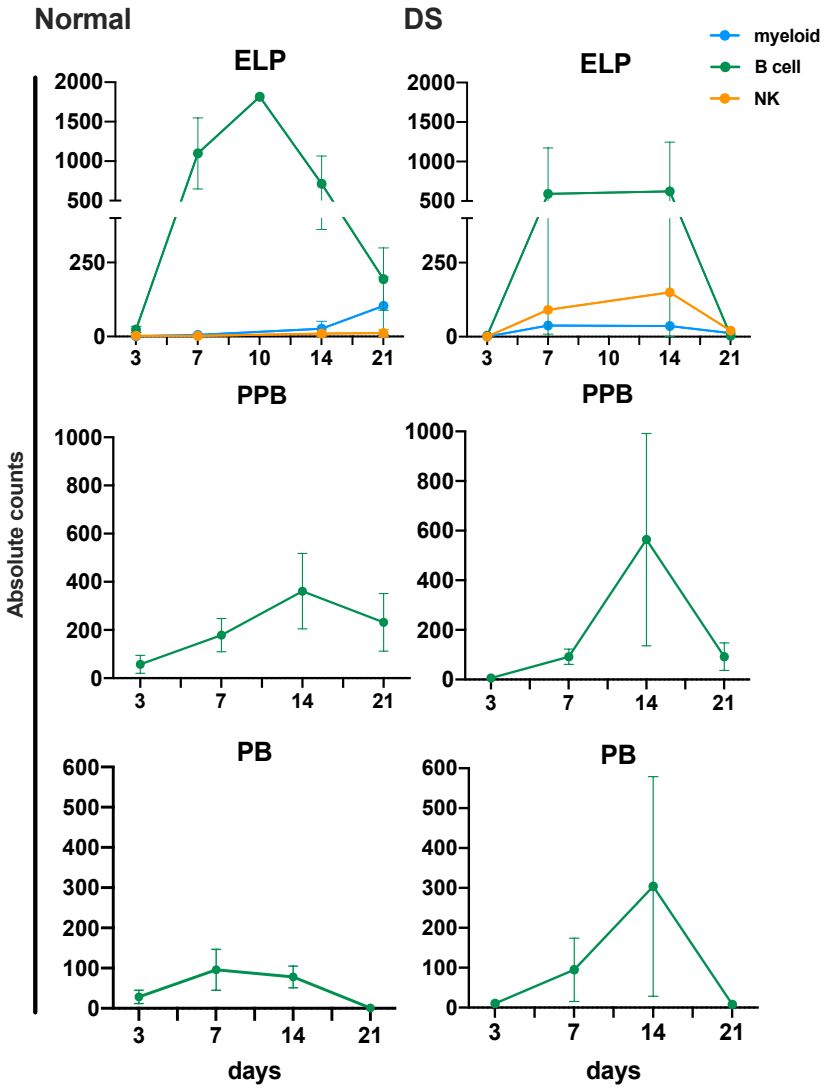


Figure 4.10 DS FBM B-progenitors do not show the same striking quantitative defect as upstream populations. DS ELPs show reduced B-cell and increased NK and myeloid absolute counts whilst DS PPB and PB show comparable or increased B-cell output relative to normal.

Differentiation assay of flow-sorted N/ DS fetal BM HSPCs co-cultured on MS-5 stromal cells with cytokines (FLT3L, SCF, IL-7, IL-2). Absolute mean counts are shown for myeloid, B- and NK- lineages, with error bars showing +/- SEM for each time point. Normal FBM n= 4-5, DS FBM n= 2. Data was not analysed where hCD45+ events <10, leading to sample exclusion.
Note: normal FBM absolute counts data also features in chapter 3.

myeloid= Lineage +, Lin cocktail = CD2,3,11b,14,235a
B-cell= Lin-CD34-CD19+
NK-cell=Lin-CD34-CD19-CD56+/CD16+

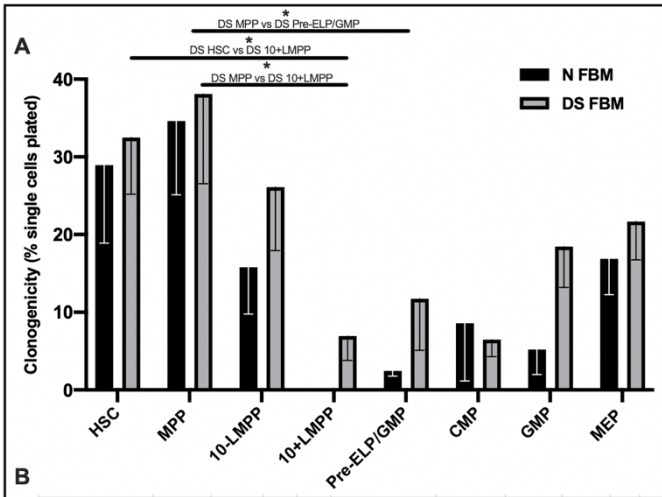
4.3.2 DS FBM HSPCs show increased clonogenicity in methylcellulose, with HSCs and MPPs showing megakaryocyte-erythroid bias.

Having observed an increased frequency of MEPs in DS FBM HSC and MPP MS-5 co-cultures (Figure 4.6), a system designed to support B, NK and myeloid cell differentiation, I wanted to see if a mega-erythroid skew was observable in methylcellulose assays. Populations were single-cell sorted in parallel with gestation-matched normal FBM across several biological replicates, in order to best capture the heterogeneity within immunophenotypically defined HSPC populations.

Methocult assays revealed the increased clonogenicity of all DS FBM early and intermediate, progenitors with myeloid potential compared with normal, with the exception of CMPs (Figure 4.11), however none of these increases were statistically significant. As was the case for normal FBM (Figure 4.11), DS FBM HSCs and MPPs displayed the highest clonogenicity of all assessed progenitors (32.5 ± 7.3% and 38.1 ±11.5%, respectively). Comparing first within the DS FBM HSPCs, both DS HSC and MPP showed significantly higher clonogenicity than CD10+LMPP (32.5 ±7.3% vs 26.1± 8.2% P= 0.035 and 38.1 ±11.5% vs 26.1± 8.2% P= 0.037, respectively), but not CD10-LMPP. DS MPPs, but not DS HSCs, showed significantly higher clonogenicity than Pre-ELP/GMP (38.1 ±11.5% vs 11.7 ±6.6%, P= 0.034). Therefore, whilst the clonogenicity of all of the HSPCs are higher in DS FBM, both DS Pre-ELP/GMP and CD10+LMPP show less myeloid potential compared with the earlier DS progenitors, as was the case in normal FBM.

The higher clonogenicity in DS FBM HSPC compared to normal FBM HSPCs was greatest for CD10-LMPP, CD10+LMPP, Pre-ELP/GMP and GMP (Figure 4.11), though none of these were statistically significant (P = 0.35, 0.11, 0.25 and 0.09, respectively). Notably, normal CD10+LMPP did not produce any colonies across 4 normal FBM biological samples, in line with the observations from MS-5 B-differentiation assays that this population are lymphoid restricted in normal FBM (see chapter 3), whereas in DS FBM, almost 7% of CD10+LMPP plated generated colonies (Figure 4.11). Whilst analysis of the clonogenicity of individual HSPC pairs (e.g. N HSC vs DS HSC) did not detect statistical significance, an overall paired t-test comparing the mean clonogenicity across all normal vs DS all HSPCs detected significance between the conditions (** $p \leq 0.01$).

A



B

HSPC population	N FBM				change in clonogenicity (in DS FBM)	Difference (%)	DS FBM			
	Mean	SEM	n	k			Mean	SEM	n	k
HSC	28.92	10.02	5	262	increased	3.56	32.48	7.28	4	326
MPP	34.61	9.49	5	322	increased	3.48	38.09	11.53	4	189
10-LMPP	15.78	6.02	4	212	increased	10.32	26.10	8.16	4	238
10+LMPP	0.00	0.00	3	104	increased	6.937	6.94	3.14	4	123
Pre-ELP/GMP	2.45	0.66	4	197	increased	9.285	11.74	6.64	4	127
CMP	8.57	7.41	3	147	decreased	-2.095	6.48	2.19	4	139
GMP	5.21	3.24	3	160	increased	13.24	18.46	5.25	4	137
MEP	16.87	4.61	5	197	increased	4.817	21.68	4.95	4	272

Figure 4.11 Clonogenic assay of single normal and DS fetal BM HSPCs reveals increased clonogenicity of all primitive and intermediate DS FBM HSPCs, (except for common myeloid progenitors, CMP), including CD10+LMPPs, which did not produce colonies when derived from normal FBM.

Clonogenic assay of index flow-sorted single normal and DS fetal BM HSPCs cultured in methocult with cytokines (IL-3, IL-6, IL-11, SCF, FLT3L, GM-CSF, TPO, EPO), to assess myeloid/ megakaryocyte/ erythroid differentiation, assessed at day 14. Normal FBM, n=3-5 biological replicates, and DS FBM n=4. Number of single cells plated is represented by k. Error bars show SEM and statistical analyses were performed using multiple t-tests, where * indicates $p < 0.05$.

A Clonogenicity is shown as % single cells plated, calculated by: (number of colonies / number of single cells plated) x 100.

B Table showing mean clonogenicity for each normal/ DS FBM HSPC cell type, the percentage difference between each condition, the SEM for each population and total single cells plated (k).

Note, normal FBM clonogenicity data was also featured in chapter 3.

Next, I wanted to characterise the output of DS FBM HSPCs by colony type. Colonies were scored using a combination of colony morphology (Figure 4.12) with representative flow cytometry (Figure 4.13) and cytospin.

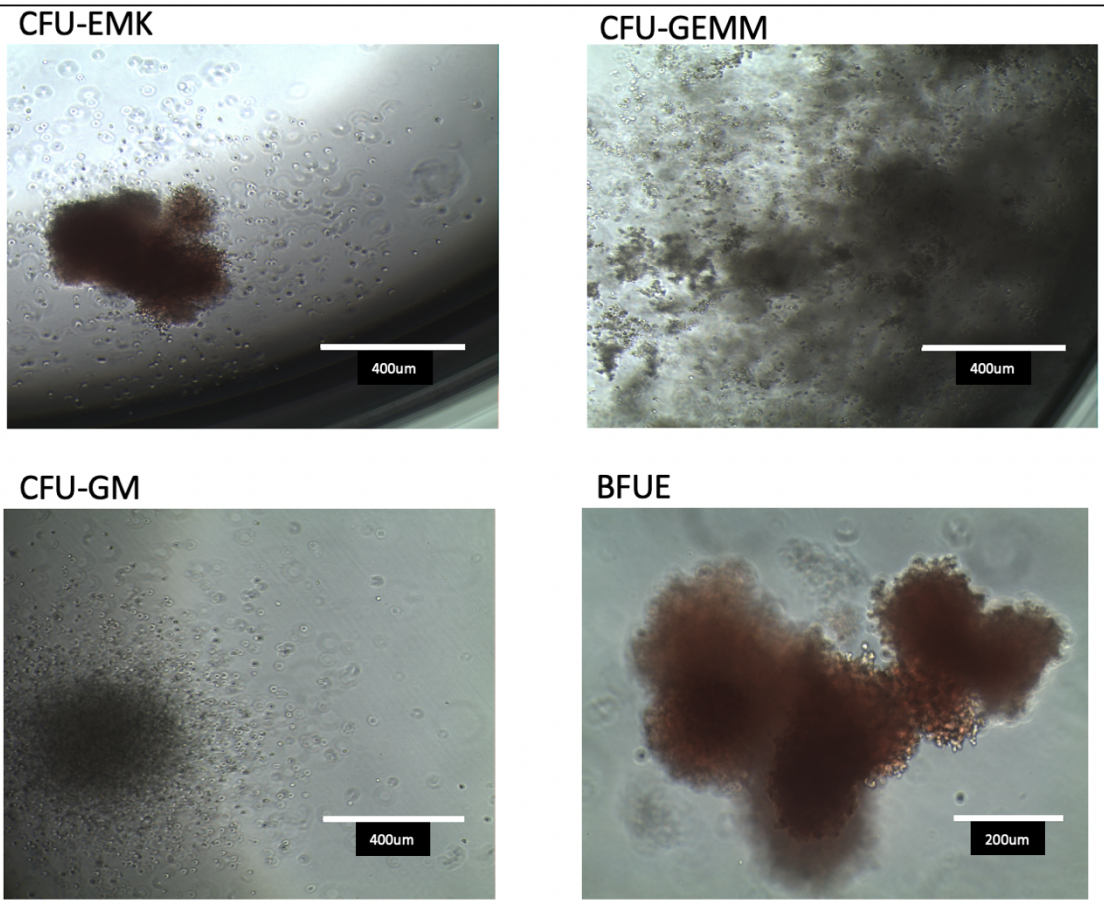


Figure 4.12 Representative images of colonies derived from clonogenic assays of sorted single DS fetal BM HSPCs in methylcellulose. White scale bar is 400um or 200um.
Original sorted HSPC: CFU-EMK (DS MEP), CFU-GEMM (DS HSC), CFU-GM (DS HSC), BFUE (DS MEP).

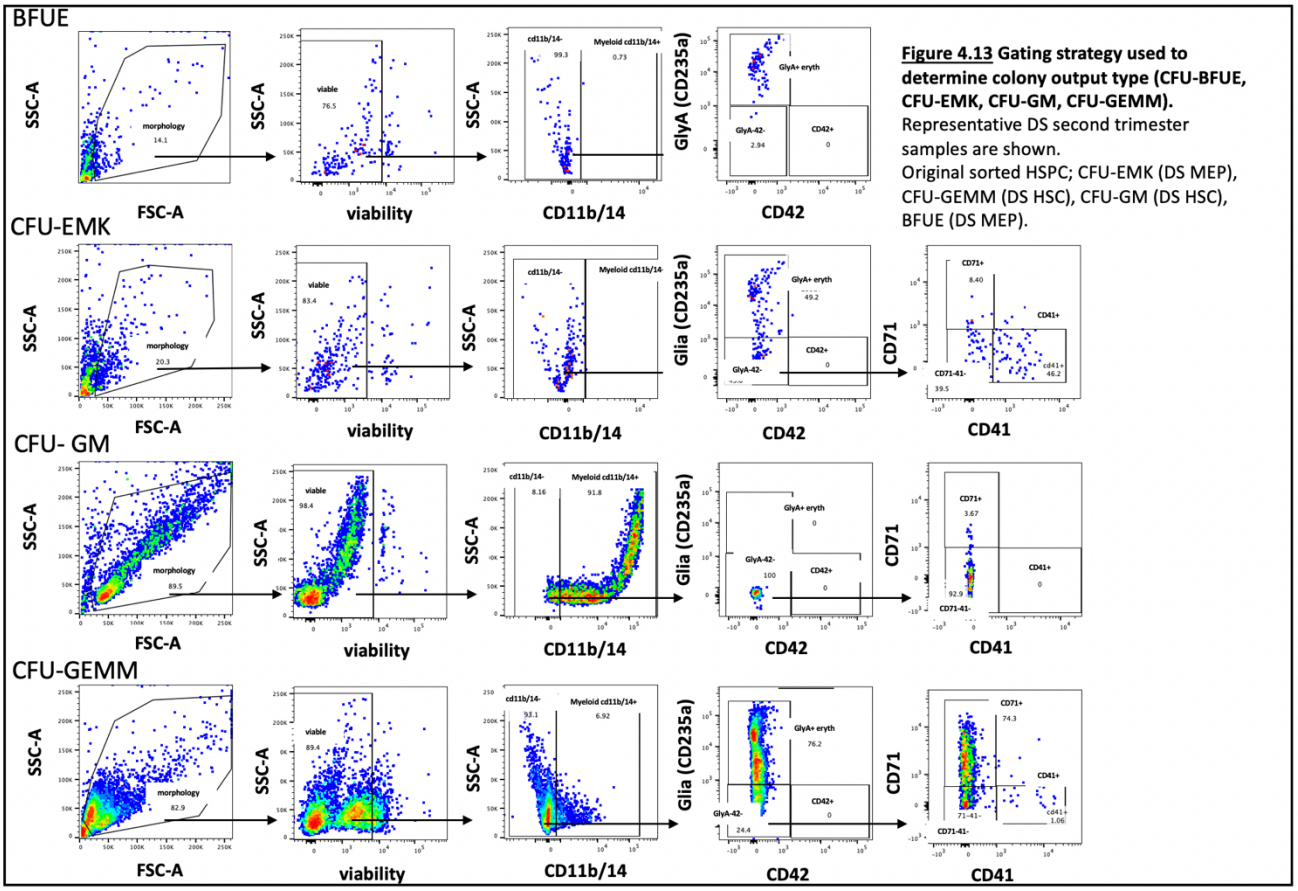


Figure 4.13 Gating strategy used to determine colony output type (CFU-BFUE, CFU-EMK, CFU-GM, CFU-GEMM).
Representative DS second trimester samples are shown.
Original sorted HSPC; CFU-EMK (DS MEP), CFU-GEMM (DS HSC), CFU-GM (DS HSC), BFUE (DS MEP).

DS HSCs and MPPs both show a significant erythroid skew relative to normal, with the most striking difference being observed at the MPP level (Figure 4.14). Comparing HSCs and MPPs, HSCs produce relatively greater GEMM and fewer erythroid colonies compared with MPPs, however in DS the proportion of mature erythroid colonies is significantly expanded (Figure 4.14).

MEPs produced exclusively erythroid and megakaryocytic output in DS FBM, whilst normal MEPs did give rise to approximately 25% myeloid output (** $p \leq 0.01$). EMK were most notably detected in DS MEP compared with HSC and MPP.

As expected, both normal and DS Pre-ELP/GMP produced myeloid colonies (Figure 4.14), however DS Pre-ELP/GMP gave rise to a small number of erythroid colonies that were not observed in normal cultures, though this was not a statistically significant finding.

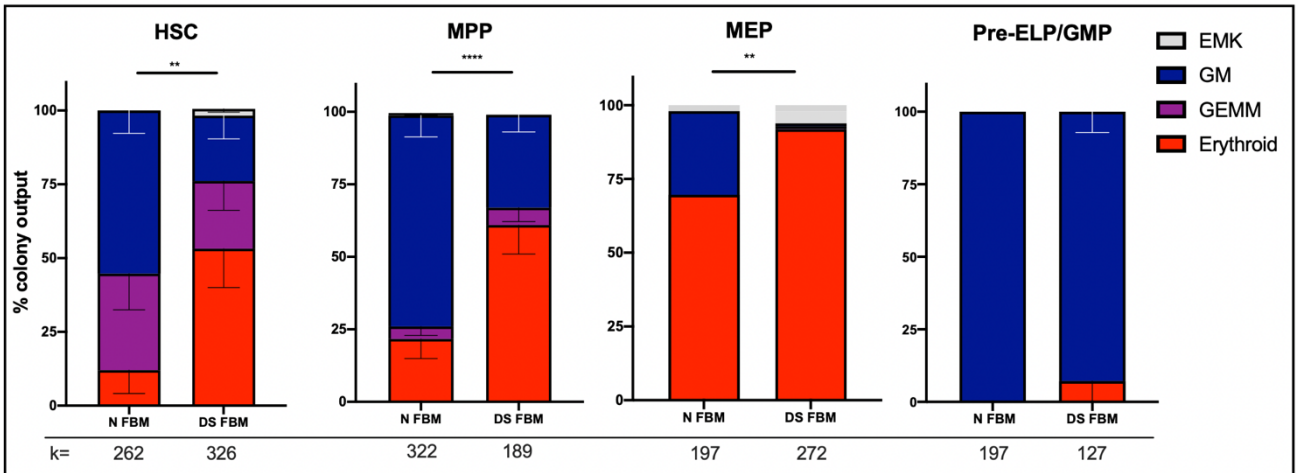


Figure 4.14 DS FBM HSCs and MPPs exhibit a significant erythroid bias in their lineage output in clonogenic assays of single normal and DS fetal BM HSPCs. DS MEPs and Pre-ELP/GMPs also show increased relative mega-erythroid and erythroid output, respectively, compared with normal counterparts.

Clonogenic assay of index flow-sorted single normal and DS fetal BM HSPCs cultured in methocult with cytokines (IL-3, IL-6, IL-11, SCF, FLT3L, GM-CSF, TPO, EPO), to assess myeloid/ megakaryocyte/ erythroid differentiation, assessed at day 14. Frequency of different colony types generated from normal FBM HSPCs, determined by morphology-based scoring and confirmatory flow cytometry/ cytospin.

Normal FBM, n=3-5 biological replicates, and DS FBM n=4. Number of single cells plated is represented by k. Error bars show SEM. Statistical analysis was performed using Two-way ANOVA (Mixed Effects analysis) with Bonferroni correction for multiple comparisons and ** $p<0.01$, **** $p<0.0001$.

Note: normal FBM colony output data was also featured in chapter 3.

4.3.3 Early and intermediate DS FBM HSPCs exhibit impaired T-cell differentiation

Given the striking B-cell defect that was observed in DS FBM HSPCs and the skew toward NK output, I wanted to further characterise lymphopoiesis in DS FBM by performing T-cell differentiation assays on DS FBM HSPCs. T-cell output was determined by flow cytometry using the same gating strategy shown in chapter 3 for normal FBM (Figure 3.10). OP9-DL1 experiments reveal reduced proportional T-lineage output for almost all of the DS FBM HSPC populations assessed (Figure 4.15 and 4.16), however this T-cell defect appears less severe than that observed for B-lymphopoiesis (Figures 4.7, 4.9, 4.10) and was not statistically significant for any of the assessed HSPCs. In parallel with the reduced T-cell output, there was a striking increase in the proportional NK output for almost all of the DS HSPCs assessed (with exception of CD10+LMPP) (Figure 4.15 and 4.16), recapitulating previous observations during B-differentiation assays (Figure 4.7), however none of the observed increased NK frequencies (Figure 4.15) were statistically significant.

Mirroring the trend observed for the impaired B-lymphopoiesis (Figures 4.7, 4.9, 4.10), upstream populations exhibited the most severe T-cell defect, with the proportion of T-cells markedly reduced in DS HSC, MPP and CD10-LMPP co-cultures (Figure 4.15) (N vs DS HSC day 14= 75.7± 7.7% vs 43.2± 5.6%, N vs DS MPP day 14= 75.8± 4.25% vs 43.8± 15.4%, N vs DS CD10-LMPP day 14= 81.8± 7.3% vs 50± 19.7%). Interestingly, CD10+LMPP did not show an obvious T-cell defect, with proportional T-cell output comparable to normal CD10+LMPP, unlike the severe B-cell defect observed for this population (Figure 4.7). As the number of replicates for normal CD10+LMPP was limited to 1 (pooled from 3 biological replicates), due

to population scarcity in normal FBM, additional assays will be needed to confirm whether or not DS FBM CD10+LMPP have reduced T-cell differentiation in vitro.

Downstream, DS Pre-ELP/GMPs showed reduced T-cell output and increased proportional NK output, most markedly at day 14 (N vs DS Pre-ELP/GMP day 14= 56.9± 18.1% vs 38.1± 7.7%, Figure 4.15), however this defect was not as striking as the B-cell impairment (see Figure 4.7). Interestingly, DS ELP also show a marked T-cell defect (N vs DS ELP day 14= 45.3± 18.1 vs 24± 3.1%) and increased NK-cell output (N vs DS ELP day 14= 13.6± 6% vs 51± 10.4%), which is as, if not more striking than the B-cell defect observed for this population in MS-5 co-culture assays (Figure 4.7).

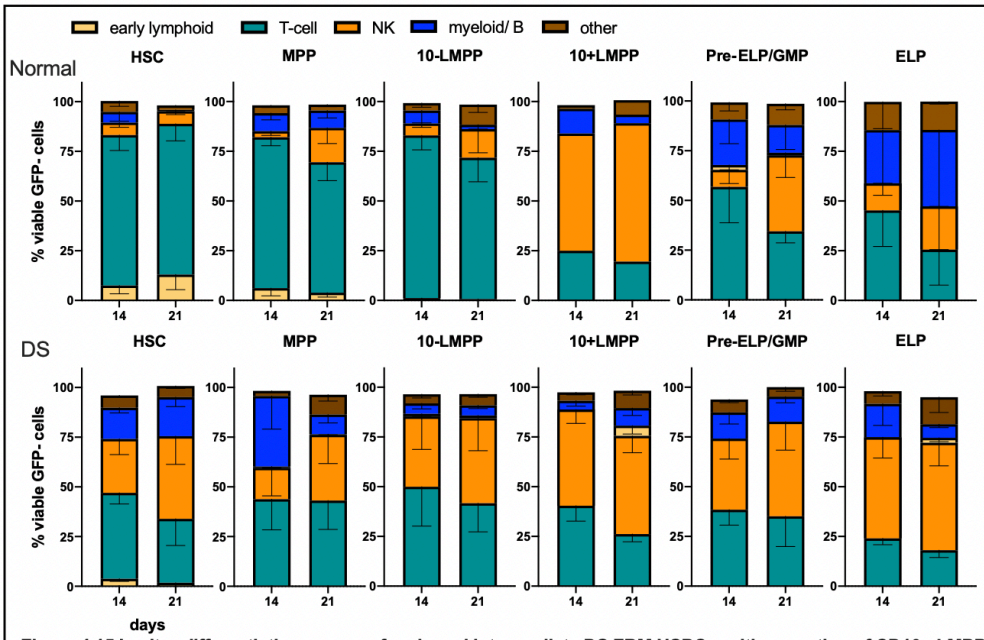


Figure 4.15 In vitro differentiation assays of early and intermediate DS FBM HSPCs, with exception of CD10+ LMPPs, reveal a moderate T-cell defect, with marked NK lineage biasing, compared with normal counterparts. Like the B-cell defect, T-lymphopoiesis is most severely impaired in upstream populations.

Differentiation assay of flow-sorted normal and DS fetal BM HSPCs co-cultured on OP9-DL1 stromal cells with cytokines (FLT3L, SCF, IL-7). Total lineage output is shown as % viable GFP- cells across the time course. Normal FBM n= 3-5 except 10+LMPP (n=1). DS FBM n= 3-4. Data was not analysed where hCD45+ events <10, leading to sample exclusion. Note: normal FBM OP9DL1 frequency data also featured in chapter 3.4.

early lymphoid= Lin-CD4-8-CD56-CD3-CD7+.
myeloid/ B= Lineage +, Lin cocktail = CD19,14,33,235a.
other = Lin-CD4-8-56-3-2-7-.

In order to discern whether, like the impaired B-lymphopoiesis observed in DS FBM (Figure 4.9 and 4.10), the T-cell defect was also a quantitative one, absolute counts were generated (Figure 4.16).

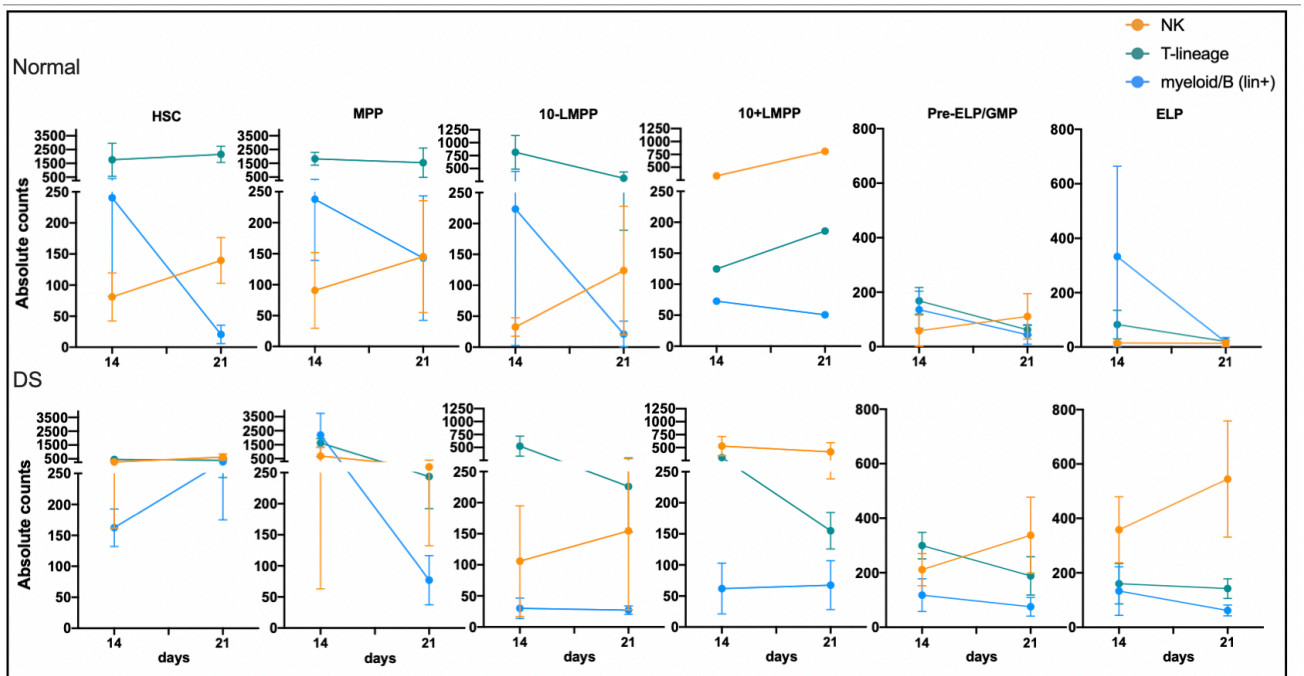


Figure 4.16 Upstream DS FBM HSPCs show reduced absolute T-cell output compared to normal counterparts, with exception of 10+LMPP, whilst NK output is increased for all DS HSPC populations. Overall trends of absolute counts are mirrored between N and DS, with T-cell output peaking in MPPs. DS Pre-ELP/GMPs and ELPs show higher numbers of T-cells than normal counterparts.

Differentiation assay of flow-sorted normal fetal BM HSPCs co-cultured on OP9-DL1 stromal cells with cytokines (FLT3L, SCF, IL-7). Data is presented as absolute T, NK and Lin+ (B/mye) counts, calculated using Countbright beads (Thermofisher). Normal FBM n= 3-5 except 10+LMPP (n=1), DS FBM n= 3-4. Data was not analysed where hCD45+ events <10, leading to sample exclusion.

myeloid/ B= Lineage +, Lin cocktail = CD19,14,33,235a.

DS HSCs presented with the most dramatic reduction in absolute T-cell counts 3.85-fold higher on day 14 and over 5-fold higher on day 21 (N vs DS HSC: day 14= 1756± 1200 vs 455± 98, and day 21= 2151± 588 vs 392± 148), though these differences were not statistically significant. Whilst the absolute T-cell output of normal and DS MPPs was comparable on day 14, by day 21 the output of DS MPPs was over 6-fold lower (N vs DS MPP: day 14= 1830± 463 vs 1630 ± 304, and day 21= 1548± 1058 vs 243± 52). The defect in

CD10-LMPPs was less marked, with a reduction of approximately 1.5-fold at both time points (N vs DS CD10-LMPP: day 14 = 813± 326 vs 526 ±193, and day 21= 312 ±122 vs 226 ±73).

Interestingly, DS CD10+LMPP produced more T-cells than normal counterparts and also more NK cells than all of the normal FBM populations assessed, however further replicates of normal 10+LMPP would be needed to confirm this.

DS Pre-ELP/GMPs and ELPs both showed higher absolute T-cell output compared with normal counterparts, unlike the B-cell defect seen for these populations during MS-5 assays (Figure 4.7).

Supporting the NK biasing observed in MS-5 co-culture assays, all of the DS FBM HSPCs assessed, with exception of CD10+LMPP, showed considerably higher absolute NK output on OP9-DL1, though none of these differences were statistically significant.
DS ELP produced the most drastic increase in absolute NK counts showing an over 20-fold increase at day 14 which increased to 38-fold by day 21 (N vs DS ELP: day 14= 15± 4 vs 358 ± 121 and day 21= 14 ±11 vs 544 ± 214, P= 0.07 and P= 0.09, respectively).

Otherwise, HSC, MPP, CD10-LMPP and Pre-ELP/GMP showed up to 7.5-fold increases in the absolute NK output (N vs DS HSC day 21= 140 ±37 vs 631 ±225 P= 0.11, N vs DS MPP day 14= 91± 61 vs 686± 623 P= 0.44, N vs DS CD10-LMPP day 14= 32± 15 vs 106 ± 89 P= 0.5 and N vs DS Pre-ELP/GMP day 14= 59 ± 57 vs 211± 59 P= 0.12).

Altogether, these findings indicate that DS FBM HSPCs are NK biased both at the expense of both B (Figure 4.7) and T output (4.15, 4.16), which is, to my knowledge, the first time this has been shown for DS fetal tissue.

4.4 Summary and discussion

Within this results chapter, I sought to build on preliminary data in our lab (Sorcha O'Byrne ASH Abstract, 2019) and further characterise the B-differentiation impairment within DS FBM. Using the normal data I generated as a reference (see chapter 3), I specifically wanted to compare the contribution of CD10- and CD10+ populations to this defect to determine the stage(s) at which the impairment originates. As previous studies have reported T- and NK-lymphoid abnormalities in individuals with DS and in DS fetal development (Cossarizza et al, 1991; Thilaganathan et al, 1993; deHingh et al, 2005; Zizka et al, 2006; Bloemers et al, 2010; Cetiner et al, 2010; Schoch et al, 2017; Waugh et al, 2019; Lambert et al, 2021; Lambert et al, 2022; Waugh et al, 2022) I also investigated T- and NK-potential of DS FBM HSPC.

The HSPC composition of DS FBM is dramatically altered, with CD10- populations particularly reduced

Using the extended progenitor panel, I immunophenotypically characterised the composition of the DS FBM HSPC compartment including the newly identified progenitors. As well as the significant expansion of HSCs and MEPs and decrease in the B-progenitors, which had previously been shown in FL (Roy et al, 2012), these experiments revealed a significant increase in the proportion of CD10+LMPP, despite the overall LMPP compartment being comparable in size to normal FBM, with a significant shift toward CD10+LMPPs in DS FBM compared with normal. The CD10- populations, PreProB and ELP, were more severely impacted when compared to CD10+ CLP and ProB. Moreover, the

proportion of CD10-LMPP and Pre-ELP/GMP were reduced in DS FBM, though not significantly.

This led me to hypothesise that CD10- and CD10+ lymphoid populations may be disparately impacted in DS FBM and that there may be a drive toward B-lymphopoiesis through CD10+ progenitors i.e. that DS FBM HSPCs may exhibit a more post-natal-like B-lymphoid differentiation phenotype.

Upstream and intermediate DS FBM HSPCs show a striking B-cell impairment and less severely abrogated T-cell differentiation, with a shift toward NK-poiesis

To characterise the differentiation potential of DS FBM HSPCs I performed MS-5, OP9-DL1 and methylcellulose assays to assess B/NK, T and myeloid/erythroid/megakaryocytic output respectively.

These data demonstrate that the B-cell defect originates at the HSC level and that B-cell differentiation is severely disrupted in upstream and intermediate progenitors. ELPs are moderately impacted whilst the downstream B-progenitors appear normal.

Whilst DS HSCs MPPs and ELPs do show reduced T-cell output, this impairment does not appear as severe as the B-cell impairment.

Across both MS-5 and OP9-DL1 assays, DS FBM HSPCs show a striking bias toward NK output, at the expense of both B- and T-lineage output and including at the level of ELPs which are B-cell restricted and show minimal residual NK potential in normal FBM.

In addition, the MS-5 absolute counts data reveal that not only do DS FBM HSPCs display reduced lineage output, but there appears to be intrinsic abnormalities in their proliferation

and expansion capacities with total hCD45+ counts consistently lower for DS FBM HPSCs. Interestingly, however, PreProBs and ProBs showed comparable or higher absolute counts in DS FBM which may indicate a compensatory proliferative drive in these populations. Despite the striking changes in lineage biasing and output in DS FBM HSPCs, the vast majority of the findings from the MS-5 and OP9-DL1 assays were not statistically significant, likely due to the inherently high sample-sample variability across primary human fetal tissue, which was exacerbated by the relatively small sample sets.

As shown previously in FL (Roy et al, 2012), DS FBM HSCs and MPPs show an erythroid bias within clonogenic assays (Jardine et al, 2021) and the clonogenicity of all DS HSPCs was consistently higher.

Altogether, these data suggest that once B-cell commitment has taken place, i.e. once cells become B-progenitors, T21 does not appear to impair progression toward a mature B-cell fate, however T21 does appear to impede the priming of earlier progenitors, such as HSCs and MPPs, that is required to initiate specification toward the B-lineage, leading to a downstream reduction in ELPs and B-progenitors. This apparent re-direction of lineage potential may represent a 'lineage steal' effect, whereby a drive toward mega-erythropoiesis results in a block in B-cell differentiation. To explore this further, it would be necessary to distinguish whether i) a specific, active block in B-cell differentiation occurs or ii) whether the re-distribution of potential toward mega-erythroid fates indirectly blocks B-lymphopoiesis, or iii) a combination of both is at play. One way this could be studied would be by surveying single normal and DS HSCs and MPPs for activating and repressive changes in mega-erythroid- and B- lineage gene networks respectively.

LMPP and Pre-ELP/GMP appear to be important branching points through which lineage biases are propagated

Whilst CD10-/+ LMPPs and Pre-ELP/GMPs are likely to contribute to the B-cell expansion in second trimester normal FBM (chapter 3), all of these populations show a striking impairment in B-cell differentiation in DS FBM. On OP9-DL1 stroma, all of the DS FBM HSPCs showed reduced T-cell output with the exception of CD10+LMPP, which showed comparable output to normal, however this must be validated as this was only performed once in normal FBM using pooled 10+LMPP from 3 biological samples due to population scarcity.

Interestingly however, there is a clear segregation in how lineage biasing presents in the CD10- and CD10+ progenitors, with DS CD10-LMPP and Pre-ELP/GMP showing markedly increased myeloid and NK output in MS-5 co-cultures (similar to upstream HSC and MPP and downstream ELP, all CD10- populations), whilst CD10+LMPP remain lymphoid restricted, as in normal FBM, but this output is almost exclusively NK. These observed biases toward the myeloid and NK lineages were also validated in methylcellulose assays where both DS CD10-LMPP and Pre-ELP/GMP generated greater numbers of myeloid colonies and within OP9-DL1 co-cultures, where increased NK-lymphopoiesis was also seen.

These disparities in the way that DS CD10-/+ progenitors are impacted suggests that the expression of CD10 is a sufficiently strong driver of lymphopoiesis that CD10 expression limits myeloid bias in DS FBM (Ichii et al, 2010; Kohn et al, 2012; Renoux et al, 2015; Karamitros et al, 2018). On the other hand, the CD10- progenitors, including the upstream

HSCs, MPPs, 10-LMPP, Pre-ELP/GMP and downstream ELPs, possess sufficient myeloid potential that a drive toward myelopoiesis is observed in DS.

Whilst the specific mechanisms for why CD10-/+ progenitors are affected differently in DS-FBM are unknown, CD10 expression has been associated with a more rapid proliferation and cycling dynamic in vitro (Cutrona et al, 2002; Mishra et al, 2016) however longer-term longevity in vitro is compromised with a propensity toward apoptosis (Cutrona et al, 2002; Ichii et al, 2010). Further, CD10 has been presented as a tumor suppressor and positive prognostic marker in both leukaemias and solid cancers (Taylor et al, 2006; Mishra et al, 2016) with the methylation and silencing of CD10 is thought to maintain leukaemic cells in a less differentiated state, when compared to normal lymphoid cells (Garcia-Manero et al, 2002; Taylor et al, 2006; Mishra et al, 2016). Briefly, one suggested model for why CD10 expression alters proliferation is thought to involve alterations in the local concentration of peptides, which CD10 hydrolyses and cells uptake to proliferate (Mishra et al, 2016). Therefore, lower CD10 expression may indicate a less lineage committed, more stem-like state, which permits the myeloid biasing observed in DS FBM CD10- HSPCs. Conversely, several studies have shown that CD10+ cells show increased levels of several lymphoid and B-lineage specific transcripts are elevated (Renoux et al, 2015; Karamitros et al, 2018; O'Byrne et al, 2019). Interestingly, the fact that CD10 expression has been associated with reduced proliferation and longevity of cells in vitro (Ichii et al, 2010) which I also observed in my co-cultures of CD10- vs 10+ LMPPs (*see chapter 3*), may explain why DS HSPCs do not expand as well in culture if they assume a more CD10+ post-natal like phenotype.

The NK lineage is an evolutionarily older component of human immunity, onto which adaptive immune programmes (B/ T) were later layered (Sun and Lanier, 2009; Cichocki et

al, 2019). The finding that DS FBM HSPCs consistently skew toward NK-lymphopoiesis adds to a complex and emerging picture of alterations to the NK lineage in DS, with some groups reporting an reduced frequencies and numbers of NK cells in fetuses and children with DS (Thilaganathan et al, 1993; deHingh et al, 2005; Bloemers et al, 2010), whilst others claim the converse (Cossarizza et al, 1991; Zizka et al, 2006; Cetiner et al, 2010; Schoch et al, 2017; Waugh et al,2019; Lambert et al, 2021). In the context of the data presented in this chapter, it is tempting to speculate that when B/T-cell differentiation programmes are not sufficiently activated, ancestral NK/myeloid programmes may become the default (Cichocki et al, 2019).

Altogether, these results indicate that this defect and associated lineage biases is propagated through LMPPs and Pre-ELP/GMPs, populations which I showed to be important in the B-cell expansion in normal FBM.

Refined models for B-lymphopoiesis in normal and DS FBM, summarising the differences between normal and DS are depicted in Figure 4.17.

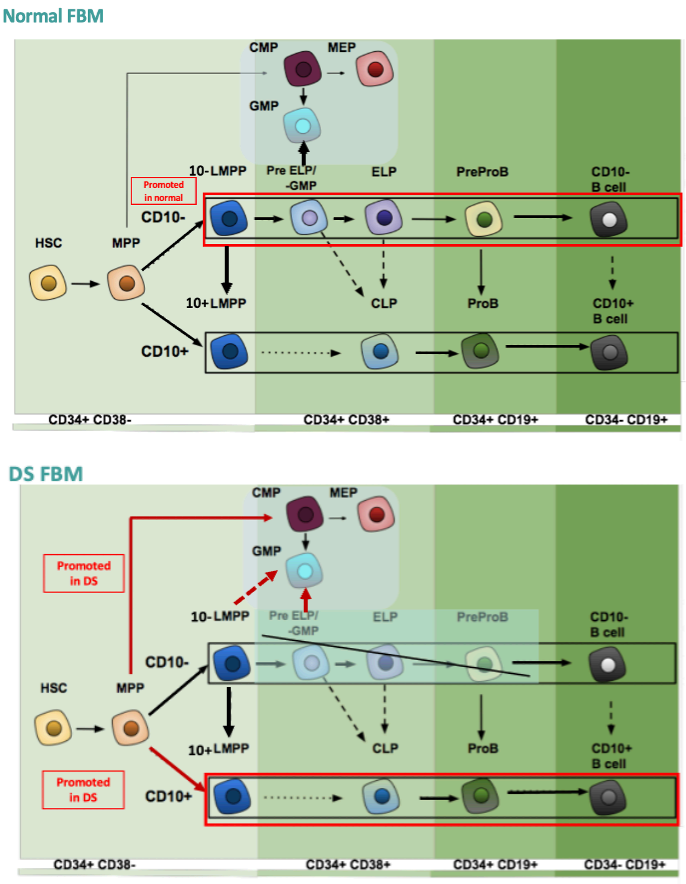


Figure 4.17 Fetal B-lymphopoiesis in normal vs DS FBM
Diagram depicting the newly refined fetal B-lymphopoiesis pathway, resolved through functional assays, in normal and DS FBM. Red annotations highlight the main differences between normal and DS FBM.

DS FBM HSCs and MPPs show increased clonogenicity in methylcellulose assays, most significantly of the erythroid lineage, suggesting a diversion toward myeloid and erythroid fates at the apex of the haematopoietic hierarchy.

Functional studies suggest that the proposed CD10- pathway of B-lymphopoiesis is promoted in normal FBM.
By contrast, in DS FBM, several CD10- progenitors are significantly reduced, including ELP and PreProBs, and several upstream progenitors show a striking B-cell defect, suggesting an upstream block in the CD10- pathway which produces these B-progenitors.
Like HSCs and MPPs, DS CD10-LMPPs and Pre-ELP/GMP show increased myeloid output in both methylcellulose and MS-5 assays, suggesting lineage biases are propagated through intermediate lymphomyeloid progenitors.

By contrast, CD10+ progenitors make up a greater proportion of HSPCs in DS compared with normal and CD10+ B-progenitors are less severely reduced than CD10- counterparts, suggesting CD10+ pathways of B-lymphopoiesis may be promoted in DS FBM.

Arrows depict established differentiation transitions of HSPCs and dashed arrows represent transitions for which preliminary evidence exists.

Future work

Whilst these data show striking lineage skewing of DS FBM HSPCs, to draw conclusions on lineage biasing in specific HSPCs, single cell functional assays would be required. Interestingly, a comprehensive single cell study of FL, CB and ABM revealed that HSPCs in fetal life are far more multipotent than post-natal HSPCs which are predominantly oligo/unipotent (Notta et al, 2016). This suggests that in DS, multi-potent fetal progenitors are primed toward myelo-erythroid and NK outputs. To address these possibilities and deepen our understanding of these differentiation defects, single cell transcriptomic studies of DS FBM HSPCs would also be valuable.

Currently, these observations of lineage biases and differentiation defects in DS HSPCs are limited to the purview of artificial co-culture systems. Specifically, the culture of HSPCs within specialised culture systems (MS-5, methylcellulose and OP9-DL1) has allowed me, within artificially perturbed conditions, to reveal the multipotentiality of progenitors – and intrinsic differentiation biases and defects in the case of DS.

For instance, MS-5 stroma are a well-established system for the in vitro study of B-cell differentiation because, through the supply of exogenous cytokines such as IL-7, this system artificially promotes B-lymphopoiesis. Accordingly, this system allows us to investigate whether progenitors possess B-lineage potential within a strongly B-primed environment, and therefore, allows us to unmask an intrinsic defect in B-lymphopoiesis within DS cultures.

However, it is important to recognise the caveat that artificially primed systems cannot recapitulate the more complex scenario in vivo. Firstly, local cytokine concentrations are likely to be spatially and temporarily variable in vivo and different than those simulated in the lab. Secondly, in situ, the FBM is under more dynamic exogenous regulation than our simplified culture system where cytokine concentrations are kept strictly controlled. Finally, MS-5 stroma are murine-derived and there are likely to be significant differences between human and murine stromal cells, therefore MS-5s are unlikely to faithfully recapitulate the complex human FBM microenvironment.

However, the inclusion of several specialised culture systems, has allowed me to compare and contrast the differentiation potential of fetal HSPCs down multiple lineage trajectories, and importantly, has allowed me to validate findings across several systems, such as consistently increased myeloid output for DS HSPCs in both MS-5 and methylcellulose assays or increased NK output for DS HSPCs in both MS-5 and OP9-DL1 systems.

Altogether, these experiments have allowed me to assess intrinsic differences in the lineage potential of FBM HSPCs within primed conditions, however these observations in isolation cannot be directly translated to the reality in vivo.

Previous work by our lab has utilised normal and T21 FBM MSCs for co-culture of FBM HSPCs (Sorcha O'Byrne ASH abstract, 2019). Expansion of this refined system using the newly refined panels I have created to simultaneously assess B, myeloid and NK differentiation, would be an improved system to conduct further investigations. However, culture of FBM HSPCs on non-immortalised stroma poses technical challenges. Recent work indicates that the HS-5 stromal cell line may faithfully recapitulate human BM MSCs both in terms of their surface expression and ability to secrete cytokines to generate an enriched environment for human haematopoeitic cell growth (Adamo et al, 2020). However, distinctions in the colony supporting potential of HS-5 and other human BM stromal lines such as HS-27 indicate the variability between cell lines, which likely represent functionally distinct players within the bone marrow microenvironment (Adamo et al, 2020). Therefore, whilst human stromal cell lines probably better recreate the scenario in vivo, thorough optimisation will be required for their use in vitro.

These data show trends of differentiation potential at the functional level, but they do not indicate whether the mature outputs of these assays, for instance mature B-cells or NK-cells, are functionally altered. It would be interesting to see the results of functional assays designed to assess whether the immune cells produced by DS FBM are also functionally defective. For the B-cell lineage this could involve testing antibody responses, or for NK

cells, their de-granulation activity could be measured (Boonyaratanakornkit and Taylor, 2019; Euchner et al, 2021).

Finally, it is interesting that DS-ALL rarely presents in infants under 1 year old (Roberts and Izraeli, 2014) which might indicate a later, possibly CD10+, fetal cell of origin, although an in utero origin for DS-ALL remains to be determined.

Chapter 5

The impact of trisomy 21 on the transcriptome and chromatin accessibility of fetal bone marrow B lymphopoiesis

5.1 Background

The molecular mechanisms for the impaired B-cell differentiation and increased leukaemia susceptibility observed in DS HSPCs remain elusive. Several genes on human chromosome 21 (Hsa21) have major roles in haematopoiesis and B-lymphopoiesis, e.g. *DYRK1A, HMGN1, RUNX1* and *ERG* (see Table 1.2), and their increased expression has been proposed as one possible mechanism for these abnormalities (Korbel et al, 2009; Malinge et al, 2012; Lane et al, 2014; Thompson et al, 2015; Mowery et al, 2018; Kubota et al, 2019; Laurent et al, 2020).

Interesingly however, the majority of studies on trisomic haemopoietic cells, including previous studies by our lab (Roy et al, 2012, Roy at al, 2014 ASH abstract) have revealed global abnormalities of gene expression associated with T21 as opposed to the altered expression of a single gene (Antonakaris et al, 2020). In FL, our own lab showed that upstream DS HSPCs adopted a megakaryocytic/ erythroid gene expression signature, with a down regulation of genes associated with lymphoid priming (Roy et al, 2012). A more recent study showed that alongside the mega-erythroid bias of DS FBM HSCs and MPPs in methycellulose, DS HSCs and MPPs showed altered expression of cell cycle and metabolic genes along the erythroid differentiation pseudotime, suggesting that a hyper-proliferative and altered metabolic state underpins the pro-erythroid bias (Jardine et al, 2021).

It has been proposed that the absence of the expected 1.5 fold increase in Hsa21 genes in trisomic cells is a result of protective gene dosage compensation mechanisms which ensure the embryonic viability of the fetus (Antonakaris, 2017; Stamoulis et al, 2019). Several epigenetic modifiers are expressed on chromosome 21, and it is thought that their altered expression may lead to global gene silencing in trisomic cells (Stamoulis et al, 2019; Wiemels et al, 2019; Muskens et al, 2021). For example, the over expression of *HMGN1*, a chromatin remodeller encoded on chromosome 21 seems to be sufficient to recapitulate the transcriptional changes observed in trisomic cells and recapitulates several aspects of impaired B-lymphopoiesis (Lane et al, 2014; Mowery et al, 2018). This has prompted speculation that abnormal fetal haematopoiesis and the propensity toward ALL in DS may be induced and/or regulated by epigenetic mechanisms. Less directly, the major haematopoietic transcription factor RUNX1 is known to recruit epigenetic modifiers to target genes, and therefore it has been hypothesised that dysregulation of RUNX1 activity also leads to wider epigenetic changes in both proximal and distal genes (Sood et al, 2017; Owens et al, 2022). In support of this, recent work within human cells has revealed the hypermethylation of *RUNX1,* a haematopoietic transcription factor encoded on chromosome 21, in DS-ALL but not non-DS ALL (Kubota et al, 2019) and in blood spots of neonates with DS but not in normal controls (Muskens et al, 2021).

To gain a more detailed picture of the molecular mechanisms underpinning the abnormal phenotypes in DS fetal HSPCs, a multi-omics approach is required. To date, no systematic and integrated study of the transcriptomic and epigenetic landscape of DS-FBM has yet been performed. Therefore, to understand the striking differences in functional output

between normal and DS FBM, shown in chapter 4, at the molecular level, I used both RNA and ATAC sequencing to infer the impact of epigenetic changes on the transcriptomic profile of DS FBM HSPCs.

Aims

1. Molecularly characterise the newly described CD10- and CD10+ FBM progenitors presented in this thesis within the context of the known human fetal HSPC hierarchy using ATAC and RNA sequencing.
2. Explore how changes in chromatin accessibility and transcription in DS FBM HSPCs underlie the functional differences and lineage skewing observed in DS FBM.

5.2 Molecular characterisation of normal fetal bone marrow HSPCs by bulk RNA sequencing and ATAC sequencing

To assess the impact of T21 on the transcriptome and chromatin accessibility of DS FBM HSPCs, I needed to first characterise molecularly, the normal FBM HSPCs, with a particular focus on profiling CD10-/+ LMPPs and Pre-ELP/GMPs. The approach for these experiments is summarised in Figure 5.1. In addition to HSCs, MPPs, LMPPs, Pre-ELP/GMPs, B-progenitors and pre-B-cells, I also sorted CMP, GMP and MEPs as a point of reference for the myeloid and erythroid lineages. In doing so, I was able to compare the new progenitors with progenitors of both B- and myeloid lineages (Figure 5.1).

Due to the scarcity of samples, especially for DS, and the rarity of several populations e.g. ELP, I utilised protocols adapted for small cell numbers (Corces et al, 2016; O'Byrne et al, 2019; Rodriguez-Meira et al, 2020). Due to their low frequencies in N FBM, I was unable to sort sufficient CD10+LMPP for ATACseq (1000 cells needed), therefore for these experiments I sorted total LMPPs. Ideally, ATACseq and RNAseq would have been performed on the same single cells, for example using the 10X system, rather than bulk, however this was not possible at the time of my experiments.

Gestation matched N FBM biological samples were used (n=3 for both RNAseq and ATAC seq, all 19 pcw). For RNASeq, samples were sorted across as few dates as possible to minimise batch effect and samples were stored at -80 °C post-sorting for the minimal time possible to prevent degradation. All cDNA libraries were generated on the same day to minimise batch effect. Further details of the quality control and the analyses performed on RNA and ATAC sequencing data are provided in Methods (chapter 2).

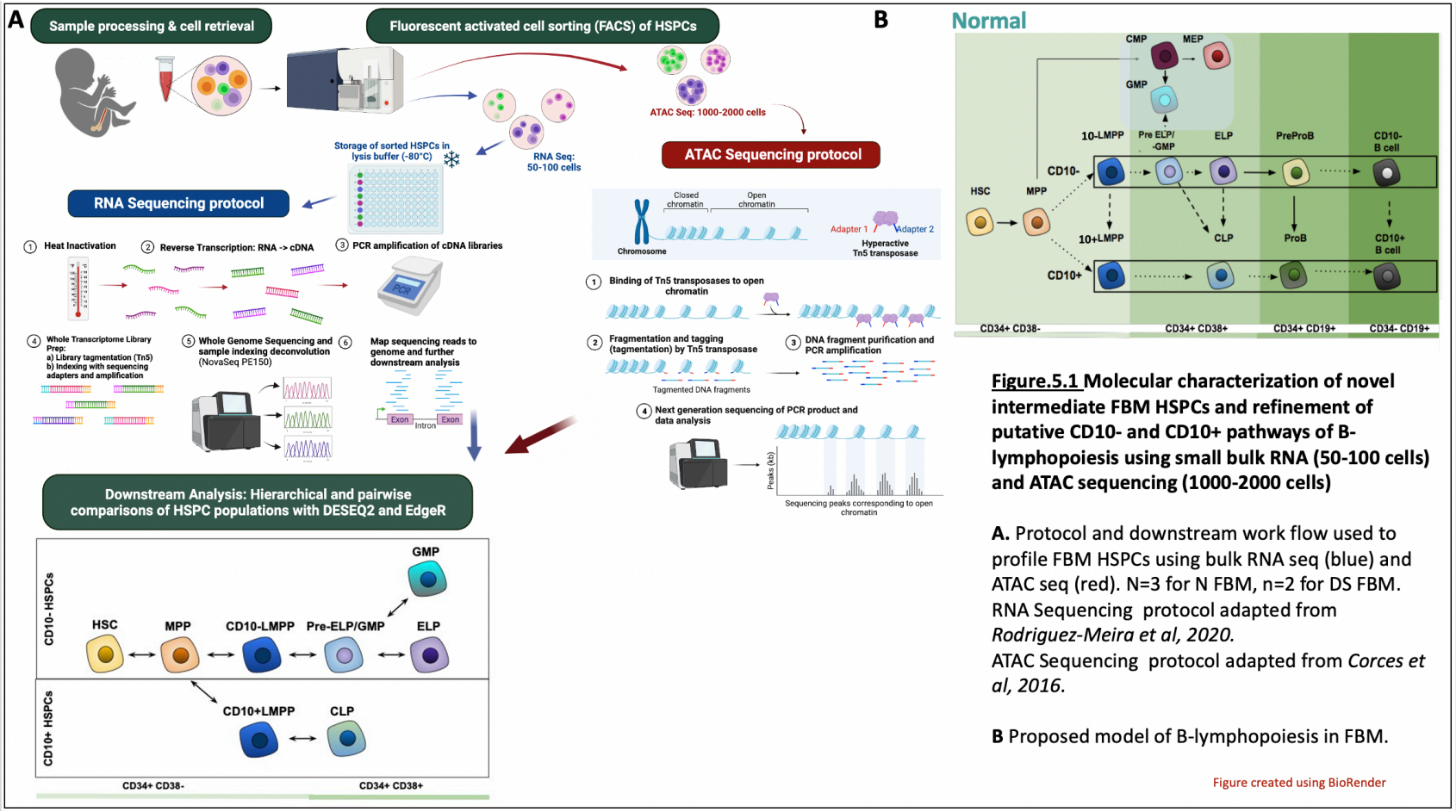


Figure.5.1 Molecular characterization of novel intermediate FBM HSPCs and refinement of putative CD10- and CD10+ pathways of B-lymphopoiesis using small bulk RNA (50-100 cells) and ATAC sequencing (1000-2000 cells)

A. Protocol and downstream work flow used to profile FBM HSPCs using bulk RNA seq (blue) and ATAC seq (red). N=3 for N FBM, n=2 for DS FBM. RNA Sequencing protocol adapted from *Rodriguez-Meira et al, 2020.* ATAC Sequencing protocol adapted from *Corces et al, 2016.*

B Proposed model of B-lymphopoiesis in FBM.

Figure created using BioRender

Hierarchical analysis of normal FBM HSPCs

A principal component analysis (PCA) of the total and top 500 most variably expressed genes (Figure 5.2 B), which I presumed would be more likely to include haematopoietic genes, reproduced the expected relationships between normal HSPC populations (Figure 5.1B). Validating these observations based on the most variably expressed genes, the same clustering distribution of populations is broadly retained when PCA was performed on all genes (Figure 5.2 A).

Briefly, the upstream progenitors, (HSC, MPP and all LMPPs), cluster closely together (blue cluster). Pre-ELP/GMPs, ELPs and the B-progenitors cluster together (green), whilst the myelo-erythroid progenitors cluster separately along PC2. This supports the in vitro data (see chapter 3) which showed relative B-cell restriction of normal FBM Pre-ELP/GMPs despite their having capacity to also produce GMPs. As expected, all LMPPs (CD10-/ CD10+/ total) clustered closely together, which reflects their close similarity relative to all of the other HSPCs.

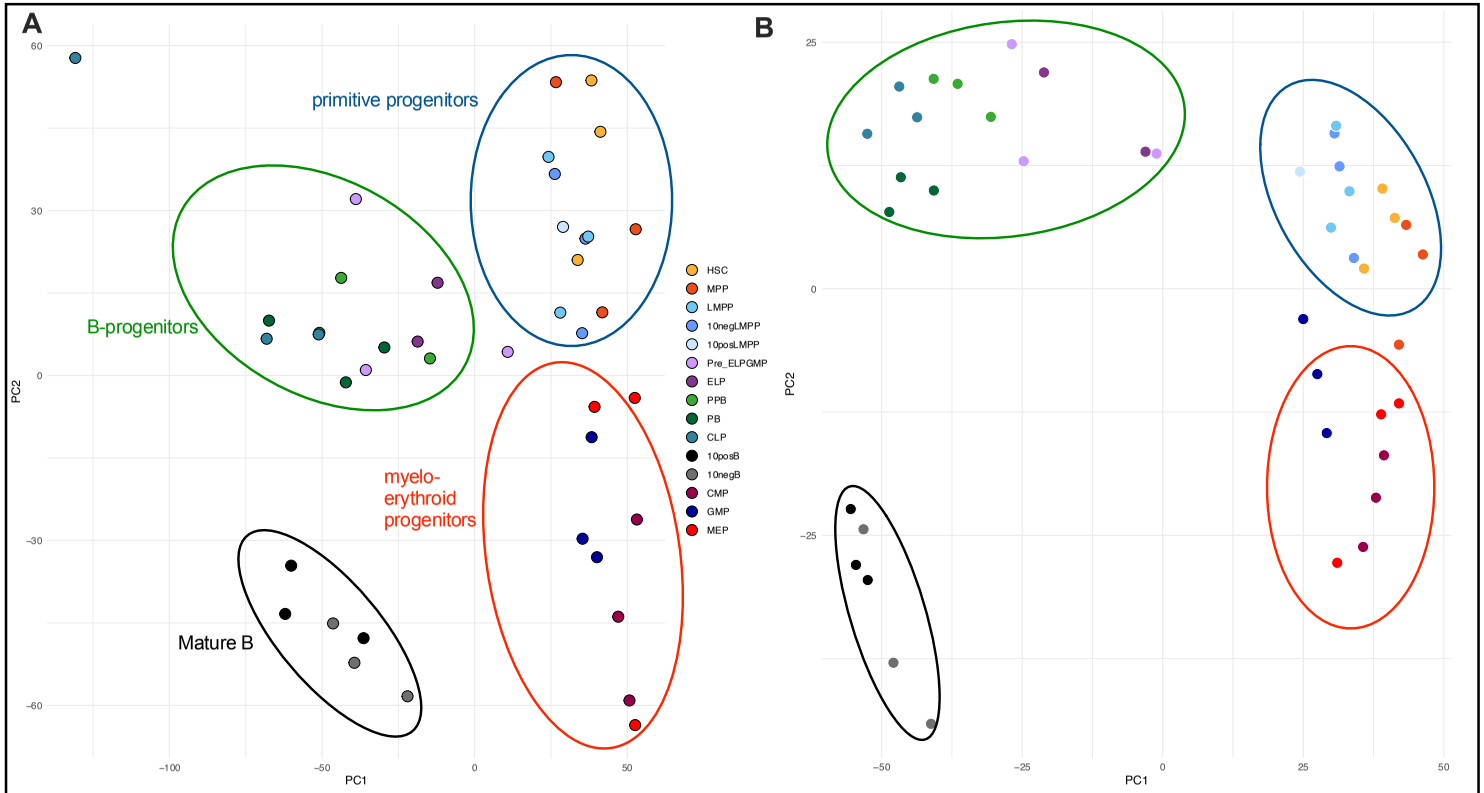


Figure 5.2 Principle Component Analysis of all genes (A) and the top 500 variably expressed (B) genes in normal FBM HSPCs (50-100 cells/population) by RNASeq resolves 4 clusters according to lineage: primitive progenitors (blue), B-progenitors (green), mature B (black) and myelo-erythroid progenitors (red). N FBM n=3, except 10posLMPP (n=1) and ELP (n=2) . PCA was performed on variant stabilised transformed normalised CPM counts.

HSPCs also cluster according to the expected progenitor hierarchy within hierarchically clustered heatmaps of the top 500 variably expressed genes (Figure 5.3) which I chose to feature as I presumed these would be predominantly haematopoietic genes.

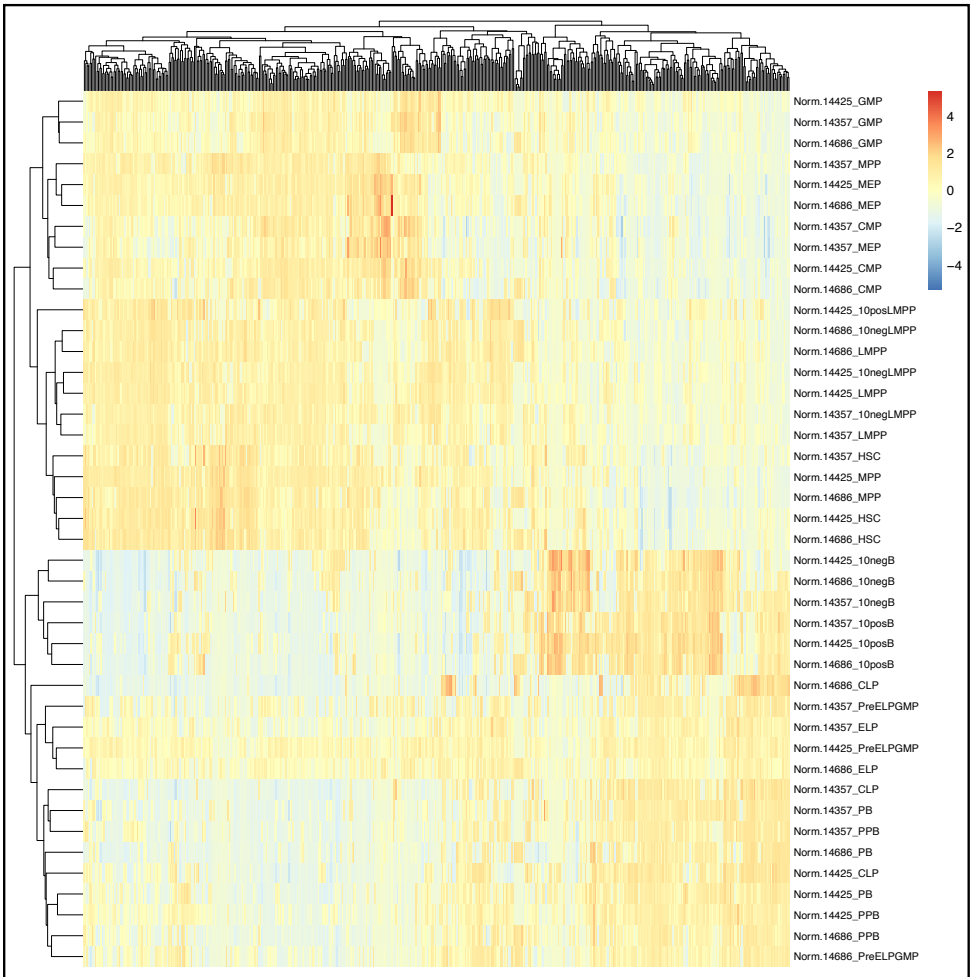


Figure 5.3 Normal FBM HSPCs cluster according to the expected progenitor hierarchy within hierarchically clustered heatmaps of the top 500 variably expressed genes across all populations (FDR <0.001, ANOVA), by RNAseq (50-100 cells/population), with clearly defined myelo-erythroid, LMPP, HSC/MPP, mature-B and B-progenitor clusters visible.
Heatmaps feature normalised CPM counts (scaled by gene). n=3 for normal FBM, except for ELP and 10pos LMPP (n=2 and 1 respectively). All analysis was performed using EdgeR.

As was the case for the gene expression data, analysis of my ATACseq data shows that upstream progenitors cluster closely (blue), whilst a B-differentiation cluster from Pre-ELP/GMP to ProB progenitors is clearly defined, as is the myelo/erythroid cluster (Figure

5.4). Pre-ELP/GMPs cluster between B-cell progenitors and myeloid progenitors, in line with their observed lymphomyeloid potential during culture assays (see chapter 3). DESEQ2 was used to generate

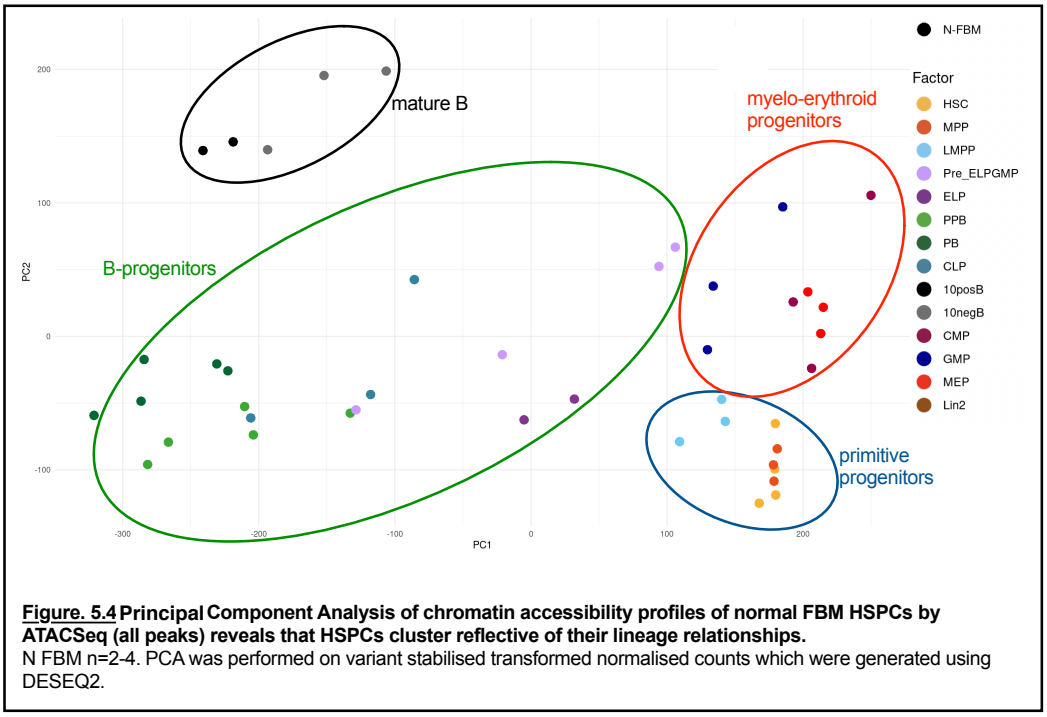


Figure. 5.4 Principal Component Analysis of chromatin accessibility profiles of normal FBM HSPCs by ATACSeq (all peaks) reveals that HSPCs cluster reflective of their lineage relationships.
N FBM n=2-4. PCA was performed on variant stabilised transformed normalised counts which were generated using DESEQ2.

normalised counts for ATACseq data due to it's favourable performance when considering biological sample size and false-positive rate (Gontarz et al, 2020), as well as compatibility with other ATACseq analysis packages such as DiffBind. ANOVA-based tests of RNAseq and ATACseq data was performed using EdgeR.

Next, I performed ANOVA-like tests across all the HSPC populations to determine the top differentially accessible genes by FDR (<0.001) with peak annotation based on nearest gene linkage (Figure 5.5). Overall, these data are consistent with the culture data presented in chapter 3. B-cell progenitors show more similar chromatin accessibility profiles as the PreB cells (10negB/10posB) (Figure 5.5), whilst the CMPs, GMPs and MEPs show a clearly distinct profile which is most similar to the earlier, upstream progenitors (HSC-LMPP), (Figure 5.5). This may reflect that i) both myelo-erythroid progenitors and upstream HSPCs lack the chromatin accessibility profile of the other HSPCs which have a stronger B-cell signature and ii) there is a greater degree of non-lymphoid priming in both population groups, relative to the B-progenitors.

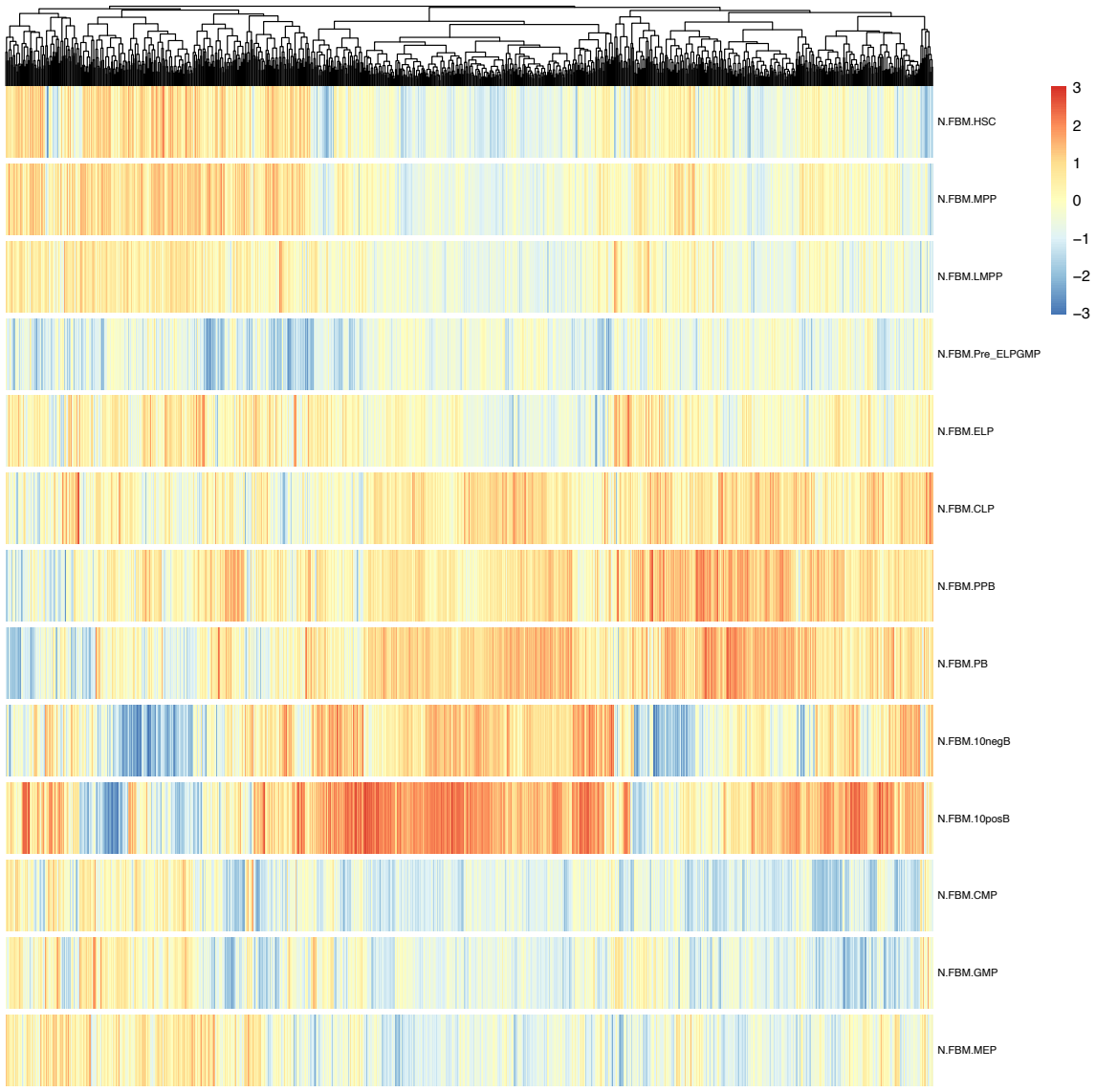


Figure 5.5 Forced clustering of normal FBM HSPC chromatin accessibility profiles by ATACseq (1000-2000 cells/pop) reveal similarities in chromatin accessibility profiles between lineage-associated progenitors. Heatmaps feature log2FC of the most differentially accessible genes determined by ANOVA (FDR <0.001) and are scaled by gene. For easier visual comparison, progenitors were forced to cluster based on their order within the proposed B-differentiation hierarchy. n= 2- 4 for each normal FBM HSPC population which were then grouped by cell type, e.g. N.FBM HSC. Normalisation of ATACseq data was performed in DESEQ2 and subsequent statistical analysis was performed using EdgeR.

Having preliminarily characterised FBM HSPCs based on their broad gene expression and chromatin accessibility signatures, I next wanted to assess the clustering of normal FBM HSPCs by the expression of specific haematopoietic lineage -associated genes.

To do this, I reviewed the literature on genes associated with the major haematopoietic lineages to create lists of genes of interest (GOI) and used these lists to filter the normalised

CPM counts of the gene expression data (Popescu et al, 2019; Jardine et al, 2021; Roy et al, 2021). Heatmaps and boxplots feature the normalised expression of lineage GOI and heatmaps are scaled by gene across the HSPCs included in the given heatmap.

B-lineage associated genes:

Looking first at the B-lineage associated genes, hierarchical clustering (Figure 5.6 A) resolves the expected relationships between progenitor populations. Early progenitors (HSC, MPP, LMPPs), cluster together and show expression of FLT3 as expected as well as relatively low expression of B-lineage genes (Figure 5.6 A). Pre-ELP/GMPs cluster with the PreProB and ProB B-cell progenitors and this sub-group collectively show moderate expression of all of the B-cell genes, both those with roles in early lineage specification (*EBF1, DNTT*) and later B-lineage commitment e.g. *CD19, CD79B, RAG1* (Figure 5.6, A/B). Finally, as expected Pre-B cells (10negB/ 10posB) show the greatest expression of late B-lymphoid genes (Figure 5.6, A).

Forced clustering of HSPCs shows the progressive increase in expression of B-lineage genes (Figure 5.6, B) along the proposed B-differentiation hierarchy. The transition from LMPP to Pre-ELP/GMP is accompanied by a clear increase in the expression of *EBF1*, an early B-lymphoid specification gene which increases through to B-progenitor stages before decreasing in Pre-B cells (Figure 5.6, C). Similarly, the expression of the later B-lineage gene *PAX5* is not detected until the Pre-ELP/GMP stage, although it's expression goes on to increase through to Pre-Bs (Figure 5.6, C). These findings support the in vitro data (chapter 3), which indicate Pre-ELP/GMP are functionally markedly more B-lineage restricted than their CD10-LMPP precursors.

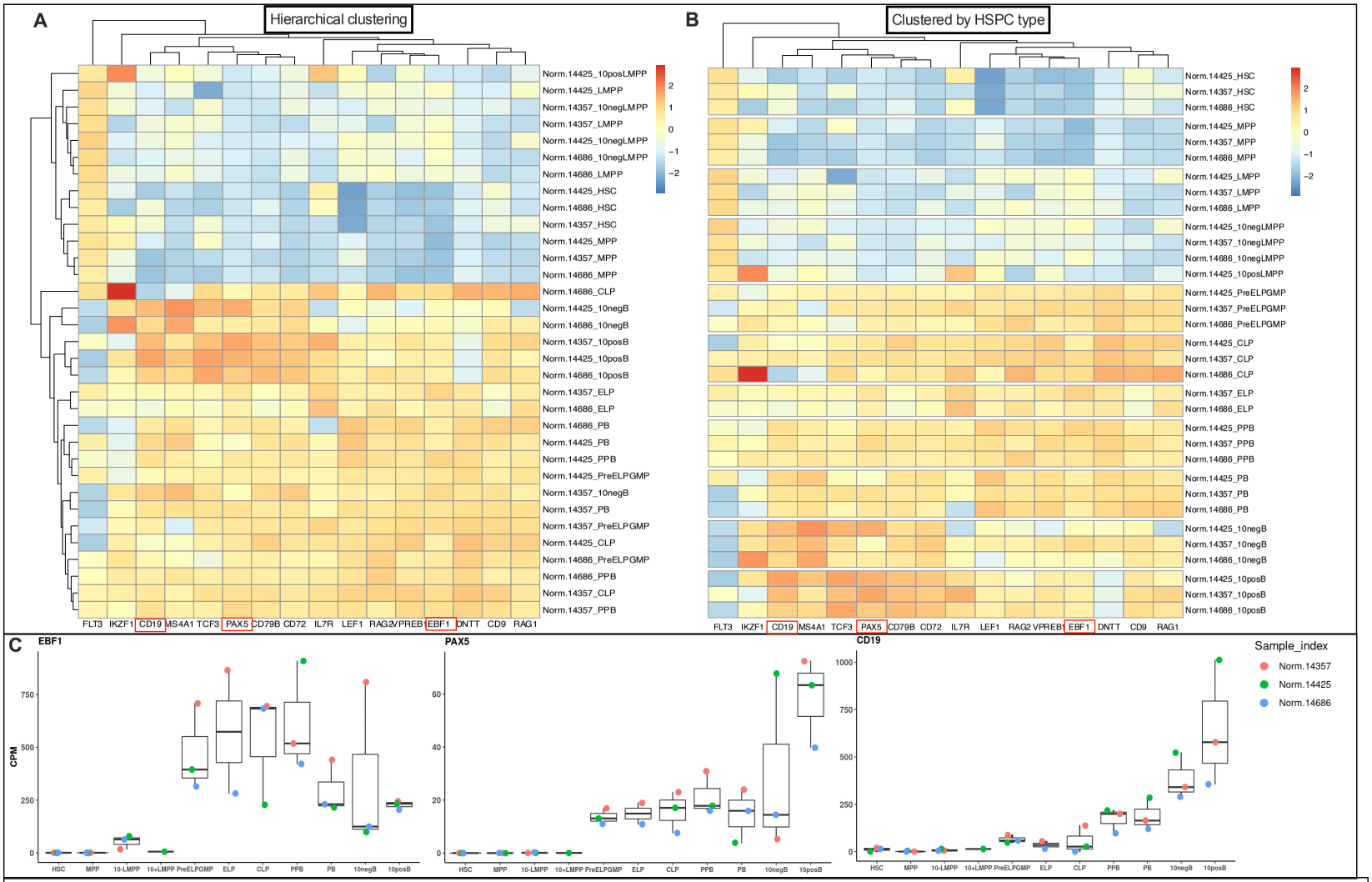


Figure 5.6 Expression of B-cell lineage-associated genes (normalised CPM, scaled by gene) in normal FBM HSPCs by RNA Seq (50-100 cells), mirrors their position in the B-cell hierarchy.
A. Hierarchical clustering of normal FBM HSPCs based on B-lineage associated GOI reveals Pre-ELP/GMPs cluster closely with B-progenitors, whilst CD10-/+ LMPPs cluster together, with mpre primitive HSCs and MPPs. **B.** Forced clustering based on HSPC type and position in the proposed B-differentiation pathway reveals a clear trend in the expression B-lineage associated genes, which gets progressively higher throughout differentiation. **C.** Normalised CPM counts of selected genes (*EBF1, PAX5, CD19)* reveals that Pre-ELP/GMP are the first early rogenitor in which the early B-lymphoid specification gene *EBF1* can be detected and later decreases in Pre-B cells, whilst levels of the B-lymphoid commitment genes PAX5 and CD19 show continual increase through to the Pre-B cell stage. All analysis was performed using EdgeR.

Similarly, the chromatin accessibility traces of selected B-lineage associated genes within normal FBM HSPCs, visualised using the UCSC browser, supports the gene expression data (Figure 5.7). Broadly speaking, B-lineage genes become more accessible down the lineage trajectory, i.e. in pre-B cells compared with HSCs (Figure 5.7)

This is particularly evident at highly conserved regions (indicated by the conservation track at the bottom of gene traces), which are thought to correlate with regulatory elements, such as promoters or enhancers. For example, two intragenic regions within *MME,* the gene encoding CD10, which are listed as gene regulatory elements on both Ensembl and GeneCards gene assembly tools, appear more accessible in the immunophenotypically CD10+ HSPCs, namely CLP, ProB and CD10+ Pre-B, when compared to CD10- Pre-ELP/GMP, ELP and Pre-ProB (Figure 5.7).

These profiles reveal that Pre-ELP/GMP exhibits greater accessibility in the selected B-cell genes than upstream precursors (HSC – LMPP) (Figure 5.7). Greater chromatin accessibility could explain the greater expression of several B-cell genes in Pre-ELP/GMPs compared with earlier progenitors (Figure 5.6).

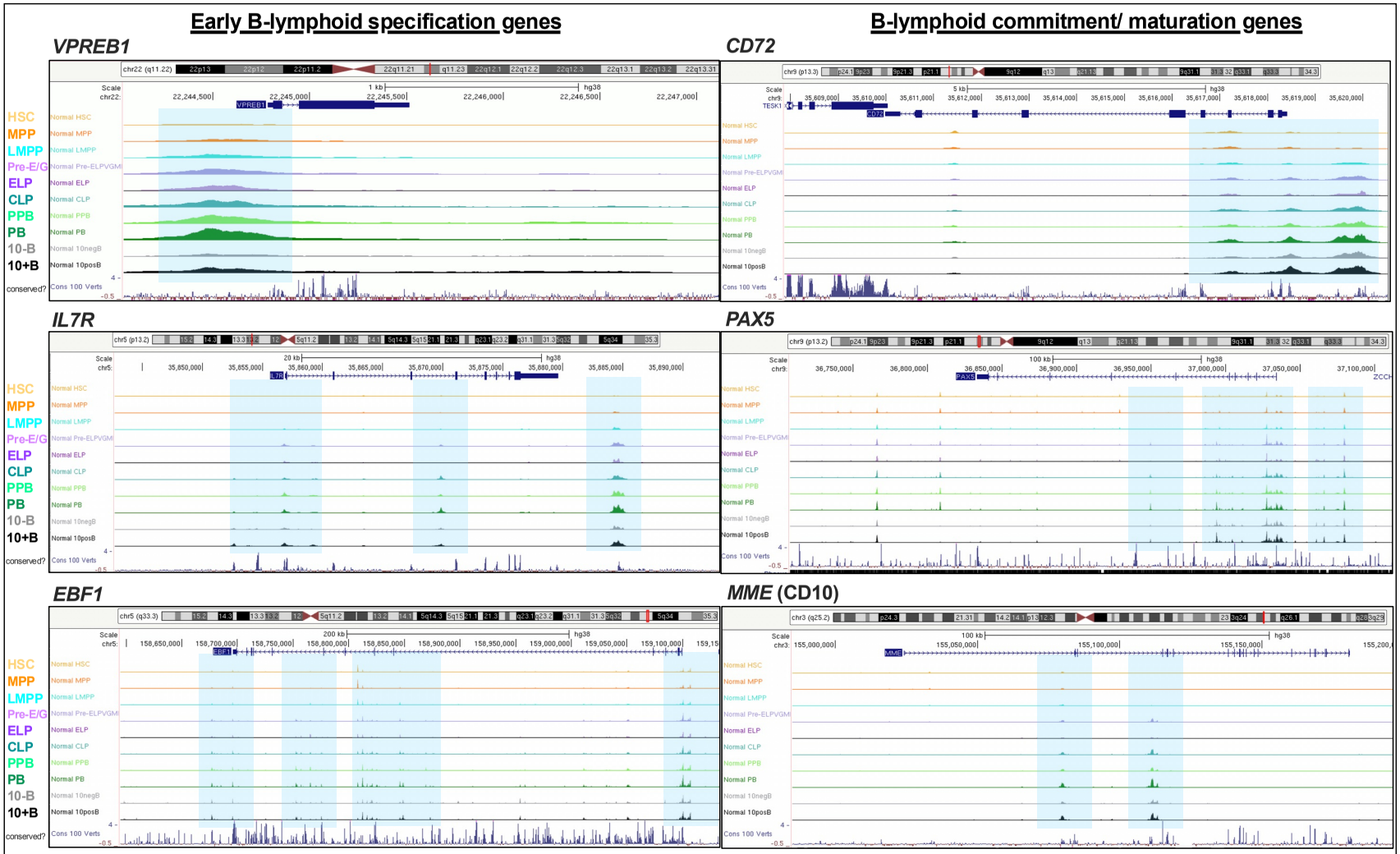


Figure 5.7 Chromatin accessibility profiles of selected B-lineage-associated genes of normal FBM HSPCs ATAC Seq (1000-2000 cells/population), reveals greater accessibility in more B-lymphoid restricted populations, correlating with expression profiles from RNA Seq (50-100 cells). Profiles were visualised in the UCSC browser, with representative merged traces shown. Selected genes with early and late roles in B-lymphopoiesis are shown on the left and right, respectively. Progenitors are listed from least (HSC) to most B-lineage restricted (10-/+ Pre-B cells), with a coloured key shown (left). Blue highlighted regions indicate visually differentially accessible peaks between HSPCs. Transcript assembly is shown at the top of each frame (Hg38), with transcription start site (TSS) indicated and direction of transcription shown using arrows. Degree of conservation across 100 verterbrate classes across the transcript is indicated by peak height.

Next, I wanted to explore the non B-lineages, given that the newly described progenitors presented in this thesis were also able to give rise to myeloid, NK- and T-cells in vitro (see chapter 3). For these heatmaps, I forced progenitors to cluster by their position within the proposed differentiation hierarchy for easier visual appraisal of expression of lineage associated genes across different HSPC populations. Heatmaps and boxplots feature the normalised expression of lineage GOI and heatmaps are scaled by gene across the HSPCs included in the given heatmap.

Myeloid lineage associated genes:

CMPs and GMPs showed the greatest expression for GOI associated with myelopoiesis, as expected (Figure 5.8 A/B).

HSCs and MPPs expressed relatively low levels of most of the myeloid-associated genes (Figure 5.8 A/B). However, PU.1 (*SPI1*), the master regulator responsible for directing multipotent progenitors toward the myeloid lineage, is detectable in HSCs and even more so in MPPs (Figure 5.8 B). Similarly, *FLT3* which has known roles in early myeloid and lymphoid specification, is also expressed (Figure 5.8 A).

Several myeloid genes show increased expression in LMPPs and CD10-LMPPs relative to HSCs and MPPs including *MPO* and *CEBPA (*Figure 5.8 A/B), though these findings were not significant. Profiles of LMPPs and CD10-LMPPs are highly similar, which likely reflects the fact that the majority of LMPPs in normal FBM are CD10- (HSPC frequencies, chapter 3), (Figure 5.8 A). For some of the myeloid GOI, Pre-ELP/GMPs show comparable or higher expression, such as *AZU1, PRTN3* and *MPO*, however the expression of several others

(*CEBPA, RUNX2, CSF1R, CSF3R, FLT3*) is higher in the LMPPs which would be consistent with their greater in vitro myeloid potential (Figure 5.8 A).

Whilst Pre-ELP/GMP do produce a small amount of GMPs in vitro (chapter 3), the myeloid expression profile of Pre-ELP/GMPs in normal FBM much more closely resembles CD10- LMPPs and ELP than GMP, which may suggest myeloid potential but a lack of strong myeloid priming (Figure 5.8 A). This could also suggest switching off of myeloid programmes as Pre-ELP/GMPs skew toward an ELP in normal FBM (chapter 3).

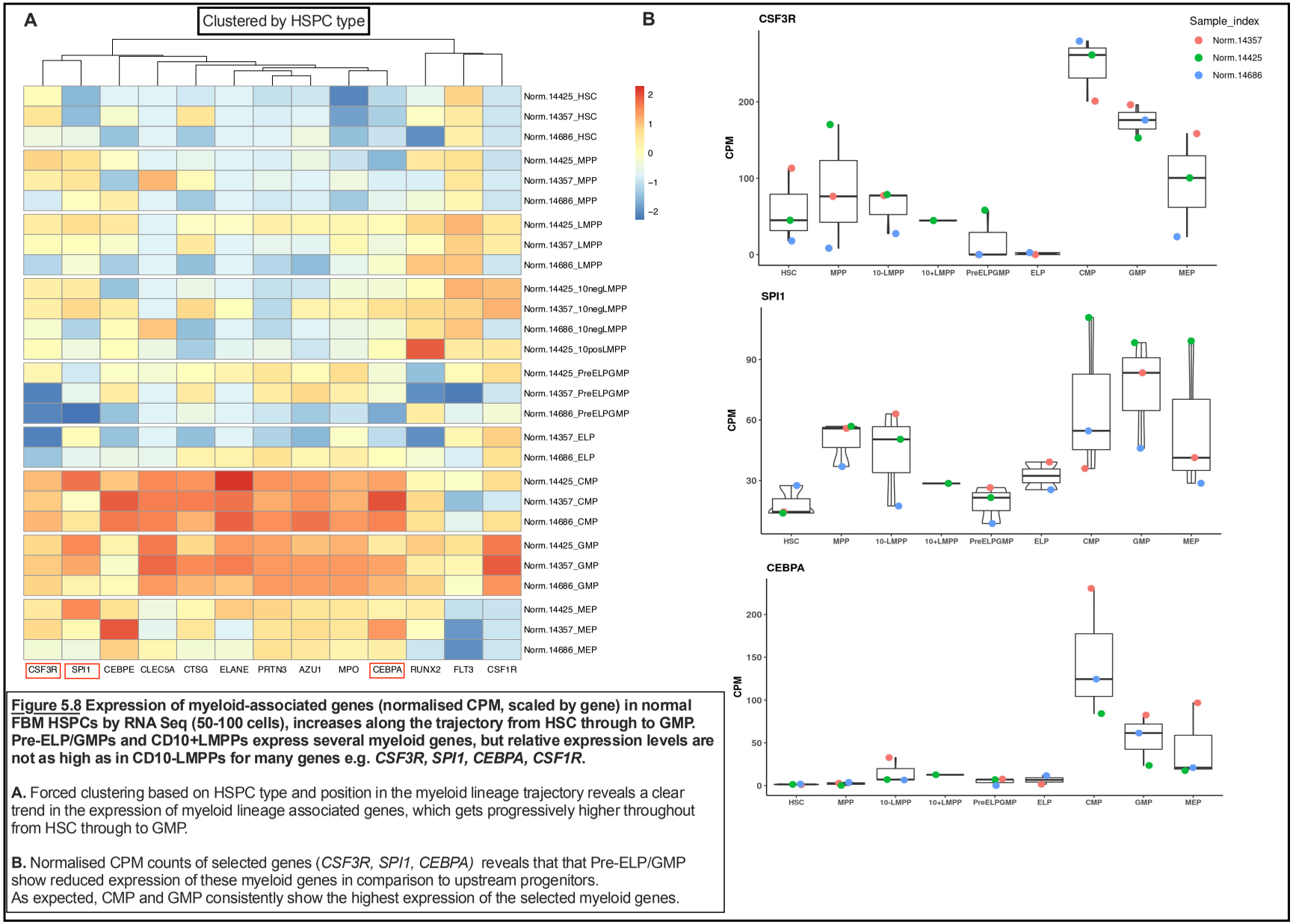


Figure 5.8 Expression of myeloid-associated genes (normalised CPM, scaled by gene) in normal FBM HSPCs by RNA Seq (50-100 cells), increases along the trajectory from HSC through to GMP. Pre-ELP/GMPs and CD10+LMPPs express several myeloid genes, but relative expression levels are not as high as in CD10-LMPPs for many genes e.g. *CSF3R, SPI1, CEBPA, CSF1R*.

A. Forced clustering based on HSPC type and position in the myeloid lineage trajectory reveals a clear trend in the expression of myeloid lineage associated genes, which gets progressively higher throughout from HSC through to GMP.

B. Normalised CPM counts of selected genes (*CSF3R, SPI1, CEBPA)* reveals that that Pre-ELP/GMP show reduced expression of these myeloid genes in comparison to upstream progenitors.
As expected, CMP and GMP consistently show the highest expression of the selected myeloid genes.

Chromatin accessibility traces of selected myeloid genes (Figure 5.9) supported the gene expression trends observed in normal FBM HSPCs. Accessibility at the *CEBPA* TSS increases between HSC to LMPP and then becomes less accessible between LMPP > Pre-ELP/GMP > ELP, supporting the expression trends observed (Figure 5.9). Similarly for the early myeloid specification gene *CSF3R*, accessibility proximal to the TSS is reduced in Pre-ELP/GMPs, ELPs and MEPs, relative to upstream multipotent progenitors and CMPs and GMPs (Figure 5.9), the same trend that was observed at the transcriptional level (Figure 5.8, B). Both the accessibility and expression of *MPO* increases between HSC and Pre-ELP/GMP (Figure 5.9), and subsequently decreases in ELPs. The peak proximal to the TSS of *PRTN3*, a granulocyte-specification gene, is most distinguishable in the CMP and GMP traces (Figure 5.9).

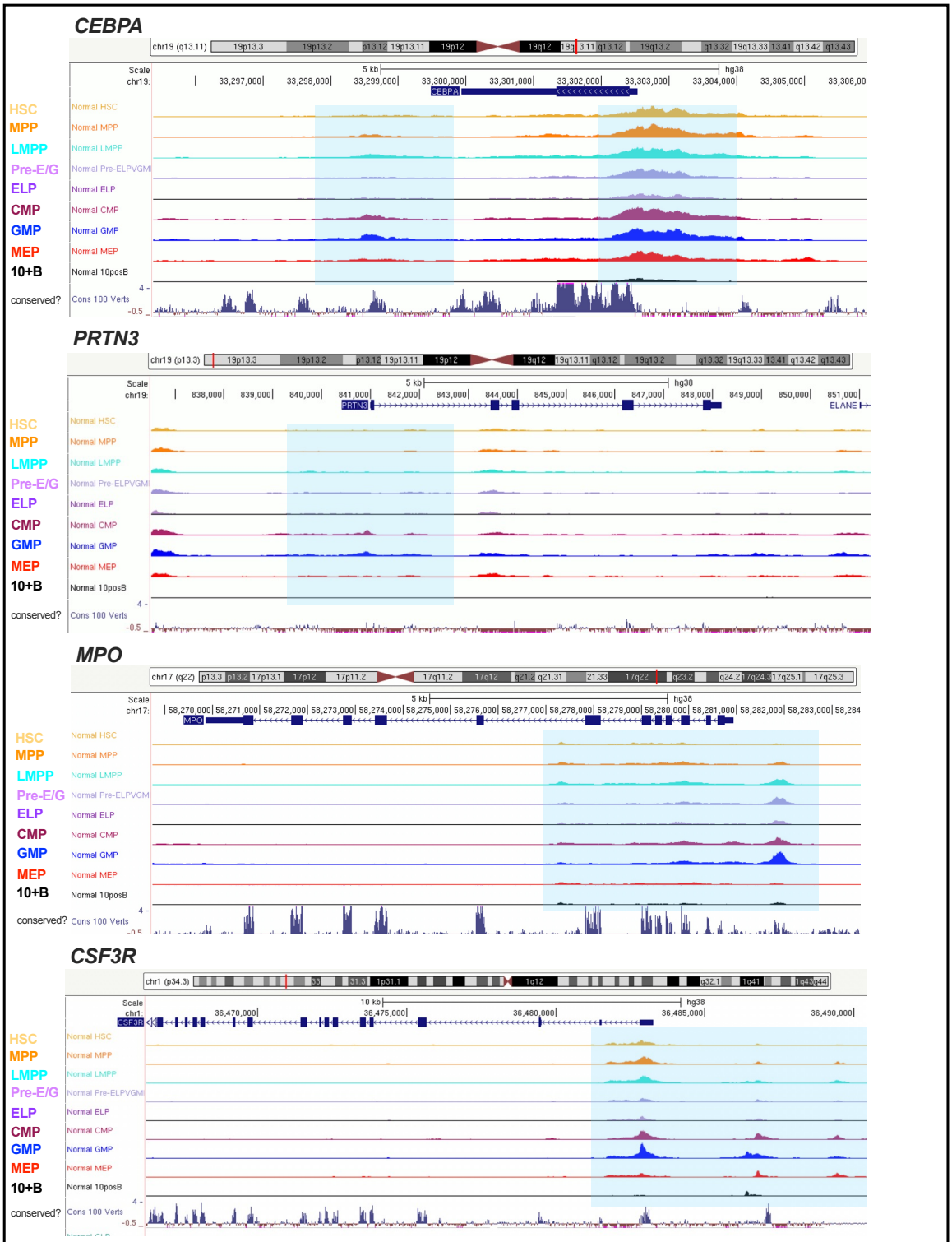


Figure 5.9 Chromatin accessibility profiles of selected genes associated with myelopoiesis within normal FBM HSPCs by ATAC Seq (1000-2000 cells/population), reveals greater accessibility in more myeloid restricted populations, correlating with expression profiles from RNA Seq (50-100 cells). Profiles were visualised in the UCSC browser, with representative merged traces shown. Transcript assembly is shown at the top of each frame (Hg38), with transcriptional start site (TSS) indicated and direction of transcription shown using arrows. Blue highlighted regions indicate visually differentially accessible peaks between HSPCs. Degree of conservation across 100 verterbrate classes across the transcript is indicated by peak height.

NK and T- lineage associated genes

Looking at genes associated with the NK and T-lineage (Figure 5.10 A), at the LMPP stage, expression of several NK-associated genes become detectable, including *ILR15A, TOX, NKG7* and *TYROPB,* with CD10-/+ populations showing similar expression levels (Figure 5.10 A). Downstream, within Pre-ELP/GMPs, a subset of additional genes appear to be switched on, including *PRMD1, ZEB2, ID2/3* and *FOXO1.* Both *PRMD1* and *FOXO1* are negative regulators of NK differentiation (Smith et al, 2010; Deng et al 2015) therefore their increased expression in Pre-ELP/GMPs relative to LMPPs may represent lymphoid potential being directed toward a more B-primed state, with NK programmes being repressed.

Similarly to the pattern observed for NK-associated genes, LMPPs represent the first progenitor type in which several T-lineage specific genes are expressed, including *SATB1,* which is involved in specifying progenitors toward the T-lineage, as well as *TCF12* which encodes HEB, a master regulator of T-cell differentiation (Figure 5.10 B). Like the NK associated genes, Pre-ELP/GMPs show similar, if slightly reduced overall expression of T-lineage genes compared to LMPP, for example of *SATB1* (Figure 5.10 B), which might suggest the diversion of lymphoid potential away from T (and NK) fates toward the B-lineage, supporting the in vitro data which showed strong B-cell priming (chapter 3).
In later B-progenitors and mature B-cells, the expression of T-lineage specific genes is reduced, whilst the expression of genes with roles in multi-lymphoid differentiation e.g. *IL7-R* and *IKZF1* are maintained (Figure 5.10 B).

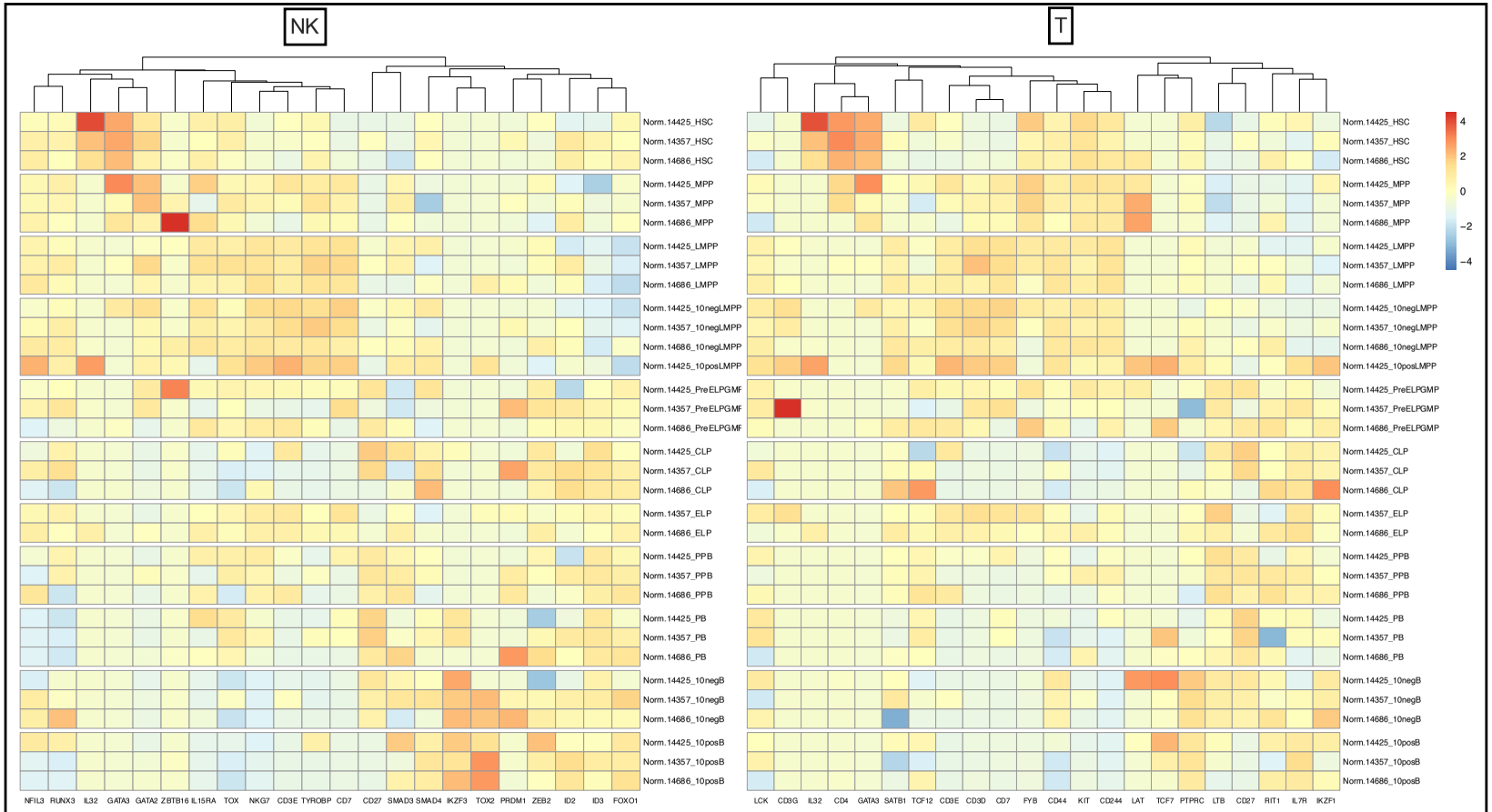


Figure 5.10 Expression of NK and T-lineage- associated genes (normalised CPM, scaled by gene) in normal FBM HSPCs by RNA Seq (50-100 cells) reveals that the expression of several GOI peaks at the LMPP stage and begins to decrease from Pre-ELP/GMPs onwards, presumably as progenitors adopt a more B-lineage primed state.
Forced clustering based on HSPC type and position in the NK/T lineage trajectory. Scaling was the same due to similar expression levels of GOI for each lineage, hence one scale bar is shown (top right). Due to their common upstream progenitor (CLP) and similar downstream immune functions, some GOI for NK and T-cells overlap, however the majority of GOI presented here are unique to either lineage.

A. NK-lineage associated genes
B. T-lineage associated genes

Pairwise comparisons normal FBM HSPCs

To identify which genes are differentially expressed during differentiation transitions e.g. CD10-LMPP to Pre-ELP/GMP, I used EdgeR to perform pairwise comparisons (Figure 5.11) and determine the DEG between selected HSPC populations of interest.

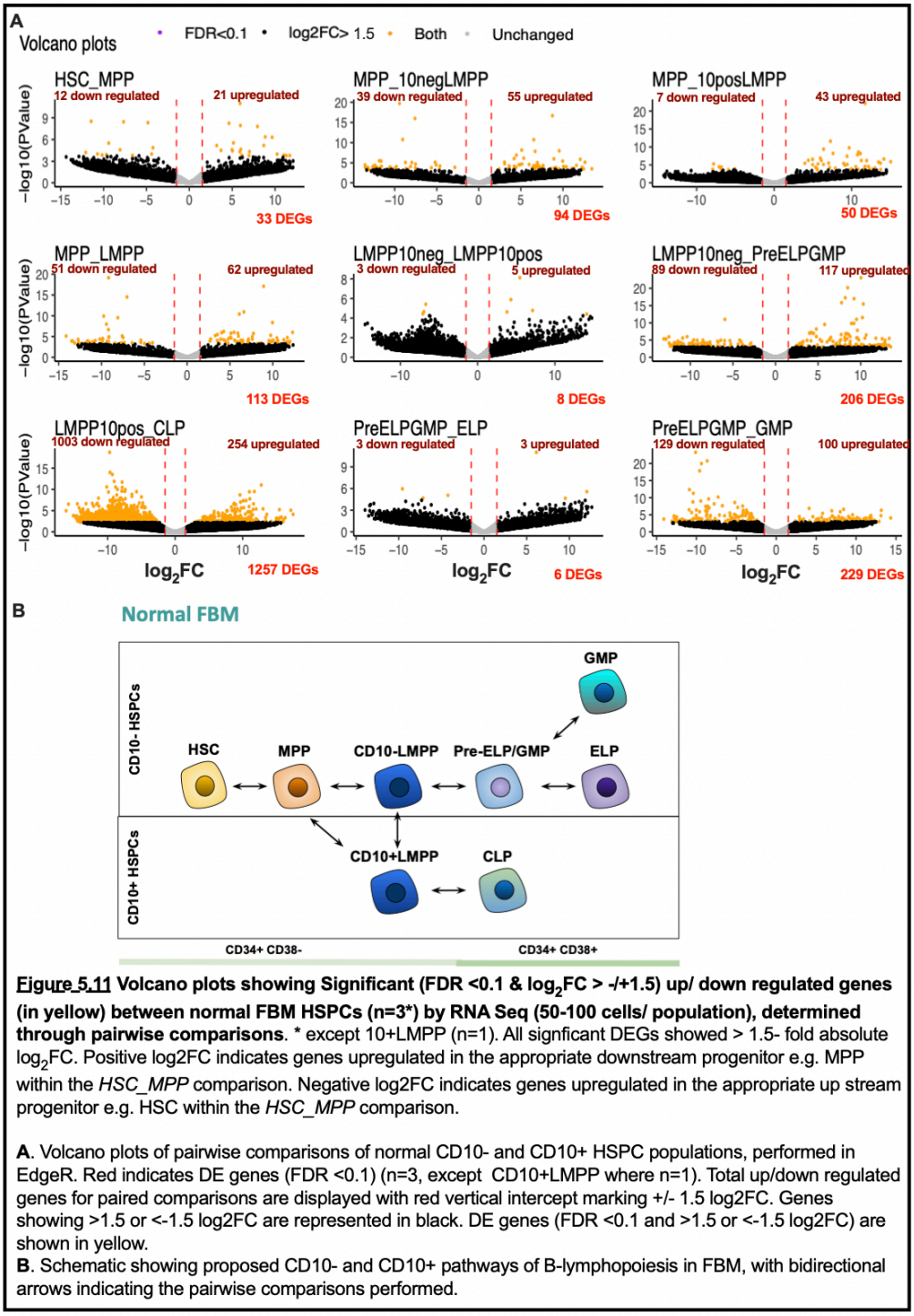


Figure 5.11 Volcano plots showing Significant (FDR <0.1 & log_2FC > -/+1.5) up/ down regulated genes (in yellow) between normal FBM HSPCs (n=3*) by RNA Seq (50-100 cells/ population), determined through pairwise comparisons. * except 10+LMPP (n=1). All signficant DEGs showed > 1.5- fold absolute log_2FC. Positive log2FC indicates genes upregulated in the appropriate downstream progenitor e.g. MPP within the *HSC_MPP* comparison. Negative log2FC indicates genes upregulated in the appropriate up stream progenitor e.g. HSC within the *HSC_MPP* comparison.

A. Volcano plots of pairwise comparisons of normal CD10- and CD10+ HSPC populations, performed in EdgeR. Red indicates DE genes (FDR <0.1) (n=3, except CD10+LMPP where n=1). Total up/down regulated genes for paired comparisons are displayed with red vertical intercept marking +/- 1.5 log2FC. Genes showing >1.5 or <-1.5 log2FC are represented in black. DE genes (FDR <0.1 and >1.5 or <-1.5 log2FC) are shown in yellow.
B. Schematic showing proposed CD10- and CD10+ pathways of B-lymphopoiesis in FBM, with bidirectional arrows indicating the pairwise comparisons performed.

For the novel progenitors, only 8 DEGs were detected between CD10-/+ LMPPs (Figure 5.11) although the power of this analysis is limited because of the single CD10+ LMPP sample available. Interestingly, however, I detected over 200 DEGs between 10-LMPP and Pre-ELP/GMP, showing that these are distinct progenitor populations. Moreover, this may indicate that the CD10-LMPP > Pre-ELP/GMP shift is a major transition point in differentiation or possibly that these cell populations are not as close in the differentiation trajectory as anticipated (Figure 5.11).

229 DEGs were detected between Pre-ELP/GMPs and GMPs, whilst there were only 6 DEGs between Pre-ELP/GMPs and ELPs. This disparity helps explain the in vitro data which showed Pre-ELP/GMPs producing a greater proportion of ELPs than GMPs (see chapter 3), and that the output of Pre-ELP/GMPs and ELPs were similar (B-progenitors and Pre-B cells) (see chapter 3). The high number of DEGs between CD10+LMPP and CLP (also CD10+) (Figure 5.11) is potentially interesting but is difficult to interpret given the single CD10+ LMPP sample.

I went on to explore further by prioritising the newly described progenitors and their upstream progenitors and filtering DEG based on their relevance in haematopoiesis.

Of the 33 DEG between HSC/MPP, 24 had a known role in haematopoiesis (15 were upregulated in MPP and 9 were downregulated). Most of the DEGs in the HSC/MPP comparison were involved in megakaryopoiesis, erythropoiesis and myelopoiesis and only four had known links to B-lymphopoiesis (*CD9, LEF1, RAG1, IL7R)* (Figure 5.12). *CD9* has dual roles in both B-lymphopoiesis and megakaryopoiesis.

By contrast, comparison of MPPs and CD10-LMPP showed that the majority of the upregulated haemopoiesis-associated DEGs in CD10-LMPP (18/30) are those associated with

B-lymphopoiesis and several others with pan-lymphopoiesis or T/NK differentiation. The upregulated B-lymphoid gene subset includes genes involved in both early B-lineage specification (*EBF1, VPREB1)* and those associated with a more B-cell committed phenotype (*CD10, RAG1, CD72) (*Figure 5.12). As expected, the majority of downregulated genes are those associated with stemness and self-renewal (yellow) and megakaryo/erythropoiesis (Figure 5.12).

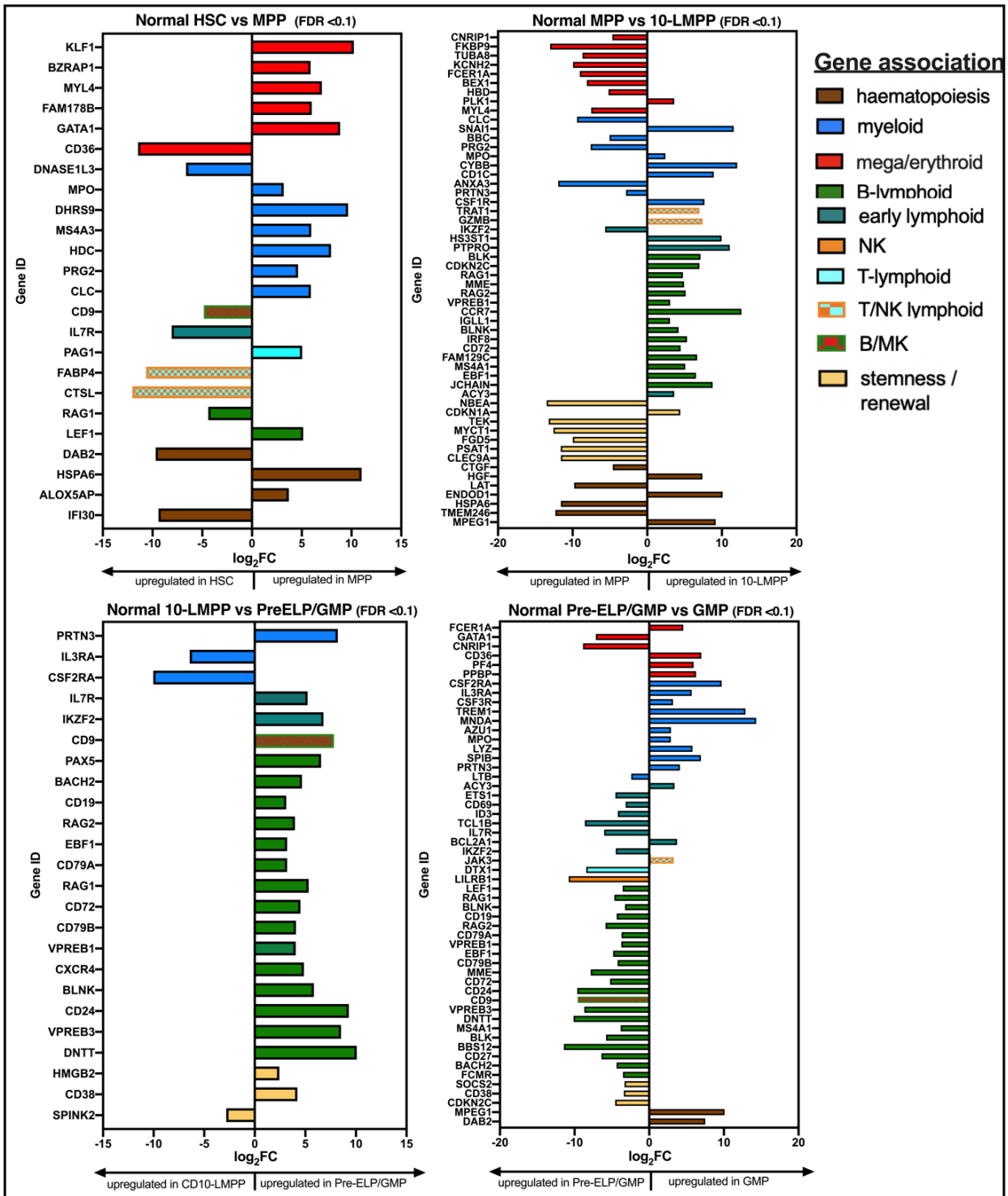


Figure 5.12 Significantly differentially expressed genes (DEGs) with known haematopoietic roles, in flow-sorted normal FBM HSPCs by RNA Seq (FDR <0.1, log_2FC >1.5).

Pairwise comparisons were performed using EdgeR. Positive log2FC indicates genes upregulated in the downstream progenitor e.g. MPP within the *HSC_MPP* comparison. Negative log2FC indicates genes upregulated in the upstream progenitor e.g. HSC within the *HSC_MPP* comparison. N=3 for normal FBM.

Colour key:

Brown: genes associated with multi-lineage haematopoiesis, **blue**: genes associated with myelopoiesis, **red**: genes associated with erythropoiesis/megakaryopoiesis, **green**: genes associated with B-lymphopoiesis, **teal**: genes associated with early pan-lymphopoiesis, **orange**: genes associated with NK-poiesis, **pale green**: genes associated with T-lymphopoiesis, **pale green with orange**: T/NK associated genes, **red with green**: B/megakayopoiesis associated genes, **yellow:** stemness / self renewal associated genes.

Of the 206 DEG between Pre-ELP/GMPs and CD10-LMPPs, I identified 24 haematopoiesis-associated genes, 21 of which were upregulated in Pre-ELP/GMPs, including 18 B-lineage associated genes (Figure 5.12). By contrast, of the 3 myeloid DEG, *CSF2RA* and *IL3RA* were downregulated in Pre-ELP/GMPs (Figure 5.12), supporting the minimal functional myeloid output observed in methylcellulose assays (see chapter 3). The lower expression of the stem gene *SPINK2* would be consistent with the downstream position of Pre-ELP/GMPs relative to CD10-LMPPs (Figure 5.12).

Of the 229 DEG during the transition from Pre-ELP/GMPs to GMPs, 54 genes with known haematopoietic function are differentially expressed (Figure 5.12). This includes a marked decrease in expression of several genes associated with B-lymphopoiesis including *BACH2, VPREB1, LEF1 CD10, CD19* and concurrent upregulation of several myeloid genes including *SPIB, IL3RA, MPO* and *CSF2RA* (Figure 5.12).

By contrast, only 6 DEGs were detected between Pre-ELP/GMPs and ELPs: 3 genes were upregulated in ELP (*CLC, TNFSF9, TNFRSF25*) and 3 were downregulated (*TCL1B, CD9, ZNF44*). *CD9* is expressed in both megakaryocytes and later stage B-lymphopoiesis, so this decrease in its expression could represent a decrease in MK or B-priming. *TCL1B,* which plays a role in T-cell development, was markedly downregulated in ELP (log2FC = -9.57, FDR= 0.011) which may indicate a downregulation of other lymphoid programmes to allow B-cell priming in normal FBM ELPs.

Unfortunately, pairwise comparisons of CD10-/+ LMPPs yielded only 8 DEGs (Figure 5.12) but the availability of a single CD10+ LMPP sample due to population scarcity in normal FBM makes it difficult to draw conclusions.

5.3 The impact of T21 on the transcriptome and chromatin accessibility of FBM HSPCs

Next, I performed comparative analysis with the progenitor populations from DS FBM to try and gain a molecular insight into the striking B-cell defect and lineage bias observed during functional assays of DS FBM HSPCs (see chapter 4).

Hierarchical analysis of normal vs DS FBM HSPCs

To get an overview of the hierarchical relationships between DS FBM HSPCs I performed several kinds of dimensionality reduction analyses. Initial PCA of all expressed genes resolved 4 clusters: early progenitors, B-progenitors, myelo-erythroid progenitors and mature B-cells (Figure 5.13). The most surprising finding was that DS Pre-ELP/GMP clustered with the myelo-erythroid progenitors.

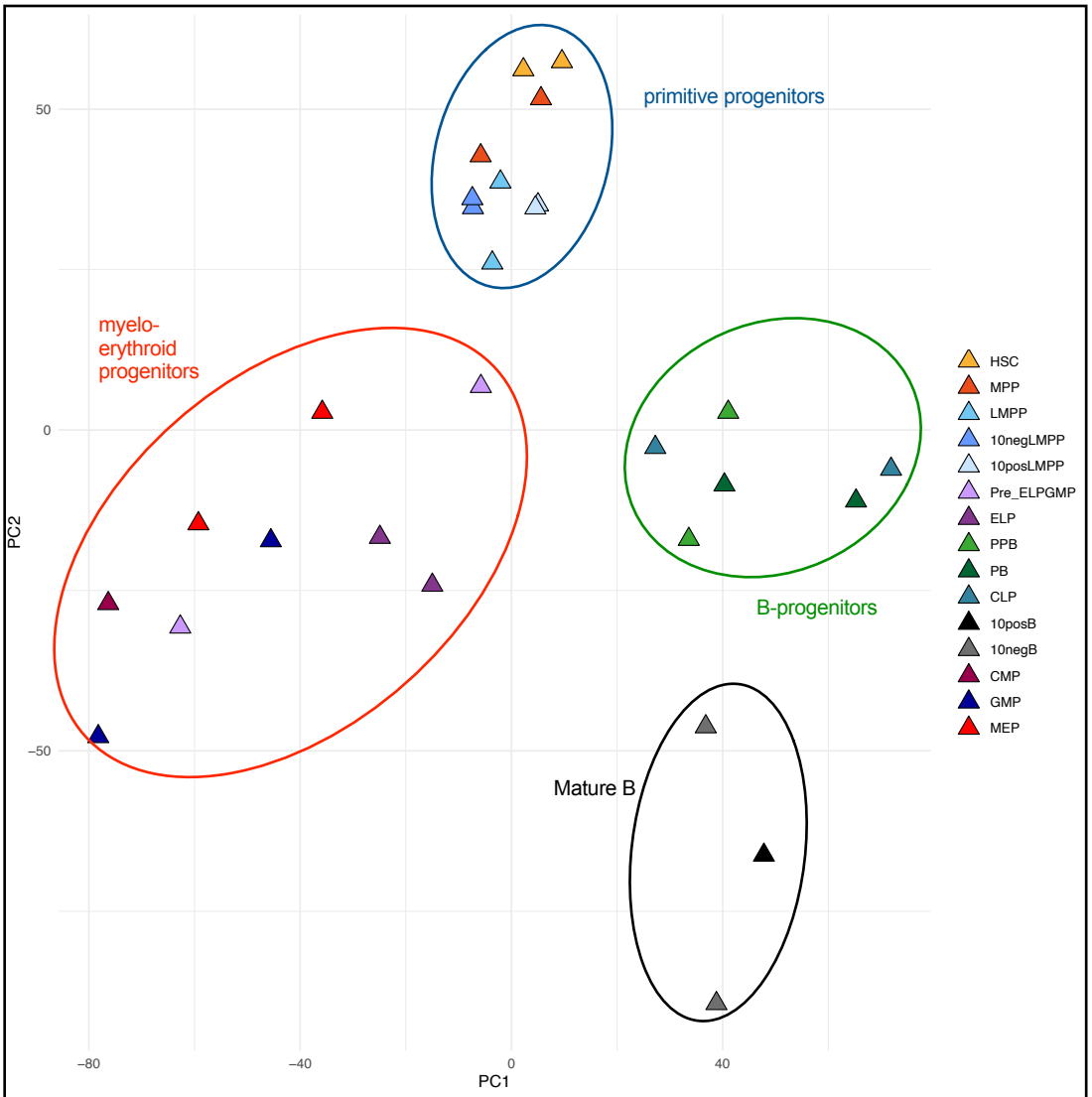


Figure 5.13 Principal Component Analysis of all expressed genes in DS FBM HSPCs (50-100 cells/population) by RNASeq demonstrates HSPCs cluster according to lineage, with DS ELPs and PreELP/GMPs clustering more closely with myelo-erythroid progenitors. Clusters are labelled according to their lineage: primitive progenitors (blue), B-progenitors (green), mature B-cells (black), and myelo-erythroid progenitors (red).
DS FBM n=2, except 10posB and CMP (n=1). PCA was performed on variant stabilised transformed normalised read counts across all genes.

Having observed that DS Pre-ELP/GMP and ELPs clustered closely with CMPs, GMPs and MEP during PCA, I performed PCA on the top 500 variably expressed genes (Figure 5.14), which I presumed would be more likely to include haematopoietic genes, to determine whether Pre-ELP/GMPs and ELPs continued to display the same clustering pattern.

As expected, PCA of the most variably expressed genes more clearly resolved the expected haematopoietic lineages (Figure 5.14), however both Pre-ELP/GMPs and ELPs fell between the B-progenitor cluster and GMPs, suggesting shared similarities with both lineages in DS FBM.

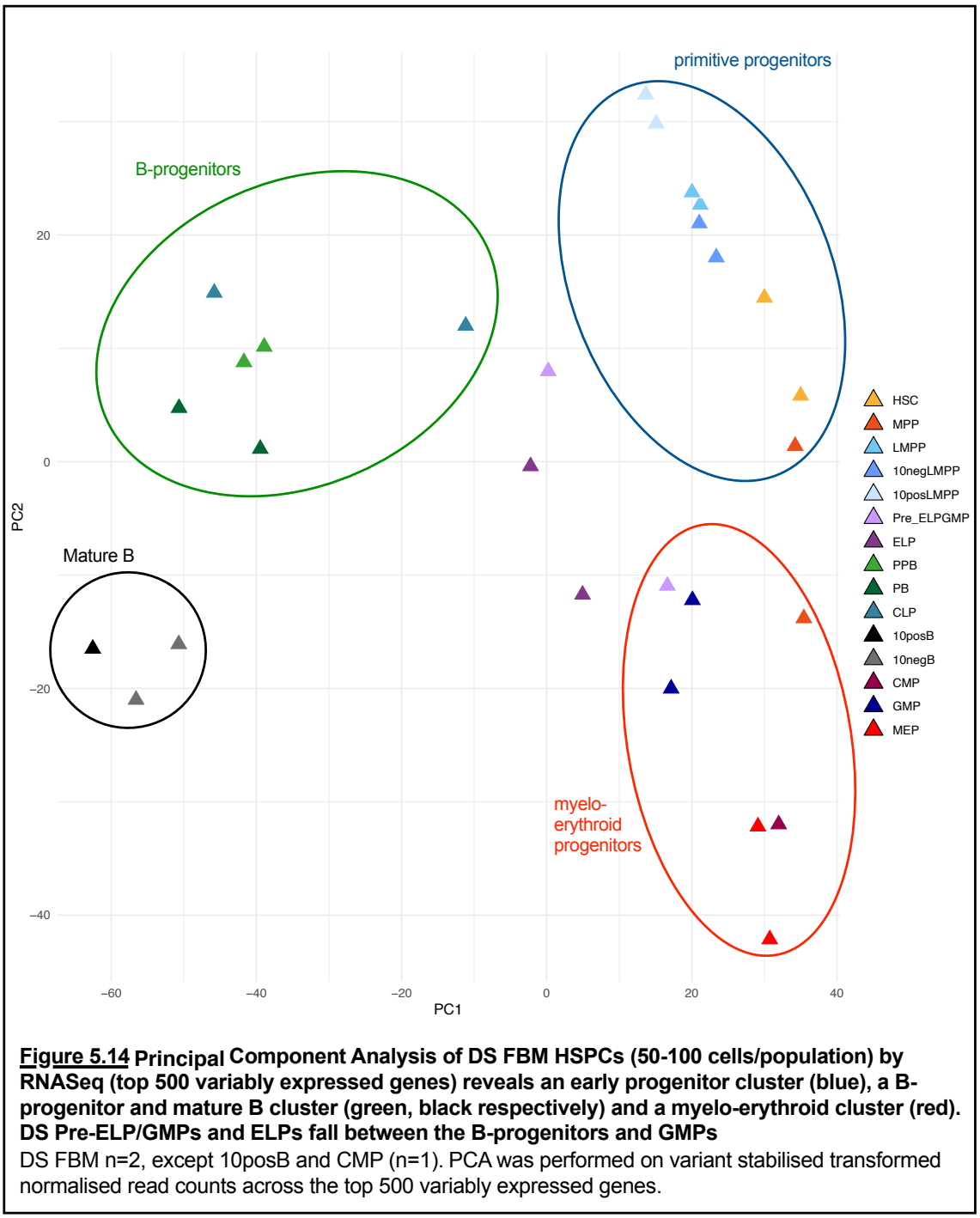


Figure 5.14 Principal Component Analysis of DS FBM HSPCs (50-100 cells/population) by RNASeq (top 500 variably expressed genes) reveals an early progenitor cluster (blue), a B-progenitor and mature B cluster (green, black respectively) and a myelo-erythroid cluster (red). DS Pre-ELP/GMPs and ELPs fall between the B-progenitors and GMPs

DS FBM n=2, except 10posB and CMP (n=1). PCA was performed on variant stabilised transformed normalised read counts across the top 500 variably expressed genes.

This is in contrast to normal FBM where Pre-ELP/GMP and ELP cluster with the B progenitors, (Figure 5.15). These clustering patterns were observed both when all genes and when top 500 variably expressed genes were included in analyses (Figure 5.15 A, B respectively).

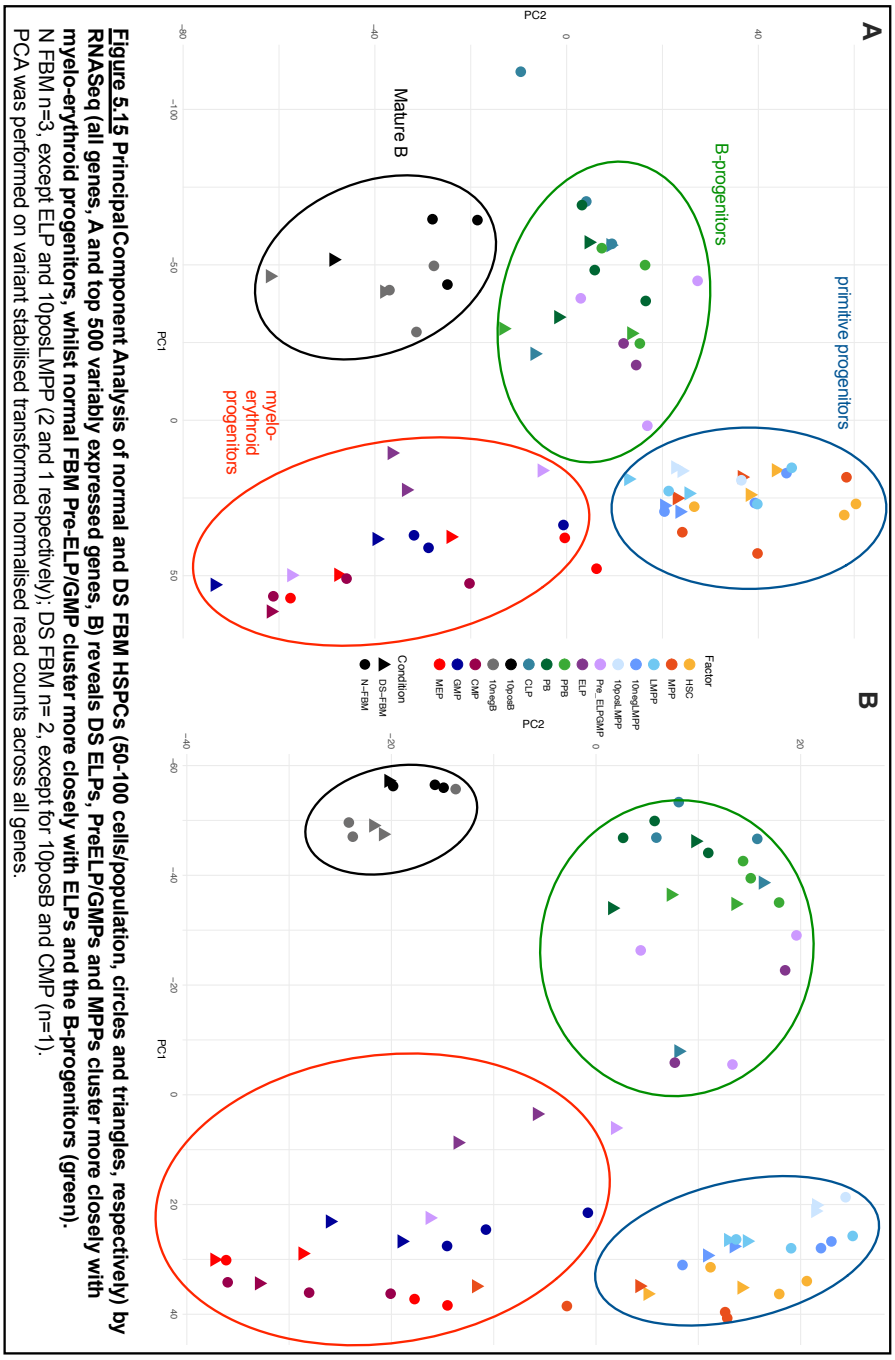


Figure 5.15 Principal Component Analysis of normal and DS FBM HSPCs (50-100 cells/population, circles and triangles, respectively) by RNASeq (all genes, A and top 500 variably expressed genes, B) reveals DS ELPs, PreELP/GMPs and MPPs cluster more closely with myelo-erythroid progenitors, whilst normal FBM Pre-ELP/GMP cluster more closely with ELPs and the B-progenitors (green).
N FBM n=3, except ELP and 10posLMPP (2 and 1 respectively); DS FBM n= 2, except for 10posB and CMP (n=1). PCA was performed on variant stabilised transformed normalised read counts across all genes.

Hierarchical based clustering also showed DS Pre-ELP/GMP and ELPs clustered closer to GMPs than normal counterparts, with the expression profiles in the 2 DS samples showing differences both between each other and with their normal counterparts as seen in the PCA (Figure 5.16). By contrast, DS CD10-LMPPs showed very similar profiles to normal and segregated within a large LMPP cluster (Figure 5.16). Whilst DS HSCs and MPPs clustered closely to normal counterparts, their profiles showed subtle differences (Figure 5.16).

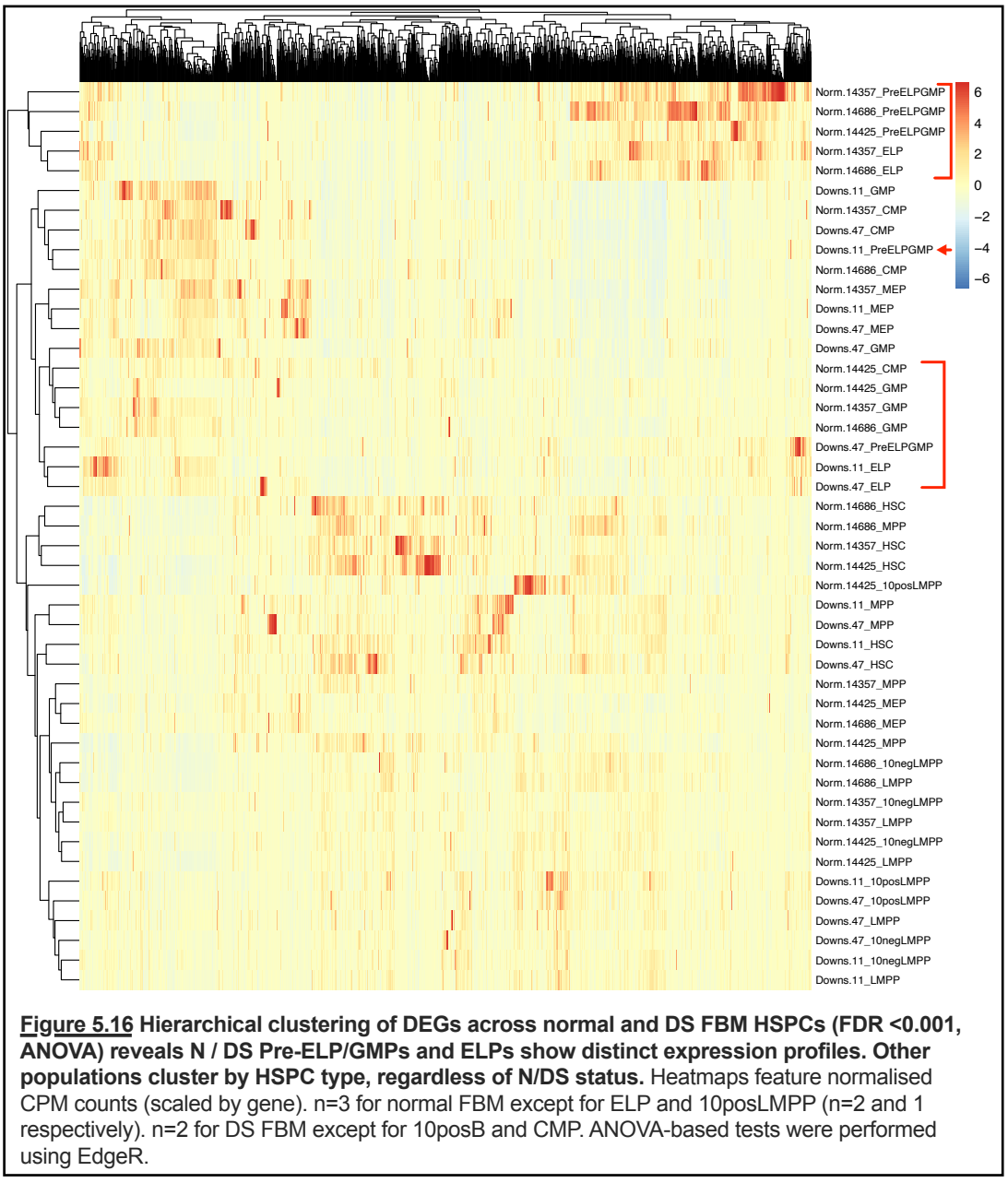


Figure 5.16 Hierarchical clustering of DEGs across normal and DS FBM HSPCs (FDR <0.001, ANOVA) reveals N / DS Pre-ELP/GMPs and ELPs show distinct expression profiles. Other populations cluster by HSPC type, regardless of N/DS status. Heatmaps feature normalised CPM counts (scaled by gene). n=3 for normal FBM except for ELP and 10posLMPP (n=2 and 1 respectively). n=2 for DS FBM except for 10posB and CMP. ANOVA-based tests were performed using EdgeR.

I next wanted to see whether these differences in progenitor clustering were consistent based on chromatin accessibility. I first confirmed that libraries derived from trisomic cells showed the expected 1.5-fold increase in chr21 mapped reads; indeed, chr21-mapped reads were 1.51-fold enriched in DS libraries relative to normal (mean proportional read contribution: 1.71% in DS and 1.13% in N FBM HSPCs) (Figure 5.17). Validating this, the relative proportion of non Chr21-mapped reads in normal/ DS was comparable for chr7 and other assessed chromosomes (Figure 5.17).

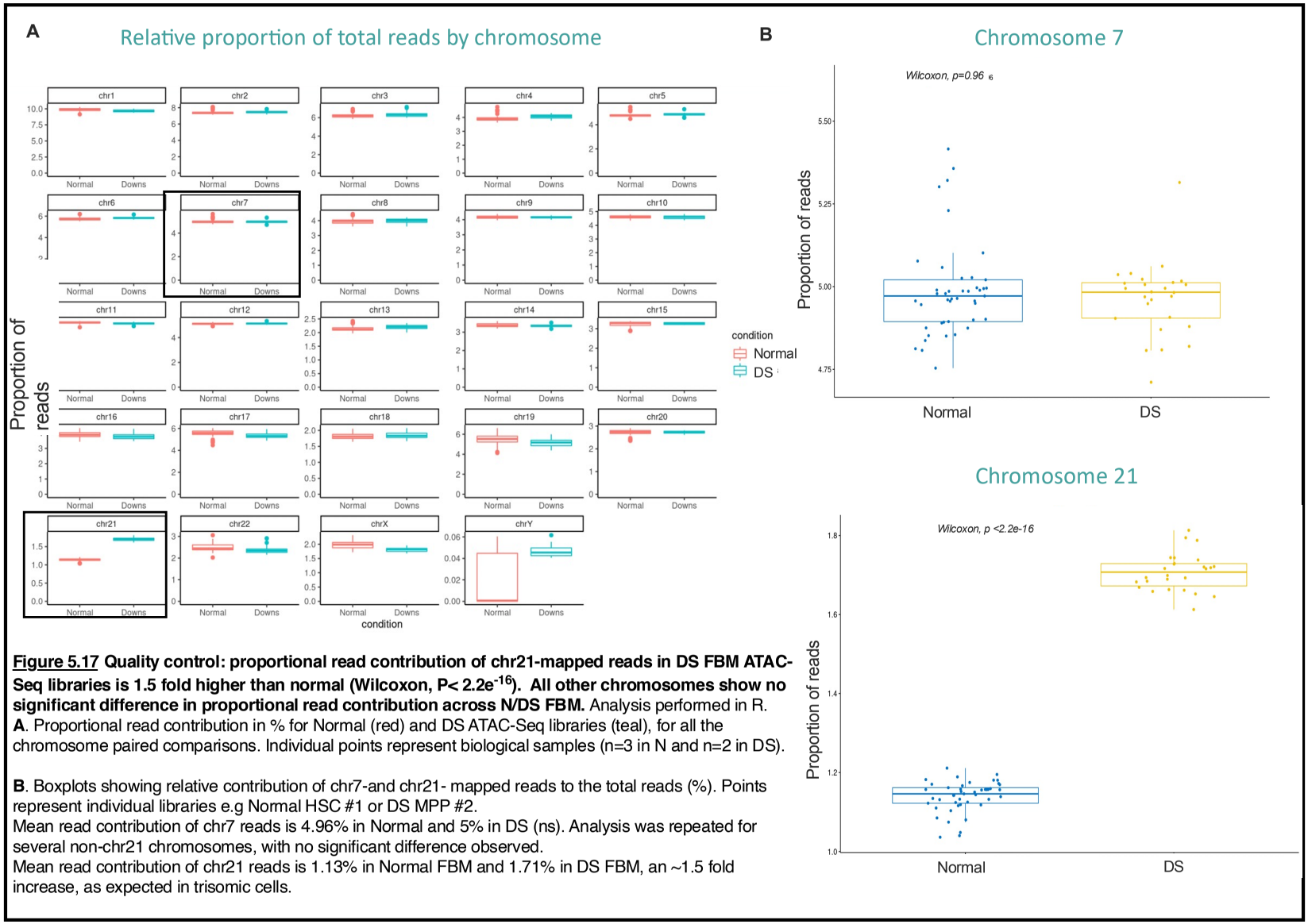


Figure 5.17 Quality control: proportional read contribution of chr21-mapped reads in DS FBM ATAC-Seq libraries is 1.5 fold higher than normal (Wilcoxon, P< $2.2e^{-16}$). All other chromosomes show no significant difference in proportional read contribution across N/DS FBM. Analysis performed in R.
A. Proportional read contribution in % for Normal (red) and DS ATAC-Seq libraries (teal), for all the chromosome paired comparisons. Individual points represent biological samples (n=3 in N and n=2 in DS).

B. Boxplots showing relative contribution of chr7-and chr21- mapped reads to the total reads (%). Points represent individual libraries e.g Normal HSC #1 or DS MPP #2.
Mean read contribution of chr7 reads is 4.96% in Normal and 5% in DS (ns). Analysis was repeated for several non-chr21 chromosomes, with no significant difference observed.
Mean read contribution of chr21 reads is 1.13% in Normal FBM and 1.71% in DS FBM, an ~1.5 fold increase, as expected in trisomic cells.

PCA of DS FBM HSPCs by chromatin accessibility broadly resolved the same lineage clusters (Figure 5.18) as were observed in by gene expression. However, Pre-ELP/GMPs clustered closely with GMPs in DS FBM, even more strikingly than at the transcriptional level (Figure 5.18), and MPPs also clustered toward the myelo-erythroid progenitors rather than HSCs and LMPPs, which was also visible, though less strikingly, in the PCA of the top 500 variably expressed genes between normal and DS FBM HSPCs (Figure 5.15 B).

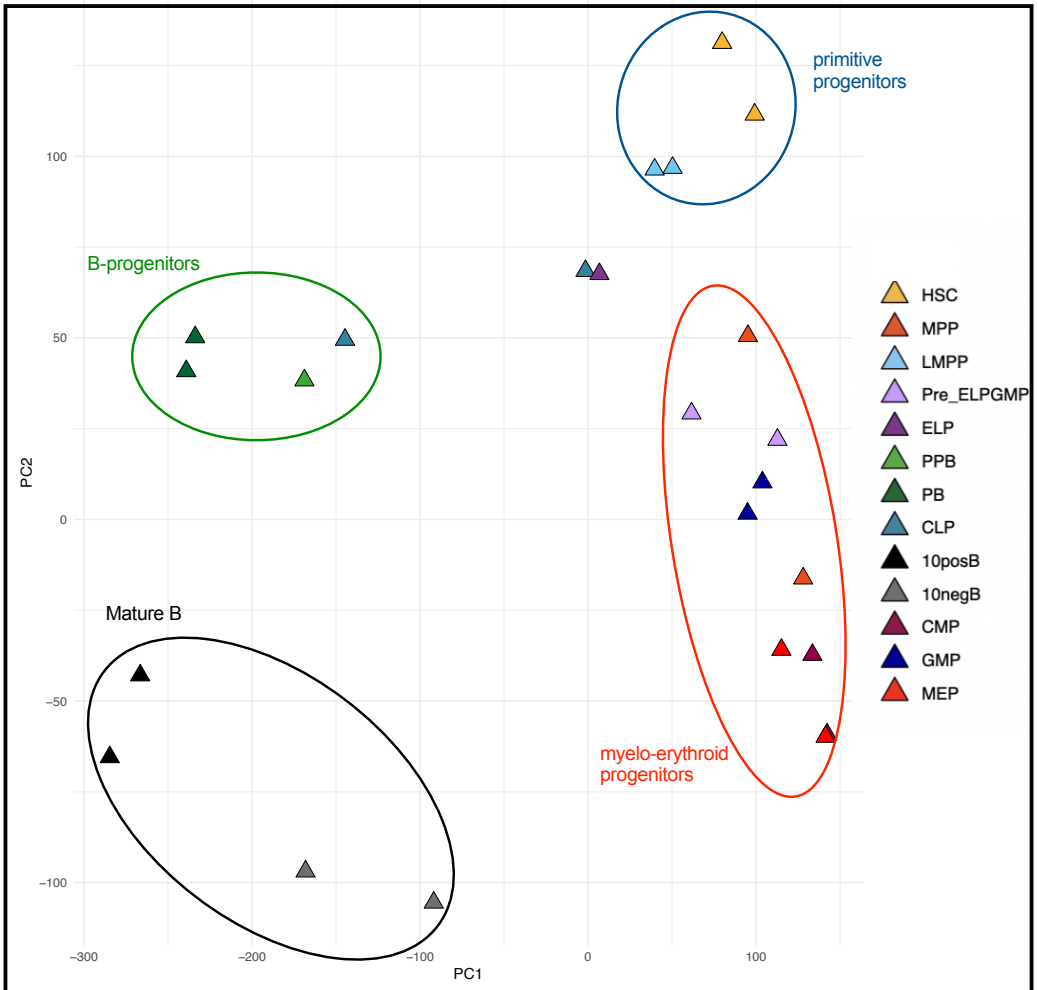


Figure 5.18 Principal Component Analysis (PCA) of all peaks in DS FBM HSPCs (1000-2000 cells/population) by ATACSeq resolves lineage clusters, however DS MPP and DS Pre-ELP/GMP cluster closely with MEPs and GMPs respectively. Clusters are labelled according to their lineage: primitive progenitors (blue), B-progenitors (green), mature B-cells (black), and myelo-erythroid progenitors (red). DS FBM n=2, except ELP (n=1). PCA analysis was performed on variant stabilised transformed normalised read counts which were generated using DESEQ2.

I then directly compared clustering of normal and DS populations according to their chromatin accessibility using PCA and UMAP-based clustering (Figure 5.19). These analyses revealed that DS FBM Pre-ELP/GMPs do cluster closely with GMPs by their chromatin accessibility, however 2/4 Pre-ELP/GMPs in normal FBM also clustered more closely to the myeloid progenitors than the other normal replicates (Figure 5.19). These were 2 replicates of the same normal biological sample, so this likely represents sample-sample variability.

UMAP based clustering showed that DS MPP cluster much more closely with MEPs than normal counterparts (Figure 5.19), consistent with the significant erythroid bias observed in functional assays of DS FBM MPPs relative to normal (see chapter 4).

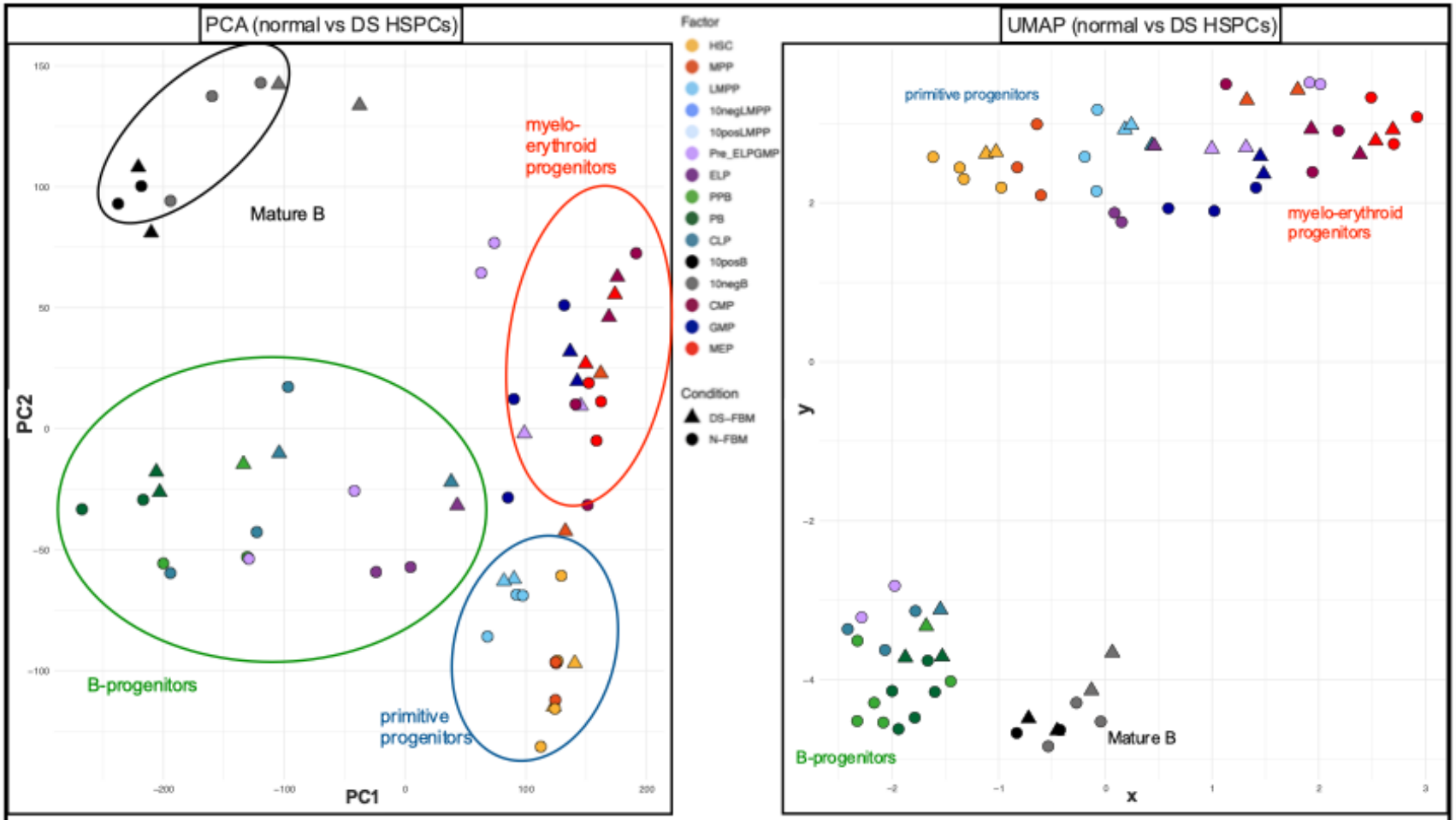


Figure 5.19 Principal Component analysis (PCA) and UMAP-based clustering of all expressed genes in normal vs DS FBM HSPCs (1000-2000 cells/population) by ATACSeq demonstrates HSPCs cluster according to both lineage and their position in the proposed hierarchy. However, DS MPPs and Pre-ELP/GMPs cluster more closely with the myelo-erythroid progenitors than normal counterparts. Clusters are labelled according to their lineage: primitive progenitors (blue), B-progenitors (green), mature B-cells (black), and myelo-erythroid progenitors (red). N FBM= 2-4. DS FBM n=2, except ELP (n=1). PCA/UMAP analyses were performed on variant stabilised transformed normalised read counts, generated using DESEQ2, across all genes.

I next compared the hierarchical clustering of normal and DS HSPCs based on the expression (normalised CPM counts) of lineage-associated genes, using the same GOI lists I generated for normal FBM.

To generate these heatmaps, I forced normal and DS HSPCs to cluster by their position within the proposed differentiation hierarchy for easier visual appraisal of expression of lineage associated genes across normal vs DS HSPC populations. Heatmaps and boxplots feature the normalised expression of lineage GOI and heatmaps are scaled by gene across the HSPCs included in the given heatmap. Results of statistical pairwise comparisons of normal and DS HSPCs, showing only DEG, rather than all lineage-associated genes (including non DEGs), can be found from Figure 5.26- 5.31.

Comparison of B-lineage associated genes suggested that DS Pre-ELP/GMPs had reduced expression of several B-cell genes involved in both early (*DNTT, LEF1, IL7-R)* and late lineage commitment (*CD19, RAG1)* (Figure 5.20), with some of these differences (*DNTT, CD9)* found to be statistically significant during subsequent pairwise comparison (Figure 5.26). Similarly, although some genes linked to lymphoid priming such as *FLT3, IKZF1* and the *IL7-R*, tended to have lower expression in DS MPP/LMPP these differences were not significant (Figure 5.20). In line with the in vitro observations that downstream B-cell output of DS B-progenitors was comparable to normal (*s*ee chapter 4), there was no apparent difference in expression of B-lineage genes between normal and DS PPB and ProB progenitors (Figure 5.20).

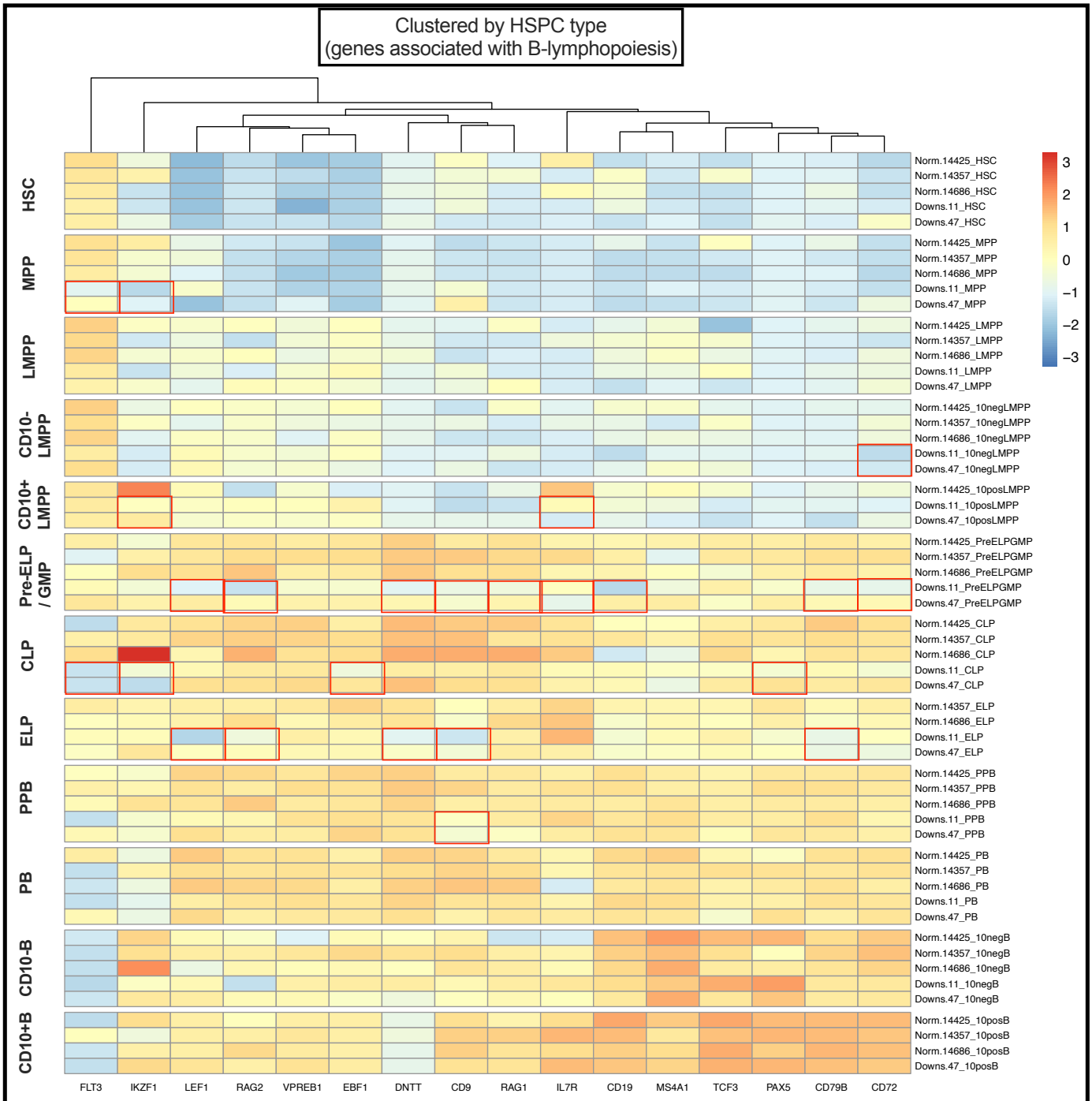


Figure 5.20 Expression of B-cell lineage-associated genes (normalised CPM, scaled by gene) in normal vs DS FBM HSPCs by RNA Seq (50-100 cells), reveals lower expression of several B-cell genes in DS HSPCs, most markedly Pre-ELP/GMPs and ELPs.
Forced clustering based on HSPC type and position in the proposed B-differentiation pathway reveals a clear trend in the expression B-lineage associated genes, which gets progressively higher throughout differentiation. Red highlights indicate genes showing markedly different expression between N/DS counterparts. Normalised CPM counts were generated using EdgeR.

The expression of several NK genes was higher in DS FBM HSPCs compared to normal (Figure 5.21), supporting in vitro observations of increased NK output in vitro (chapter 4). Although expression of several NK-associated genes, such as *IL32, ZBTB1,* and *TOX2* appeared to be higher in DS Pre-ELP/GMPs (Figure 5.21) only the upregulation of *NCR3* and *PVRIG* reached statistical significance (Figure 5.26).

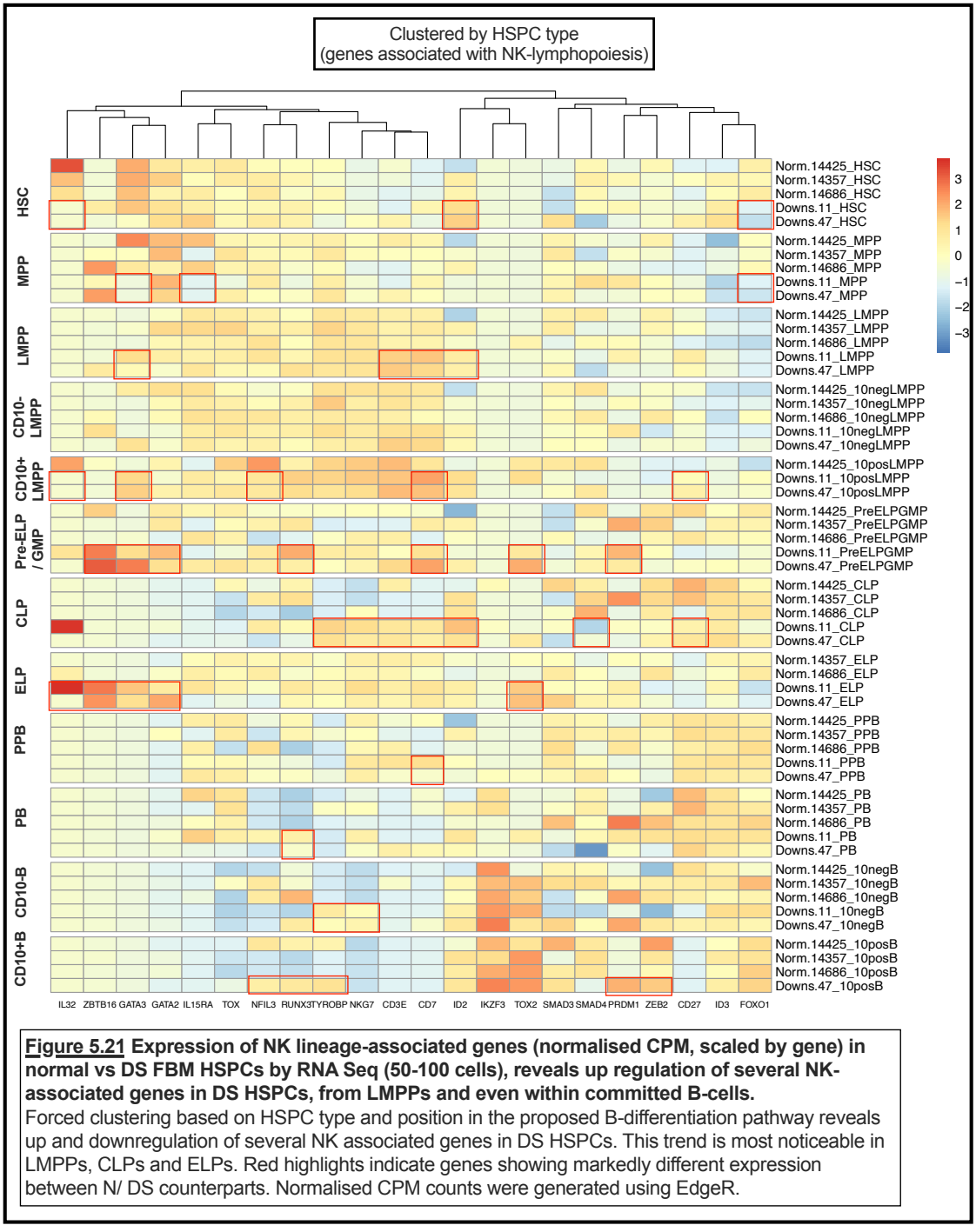


Figure 5.21 Expression of NK lineage-associated genes (normalised CPM, scaled by gene) in normal vs DS FBM HSPCs by RNA Seq (50-100 cells), reveals up regulation of several NK-associated genes in DS HSPCs, from LMPPs and even within committed B-cells.
Forced clustering based on HSPC type and position in the proposed B-differentiation pathway reveals up and downregulation of several NK associated genes in DS HSPCs. This trend is most noticeable in LMPPs, CLPs and ELPs. Red highlights indicate genes showing markedly different expression between N/ DS counterparts. Normalised CPM counts were generated using EdgeR.

The myeloid expression pattern of DS Pre-ELP/GMPs seemed to more closely resemble that of GMPs compared with CD10-LMPPs or ELPs (Figure 5.22) and several myeloid genes were significantly upregulated in DS Pre-ELP/GMP when pairwise comparisons were performed (Figure 5.26).

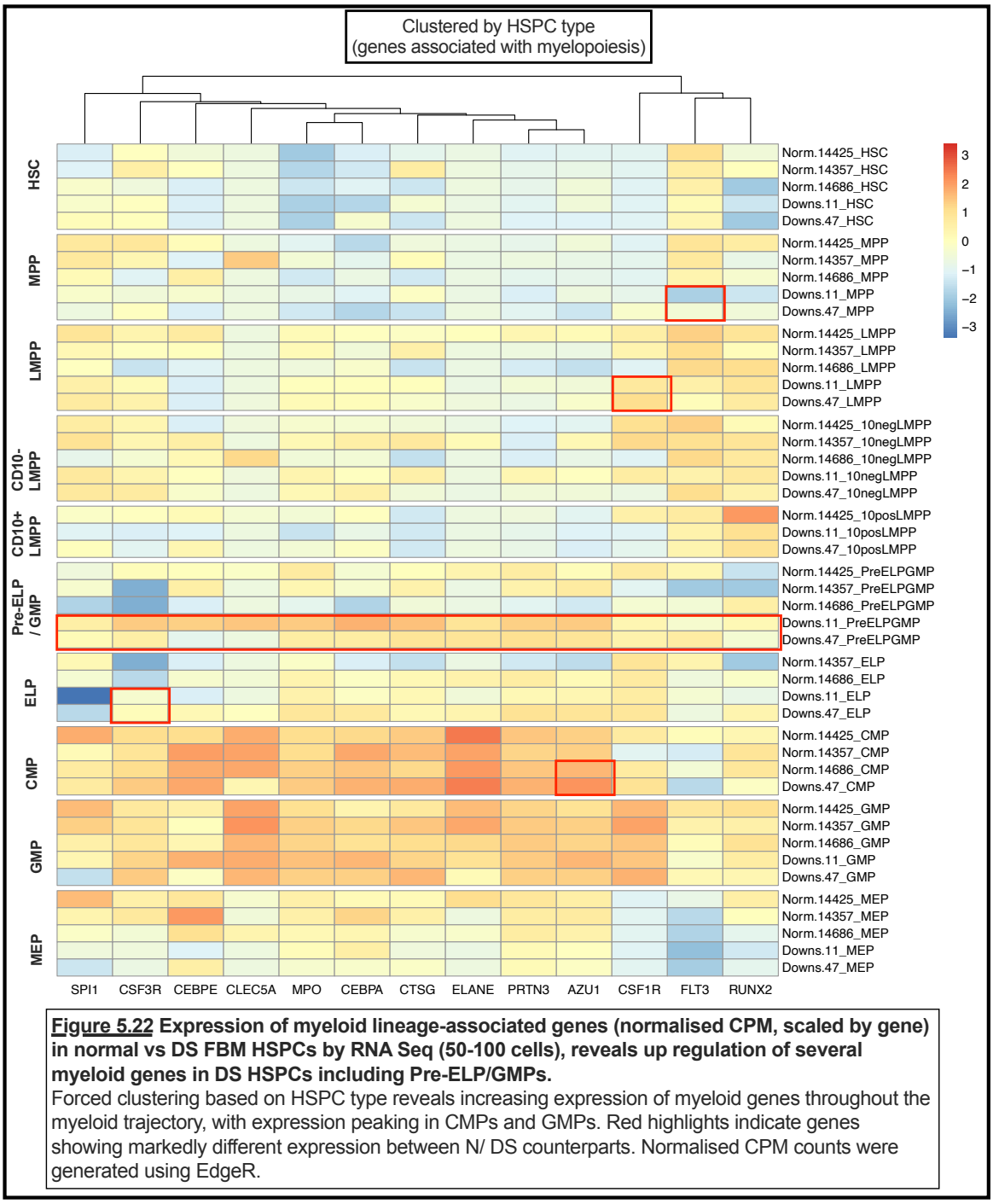


Figure 5.22 Expression of myeloid lineage-associated genes (normalised CPM, scaled by gene) in normal vs DS FBM HSPCs by RNA Seq (50-100 cells), reveals up regulation of several myeloid genes in DS HSPCs including Pre-ELP/GMPs.
Forced clustering based on HSPC type reveals increasing expression of myeloid genes throughout the myeloid trajectory, with expression peaking in CMPs and GMPs. Red highlights indicate genes showing markedly different expression between N/ DS counterparts. Normalised CPM counts were generated using EdgeR.

Several erythroid and megakaryocytic genes also appeared to be expressed at higher levels in DS HSCs and MPPs (Figure 5.23 and 5.24) as has been reported previously for FL and FBM (Roy et al, 2012; Jardine et al, 2021), with pairwise comparisons showing significantly increased expression of several of these genes (Figure 5.29 and 5.30).

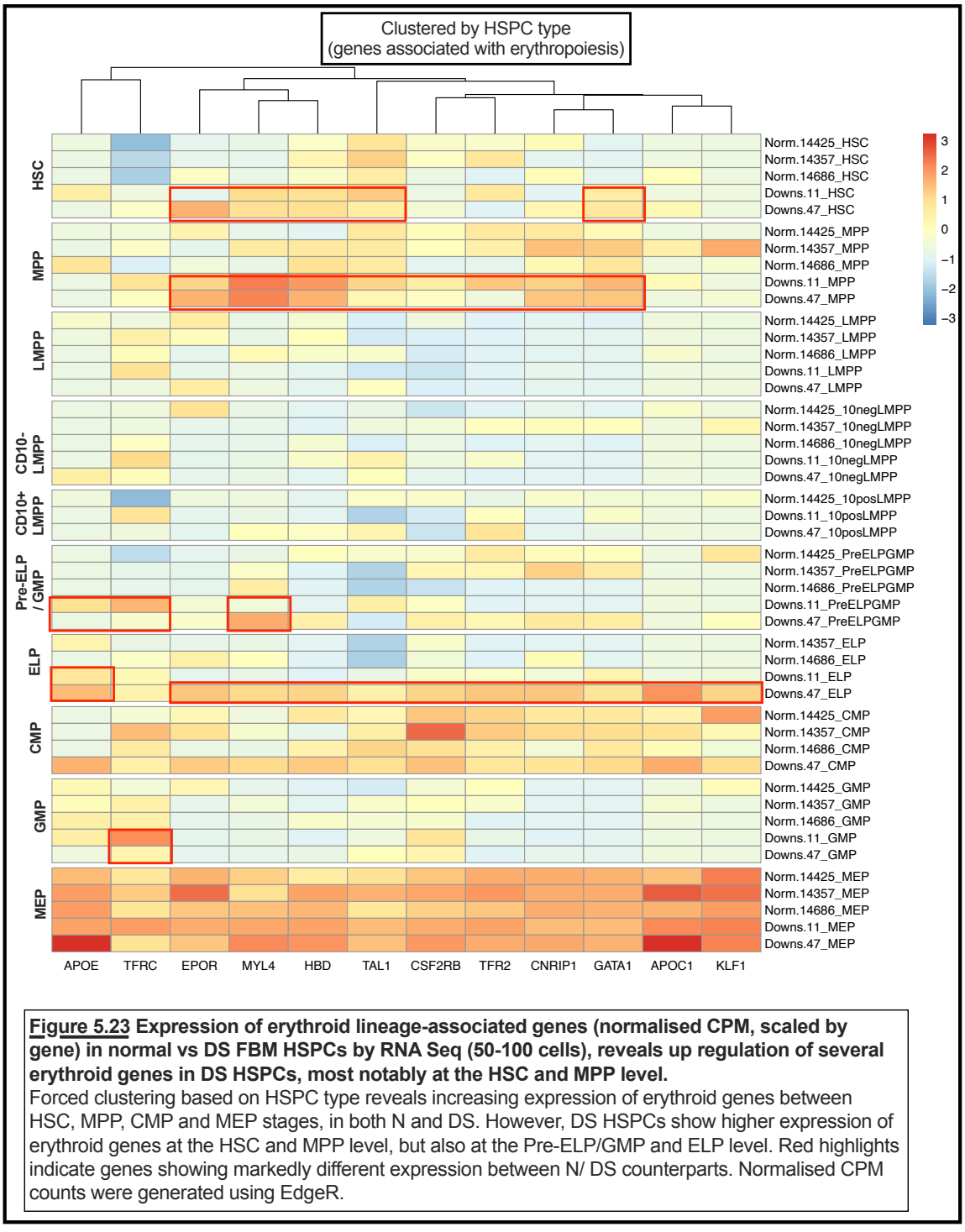


Figure 5.23 Expression of erythroid lineage-associated genes (normalised CPM, scaled by gene) in normal vs DS FBM HSPCs by RNA Seq (50-100 cells), reveals up regulation of several erythroid genes in DS HSPCs, most notably at the HSC and MPP level.
Forced clustering based on HSPC type reveals increasing expression of erythroid genes between HSC, MPP, CMP and MEP stages, in both N and DS. However, DS HSPCs show higher expression of erythroid genes at the HSC and MPP level, but also at the Pre-ELP/GMP and ELP level. Red highlights indicate genes showing markedly different expression between N/ DS counterparts. Normalised CPM counts were generated using EdgeR.

It was interesting and surprising, to see expression of some megakaryocyte/erythroid genes in DS Pre-ELP/GMP and ELP (Figure 5.23 and 5.24) which was confirmed by pairwise comparisons e.g. *ITGA2B, GFI1B, SLC22A4, FCER1A* (Figure 5.26 and 5.31), which suggests that although these cells do not give rise to erythroid colonies in vitro, they may retain residual erythroid gene expression.

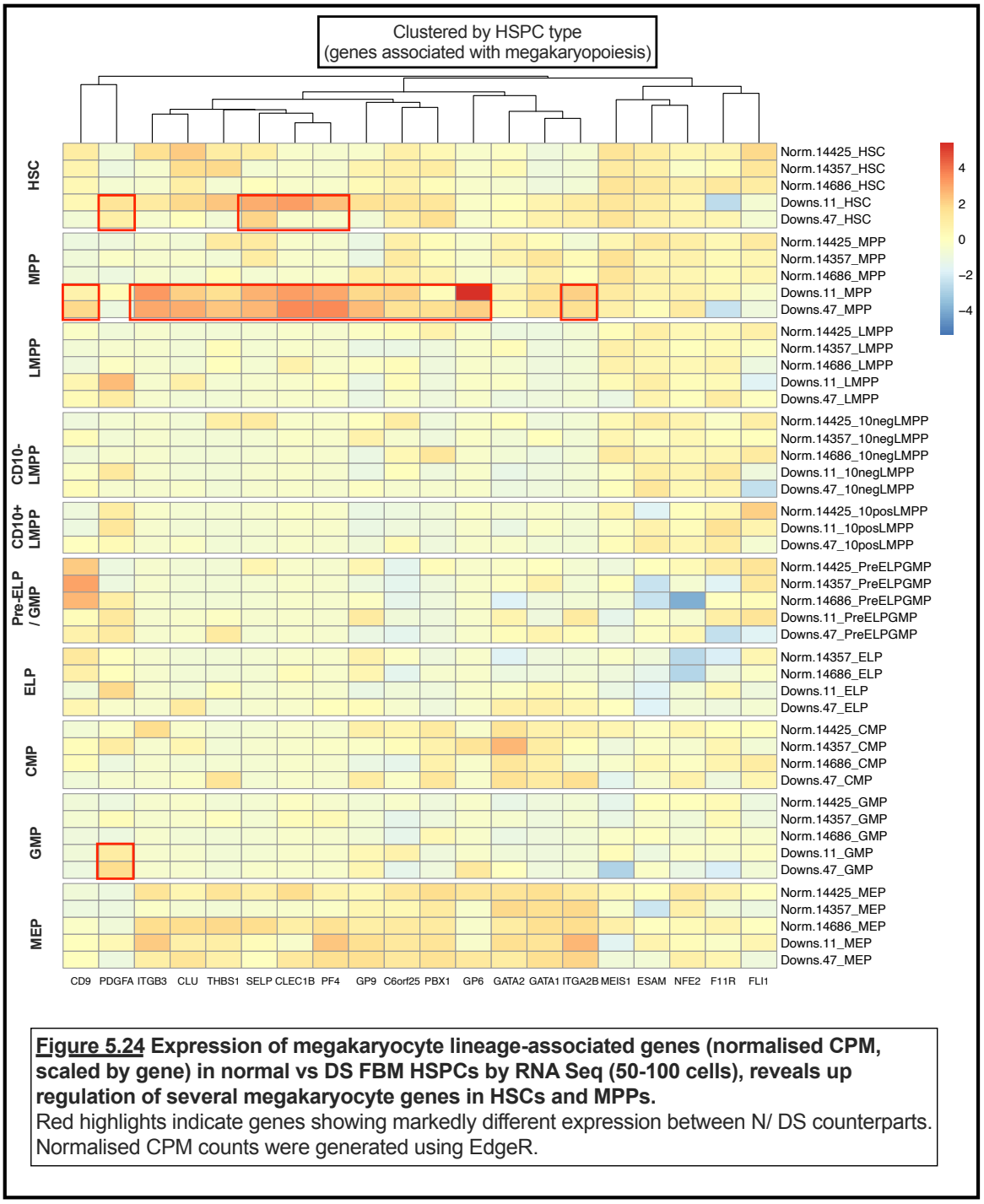


Figure 5.24 Expression of megakaryocyte lineage-associated genes (normalised CPM, scaled by gene) in normal vs DS FBM HSPCs by RNA Seq (50-100 cells), reveals up regulation of several megakaryocyte genes in HSCs and MPPs.
Red highlights indicate genes showing markedly different expression between N/ DS counterparts. Normalised CPM counts were generated using EdgeR.

Pairwise comparisons of gene expression patterns of N and DS FBM HSPCs

Overall, Pre-ELP/GMPs showed the greatest number of DEGs between N and DS (105, FDR <0.1 and absolute log_2FC >1.5) (Fig 5.25 A), whilst total LMPPs and CD10-LMPPs showed few or no DEGs (Fig 5.25 A). CD10+LMPPs showed 20 DEGs (Fig 5.25 A) but limited conclusions can be drawn from these, given that n=1 for normal.

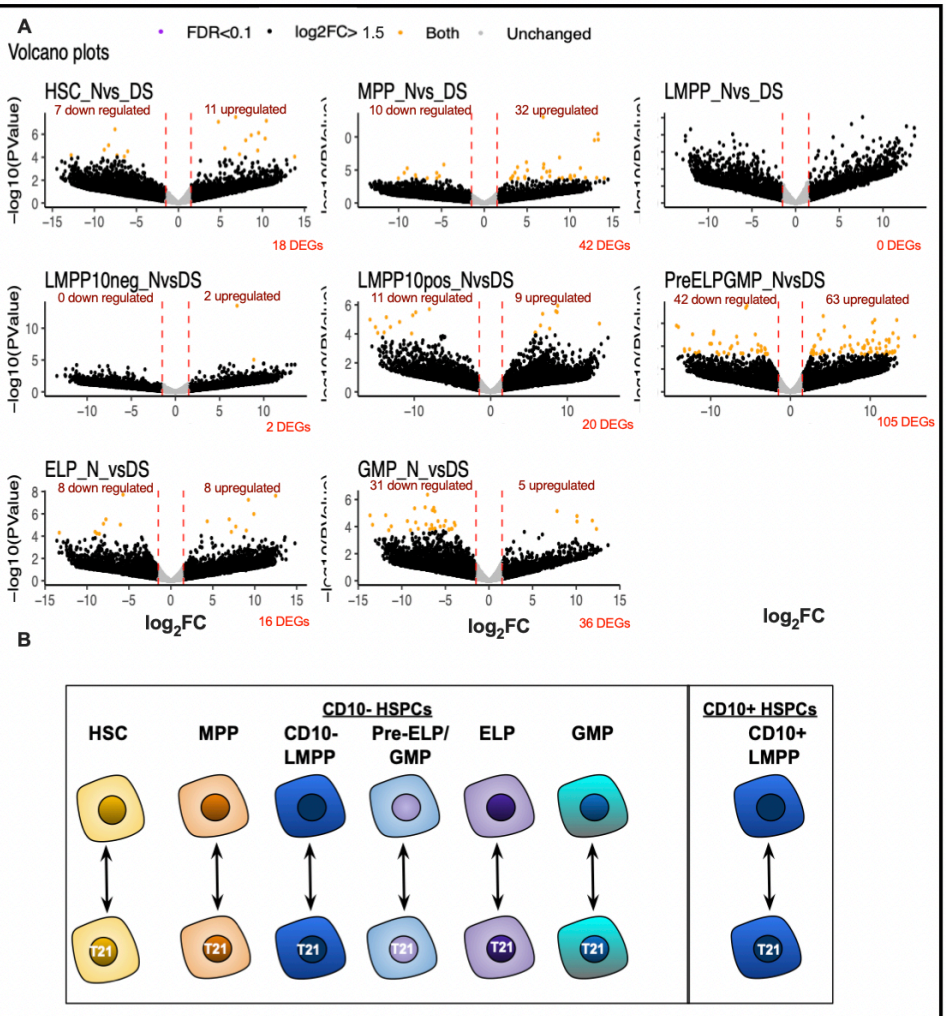


Figure 5.25 Volcano plots showing significant (FDR <0.1 & log_2FC > -/+1.5) up and down regulated genes (in yellow) between normal and DS FBM HSPCs by RNA Seq (50-100 cells/ population), determined through pairwise comparisons (n=1-3). All signficant DE genes showed greater than 1.5 absolute log_2FC. Positive log_2FC indicates genes upregulated in DS HSPCs, negative log_2FC indicates genes upregulated in normal.

A. Volcano plots of pairwise comparisons of N vs DS FBM CD10- and CD10+ HSPC populations, performed in EdgeR. Red indicates DE genes (FDR <0.1). N=3 for normal, except CD10+LMPP (n=1) and n=2 for DS. Total up/down regulated genes are displayed with red vertical intercept marking +/- 1.5 log_2FC. Genes showing >1.5 or <-1.5 log_2FC are represented in black. DE genes (FDR <0.1 and >1.5 or <-1.5 log_2FC) are shown in yellow.

B. Schematic showing pairwise comparisons of N and DS CD10- and CD10+ progenitors in FBM. DS HSPCs are indicated by 'T21' labels. Arrows indicate pairwise comparisons performed using EdgeR

Focusing first on the novel progenitors, of the 105 DEG between N and DS Pre-ELP/GMPs, there was increased expression of several myeloid genes including *AZU1, TREML1* and *PRTN3* (Figure 5.26)*,* mirroring methylcellulose assays which showed higher myeloid clonogenicity of DS Pre-ELP/GMPs (see chapter 4). In addition, the DNA binding protein *ID1,* which is known to promote myeloid differentiation and inhibit B-cell differentiation, is significantly upregulated in DS FBM Pre-ELP/ GMPs (log_2FC= 3.95) (Figure 5.26).

Concurrently, there is a significant downregulation of B-lineage associated genes in DS Pre-ELP/GMP including *VPREB3, DNTT, CD24, TCL1A, CD9* and *IRF4* (Figure 5.26). Interestingly, there was a significant increase in several genes known to play a role in NK development (*JAK3, NCR3, PVRIG, TNFSF9)* (Figure 5.26). Altogether, the disparities in B/NK gene expression directly support in vitro observations of increased NK output and impaired B-cell differentiation (see chapter 4). In addition, several genes involved in erythropoiesis were upregulated in DS Pre-ELP/GMPs, with downregulation of two negative regulators of erythropoiesis *ATGA4* and *ZNF613* (Figure 5.26) suggesting that the normal silencing of the erythroid programme may be inefficient in these cells.

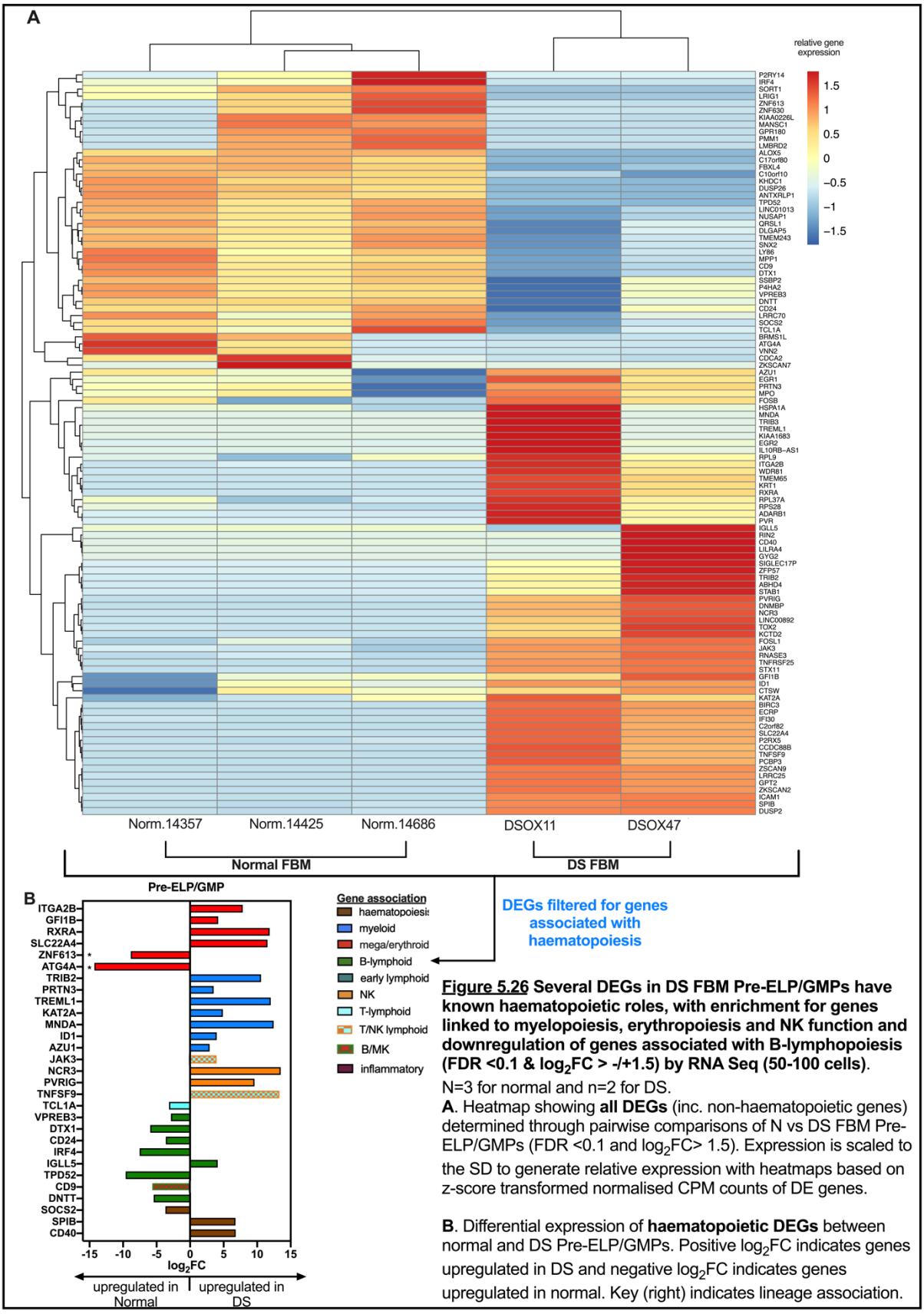


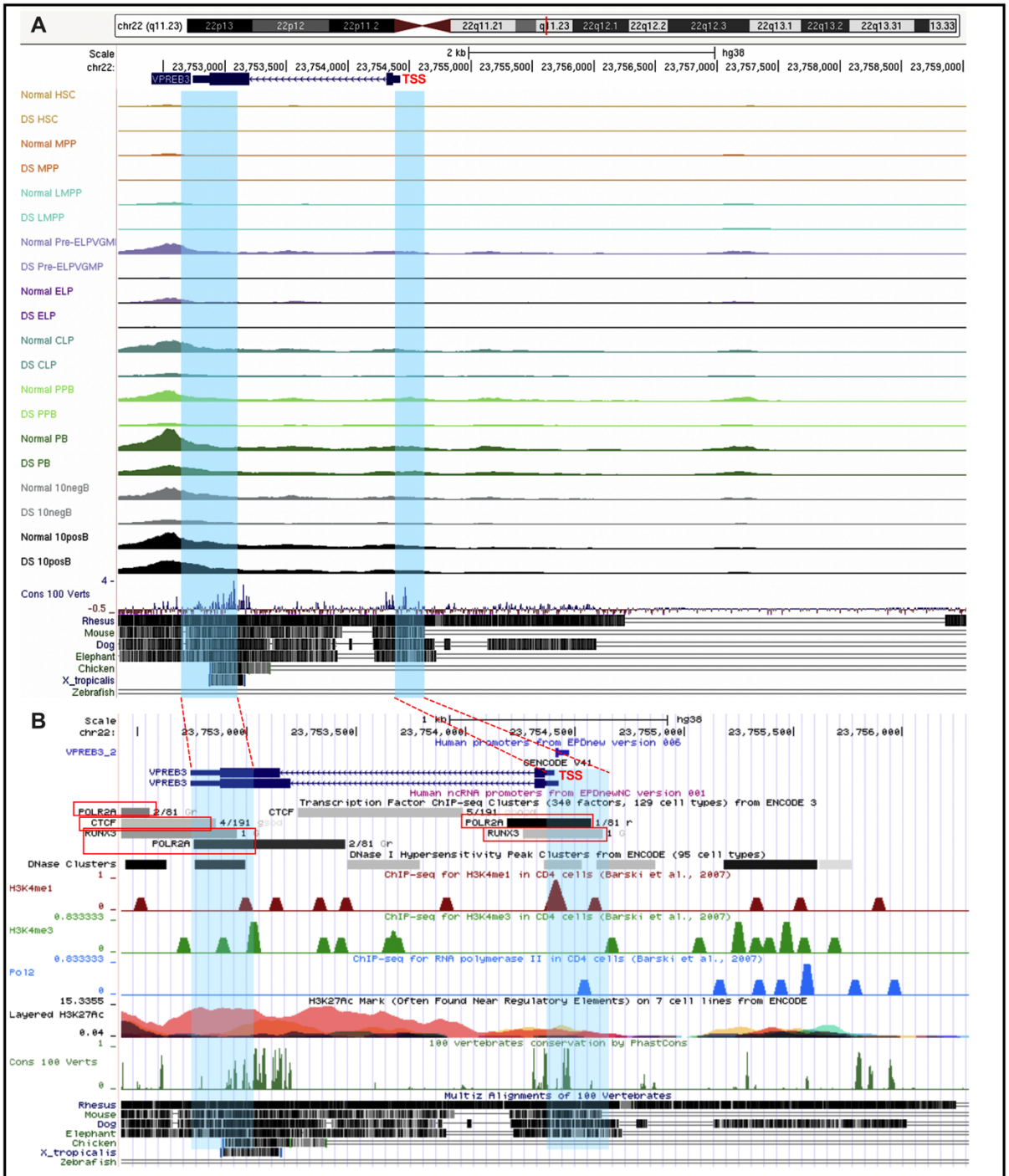
Figure 5.26 Several DEGs in DS FBM Pre-ELP/GMPs have known haematopoietic roles, with enrichment for genes linked to myelopoiesis, erythropoiesis and NK function and downregulation of genes associated with B-lymphopoiesis (FDR <0.1 & log_2FC > -/+1.5) by RNA Seq (50-100 cells).

N=3 for normal and n=2 for DS.

A. Heatmap showing **all DEGs** (inc. non-haematopoietic genes) determined through pairwise comparisons of N vs DS FBM Pre-ELP/GMPs (FDR <0.1 and log_2FC> 1.5). Expression is scaled to the SD to generate relative expression with heatmaps based on z-score transformed normalised CPM counts of DE genes.

B. Differential expression of **haematopoietic DEGs** between normal and DS Pre-ELP/GMPs. Positive log_2FC indicates genes upregulated in DS and negative log_2FC indicates genes upregulated in normal. Key (right) indicates lineage association.

Having identified that Pre-ELP/GMPs appear to be a key stage at which lineage biases are propagated in DS FBM, from both the functional (chapter 4) and molecular data, I wanted to identify whether the DEGs of Pre-ELP/GMPs showed altered chromatin accessibility. *VPREB3* is a member of the VPREB family, which have been associated with BCR expression and B-cell differentiation (Martensson et al, 2007; Reth and Nielsen, 2014). *VPREB3* is a highly conserved member of the VPREB family with less well-defined functions, however it has been hypothesised to function intracellularly within cells of the B-lineage by binding nascent immunoglobulin and it has also been linked to the function and expression of the BCR (Rosnet et al, 1999; Rosnet et al, 2004; Rodig et al, 2010; Wang et al, 2012). *VPREB3* is expressed throughout B-cell differentiation and was one of the significantly downregulated genes between normal and DS Pre-ELP/GMPs (Figure 5.26), as well as normal Pre-ELP/GMPs and normal GMPs (Figure 5.12). Visual appraisal of UCSC traces of normal vs DS FBM Pre-ELP/GMPs reveals reduced accessibility of VPREB3 at two highly conserved regions which map to known regulatory elements, both RUNX3 binding sites (*Eukaryotic Promoter Database*) (Figure 5.27). The TSS- proximal region is a known VPREB3 promoter, whilst the downstream element is thought to be an enhancer due to the co-occurrence of H3K4me1 and H3K27Ac around the region, which are used to distinguish activating enhancers from poised promoters (Creyghton et al, 2010; Bae and Lesch, 2020).



<u>Figure 5.27</u> ATACSeq (1000-2000 cells) of normal vs DS FBM HSPCs reveals reduced accessiblity in regions of the *VPREB3* gene, which is expressed in several stages of B-cell differentiation and has known roles in BCR formation. These differences are most striking in Pre-ELP/GMP, CLP, ELP and PreProB.

A Representative peak traces annotated to the *VPREB3* gene, viewed on the UCSC Genome Browser for HSPCs within the B-cell differentiation hierarchy in N and DS FBM. Blue highlighted regions indicate highly conserved regions which show visibly differential accessibility between N and DS HSPCs. Merged representative traces are shown for N and DS HSPCs.

B Closer assessment of highlighted regions using the Eukaryotic Promoter Database (EPD) tool reveals 2 clusters of highly conserved RUNX3, RNA Polymerase II and CTCF binding sites. The upstream site proximal to the TSS is a known promoter for *VPREB3*, as indicated in blue (EPD version 6). Highlighted regions are flanked by DNA hypersensitivity peaks. The co-occurence of both H3K4me1 and elevated H3K27Ac levels is known to distinguish activating (H3K27Ac presence) regulaotory elements from poised (H3K4me1 presence) regulatory elements (Creygthon et al, 2010; Bae and Lesch, 2020).

In contrast to the Pre-ELP/GMP comparison, there were only 2 DEG between normal and DS CD10-LMPPs was much smaller; of these the only haematopoietic associated DEG was the myeloid gene *PRTN3,* which showed a 6.97 log_2FC increase in expression within DS CD10-LMPPs.

DS CD10+LMPPs showed significantly reduced expression of B-lineage associated genes *CEACAM1* and *ZNF609* and increased expression of genes linked to myelopoiesis and inflammation (Figure 5.28), in line with previous reports of a DS FBM HSPCs showing an inflammatory phenotype (Sorcha O'Byrne ASH abstract, 2019). However, findings from CD10+LMPPs cannot be confidently interpreted at this stage, due to only having n=1 for normal due to population scarcity.

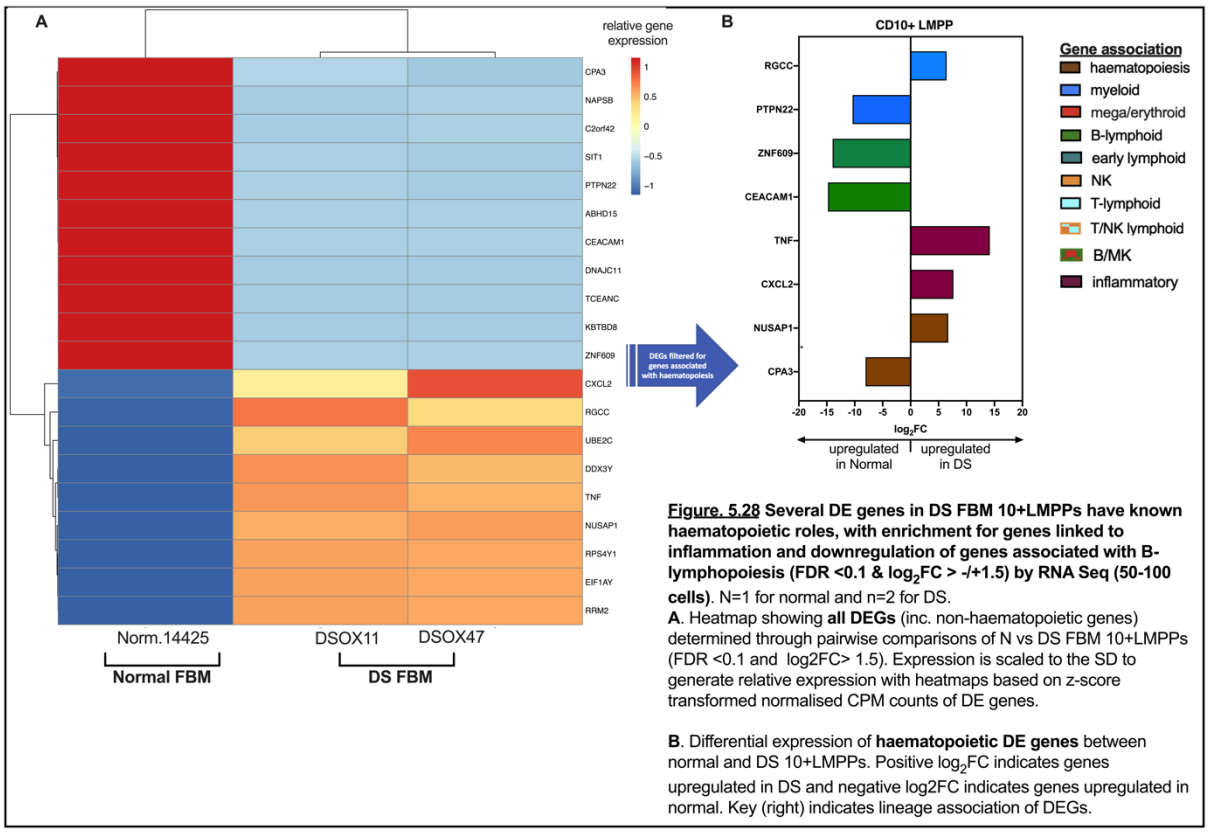


Figure. 5.28 Several DE genes in DS FBM 10+LMPPs have known haematopoietic roles, with enrichment for genes linked to inflammation and downregulation of genes associated with B-lymphopoiesis (FDR <0.1 & log_2FC > -/+1.5) by RNA Seq (50-100 cells). N=1 for normal and n=2 for DS.
A. Heatmap showing **all DEGs** (inc. non-haematopoietic genes) determined through pairwise comparisons of N vs DS FBM 10+LMPPs (FDR <0.1 and log2FC> 1.5). Expression is scaled to the SD to generate relative expression with heatmaps based on z-score transformed normalised CPM counts of DE genes.

B. Differential expression of **haematopoietic DE genes** between normal and DS 10+LMPPs. Positive log_2FC indicates genes upregulated in DS and negative log2FC indicates genes upregulated in normal. Key (right) indicates lineage association of DEGs.

Of the 18 DEG in DS FBM HSCs compared to normal FBM HSCs, 9 were upregulated, including 6 megakaryocyte erythroid genes: *GATA1, FCER1A, MYL4, PPBP, PF4 AND CLEC1B* (Figure 5.29). Expression of two lymphoid associated genes (*CD72* and IGLL1) was also slightly increased in DS HSC but expression of all the other lymphoid associated genes was not significantly different in DS compared to normal FBM HSC.

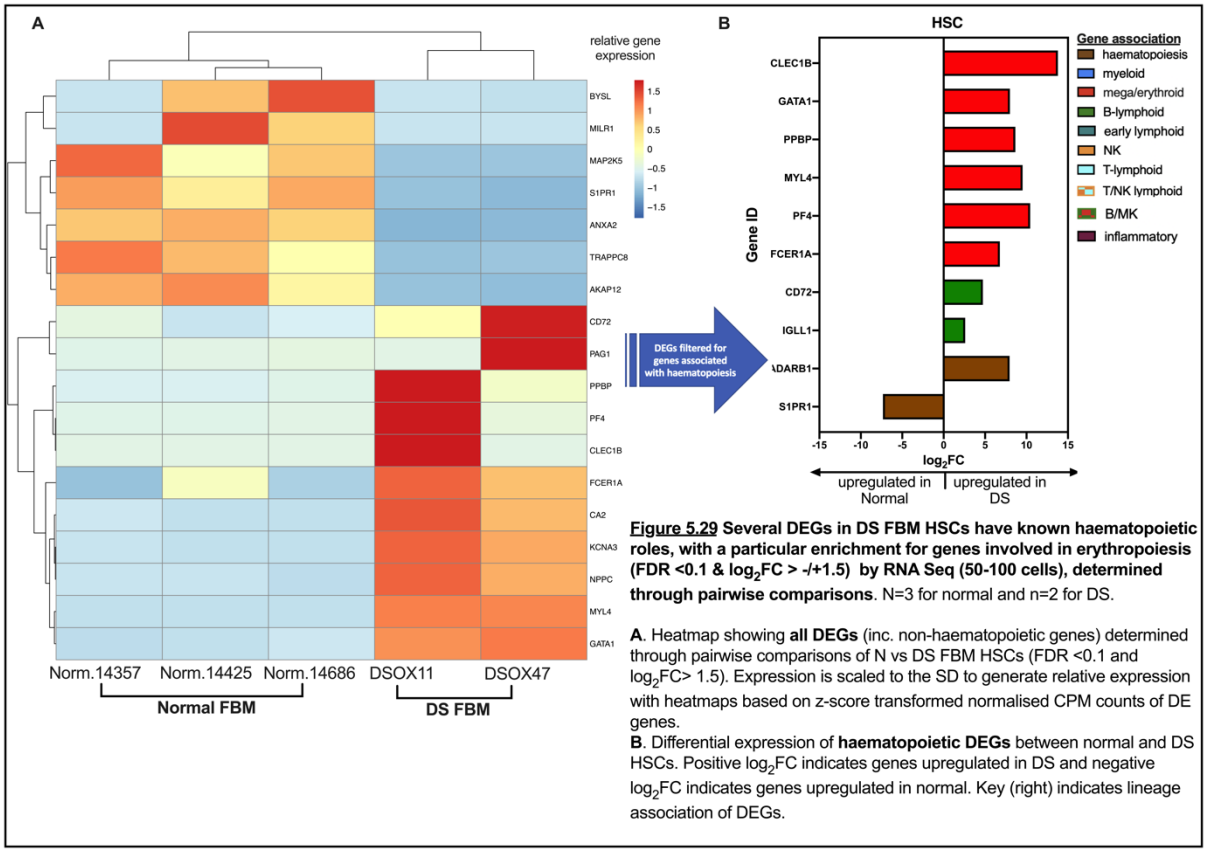


Figure 5.29 Several DEGs in DS FBM HSCs have known haematopoietic roles, with a particular enrichment for genes involved in erythropoiesis (FDR <0.1 & log_2FC > -/+1.5) by RNA Seq (50-100 cells), determined through pairwise comparisons. N=3 for normal and n=2 for DS.

A. Heatmap showing **all DEGs** (inc. non-haematopoietic genes) determined through pairwise comparisons of N vs DS FBM HSCs (FDR <0.1 and log_2FC> 1.5). Expression is scaled to the SD to generate relative expression with heatmaps based on z-score transformed normalised CPM counts of DE genes.
B. Differential expression of **haematopoietic DEGs** between normal and DS HSCs. Positive log_2FC indicates genes upregulated in DS and negative log_2FC indicates genes upregulated in normal. Key (right) indicates lineage association of DEGs.

Of the 42 DEG in DS FBM MPPs, 32 were upregulated in DS MPP, including 10 megakaryocyte-erythroid genes (*CLU, PLK1, FCER1A, PF4, CD36, CLEC1B*, *RGS16, TRPC6, CA1* and *HBG2*) (Figure 5.25).

Downstream DS MPPs show decreased expression of several B-lymphoid genes including *HLA-DOA, FCMR* and *ZBTZ5*, however they also show increased expression of *JCHAIN* and *CD72* (Figure 5.30). Altogether these observations indicate that whilst a small number of B-

lymphoid genes are downregulated in DS HSCs and MPPs, the majority appear to be unchanged.

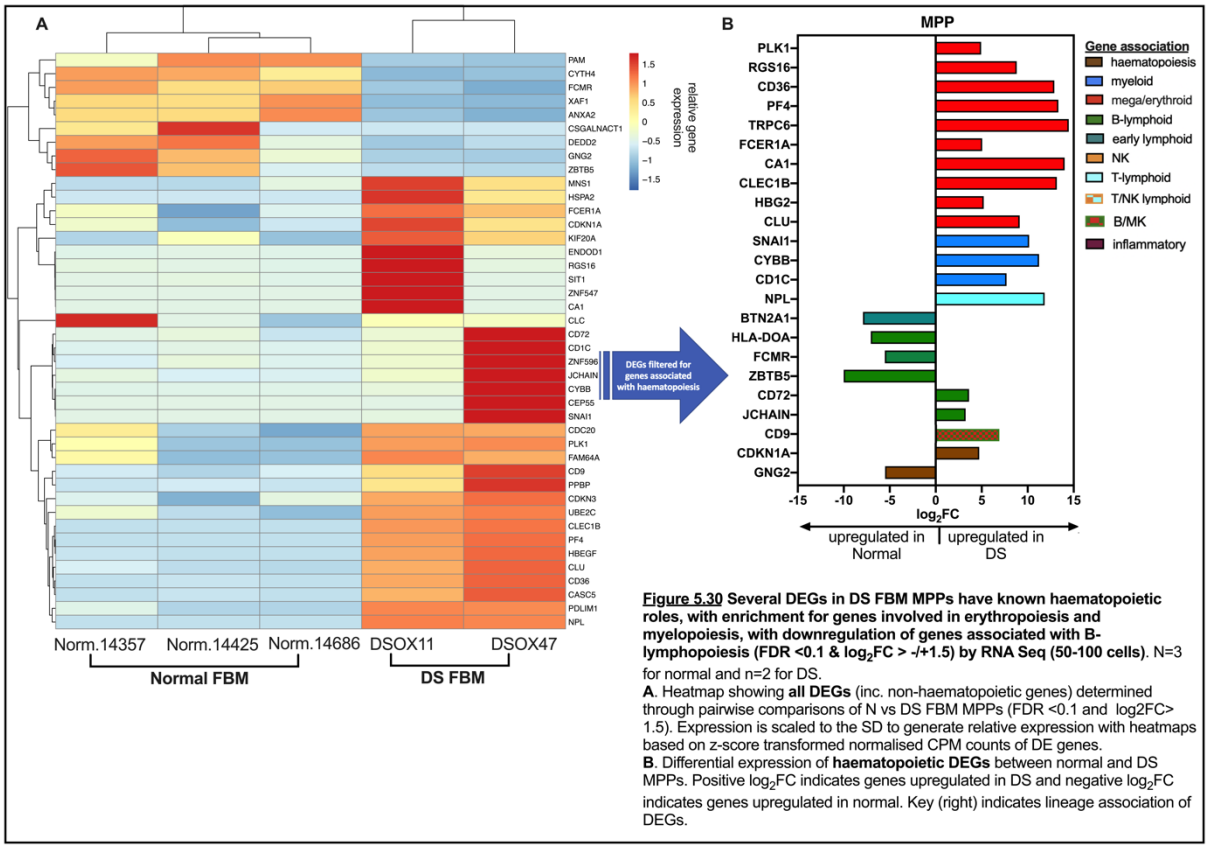


Figure 5.30 Several DEGs in DS FBM MPPs have known haematopoietic roles, with enrichment for genes involved in erythropoiesis and myelopoiesis, with downregulation of genes associated with B-lymphopoiesis (FDR <0.1 & log_2FC > -/+1.5) by RNA Seq (50-100 cells). N=3 for normal and n=2 for DS.
A. Heatmap showing **all DEGs** (inc. non-haematopoietic genes) determined through pairwise comparisons of N vs DS FBM MPPs (FDR <0.1 and log2FC> 1.5). Expression is scaled to the SD to generate relative expression with heatmaps based on z-score transformed normalised CPM counts of DE genes.
B. Differential expression of **haematopoietic DEGs** between normal and DS MPPs. Positive log_2FC indicates genes upregulated in DS and negative log_2FC indicates genes upregulated in normal. Key (right) indicates lineage association of DEGs.

Of the 16 DEG between normal and DS FBM ELPs (Figure 5.25), there was significant upregulation of several genes associated with erythropoiesis (Figure 5.31) and downregulation of B-lymphoid genes including *DNTT* which was also downregulated in DS Pre-ELP/GMP (Figure 5.26). Interestingly, *IGLL5*, a B-cell specific gene and known target of PAX5 (Pridans et al, 2008), was one of the only upregulated B-cell genes in both DS Pre-ELP/GMP and ELP compared to their normal counterparts (Figure 5.26, 5.31).

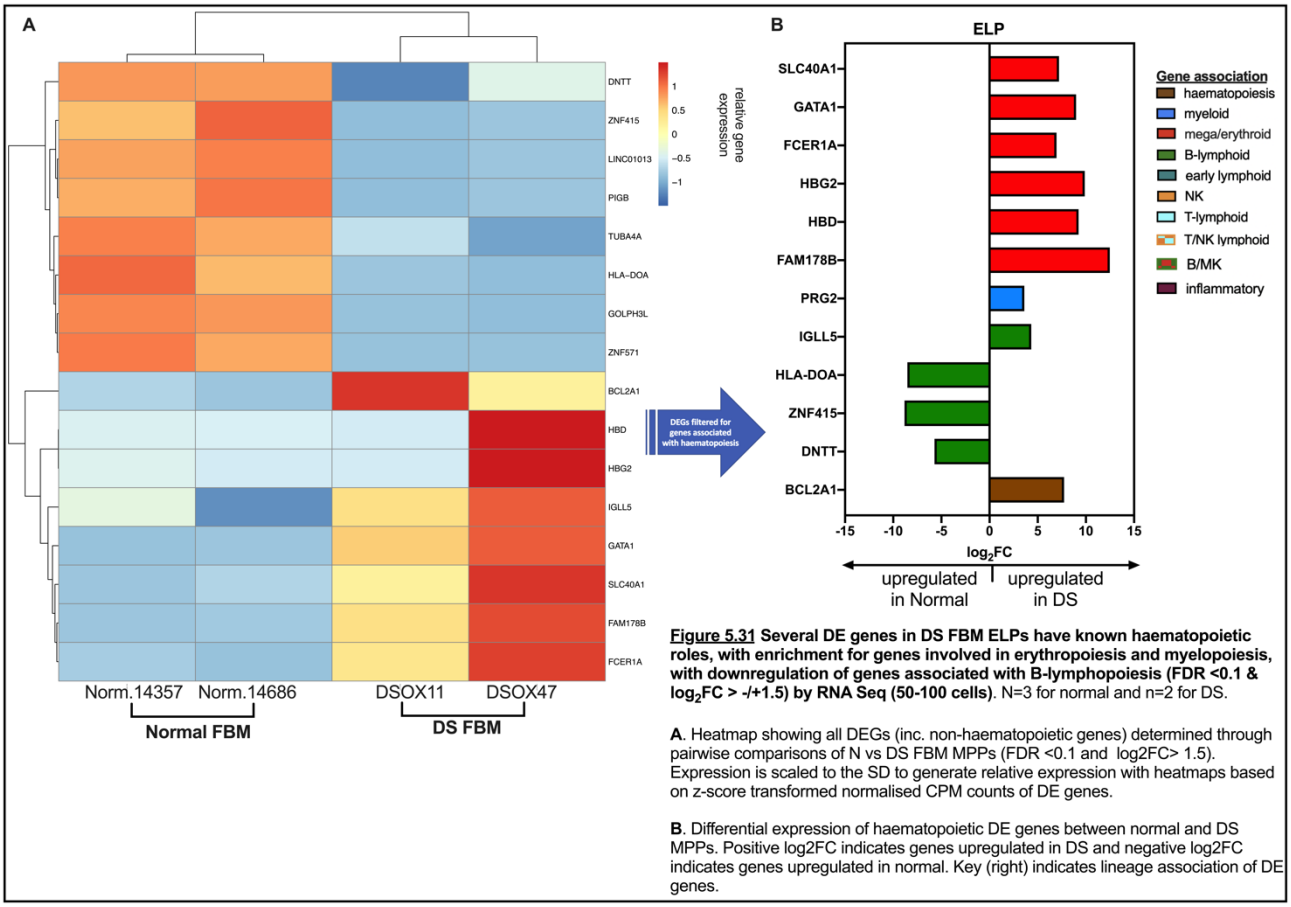


Figure 5.31 Several DE genes in DS FBM ELPs have known haematopoietic roles, with enrichment for genes involved in erythropoiesis and myelopoiesis, with downregulation of genes associated with B-lymphopoiesis (FDR <0.1 & log_2FC > -/+1.5) by RNA Seq (50-100 cells). N=3 for normal and n=2 for DS.

A. Heatmap showing all DEGs (inc. non-haematopoietic genes) determined through pairwise comparisons of N vs DS FBM MPPs (FDR <0.1 and log2FC> 1.5). Expression is scaled to the SD to generate relative expression with heatmaps based on z-score transformed normalised CPM counts of DE genes.

B. Differential expression of haematopoietic DE genes between normal and DS MPPs. Positive log2FC indicates genes upregulated in DS and negative log2FC indicates genes upregulated in normal. Key (right) indicates lineage association of DE genes.

5.4 Summary and discussion

Within this results chapter, I sought to understand the striking B-cell impairment and lineage biasing I had uncovered in DS FBM HSPCs (chapter 4), at the molecular level.
In order to do this, I had to first characterise normal FBM HSPCs, both at the transcriptomic and chromatin accessibility level. I chose to focus on the novel progenitors I'd described in FBM for the first time, to build on previous molecular data in the lab from FL and FBM (Roy et al, 2012; Anindita Roy ASH Abstract, 2014; O'Byrne et al, 2019; Sorcha O'Byrne ASH Abstract, 2019). As my data indicated a T-cell defect presented in DS FBM (chapter 4), though this was less severe than the B-cell impairment, and consistent strong NK bias, I wanted to explore genes associated with these lineages in my analyses.

Molecular Characterisation of normal FBM HSPCs supports functional observations
In support of the proposed differentiation model (Figure 5.1, B), the expression of lineage associated genes in normal FBM HSPCs reflects their position of progenitors within the proposed lineage hierarchy. Namely, the expression of B-lineage associated genes increases from HSCs through to Pre-B cells and the same trend is observed for myeloid and mega-erythroid associated genes in early HSPCs and CMPs/ GMPs/ MEPs, mirroring a recent single cell study of human FBM (Jardine et al, 2021).

As expected, LMPPs were the first population in which lymphoid expression begins to take off. CD10-LMPPs and total LMPPs were indistinguishable in normal FBM, probably due to the fact that the vast majority of these total LMPPs will be CD10- (see chapter 3). Broadly speaking however, CD10-LMPPs retained expression of myeloid genes along with the

increase in B, NK and T-lymphoid expression relative and showed reduced levels of mega-erythroid genes compared with HSC and MPP, supporting my in vitro data (chapter 3) and previous findings for $CD10^{-/low}$ LMPPs in human CB (Karamitros et al, 2018).
Unfortunately, conclusions cannot be drawn on the normal CD10+LMPP data due to their only being n=1 due to the scarcity of this population in normal FBM.

Pre-ELP/GMP, however, showed a clearly distinct expression profile and clustering pattern from CD10-LMPP, at the transcriptomic and chromatin accessibility level, demonstrating these are two distinct progenitor populations. Confirming in vitro observations, Pre-ELP/GMP showed significantly increased expression of B-cell genes compared to both upstream CD10-LMPPs and downstream GMPs. There were few DEGs between Pre-ELP/GMP and ELP, which supports their similar output in vitro (B-progenitors and PreB-cells, chapter 3). Pre-ELP/GMP and GMP showed markedly different expression and accessibility profiles, which indicates that although normal Pre-ELP/GMP can give rise to GMP, these are very differently primed populations (B and myeloid, respectively).

DS FBM HSPCs exhibit significant dysregulation of B- myeloid- and mega-erythroid associated genes and, to a lesser degree, NK genes

Despite alterations in the expression profiles in DS FBM HSPCs, populations also broadly resolve the proposed lineage hierarchy, both transcriptomically and by chromatin accessibility.
However, several populations showed a distinct clustering pattern from normal FBM which supports the functional data presented in this thesis. Similar to previous observations in FL and FBM (Roy et al, 2012; Anindita Roy 2014 ASH Abstract), DS FBM HSCs and MPPs showed a significant upregulation of several genes associated with myelo-, mega- and

erythropoiesis, directly supporting my observations in methylcellulose (chapter 4). Moreover, the DS MPPs clustered more closely to DS MEP than normal counterparts based on their chromatin accessibility, further supporting these findings.

Downstream, CD10-/+LMPPs, Pre-ELP/GMPs and ELPs showed significant downregulation of genes associated with both early B-lineage commitment including *DNTT, EBF1,* and those associated with later B-cell maturation (*CD19, CD9)*, supporting the striking B-cell defect observed for these populations during MS-5 co-culture assays (chapter 4). Visual appraisal of the B-lineage associated gene *VPREB3*, which was significantly upregulated in the transition from CD10-LMPP to Pre-ELP/GMP and contrastingly was significantly downregulated in DS FBM Pre-ELP/GMPs, revealed this gene was less accessible in DS Pre-ELP/GMP, PreProB, ELP and CLP. Exploration of these regions using the Eukaryotic Promoter Database tool (epd.epfl.ch) revealed the peaks of interest correlated to the VPREB3 promoter and a second regulatory element, possibly an enhancer.

Concurrently, these populations all showed, to different degrees, significant upregulation of genes associated with myelopoiesis. These differences were also clear during PCA-, UMAP and hierarchical clustering -based analysis of normal vs DS HSPCs, which consistently suggested DS Pre-ELP/GMPs show a greater similarity to GMP, whilst those in normal FBM are more similar to ELP. In fact, many of the DEGs between normal and DS Pre-ELP/GMPs were shared with the upregulated DEGs in normal GMPs compared with normal Pre-ELP/GMPs. Interestingly, DS ELPs also showed a significant upregulation of genes associated with erythropoiesis, despite this not translating functionally.

DS Pre-ELP/GMP did show a significant upregulation of 2 genes associated with NK lymphopoiesis, *PVRIG* and *NCR3*.

The absence of any extensive significant upregulation of NK genes in other HSPCs, despite such a striking functional phenotype (chapter 4), may suggest that rather than a specific push toward NK fates, in the absence of sufficient B-cell programmes, such as in DS FBM, NK becomes the default cell type, as others have suggested due to the NK lineage being a residual ancestral adaptive programme (Sun and Lanier, 2009; Cichocki et al, 2019).

Future work

Similar to the functional studies, one of the major limitations to this work was sample availability, with primary DS fetal samples at sufficient cell numbers particularly scarce. Given that the Pre-ELP/GMP yielded some of the most exciting data from this project, and that CD10+LMPP were unable to be fully molecularly characterised due to their scarcity in normal FBM, it is important that these experiments are repeated to confirm these preliminary findings. Adoption of a single cell approach, such as that published recently published for FL and FBM (Popescu et al, 2019; Jardine et al, 2021; Ranzoni et al, 2021; Roy et al, 2021), would circumvent some of the issues presented by rarer populations and low numbers of biological samples. In addition, this approach would provide a more accurate picture of HSPC lineage potential given the considerable heterogeneity of HSPC compartments (Notta et al, 2016; Karamitros et al, 2018; Ranzoni et al, 2021).

It was important to characterise the newly described progenitors which I have identified during my project, molecularly. Within the scope of my project and timescale, analysis was

limited to predominantly the RNA sequencing data and hierarchical ATAC analyses, which enabled me to confirm my functional observations and place these new progenitors within the proposed hierarchy.

It would be interesting to see the results of further exploration of the ATAC sequencing data, combined with a broader epigenetic approach.

Going forward, other ways in which these new ATAC data could be analysed include pairwise comparisons of normal vs DS HSPC chromatin accessibility profiles, similar to those I performed on the RNA sequencing data. A combination of DESEQ2 and DiffBind, which I used to normalise my ATAC sequencing libraries and manipulate annotated binding matrices, is commonly used to compare accessibility of small, highly variably sample sets with minimal false positives (Gontarz et al, 2020). Subsequently, EdgeR could be used to perform pairwise statistical comparisons of the normalised CPM, Log_2FC and FDR of outputs of these analyses. Due to the sheer number of possible comparisons across 14 HSPC populations and 2 conditions, it would be important to prioritise populations based on interest. DS Pre-ELP/GMP appear to propagate lineage biases functional and this was supported by significant alterations to the expression of B-, NK- and myeloid-associated genes, so this would be a pertinent starting point.

Once the significant DARs for HSPCs are identified, it would be interesting to perform a motif analysis, for example using the HOMER package, to determine whether particular transcription factor (TF) binding sites are over-represented in the DARs e.g. the Hsa21 encoded master regulator *RUNX1*. These analyses would not just be limited to TFs, if DARs can be correlated to other chromatin regulators e.g. *HMGN1,* a chromatin remodeller also

encoded on Hsa21 which has also been implicated in the B-cell phenotype of DS (Lane et al, 2014; Mowery et al, 2018).

These kinds of approaches could help to identify key players controlling and of the alterations in the transcriptome of DS FBM HSPCs. When combined with other packages and tools, these data could be used to build a Gene Regulatory Network, similar to that recently generated to explore ALL (Harman et al, 2021), in order to gain a mechanistic understanding of how T21 caused molecular changes in FBM HSPCs.

To address the key questions and aims of this project, I focused on haematopoiesis-associated genes, however for both the transcriptomic and ATAC data, it would be interesting to explore the expression and accessibility of genes not involved in haematopoiesis, for instance those with roles in cell cycling and apoptosis. Several of the genes that were shown to be differentially expressed across several HSPC populations had roles in cell cycle control, expanding on previous work in our lab which showed an over-expression of several cell cycle genes in DS B-progenitors (Sorcha O'Byrne ASH Abstract, 2019). Given that upstream DS FBM HSPCs presented intrinsic deficiencies in vitro, most notably within MS-5 co-culture but downstream progenitors appeared to be spared this defect (chapter 4), this could represent a proliferative drive to compensate for impaired upstream specification into the B-lineage. To clarify this, it would be interesting to explore these further and properly characterise the changes in cell cycle genes at different stages of the hierarchy. Specifically, it would be of interest to see whether the cell cycle dynamics of DS HSPCs differ from normal, such as acceleration through specific cycle stages. It would also be of interest to assess whether cell cycle regulators, such as checkpoint regulators such as Cdc (cell division control) proteins or cyclin dependent kinases, are expressed at

normal functional levels, as this might give some clues to the propensity toward leukaemic transformation if the cell cycle isn't being controlled appropriately. To gain a fuller picture of the growth dynamic of DS HSPCs, it would also be interesting to look at both pro and anti-apoptotic proteins, such as members of the Bcl-2 family, alongside cycle regulators.

Considering epigenetic mechanisms more broadly, studies have shown genome wide changes in DNA methylation in cells harbouring T21, including within human neonates (Wiemels et al, 2019; Muskens et al, 2021), suggesting these alterations originate before birth.

At present, whilst Bisulfite-based sequencing is the gold-standard for DNA methylation analyses, these protocols can be astringent and lead to cell loss (Olova et al, 2018), which may not be appropriate for rare and precious primary DS fetal samples. Currently, protocols exist for small input non-bilsufite whole genome DNA methylation analyses which have been successfully applied to leukaemic cells (Liu et al, 2019; Li et al, 2020) and it would be exciting to see this system used to study normal and DS FBM HSPCs, including the newly described progenitors.

Chapter 6

Discussion

6.1 Background

Individuals with DS present with striking T- and, most markedly, B-cell defects throughout their lives, leading DS to be considered by some as an immunodeficiency with both quantitative and functional lymphocytopenia causing recurrent infection (Kusters et al, 2009; Carsetti et al, 2015). The B-cell defects have been shown to originate before birth (Roy et al, 2012; Roy ASH Abstract, 2014; O'Byrne ASH Abstract, 2019; Jardine et al, 2021).

Our lab recently delineated the B-differentiation pathway in FBM for the first time and showed that although B-progenitors initially emerge in the FL, the FBM is the key site of B-cell expansion from 11pcw onwards (O'Byrne et al, 2019). This study identified fetal-specific B-progenitors that expressed a developmental-stage specific gene expression programme (O'Byrne et al, 2019). More recently, the cellular landscape of normal and DS FBM was described in detail at a single cell level (Jardine et al, 2021).

Within DS FL, multi-lineage perturbation of haematopoiesis has been documented (Tunstall-Pedoe et al, 2008; Roy et al, 2012). B-cell progenitors are significantly depleted and there is a concurrent expansion of HSCs and MEPs and B-cell differentiation assays revealed a striking impairment (Roy et al, 2012). Moreover, these immunophenotypic and functional changes were accompanied by a pro-megakaryocytic/ erythroid gene expression signature

and genes involved in early lymphoid priming failed to be upregulated in DS FL HSCs, MPPs and LMPPs (Roy et al, 2012). Preliminary investigations within DS FBM suggested a similar block in B-cell differentiation suggest this defect is exacerbated within the FBM, limiting B-cell expansion before birth (Sorcha O'Byrne, DPhil thesis; O'Byrne ASH Abstract, 2019).

Whilst there is evidence that T21 alters the FBM microenvironment (Sorcha O'Byrne, DPhil thesis; O'Byrne ASH Abstract, 2019), further work was needed to understand the impact of T21 on FBM HSPCs and the process of normal B-lymphopoiesis itself for several reasons. Refining our models of B-lymphopoiesis within the normal FBM will, alongside prior work in FL, enable researchers to distinguish and compare the impact of T21 on each of these key haematopoietic sites and on the specific aspects of B-cell production each site is responsible for. Secondly, assessing additional intermediary HSPC populations within FBM, allows more precise identification of the stage at which B-cell differentiation is blocked in DS and whether there is also disruption to both fetal T- and NK-lymphocyte development in DS.

Finally, there is a significantly increased risk of children with DS developing ALL (Buitenkamp et al, 2014; Hasle et al, 2016). It is known that many, potentially the majority, of childhood ALL cases originate before birth (Wiemels et al, 1999; Rice et al, 2021), though this has not been proven for DS-ALL. Further understanding of the impact of T21 on FBM HSPCs prior to ALL initiation could provide insights into the pre-leukaemic transcriptional and epigenetic programmes that are dysregulated and leave these cells vulnerable to subsequent transformation.

In this thesis I aimed to address these gaps in our present knowledge and understanding by performing functional and molecular characterisation of HSPCs of the major sub-lineages: lymphoid, myeloid and mega-erythroid, in both normal and DS FBM.

6.2 Refining existing models of human fetal BM B-lymphopoiesis

Immunophenotypic and functional characterisation

According to the classical model, normal B-cell development in adults arises through an LMPP -> CLP -> B-cell transition (the earlier two are also believed to be precursors involved in the production of T-cells and NK). The recent identification of CD10- B-progenitors, nominally ELP and PreProB, which are unique to fetal life (O'Byrne et al, 2019), led me to hypothesise that pathways of fetal B-lymphopoiesis may assume a more CD10- phenotype compared with a more CD10+ post-natal process.

To begin to address this hypothesis, I wanted to characterise the populations present in the HSPC compartment of FBM in greater detail. To do this I designed and optimised a 12-colour flow panel to simultaneously measure the frequencies of progenitors of each of the major sub-lineages. These initial experiments revealed new, previously undescribed intermediate populations; immunophenotypic LMPPs either negative or positive for the B-cell marker CD10 (CD10-LMPP/ CD10+LMPP respectively), and an unknown progenitor which immunophenotypically resembled a CD38+ mature LMPP, later named Pre-ELP/GMP based on its functional output.

To my knowledge, this thesis presents the first characterisation of distinct CD10-/+ LMPPs in fetal tissue. Recently, progenitors named multi-lineage progenitors (MLP), with a similar immunophenotype to the CD10+ LMPP presented here ($CD34^{+}CD38^{-}Thy\text{-}1^{neg-lo}CD45RA^{+}Flt3^{+}CD7^{-/+}CD10^{+}$) and distinct populations of LMPP based on CD10 expression ($LMPP^{Ly}$ and $LMPP^{mix}$) had been described in CB and adult bone marrow (ABM) (Karamitros et al, 2018). By comprehensively characterising the functional output and transcriptome of CB LMPPs and MLPs, this recent study provided compelling evidence that the human LMPP

compartment was more heterogeneous than previously appreciated and also expanded on earlier studies which had reported human LMPPs and MLPs (Doulatov et al, 2010; Goardon et al, 2011; Laurenti et al, 2013; Farlik et al, 2016).

Briefly, the vast majority of total LMPPs in FBM were CD10-, with CD10+ LMPPs making up a scarce population compared with CD10-LMPPs and Pre-ELP/GMPs. Interestingly, in CB the frequency of Pre-ELP/GMPs was markedly reduced compared to FBM, which may suggest these are enriched in fetal life. Within CB, I also showed that a greater proportion of the total LMPPs were CD10+, and the frequencies of CD10-LMPP and CD10+LMPP were similar to the previous reported frequencies of LMPP and MLP in CB, respectively (Karamitros et al, 2018). These findings may indicate that the transition into post-natal lymphopoeisis involves a more CD10+ phenotype, however these experiments must be repeated in ABM to confirm this.

Functionally, I showed that CD10-LMPP give rise to both CD10+LMPP and Pre-ELP/GMP and the downstream B-progenitors, whilst Pre-ELP/GMP fail to produce any LMPPs but do give rise to ELPs, GMPs and the B-progenitors. In terms of their mature output, all 3 populations gave rise to B, NK and T-cells. CD10-LMPPs showed the greatest myeloid potential on methylcellulose, mirroring early observations by Goardon et al, using ABM, that showed CD10- 'LMPP-like' progenitors with the same immunophenotype could produce all of the major lymphoid lineages whilst retaining myeloid output in vitro (Goardon et al, 2011). In terms of lymphoid output, Pre-ELP/GMP were almost entirely B-restricted and CD10+LMPPs were lymphoid restricted and gave rise to proportionally greater NK cells than both other populations. These findings align with the observations from CB that $CD10^{low/neg}$ LMPPs

designated LMPP^{mix} showed greater myeloid potential, whilst an increase in CD10 expression, such as within the CD10$^{mod/high}$ LMPP^{Ly} and CD10+ MLP populations, is associated with lineage restriction and a loss of myeloid output (Doulatov et al, 2010; Karamitros et al, 2018). Similarly, LMPP^{Ly} in CB showed greater proportional NK output in MS5-DL1 culture assays compared to their CD10- counterparts (Karamitros et al, 2018), as was the case for CD10-/+ FBM LMPPs in my functional experiments.

Altogether these findings in human fetal BM, lend support to the growing body of work that shows CD10 is a faithful marker of lymphoid commitment (Ichii et al, 2010; Kohn et al, 2012; Karamitros et al, 2018). The association between increasing CD10 expression and lineage restriction from the data presented in this thesis and the Karamitros paper, suggest that CD10-LMPP are more multipotent and less differentiated than their more CD10+ downstream counterparts. This is further supported by the absolute counts data which showed that CD10-LMPPs produced the greatest absolute output for all measured lineages and Pre-ELP/GMP the lowest, suggesting that CD10-LMPP may possess greater self-renewal and expansion capacity, whilst CD10+LMPP and Pre-ELP/GMP appear more differentiated.

Molecular findings

These functional observations were mirrored by the molecular data. Pairwise comparisons showed a significant upregulation of many genes involved in B-lymphopoiesis within Pre-ELP/GMPs compared to CD10-LMPPs including *DNTT*, *PAX5, EBF1, CD72* in Pre-ELP/GMPs and a concurrent significant decrease in myeloid genes such as *CSF2RA* and *IL3RA*. These data support the almost exclusively B-lineage output of normal Pre-ELP/GMPs in MS-5 co-culture assays compared to the more multi-potent CD10-LMPPs. CD10-LMPPs show higher

expression of *FLT3* (though not significantly), which is known to support both early lymphopoiesis and myelopoiesis, suggesting that early lineage priming begins upstream of Pre-ELP/GMP. The expression profile of the FBM CD10-LMPPs in this study was similar to that of the CB LMPPs (CD10-) presented by Karamitros et al, who showed a similar co-expression of both lymphoid and myeloid genes (Karamitros et al, 2018).

Pre-ELP/GMPs do retain detectable myeloid expression e.g. *PRTN3, AZU1, MPO*, showing that whilst this does not translate to substantial functional output, these programmes are residually maintained. I also observed significantly increased expression of *CD38*, which is associated with haematopoietic maturation, in Pre-ELP/GMPs relative to CD10-LMPPs and reduced expression of the stem gene *SPINK2.*

Altogether the molecular and functional data support the hypothesis that these are two distinct populations and that Pre-ELP/GMPs appear to lie downstream of CD10-LMPPs within the differentiation hierarchy.

The expression profiles of CD10-/+ LMPPs were very similar although expression of early B-lineage tended to be higher in the CD10+ LMPP and that of myeloid genes tended to be higher in the CD10- LMPPs. These data mirror findings in CB where the expression of lymphoid associated genes was highest in MLPs (counterpart of CD10+ FBM LMPPs) and lower in LMPPs (counterpart of CD10- FBM LMPPs) with the converse was observed for myeloid-associated genes (Karamitros et al, 2018).

The molecular data support the findings from functional assays which indicated lymphoid restriction in CD10+LMPPs, however these results should be appraised with caution due to having only one normal 10+LMPP replicate due to population scarcity.

Otherwise, several NK-associated genes become detectable at the LMPP stage such as *ILR15A, TOX, NKG7* and *TYROPB,* with CD10-/+ populations showing similar expression, with most NK-associated genes showing comparable or decreased expression in Pre-ELP/GMPs. Interestingly, however the expression of *PRMD1* and *FOXO1,* which are both negative regulators of NK-lymphopoiesis, are expressed more highly in Pre-ELP/GMP than both CD10-/+ LMPPs, which may indicate a repression of NK differentiation in favour of a B-cell restricted state.

Comparing Pre-ELP/GMPs to their downstream ELP and GMP, I detected very few DEGs between Pre-ELP/GMP and ELP, mostly of non-haematopoietic function. By contrast, Pre-ELP/GMPs and GMPs showed clearly distinct expression profiles. Several B-cell genes were expressed at significantly higher levels in Pre-ELP/GMP, including *BACH2, VPREB1, LEF1 CD10, CD19*, whilst many myeloid- and erythroid-associated genes were significantly upregulated in GMPs including *SPIB, AZU1, MPO, FCER1A, PF4* in contrast to the upstream B- lineage biasing between CD10-LMPPs and Pre-ELP/GMPs. Overall, these data indicate that unlike Pre-ELP/GMPs and ELPs, Pre-ELP/GMPs and GMPs show distinct transcriptional and chromatin accessibility profiles, representing B- and myeloid- biased signatures, respectively.

Putative CD10-/+ pathways of B-lymphopoiesis within FBM

Based on these preliminary findings, I hypothesise that in FBM, B-cells can be generated through 2 pathways of B-lymphopoiesis, distinguished by CD10, and that the pathway involving the CD10- progenitors is more dominant in normal FBM (see Figure 6.1).

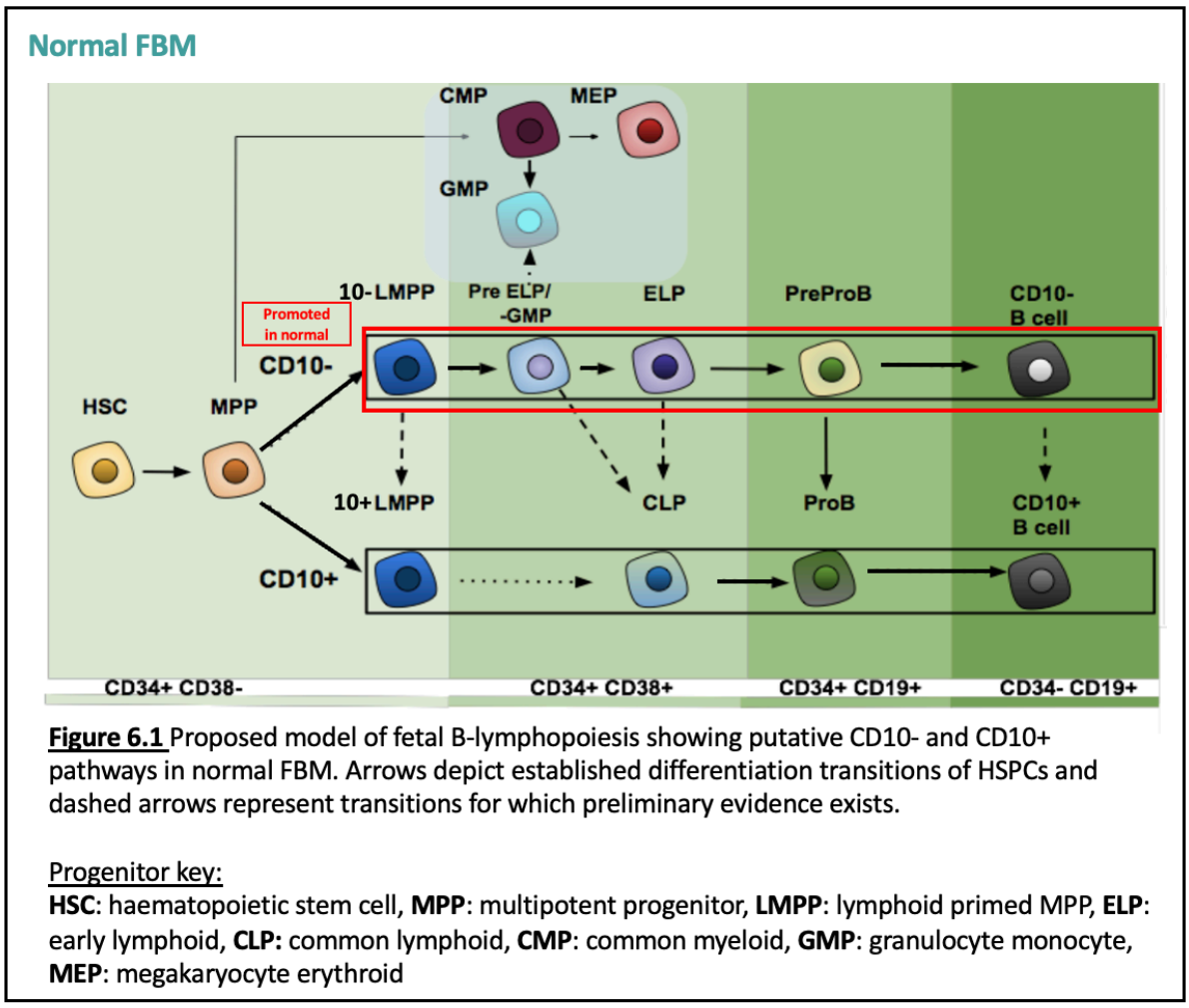


Figure 6.1 Proposed model of fetal B-lymphopoiesis showing putative CD10- and CD10+ pathways in normal FBM. Arrows depict established differentiation transitions of HSPCs and dashed arrows represent transitions for which preliminary evidence exists.

Progenitor key:
HSC: haematopoietic stem cell, **MPP**: multipotent progenitor, **LMPP**: lymphoid primed MPP, **ELP**: early lymphoid, **CLP:** common lymphoid, **CMP**: common myeloid, **GMP**: granulocyte monocyte, **MEP**: megakaryocyte erythroid

As expected, and reported previously (Sorcha O'Byrne DPhil thesis), B-cell differentiation genes increase in expression down the B-differentiation hierarchy, which is mirrored by the chromatin accessibility profiles of these genes. In contrast, genes associated with myelopoiesis and erythropoiesis are more highly expressed in upstream progenitors and the myeloid/erythroid progenitors.

LMPPs represent a key transition in early pan-lymphoid priming, and show the potential to give rise to all lymphoid lineages at both the functional and molecular level. CD10-LMPP lie upstream of both CD10+LMPP and Pre-ELP/GMP. The functional data indicate CD10+LMPPs are more differentiated than CD10-LMPP and are more lymphoid restricted, in line with

findings in CB (Karamitros et al, 2018). It has been difficult to tease apart these differences at the molecular level due to the scarcity of CD10+LMPP in normal FBM limiting replicates for these experiments. That CD10+LMPPs give rise to B-cells, would indicate that this could take place through a CD10+ pathway involving CLPs, which I did find in FBM, and ProB progenitors. It may be possible that CD10 can be transiently lost during B-lymphopoiesis, though current evidence only supports this happening at later transitional B-cell stages (Sanz et al, 2019).

These data point toward a parallel CD10- trajectory from CD10-LMPP > Pre-ELP/GMP > ELP > PreProB. Whilst Pre-ELP/GMP can give rise to GMP and do retain expression of myeloid genes, their progeny are mostly ELP and subsequently PreProB in normal FBM. As ELPs are a rare HSPC population it is possible that Pre-ELP/GMPs are able to directly produce CLPs or PreProBs either by acquiring CD10 or CD19 respectively. This direct transmission, circumventing an ELP intermediate, would explain how PreProBs are detected as early as day 3 in MS-5 co-cultures. Regardless, the transition from CD10-LMPP to Pre-ELP/GMP appears to represent an important shift toward B-cell commitment.

6.3 The functional impact of T21 on multi-lineage haematopoiesis in FBM

To characterise the functional impact of T21 on FBM haematopoiesis, I systematically sorted all of the newly described and established HSPCs of the B-differentiation hierarchy for extensive functional characterisation. Given the conflicting reports about the impact of T21 on T- and NK-lymphopoiesis (Cossarizza et al, 1991; Thilaganathan et al, 1993; deHingh et al, 2005; Zizka et al, 2006; Bloemers et al, 2010; Cetiner et al, 2010; Schoch et al, 2017; Waugh et al, 2019; Lambert et al, 2021; Lambert et al, 2022; Waugh et al, 2022), I also conducted OP9-DL1 co-culture assays to assess the differentiation of these lineages, to determine whether the previously reported B-cell defect was a specific one or a result of pan-lymphoid impairments. Where possible, I sought to gestation match normal and DS FBM samples to minimise additional potential sources of variation in already highly variable primary samples.

Immunophenotypic analysis of the DS FBM HSPC compartment revealed dramatic alterations in HSPC frequencies. Mirroring previous findings in FL and FBM, the frequencies of both HSCs and MEPs were significantly increased in DS FBM, whilst the B-progenitors, most markedly the CD10- ELP and PreProB and less strikingly the CD10+ CLP and ProB, were significantly reduced (Roy et al, 2012; Anindita Roy ASH Abstract, 2014; Sorcha O'Byrne ASH Abstract, 2019, Sorcha O'Byrne DPhil thesis, 2019). Perhaps most interesting was the significant increase in the frequency of CD10+LMPPs in DS FBM, shown in this thesis for the first time. The overall LMPP compartment was comparable in size to normal FBM, which suggests a specific shift toward a more CD10+ phenotype. The relative increase in CD10+LMPP out of the total LMPP population was comparable to that in CB. That CD10- ELP and PreProB are specific to fetal life (O'Byrne et al, 2019), and that these are most strikingly

depleted in DS FBM, combined with the significant increase in CD10+LMPP, suggests that CD10-/+ progenitors are disparately impacted by T21, and that in DS FBM a more CD10+ post-natal phenotype presents (see Figure 6.2).

In line with previous observations, (Roy et al, 2012; Sorcha O'Byrne ASH Abstract, 2019), I observed striking defects in B-lymphopoiesis within upstream and intermediate DS FBM HSPCs during MS-5 co-culture assays. Whilst normal FBM HSPCs showed robust B-cell output on MS-5 stroma, B-cell frequencies were drastically decreased from the HSC level in DS FBM. This striking defect was also observed for the newly described Pre-ELP/GMP, 10-/+LMPP, which all robustly produced B-cells in normal FBM. Interestingly, DS ELP showed a milder B-cell impairment and the output of PreProB and ProB progenitors was comparable to normal. These discrepancies in up/downstream progenitors, suggests that this defect originates upstream and represents a failure to support early B-lymphoid commitment. However, despite B-progenitors appearing to be able to successfully differentiate into mature B-cells, the earlier block prevents the accumulation of Pre-ELP/GMPs, ELPs and B-progenitors, which ultimately limits the final B-cell output.

Alongside impaired B-lymphopoiesis, I observed lineage skewing within upstream and intermediate DS FBM HSPCs, with the nature of this lineage skewing appeared to be linked to whether the HSPC population in question was CD10- or CD10+. All of the upstream CD10- progenitors (HSC, MPP, CD10-LMPP, Pre-ELP/GMP) showed a skew toward myelopoiesis on MS-5 stroma and increased clonogenicity in methylcellulose, however DS CD10+LMPP showed limited myelopoiesis. In addition, DS FBM HSCs and MPPs showed a mega-erythroid bias on methylcellulose (Jardine et al 2021), in line with previous findings in FL (Tunstall-

Pedoe et al, 2008; Roy et al, 2012). DS ELPs did show greater myeloid output than normal, however this skew was less striking than in the upstream progenitors, which might suggest limited residual myeloid potential in these lymphoid progenitors that can be translated into output.

A summary of the proposed changes to B-lymphopoiesis in DS FBM and how CD10-/+ pathways appear to be differentially blocked and promoted based on the immunophenotypic and functional data, is shown in Figure 6.2.

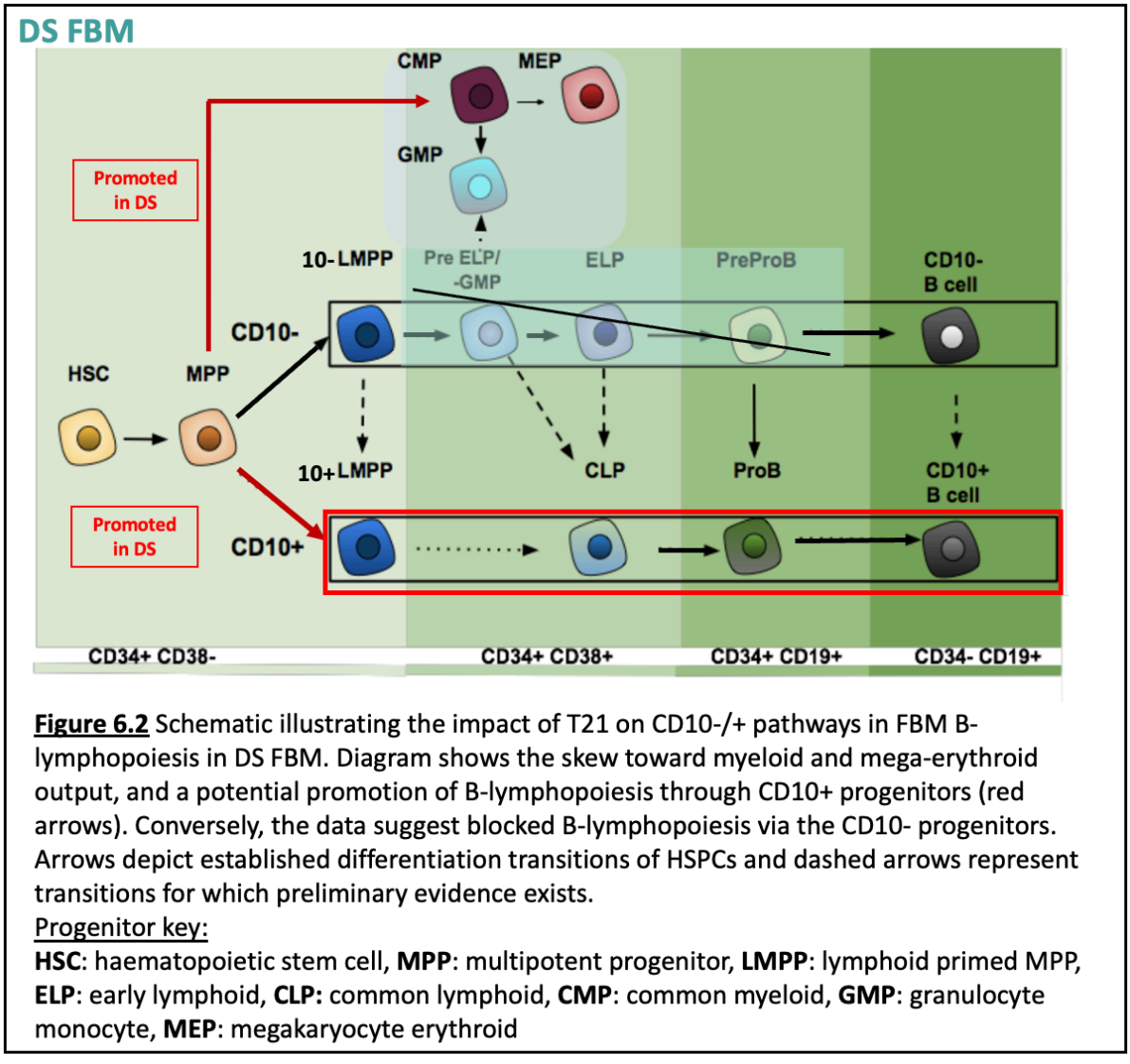


Figure 6.2 Schematic illustrating the impact of T21 on CD10-/+ pathways in FBM B-lymphopoiesis in DS FBM. Diagram shows the skew toward myeloid and mega-erythroid output, and a potential promotion of B-lymphopoiesis through CD10+ progenitors (red arrows). Conversely, the data suggest blocked B-lymphopoiesis via the CD10- progenitors. Arrows depict established differentiation transitions of HSPCs and dashed arrows represent transitions for which preliminary evidence exists.
Progenitor key:
HSC: haematopoietic stem cell, **MPP**: multipotent progenitor, **LMPP**: lymphoid primed MPP, **ELP**: early lymphoid, **CLP:** common lymphoid, **CMP**: common myeloid, **GMP**: granulocyte monocyte, **MEP**: megakaryocyte erythroid

One of the most striking observations of both MS-5 and OP9-DL1 co-culture assays, was the skew toward NK lymphopoiesis for all of the upstream and intermediate DS FBM HSPCs, including ELP. As was the case in normal FBM, CD10+LMPP are lymphoid restricted but this is toward NK cell fates, rather than B-lymphoid. This indicates that CD10 remains a driver of lymphoid restriction in DS FBM, but there is a failure to ensure B-lymphopoiesis. Similarly, DS ELP showed a skew toward NK output, suggesting potential re-direction of their lymphoid priming away from a B-cell fate, or the adoption of NK cell fates in the absence of sufficient B-cell programmes.

To my knowledge, the skew toward NK-cell fates in DS FBM HSPCs is a novel finding within fetal tissue and is consistent with previous reports of increased NK numbers and frequencies in individuals with DS, including as early as neonatal life (Cossarizza et al, 1991; Zizka et al, 2006; Cetiner et al, 2010; Schoch et al, 2017; Waugh et al,2019; Lambert et al, 2021).

There are several reasons why there might be a skew toward NK cell fates in DS. The first theory involves the increase in hyperinflammatory signalling and responsiveness, such as Interferon (IFN) and IL-6 mediated signalling in DS cells, including the FBM microenvironment (Sullivan et al, 2016; Sullivan et al, 2017; Waugh et al, 2019; O'Byrne ASH Abstract, 2019; O'Byrne DPhil thesis, 2019; Jardine et al, 2021), as illustrated in Figure 6.3. As well as an increase in the frequency of NK cells within individuals with DS, reports have highlighted an increase in hyper-activated cytotoxic NK cells (Cossarissa et al 1991; Waugh et al, 2019), which are regulated through Type I IFN signalling cascades (Paolini et al, 2015; Müller et al, 2017). Given that several IFN signalling receptors (IFNAR) are expressed on chromosome 21 (de Weerd and Nguyen, 2012) it has been hypothesised that alterations to the expression of these genes is causal in the enhanced pro-inflammatory IFN signalling

observed in DS (Waugh et al, 2019; Kong et al, 2020; Illouz et al, 2021). The IFN-mediated enhanced cytotoxicity of DS cells is believed to predispose individuals with DS to autoimmune disorders (Anwar et al, 1998; Karlsson et al, 1998; Mårild et al, 2013), and paradoxically, also impairs the development of and reduces the incidence of solid tumors, (Waugh et al, 2019; Illouz et al, 2021), another hallmark of DS (Hasle et al, 2016). In addition to the increased NK frequencies, the pro-inflammatory microenvironment in DS FBM (O'Byrne ASH Abstract, 2019), would explain the skew toward myelopoiesis observed in my experiments (Waugh et al, 2019; Huggard et al, 2020).

Another hypothesis regarding lymphoid lineage switching lies in our evolutionary understanding of innate and adaptive immunity. Evolutionary geneticists have shown that the NK lineage is an older component of human immunity that the later adaptive B- and T-immune programmes are layered onto (Sun and Lanier, 2009; Cichocki et al, 2019). It has been speculated, and would apply here, that if B-cell programmes are not adequately activated, the NK lineage would become the default (Cichocki et al, 2019).

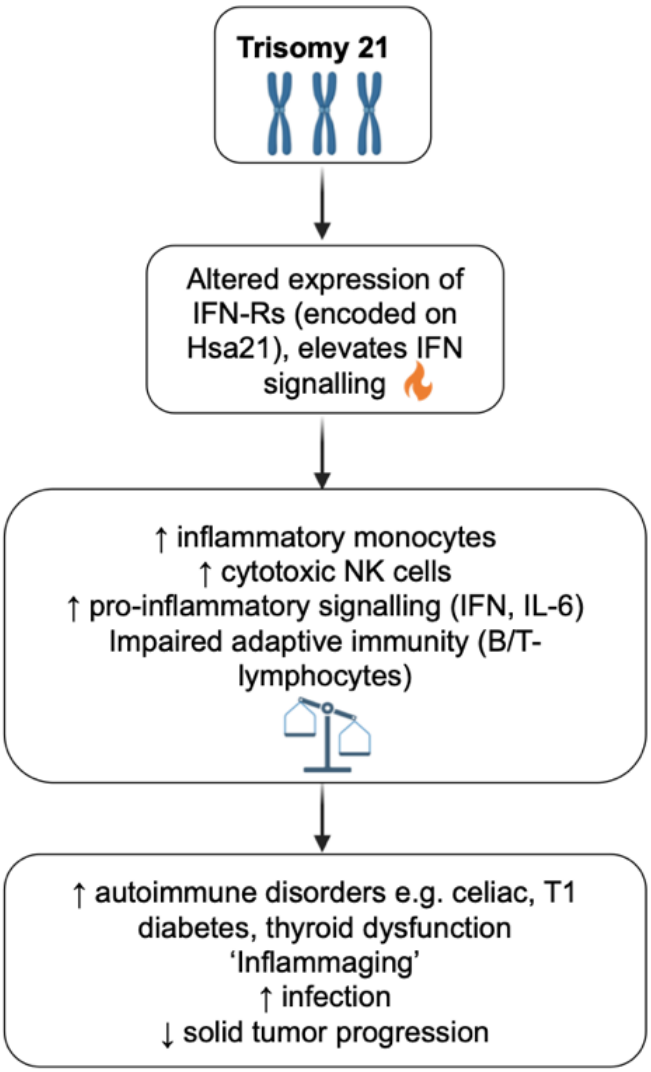


Figure 6.3 T21-driven pro-inflammatory signals are thought to unbalance the immune system in DS and may explain the myeloid/ NK skew observed during functional assays of DS FBM.

6.4 The impact of T21 on the transcriptome and chromatin accessibility of FBM HSPCs

I performed RNA and ATAC sequencing of DS FBM HSPCs in order to gain a molecular understanding of the B-cell impairment and lineage skewing observed during the functional assays.

Overall, dimensionality reduction analysis of DS-FBMs based on their chromatin accessibility and gene expression, broadly resolved the expected progenitor relationships based on HSPC lineage and position within the differentiation hierarchy, as was seen for normal. Broadly speaking, the more primitive progenitors (HSC, MPP, LMPP) clustered closely together, while the B-lymphoid and myelo/mega/erythroid committed progenitors formed 2 distinct clusters.

Interestingly however, DS Pre-ELP/GMP clustered more closely to GMPs than ELP when compared to normal Pre-ELP/GMP which clustered more closely to ELPs and B-progenitors, in line with the myeloid skew observed for this population in both MS-5 and methycellulose assays. Furthermore, DS MPP also clustered more closely to the myelo-erythroid progenitors than normal MPP, which supports the significant erythroid bias observed for DS MPP in methycellulose.

Pairwise comparisons of normal and DS HSPCs further supported the functional observations. Mirroring my observations for FBM in methylcellulose (Jardine et al, 2021), and previous findings in DS FL (Tunstall-Pedoe et al, 2008; Roy et al, 2012), both DS FBM HSCs/MPPs showed significantly higher expression of several megakaryocytic and erythroid genes compared with normal counterparts. Interestingly, DS Pre-ELP/GMP produced a small

number of erythroid colonies on methylcellulose, which was not observed for normal counterparts. Supporting this functional observation, pairwise comparisons of the transcriptome of normal/DS Pre-ELP/GMPs revealed a significant increase in several mega-erythroid lineage associated genes including *ITGA2B* and *GFI1B.*

Interestingly, only one DEG with known haematopoietic function could be determined between pairwise comparisons of N and DS CD10-LMPPs, which was the myeloid gene *PRTN3*, which was over expressed in DS. The expression of some genes associated with B-lymphopoiesis were reduced in DS CD10-LMPPs, such as *CD72*, whilst genes associated with myelopoiesis and NK-lymphopoiesis, such as *MPO* and *ID2* were increased, but none of these changes were statistically significant.

Conclusions from comparisons of normal and DS CD10+LMPPs cannot be confidently interpreted at this stage due to only having n=1 for normal, however CD10+LMPPs did show significantly reduced expression of B-lineage associated genes *CEACAM1* and *ZNF609* and significantly increased expression of genes linked to myelopoiesis and inflammation in DS FBM, which supports previous observations of a pro-inflammatory phenotype in DS FBM (Sorcha O'Byrne ASH abstract, 2019). In addition, I did observe increased expression of genes associated with NK-lymphopoiesis, such as *NFIL3* and *ID2* in DS CD10+LMPPs, supporting functional observations.

Comparisons of Pre-ELP/GMPs in normal and DS FBM revealed a significant downregulation of several genes associated with B-lymphopoiesis in DS, mirroring observations from MS-5 co-culture assays. Concurrently, several genes associated with myelopoiesis, such as *ID1,*

AZU1 and *PRTN3* and NK-lymphopoiesis, such as *NCR3* and *PVRIG* were upregulated in DS Pre-ELP/GMPs, supporting functional findings. Several of the genes that were differentially expressed between normal Pre-ELP/GMP and GMP which had roles in myelopoiesis, were also significantly upregulated in DS Pre-ELP/GMP compared to normal Pre-ELP/GMP. This suggests Pre-ELP/GMPs bear greater resemblance to their myeloid progeny in DS FBM, whereas in normal FBM Pre-ELP/GMP showed greater molecular similarity to ELP. Interestingly, despite the B-cell defects being most severe in upstream and intermediate DS FBM HSPCs, I did observe a significant decrease in the expression of B-lineage genes in DS ELPs, as well as a significant increase in the expression of megakaryocyte-erythroid associated genes even if these do not translate into erythroid output on methylcellulose.

6.5 Future work

There were unavoidable technical limitations incurred during this project, namely the rarity of several HSPC populations and the limited numbers of primary DS fetal samples. Whilst the preliminary findings presented in this thesis raise interesting questions and offer potential answers, such as the existence of CD10-/+ pathways of B-lymphopoiesis, this model will require validation with additional biological replicates.

Pre-ELP/GMPs are a novel discovery of this project and it is of major interest to identify whether these are specifically enriched in fetal life and perform ontogeny specific functions, as was the case for ELP and PreProB (O'Byrne et al, 2019), by comparing their frequencies in FBM with CB and ABM. It would also be of interest to identify whether Pre-ELP/GMP are present in FL and if so, whether they exhibit distinct characteristics compared to those found in FBM given recent work which has emphasised changes in lineage priming within distinct haematopoietic sites throughout ontogeny (Roy et al, 2021). Single cell atlases of FL and FBM have been recently published (Popescu et al, 2019; Jardine et al, 2021), and it would be exciting to see Pre-ELP/GMP included in such work in future.
Similarly, it is important to validate the observations of CD10-/+ LMPP in further FBM replicates, is possible, and also within other developmental stages e.g. CB and ABM. The development of single cell protocols, where feasible, would circumvent the technical limitations imposed by the scarcity of CD10+LMPP in normal FBM.

Confirming whether CD10-/+ pathways are disproportionately promoted in DS FBM, will only be possible by repeating experiments in normal and DS FBM. To make inferences about whether a more post-natal-like, CD10+ phenotype presents in DS-FBM, would involve

comparisons of normal and DS FBM with CB and ABM and ideally FL. This work would be particularly interesting as children with DS show an increased proclivity toward ALL, the non-DS version of which is thought to originate in utero. Interestingly however, DS-ALL almost never occurs in infants (Roberts and Izraeli, 2014) and it has been suggested that infant and childhood non-DS-ALL originate in distinct CD10- and CD10+ fetal progenitors respectively (O'Byrne et al, 2019; Jackson et al, 2021; Khabirova et al, 2022). If it is further clarified that DS-FBM shows a more CD10+ phenotype and a reduction in the CD10- progenitor compartment, then it may also be that a CD10+ progenitor is the cell of origin for DS-ALL.

Further exploration of the CD10- and CD10+ progenitors may give indications as to their permissiveness toward transformation compared to normal counterparts. Our lab recently developed a faithful mouse model for MLL-AF4 arranged ALL in which FL HSPCs from several stages of the B-differentiation hierarchy could be transformed through CRISPR-Cas9 editing (Rice et al, 2021). Our current understanding of the origins of DS-ALL is limited, so it would be exciting to see the results of similar investigations in DS fetal HSPCs, such as CD10-/+ LMPPs, Pre-ELP/GMPs, ELPs and the downstream B-progenitors. These longer term, translational efforts would rely on a fuller understanding of the pre-transformation background of the HSPCs involved in B-differentiation in DS FBM.

Given the emerging data suggesting epigenetic mechanisms lie behind the perturbed haematopoiesis of DS (Mowery et al, 2018, Lane et al, 2014; Muskens et al, 2021), it would be of interest to explore this further. Specifically, genome-wide alterations in DS HSPCs from neonatal blood spots was recently reported (Muskens et al, 2021) indicating that they originate before birth. Protocols exist for small input, high-sensitivity non-bisulphite DNA

methylation sequencing (Liu et al, 2019), which would be appropriate given the scarcity of these biological samples.

Finally, the functional experiments presented in this thesis were limited to in vitro assays which whilst allowing us to assess lineage output in vitro, do not accurately recapitulate the in vivo scenario. Mouse studies would enable us to first verify the functional potential of the newly described progenitors presented here, and subsequently compare the output of DS FBM HSPCs in vivo. Moreover, this would enable us to compare whether the mature immune output of DS FBM HSPCs e.g. B-cells or NK-cells, is functionally compromised, which was unfortunately beyond the scope of my project.

6.6. Conclusions

There is a growing appreciation for the heterogeneity that exists within HSPC populations of haematopoietic differentiation hierarchies. By characterising the HSPC compartment of FBM in greater detail, specifically by describing three potential new intermediate lymphomyeloid progenitors, I have refined the existing model for fetal B-cell differentiation. Ultimately, lymphoid specification and commitment occurs along a continuum and the incorporation of single cell protocols in future work will bring us closer to understanding fetal B-lymphopoiesis and other lineage trajectories.

In DS FBM, I have revealed a striking B-cell defect and lineage biasing which originates at the HSC level and is propagated through intermediate progenitors. The novel observation that NK-lymphopoiesis is increased in DS FBM highlights that there is not an indiscriminate block in lymphopoiesis, but rather implies a diversion of lymphoid potential away from the B-lineage toward NK fates, which may be linked to a T21-induced pro-inflammatory microenvironment as suggested by Jardine et al (2021).

These functional observations were supported at the molecular level, with T21 causing broad changes in both the transcriptome and chromatin accessibility of FBM HSPCs.

Bibliography

Adamo, Annalisa, Pietro Delfino, Alessandro Gatti, Alice Bonato, Paul Takam Kamga, Riccardo Bazzoni, Stefano Ugel, Angela Mercuri, Simone Caligola, and Mauro Krampera. 2020. “HS-5 and HS-27A Stromal Cell Lines to Study Bone Marrow Mesenchymal Stromal Cell-Mediated Support to Cancer Development.” *Frontiers in Cell and Developmental Biology* 8 (November): 584232.

Adkins, Becky, Claude Leclerc, and Stuart Marshall-Clarke. 2004. “Neonatal Adaptive Immunity Comes of Age.” *Nature Reviews. Immunology* 4 (7): 553–64.

Adolfsson, Jörgen, Robert Månsson, Natalija Buza-Vidas, Anne Hultquist, Karina Liuba, Christina T. Jensen, David Bryder, et al. 2005. “Identification of Flt3+ Lympho-Myeloid Stem Cells Lacking Erythro-Megakaryocytic Potential a Revised Road Map for Adult Blood Lineage Commitment.” *Cell* 121 (2): 295–306.

Ahn, Erin Eun-Young, Tsunehito Higashi, Ming Yan, Shinobu Matsuura, Christopher J. Hickey, Miao-Chia Lo, Wei-Jong Shia, Russell C. DeKelver, and Dong-Er Zhang. 2013. “SON Protein Regulates GATA-2 through Transcriptional Control of the microRNA 23a~27a~24-2 Cluster.” *The Journal of Biological Chemistry* 288 (8): 5381–88.

Akashi, K., D. Traver, T. Miyamoto, and I. L. Weissman. 2000. “A Clonogenic Common Myeloid Progenitor That Gives Rise to All Myeloid Lineages.” *Nature* 404 (6774): 193–97.

Aksöz, Merve, Grigore-Aristide Gafencu, Bilyana Stoilova, Mario Buono, Yiran Meng, Niels Asger Jakobsen, Marlen Metzner, et al. 2022. “Identification and Age-Dependent Increase of Platelet

Biased Human Hematopoietic Stem Cells." *bioRxiv*. https://doi.org/10.1101/2022.01.14.475546.

Alexandrov, Ludmil B., Philip H. Jones, David C. Wedge, Julian E. Sale, Peter J. Campbell, Serena Nik-Zainal, and Michael R. Stratton. 2015. "Clock-like Mutational Processes in Human Somatic Cells." *Nature Genetics* 47 (12): 1402–7.

Alhaj Hussen, Kutaiba, Thien-Phong Vu Manh, Fabien Guimiot, Elisabeth Nelson, Emna Chabaane, Marc Delord, Maxime Barbier, et al. 2017. "Molecular and Functional Characterization of Lymphoid Progenitor Subsets Reveals a Bipartite Architecture of Human Lymphopoiesis." *Immunity* 47 (4): 680–96.e8.

Anjos-Afonso, Fernando, Florian Buettner, Syed A. Mian, Hefin Rhys, Jimena Perez-Lloret, Manuel Garcia-Albornoz, Namrata Rastogi, Linda Ariza-McNaughton, and Dominique Bonnet. 2022. "Single Cell Analyses Identify a Highly Regenerative and Homogenous Human CD34+ Hematopoietic Stem Cell Population." *Nature Communications* 13 (1): 2048.

Antonarakis, Stylianos E. 2017. "Down Syndrome and the Complexity of Genome Dosage Imbalance." *Nature Reviews. Genetics* 18 (3): 147–63.

Antonarakis, Stylianos E., Brian G. Skotko, Michael S. Rafii, Andre Strydom, Sarah E. Pape, Diana W. Bianchi, Stephanie L. Sherman, and Roger H. Reeves. 2020. "Down Syndrome." *Nature Reviews. Disease Primers* 6 (1): 9.

Anwar, A. J., J. D. Walker, and B. M. Frier. 1998. "Type 1 Diabetes Mellitus and Down's Syndrome: Prevalence, Management and Diabetic Complications." *Diabetic Medicine: A Journal*

of the British Diabetic Association 15 (2): 160–63.

Arinobu, Yojiro, Shin-Ichi Mizuno, Yong Chong, Hirokazu Shigematsu, Tadafumi Iino, Hiromi Iwasaki, Thomas Graf, et al. 2007. "Reciprocal Activation of GATA-1 and PU.1 Marks Initial Specification of Hematopoietic Stem Cells into Myeloerythroid and Myelolymphoid Lineages." *Cell Stem Cell* 1 (4): 416–27.

Awong, Génève, Ross N. La Motte-Mohs, and Juan Carlos Zúñiga-Pflücker. 2008. "In Vitro Human T Cell Development Directed by Notch-Ligand Interactions." *Methods in Molecular Biology* 430: 135–42.

Bae, Sunhee, and Bluma J. Lesch. 2020. "H3K4me1 Distribution Predicts Transcription State and Poising at Promoters." *Frontiers in Cell and Developmental Biology* 8 (May): 289.

Bamburg, James R., and George S. Bloom. 2009. "Cytoskeletal Pathologies of Alzheimer Disease." *Cell Motility and the Cytoskeleton* 66 (8): 635–49.

Barber, Chad L., Encarnacion Montecino-Rodriguez, and Kenneth Dorshkind. 2011. "Reduced Production of B-1–specified Common Lymphoid Progenitors Results in Diminished Potential of Adult Marrow to Generate B-1 Cells." *Proceedings of the National Academy of Sciences* 108 (33): 13700–704.

Basha, Saleem, Naveen Surendran, and Michael Pichichero. 2014. "Immune Responses in Neonates." *Expert Review of Clinical Immunology* 10 (9): 1171–84.

Beaudin, Anna E., Scott W. Boyer, Jessica Perez-Cunningham, Gloria E. Hernandez, S. Christopher Derderian, Chethan Jujjavarapu, Eric Aaserude, Tippi MacKenzie, and E. Camilla Forsberg. 2016. “A Transient Developmental Hematopoietic Stem Cell Gives Rise to Innate-like B and T Cells.” *Cell Stem Cell* 19 (6): 768–83.

Belluschi, Serena, Emily F. Calderbank, Valerio Ciaurro, Blanca Pijuan-Sala, Antonella Santoro, Nicole Mende, Evangelia Diamanti, et al. 2018. “Myelo-Lymphoid Lineage Restriction Occurs in the Human Haematopoietic Stem Cell Compartment before Lymphoid-Primed Multipotent Progenitors.” *Nature Communications* 9 (1): 4100.

Béné, Marie C. 2005. “Immunophenotyping of Acute Leukaemias.” *Immunology Letters* 98 (1): 9–21.

Benz, Claudia, Michael R. Copley, David G. Kent, Stefan Wohrer, Adrian Cortes, Nima Aghaeepour, Elaine Ma, et al. 2012. “Hematopoietic Stem Cell Subtypes Expand Differentially during Development and Display Distinct Lymphopoietic Programs.” *Cell Stem Cell* 10 (3): 273–83.

Berardi, A. C., E. Meffre, F. Pflumio, A. Katz, W. Vainchenker, C. Schiff, and L. Coulombel. 1997. “Individual CD34+CD38lowCD19-CD10- Progenitor Cells from Human Cord Blood Generate B Lymphocytes and Granulocytes.” *Blood* 89 (10): 3554–64.

Berland, Robert, and Henry H. Wortis. 2002. “Origins and Functions of B-1 Cells with Notes on the Role of CD5.” *Annual Review of Immunology* 20: 253–300.

Birger, Yehudit, Liat Goldberg, Timothy M. Chlon, Benjamin Goldenson, Inna Muler, Ginette Schiby, Jasmin Jacob-Hirsch, Gideon Rechavi, John D. Crispino, and Shai Izraeli. 2013. "Perturbation of Fetal Hematopoiesis in a Mouse Model of Down Syndrome's Transient Myeloproliferative Disorder." *Blood* 122 (6): 988–98.

Bloemers, Beatrijs L. P., Grada M. van Bleek, Jan L. L. Kimpen, and Louis Bont. 2010. "Distinct Abnormalities in the Innate Immune System of Children with Down Syndrome." *The Journal of Pediatrics* 156 (5): 804–9, 809.e1–809.e5.

Blokzijl, Francis, Joep de Ligt, Myrthe Jager, Valentina Sasselli, Sophie Roerink, Nobuo Sasaki, Meritxell Huch, et al. 2016. "Tissue-Specific Mutation Accumulation in Human Adult Stem Cells during Life." *Nature* 538 (7624): 260–64.

Bohnstedt, C., M. Levinsen, S. Rosthøj, B. Zeller, M. Taskinen, S. Hafsteinsdottir, H. Björgvinsdóttir, M. Heyman, K. Schmiegelow, and Nordic Society of Pediatric Hematology and Oncology (NOPHO). 2013. "Physicians Compliance during Maintenance Therapy in Children with Down Syndrome and Acute Lymphoblastic Leukemia." *Leukemia* 27 (4): 866–70.

Böiers, Charlotta, Joana Carrelha, Michael Lutteropp, Sidinh Luc, Joanna C. A. Green, Emanuele Azzoni, Petter S. Woll, et al. 2013. "Lymphomyeloid Contribution of an Immune-Restricted Progenitor Emerging prior to Definitive Hematopoietic Stem Cells." *Cell Stem Cell* 13 (5): 535–48.

Böiers, Charlotta, Simon E. Richardson, Emma Laycock, Alya Zriwil, Virginia A. Turati, John Brown, Jason P. Wray, et al. 2018. "A Human IPS Model Implicates Embryonic B-Myeloid Fate Restriction as Developmental Susceptibility to B Acute Lymphoblastic Leukemia-Associated

ETV6-RUNX1." *Developmental Cell* 44 (3): 362–77.e7.

Boonyaratanakornkit, Jim, and Justin J. Taylor. 2019. "Techniques to Study Antigen-Specific B Cell Responses." *Frontiers in Immunology* 10 (July): 1694.

Brault, Véronique, Arnaud Duchon, Caroline Romestaing, Ignasi Sahun, Stéphanie Pothion, Mona Karout, Christelle Borel, et al. 2015. "Opposite Phenotypes of Muscle Strength and Locomotor Function in Mouse Models of Partial Trisomy and Monosomy 21 for the Proximal Hspa13-App Region." *PLoS Genetics* 11 (3): e1005062.

Brault, Veronique, Caroline Romestaing, Ignasi Sahun, Mona Karout, and Yann Herault. 2015. "Locomotor dysfunction and hypotonia in Down syndrome mouse models for the HSPA13-APP region as a consequence of dosage sensitive genes controlling muscular metabolism and mitochondrial function." *Acta Physiologica* 214 (May): 11–12.

Broers, Chantal J. M., Reinoud J. B. J. Gemke, Michel E. Weijerman, Koen F. van der Sluijs, and A. Marceline van Furth. 2012. "Increased pro-Inflammatory Cytokine Production in Down Syndrome Children upon Stimulation with Live Influenza A Virus." *Journal of Clinical Immunology* 32 (2): 323–29.

Bruijn, Marella F. T. R. de, Xiaoqian Ma, Catherine Robin, Katrin Ottersbach, Maria-Jose Sanchez, and Elaine Dzierzak. 2002. "Hematopoietic Stem Cells Localize to the Endothelial Cell Layer in the Midgestation Mouse Aorta." *Immunity* 16 (5): 673–83.

Buitenkamp, Trudy D., Shai Izraeli, Martin Zimmermann, Erik Forestier, Nyla A. Heerema, Marry

M. van den Heuvel-Eibrink, Rob Pieters, et al. 2014. “Acute Lymphoblastic Leukemia in Children with Down Syndrome: A Retrospective Analysis from the Ponte Di Legno Study Group.” *Blood* 123 (1): 70–77.

Bull, Marilyn J. 2020. “Down Syndrome.” *The New England Journal of Medicine* 382 (24): 2344–52.

Bunis, Daniel G., Yelena Bronevetsky, Elisabeth Krow-Lucal, Nirav R. Bhakta, Charles C. Kim, Srilaxmi Nerella, Norman Jones, et al. 2021. “Single-Cell Mapping of Progressive Fetal-to-Adult Transition in Human Naive T Cells.” *Cell Reports* 34 (1): 108573.

Burjanivova, Tatiana, Jozef Madzo, Katerina Muzikova, Claus Meyer, Björn Schneider, Jan Stary, Rolf Marschalek, Jan Trka, and Jan Zuna. 2005. “In-Utero Origin of Childhood Acute Leukaemias.” *Blood* 106 (11): 1445–1445.

Burt, Trevor D. 2013. “Fetal Regulatory T Cells and Peripheral Immune Tolerance in Utero: Implications for Development and Disease.” *American Journal of Reproductive Immunology* 69 (4): 346–58.

Byrska-Bishop, Marta, Daniel VanDorn, Amy E. Campbell, Marisol Betensky, Philip R. Arca, Yu Yao, Paul Gadue, et al. 2015. “Pluripotent Stem Cells Reveal Erythroid-Specific Activities of the GATA1 N-Terminus.” *The Journal of Clinical Investigation* 125 (3): 993–1005.

Canque, B., S. Camus, A. Dalloul, E. Kahn, M. Yagello, C. Dezutter-Dambuyant, D. Schmitt, C. Schmitt, and J. C. Gluckman. 2000. “Characterization of Dendritic Cell Differentiation Pathways

from Cord Blood CD34(+)CD7(+)CD45RA(+) Hematopoietic Progenitor Cells." *Blood* 96 (12): 3748–56.

Canzonetta, Claudia, Claire Mulligan, Samuel Deutsch, Sandra Ruf, Aideen O'Doherty, Robert Lyle, Christelle Borel, et al. 2008. "DYRK1A-Dosage Imbalance Perturbs NRSF/REST Levels, Deregulating Pluripotency and Embryonic Stem Cell Fate in Down Syndrome." *American Journal of Human Genetics* 83 (3): 388–400.

Carrel, S., F. Buchegger, D. Heumann, C. Girardet, C. Barras, G. Losa, J. P. Mach, and V. von Fliedner. 1984. "Detection of the Common Acute Lymphoblastic Leukemia Antigen in the Serum of Leukemia Patients." *The Journal of Clinical Investigation* 74 (5): 1882–85.

Carrelha, Joana, Yiran Meng, Laura M. Kettyle, Tiago C. Luis, Ruggiero Norfo, Verónica Alcolea, Hanane Boukarabila, et al. 2018. "Hierarchically Related Lineage-Restricted Fates of Multipotent Haematopoietic Stem Cells." *Nature* 554 (7690): 106–11.

Carsetti, Rita, Diletta Valentini, Valentina Marcellini, Marco Scarsella, Emiliano Marasco, Ferruccio Giustini, Andrea Bartuli, Alberto Villani, and Alberto G. Ugazio. 2015. "Reduced Numbers of Switched Memory B Cells with High Terminal Differentiation Potential in Down Syndrome." *European Journal of Immunology* 45 (3): 903–14.

Cesana, Marcella, Michael H. Guo, Davide Cacchiarelli, Lara Wahlster, Jessica Barragan, Sergei Doulatov, Linda T. Vo, et al. 2018. "A CLK3-HMGA2 Alternative Splicing Axis Impacts Human Hematopoietic Stem Cell Molecular Identity throughout Development." *Cell Stem Cell* 22 (4): 575–88.e7.

Cetiner, S., O. Demirhan, T. C. Inal, D. Tastemir, and Y. Sertdemir. 2010. “Analysis of Peripheral Blood T-Cell Subsets, Natural Killer Cells and Serum Levels of Cytokines in Children with Down Syndrome.” *International Journal of Immunogenetics* 37 (4): 233–37.

Challen, Grant A., Nathan C. Boles, Stuart M. Chambers, and Margaret A. Goodell. 2010. “Distinct Hematopoietic Stem Cell Subtypes Are Differentially Regulated by TGF-beta1.” *Cell Stem Cell* 6 (3): 265–78.

Challen, Grant A., Deqiang Sun, Allison Mayle, Mira Jeong, Min Luo, Benjamin Rodriguez, Cates Mallaney, et al. 2014. “Dnmt3a and Dnmt3b Have Overlapping and Distinct Functions in Hematopoietic Stem Cells.” *Cell Stem Cell* 15 (3): 350–64.

Charbord, P., M. Tavian, L. Humeau, and B. Péault. 1996. “Early Ontogeny of the Human Marrow from Long Bones: An Immunohistochemical Study of Hematopoiesis and Its Microenvironment.” *Blood* 87 (10): 4109–19.

Chedin, Frederic, Michael R. Lieber, and Chih-Lin Hsieh. 2002. “The DNA Methyltransferase-like Protein DNMT3L Stimulates de Novo Methylation by Dnmt3a.” *Proceedings of the National Academy of Sciences of the United States of America* 99 (26): 16916–21.

Chen, Changya, Wenbao Yu, Joanna Tober, Peng Gao, Bing He, Kiwon Lee, Tuan Trieu, Gerd A. Blobel, Nancy A. Speck, and Kai Tan. 2019. “Spatial Genome Re-Organization between Fetal and Adult Hematopoietic Stem Cells.” *Cell Reports* 29 (12): 4200–4211.e7.

Chen, Michael J., Yan Li, Maria Elena De Obaldia, Qi Yang, Amanda D. Yzaguirre, Tomoko Yamada-Inagawa, Chris S. Vink, Avinash Bhandoola, Elaine Dzierzak, and Nancy A. Speck. 2011. "Erythroid/myeloid Progenitors and Hematopoietic Stem Cells Originate from Distinct Populations of Endothelial Cells." *Cell Stem Cell* 9 (6): 541–52.

Cho, Scott, and Gerald J. Spangrude. 2011. "Enrichment of Functionally Distinct Mouse Hematopoietic Progenitor Cell Populations Using CD62L." *Journal of Immunology* 187 (10): 5203–10.

Chou, Stella T., Marta Byrska-Bishop, Joanna M. Tober, Yu Yao, Daniel VanDorn, Joanna B. Opalinska, Jason A. Mills, et al. 2012. "Trisomy 21-Associated Defects in Human Primitive Hematopoiesis Revealed through Induced Pluripotent Stem Cells." *Proceedings of the National Academy of Sciences* 109 (43): 17573–78.

Christensen, Julie L., Douglas E. Wright, Amy J. Wagers, and Irving L. Weissman. 2004. "Circulation and Chemotaxis of Fetal Hematopoietic Stem Cells." *PLoS Biology* 2 (3): E75.

Chunduri, Narendra Kumar, and Zuzana Storchová. 2019. "The Diverse Consequences of Aneuploidy." *Nature Cell Biology* 21 (1): 54–62.

Chung, Il Yup, Sae Mi Hwang, and Tae Gi Uhm. 2016. "Expression and Function of Olig2 in Eosinophils." *The Journal of Immunology* 196 (1 Supplement): 52.17–52.17.

Cichocki, Frank, Bartosz Grzywacz, and Jeffrey S. Miller. 2019. "Human NK Cell Development: One Road or Many?" *Frontiers in Immunology* 10 (August): 2078.

Conrad Hal Waddington, H. Kacser. 1957. “The Strategy of the Genes: A Discussion of Some Aspects of Theoretical Biology.” *London: Allen & Unwin*.

Consolini, R., A. Legitimo, R. Rondelli, C. Guguelmi, E. Barisone, A. Lippi, A. Cantù-Rajnoldi, et al. 1998. “Clinical Relevance of CD10 Expression in Childhood ALL. The Italian Association for Pediatric Hematology and Oncology (AIEOP).” *Haematologica* 83 (11): 967–73.

Copley, Michael R., Sonja Babovic, Claudia Benz, David J. H. F. Knapp, Philip A. Beer, David G. Kent, Stefan Wohrer, et al. 2013. “The Lin28b-Let-7-Hmga2 Axis Determines the Higher Self-Renewal Potential of Fetal Haematopoietic Stem Cells.” *Nature Cell Biology* 15 (8): 916–25.

Corces, M. Ryan, Jason D. Buenrostro, Beijing Wu, Peyton G. Greenside, Steven M. Chan, Julie L. Koenig, Michael P. Snyder, et al. 2016. “Lineage-Specific and Single-Cell Chromatin Accessibility Charts Human Hematopoiesis and Leukemia Evolution.” *Nature Genetics* 48 (10): 1193–1203.

Cossarizza, A., C. Ortolani, E. Forti, G. Montagnani, R. Paganelli, M. Zannotti, M. Marini, D. Monti, and C. Franceschi. 1991. “Age-Related Expansion of Functionally Inefficient Cells with Markers of Natural Killer Activity in Down’s Syndrome.” *Blood* 77 (6): 1263–70.

Creyghton, Menno P., Albert W. Cheng, G. Grant Welstead, Tristan Kooistra, Bryce W. Carey, Eveline J. Steine, Jacob Hanna, et al. 2010. “Histone H3K27ac Separates Active from Poised Enhancers and Predicts Developmental State.” *Proceedings of the National Academy of Sciences of the United States of America* 107 (50): 21931–36.

Crooks, G. M., Q. L. Hao, D. Petersen, L. W. Barsky, and D. Bockstoce. 2000. “IL-3 Increases Production of B Lymphoid Progenitors from Human CD34+CD38- Cells.” *Journal of Immunology* 165 (5): 2382–89.

Cumano, Ana, and Isabelle Godin. 2007. “Ontogeny of the Hematopoietic System.” *Annual Review of Immunology* 25: 745–85.

Cutrona, G., P. Tasso, M. Dono, S. Roncella, M. Ulivi, E. M. Carpaneto, V. Fontana, et al. 2002. “CD10 Is a Marker for Cycling Cells with Propensity to Apoptosis in Childhood ALL.” *British Journal of Cancer* 86 (11): 1776–85.

Cyster, Jason G., and Christopher D. C. Allen. 2019. “B Cell Responses: Cell Interaction Dynamics and Decisions.” *Cell* 177 (3): 524–40.

Davisson, M. T., C. Schmidt, and E. C. Akeson. 1990. “Segmental Trisomy of Murine Chromosome 16: A New Model System for Studying Down Syndrome.” *Progress in Clinical and Biological Research* 360: 263–80.

De Silva, Nilushi S., and Ulf Klein. 2015. “Dynamics of B Cells in Germinal Centres.” *Nature Reviews. Immunology* 15 (3): 137–48.

De Vita, S., C. Canzonetta, C. Mulligan, F. Delom, J. Groet, C. Baldo, L. Vanes, et al. 2010. “Trisomic Dose of Several Chromosome 21 Genes Perturbs Haematopoietic Stem and Progenitor Cell Differentiation in Down’s Syndrome.” *Oncogene* 29 (46): 6102–14.

Delabar, J. M., D. Theophile, Z. Rahmani, Z. Chettouh, J. L. Blouin, M. Prieur, B. Noel, and P. M. Sinet. 1993. “Molecular Mapping of Twenty-Four Features of Down Syndrome on Chromosome 21.” *European Journal of Human Genetics: EJHG* 1 (2): 114–24.

Deng, Youcai, Yann Kerdiles, Jianhong Chu, Shunzong Yuan, Youwei Wang, Xilin Chen, Hsiaoyin Mao, et al. 2015. “Transcription Factor Foxo1 Is a Negative Regulator of Natural Killer Cell Maturation and Function.” *Immunity* 42 (3): 457–70.

Descatoire, Marc, Jean-Claude Weill, Claude-Agnès Reynaud, and Sandra Weller. 2011. “A Human Equivalent of Mouse B-1 Cells?” *The Journal of Experimental Medicine*.

Doulatov, Sergei, Faiyaz Notta, Kolja Eppert, Linh T. Nguyen, Pamela S. Ohashi, and John E. Dick. 2010. “Revised Map of the Human Progenitor Hierarchy Shows the Origin of Macrophages and Dendritic Cells in Early Lymphoid Development.” *Nature Immunology* 11 (7): 585–93.

Doulatov, Sergei, Faiyaz Notta, Elisa Laurenti, and John E. Dick. 2012. “Hematopoiesis: A Human Perspective.” *Cell Stem Cell* 10 (2): 120–36.

Drissen, Roy, Natalija Buza-Vidas, Petter Woll, Supat Thongjuea, Adriana Gambardella, Alice Giustacchini, Elena Mancini, et al. 2016. “Distinct Myeloid Progenitor-Differentiation Pathways Identified through Single-Cell RNA Sequencing.” *Nature Immunology* 17 (6): 666–76.

Drissen, Roy, Supat Thongjuea, Kim Theilgaard-Mönch, and Claus Nerlov. 2019. “Identification of Two Distinct Pathways of Human Myelopoiesis.” *Science Immunology* 4 (35). https://doi.org/10.1126/sciimmunol.aau7148.

Dzierzak, Elaine, and Anna Bigas. 2018. “Blood Development: Hematopoietic Stem Cell Dependence and Independence.” *Cell Stem Cell* 22 (5): 639–51.

Easterbrook, Jennifer, Stanislav Rybtsov, Sabrina Gordon-Keylock, Andrejs Ivanovs, Samir Taoudi, Richard A. Anderson, and Alexander Medvinsky. 2019. “Analysis of the Spatiotemporal Development of Hematopoietic Stem and Progenitor Cells in the Early Human Embryo.” *Stem Cell Reports* 12 (5): 1056–68.

Elagib, Kamaleldin E., Frederick K. Racke, Michael Mogass, Rina Khetawat, Lorrie L. Delehanty, and Adam N. Goldfarb. 2003. “RUNX1 and GATA-1 Coexpression and Cooperation in Megakaryocytic Differentiation.” *Blood* 101 (11): 4333–41.

Elcheva, Irina A., Tyler Wood, Kathryn Chiarolanzio, Bryan Chim, Madeline Wong, Vikash Singh, Chethana P. Gowda, et al. 2020. “RNA-Binding Protein IGF2BP1 Maintains Leukemia Stem Cell Properties by Regulating HOXB4, MYB, and ALDH1A1.” *Leukemia* 34 (5): 1354–63.

Elsaid, Ramy, Francisca Soares-da-Silva, Marcia Peixoto, Dali Amiri, Nathan Mackowski, Pablo Pereira, Antonio Bandeira, and Ana Cumano. 2020. “Hematopoiesis: A Layered Organization Across Chordate Species.” *Frontiers in Cell and Developmental Biology* 8 (December): 606642.

Elsaid, Ramy, Junjie Yang, and Ana Cumano. 2019. “The Influence of Space and Time on the Establishment of B Cell Identity.” *Biomedical Journal* 42 (4): 209–17.

Englund, Annika, Björn Jonsson, Cecilia Soussi Zander, Jan Gustafsson, and Göran Annerén.

2013. “Changes in Mortality and Causes of Death in the Swedish Down Syndrome Population.” *American Journal of Medical Genetics. Part A* 161A (4): 642–49.

Ernst, Peter B., and Anne-Ruxandra Carvunis. 2018. “Of Mice, Men and Immunity: A Case for Evolutionary Systems Biology.” *Nature Immunology* 19 (5): 421–25.

Euchner, Johanna, Jasmin Sprissler, Toni Cathomen, Daniel Fürst, Hubert Schrezenmeier, Klaus-Michael Debatin, Klaus Schwarz, and Kerstin Felgentreff. 2021. “Natural Killer Cells Generated From Human Induced Pluripotent Stem Cells Mature to CD56brightCD16+NKp80+/- In-Vitro and Express KIR2DL2/DL3 and KIR3DL1.” *Frontiers in Immunology* 12 (May): 640672.

Farlik, Matthias, Florian Halbritter, Fabian Müller, Fizzah A. Choudry, Peter Ebert, Johanna Klughammer, Samantha Farrow, et al. 2016. “DNA Methylation Dynamics of Human Hematopoietic Stem Cell Differentiation.” *Cell Stem Cell* 19 (6): 808–22.

Ferrari, Marta, and Stefano Stagi. 2021. “Autoimmunity and Genetic Syndromes: A Focus on Down Syndrome.” *Genes* 12 (2). https://doi.org/10.3390/genes12020268.

Ferster, A., A. Verhest, E. Vamos, E. De Maertelaere, and J. Otten. 1986. “Leukemia in a Trisomy 21 Mosaic: Specific Involvement of the Trisomic Cells.” *Cancer Genetics and Cytogenetics* 20 (1-2): 109–13.

Finne, P. H., and S. Halvorsen. 1972. “Regulation of Erythropoiesis in the Fetus and Newborn.” *Archives of Disease in Childhood* 47 (255): 683–87.

Ford, A. M., C. A. Bennett, C. M. Price, M. C. Bruin, E. R. Van Wering, and M. Greaves. 1998. "Fetal Origins of the TEL-AML1 Fusion Gene in Identical Twins with Leukemia." *Proceedings of the National Academy of Sciences of the United States of America* 95 (8): 4584–88.

Frame, Jenna M., Kathleen E. McGrath, and James Palis. 2013. "Erythro-Myeloid Progenitors: 'Definitive' Hematopoiesis in the Conceptus prior to the Emergence of Hematopoietic Stem Cells." *Blood Cells, Molecules & Diseases* 51 (4): 220–25.

Francis, Olivia L., Terry-Ann M. Milford, Shannalee R. Martinez, Ineavely Baez, Jacqueline S. Coats, Karina Mayagoitia, Katherine R. Concepcion, et al. 2016. "A Novel Xenograft Model to Study the Role of TSLP-Induced CRLF2 Signals in Normal and Malignant Human B Lymphopoiesis." *Haematologica* 101 (4): 417–26.

Gadalla, Ramy, Babak Noamani, Bethany L. MacLeod, Russell J. Dickson, Mengdi Guo, Wenxi Xu, Sabelo Lukhele, et al. 2019. "Validation of CyTOF Against Flow Cytometry for Immunological Studies and Monitoring of Human Cancer Clinical Trials." *Frontiers in Oncology* 9 (May): 415.

Gale, K. B., A. M. Ford, R. Repp, A. Borkhardt, C. Keller, O. B. Eden, and M. F. Greaves. 1997. "Backtracking Leukemia to Birth: Identification of Clonotypic Gene Fusion Sequences in Neonatal Blood Spots." *Proceedings of the National Academy of Sciences of the United States of America* 94 (25): 13950–54.

Galy, A., M. Travis, D. Cen, and B. Chen. 1995. "Human T, B, Natural Killer, and Dendritic Cells Arise from a Common Bone Marrow Progenitor Cell Subset." *Immunity* 3 (4): 459–73.

Gamis, Alan S., Todd A. Alonzo, Robert B. Gerbing, Joanne M. Hilden, April D. Sorrell, Mukta Sharma, Thomas W. Loew, et al. 2011. “Natural History of Transient Myeloproliferative Disorder Clinically Diagnosed in Down Syndrome Neonates: A Report from the Children’s Oncology Group Study A2971.” *Blood* 118 (26): 6752–59; quiz 6996.

Garcia-Manero, Guillermo, Jerry Daniel, Terry L. Smith, Steven M. Kornblau, Ming-Sheng Lee, Hagop M. Kantarjian, and Jean-Pierre J. Issa. 2002. “DNA Methylation of Multiple Promoter-Associated CpG Islands in Adult Acute Lymphocytic Leukemia.” *Clinical Cancer Research: An Official Journal of the American Association for Cancer Research* 8 (7): 2217–24.

Gardiner, Katheleen, Andrew Fortna, Lawrence Bechtel, and Muriel T. Davisson. 2003. “Mouse Models of Down Syndrome: How Useful Can They Be? Comparison of the Gene Content of Human Chromosome 21 with Orthologous Mouse Genomic Regions.” *Gene* 318 (October): 137–47.

Ge, Y., K. M. LaFiura, A. A. Dombkowski, Q. Chen, S. G. Payton, S. A. Buck, S. Salagrama, A. E. Diakiw, L. H. Matherly, and J. W. Taub. 2008. “The Role of the Proto-Oncogene ETS2 in Acute Megakaryocytic Leukemia Biology and Therapy.” *Leukemia* 22 (3): 521–29.

Gekas, Christos, Francoise Dieterlen-Lièvre, Stuart H. Orkin, and Hanna K. A. Mikkola. 2005. “The Placenta Is a Niche for Hematopoietic Stem Cells.” *Developmental Cell* 8 (3): 365–75.

Ghaedi, Maryam, Catherine A. Steer, Itziar Martinez-Gonzalez, Timotheus Y. F. Halim, Ninan Abraham, and Fumio Takei. 2016. “Common-Lymphoid-Progenitor-Independent Pathways of Innate and T Lymphocyte Development.” *Cell Reports* 15 (3): 471–80.

Ghosn, Eliver Eid Bou, Jeffrey Waters, Megan Phillips, Ryo Yamamoto, Brian R. Long, Yang Yang, Rachel Gerstein, Cheryl A. Stoddart, Hiromitsu Nakauchi, and Leonore A. Herzenberg. 2016. "Fetal Hematopoietic Stem Cell Transplantation Fails to Fully Regenerate the B-Lymphocyte Compartment." *Stem Cell Reports* 6 (1): 137–49.

Gilliland, D. Gary, and James D. Griffin. 2002. "The Roles of FLT3 in Hematopoiesis and Leukemia." *Blood* 100 (5): 1532–42.

Gleissner, Beate, Nicola Goekbuget, Harald Rieder, Renate Arnold, Stefan Schwartz, Helmut Diedrich, Claudia Schoch, et al. 2005. "CD10- Pre-B Acute Lymphoblastic Leukemia (ALL) Is a Distinct High-Risk Subgroup of Adult ALL Associated with a High Frequency of MLL Aberrations: Results of the German Multicenter Trials for Adult ALL (GMALL)." *Blood* 106 (13): 4054–56.

Goardon, Nicolas, Emanuele Marchi, Ann Atzberger, Lynn Quek, Anna Schuh, Shamit Soneji, Petter Woll, et al. 2011. "Coexistence of LMPP-like and GMP-like Leukemia Stem Cells in Acute Myeloid Leukemia." *Cancer Cell* 19 (1): 138–52.

Gomez Perdiguero, Elisa, Kay Klapproth, Christian Schulz, Katrin Busch, Emanuele Azzoni, Lucile Crozet, Hannah Garner, et al. 2015. "Tissue-Resident Macrophages Originate from Yolk-Sac-Derived Erythro-Myeloid Progenitors." *Nature* 518 (7540): 547–51.

Gontarz, Paul, Shuhua Fu, Xiaoyun Xing, Shaopeng Liu, Benpeng Miao, Viktoriia Bazylianska, Akhil Sharma, et al. 2020. "Comparison of Differential Accessibility Analysis Strategies for ATAC-Seq Data." *Scientific Reports* 10 (1): 10150.

Görgens, André, Stefan Radtke, Peter A. Horn, and Bernd Giebel. 2013. “New Relationships of Human Hematopoietic Lineages Facilitate Detection of Multipotent Hematopoietic Stem and Progenitor Cells.” *Cell Cycle* 12 (22): 3478–82.

Greaves, M. 1999. “Molecular Genetics, Natural History and the Demise of Childhood Leukaemia.” *European Journal of Cancer* 35 (2): 173–85.

Greaves, Mel F., Ana Teresa Maia, Joseph L. Wiemels, and Anthony M. Ford. 2003. “Leukemia in Twins: Lessons in Natural History.” *Blood* 102 (7): 2321–33.

Griffin, Daniel O., Nichol E. Holodick, and Thomas L. Rothstein. 2011. “Human B1 Cells in Umbilical Cord and Adult Peripheral Blood Express the Novel Phenotype CD20+ CD27+ CD43+ CD70-.” *The Journal of Experimental Medicine* 208 (1): 67–80.

Grimm, Juliane, Dirk Heckl, and Jan-Henning Klusmann. 2021. “Molecular Mechanisms of the Genetic Predisposition to Acute Megakaryoblastic Leukemia in Infants With Down Syndrome.” *Frontiers in Oncology* 11 (March): 636633.

Groet, Jürgen, Suzanne McElwaine, Monica Spinelli, Andrea Rinaldi, Ingo Burtscher, Claire Mulligan, Afua Mensah, et al. 2003. “Acquired Mutations in GATA1 in Neonates with Down’s Syndrome with Transient Myeloid Disorder.” *The Lancet* 361 (9369): 1617–20.

Gruhn, B., J. W. Taub, Y. Ge, J. F. Beck, R. Zell, R. Häfer, F. H. Hermann, K-M Debatin, and D. Steinbach. 2008. “Prenatal Origin of Childhood Acute Lymphoblastic Leukemia, Association with

Birth Weight and Hyperdiploidy." *Leukemia* 22 (9): 1692–97.

Gu, Yue, Amanda E. Jones, Wei Yang, Shanrun Liu, Qian Dai, Yudong Liu, C. Scott Swindle, et al. 2016. "The Histone H2A Deubiquitinase Usp16 Regulates Hematopoiesis and Hematopoietic Stem Cell Function." *Proceedings of the National Academy of Sciences of the United States of America* 113 (1): E51–60.

Guffroy, Aurélien, Yannick Dieudonné, Beatrice Uring-Lambert, Joelle Goetz, Yves Alembik, and Anne-Sophie Korganow. 2019. "Infection Risk among Adults with down Syndrome: A Two Group Series of 101 Patients in a Tertiary Center." *Orphanet Journal of Rare Diseases* 14 (1): 15.

Haas, Jan D., Sarina Ravens, Sandra Düber, Inga Sandrock, Linda Oberdörfer, Elham Kashani, Vijaykumar Chennupati, et al. 2012. "Development of Interleukin-17-Producing γδ T Cells Is Restricted to a Functional Embryonic Wave." *Immunity* 37 (1): 48–59.

Haas, Simon, Jenny Hansson, Daniel Klimmeck, Dirk Loeffler, Lars Velten, Hannah Uckelmann, Stephan Wurzer, et al. 2015. "Inflammation-Induced Emergency Megakaryopoiesis Driven by Hematopoietic Stem Cell-like Megakaryocyte Progenitors." *Cell Stem Cell* 17 (4): 422–34.

Haddad, Rima, Philippe Guardiola, Brigitte Izac, Christelle Thibault, Jerry Radich, Anne-Lise Delezoide, Claude Baillou, et al. 2004. "Molecular Characterization of Early Human T/NK and B-Lymphoid Progenitor Cells in Umbilical Cord Blood." *Blood* 104 (13): 3918–26.

Hadjur, S., K. Ung, L. Wadsworth, J. Dimmick, E. Rajcan-Separovic, R. W. Scott, M. Buchwald, and F. R. Jirik. 2001. "Defective Hematopoiesis and Hepatic Steatosis in Mice with Combined

Deficiencies of the Genes Encoding Fancc and Cu/Zn Superoxide Dismutase." *Blood* 98 (4): 1003–11.

Hadland, Brandon, and Momoko Yoshimoto. 2018. "Many Layers of Embryonic Hematopoiesis: New Insights into B-Cell Ontogeny and the Origin of Hematopoietic Stem Cells." *Experimental Hematology* 60 (April): 1–9.

Hao, Q. L., J. Zhu, M. A. Price, K. J. Payne, L. W. Barsky, and G. M. Crooks. 2001. "Identification of a Novel, Human Multilymphoid Progenitor in Cord Blood." *Blood* 97 (12): 3683–90.

Hardy, R. R., and K. Hayakawa. 1991. "A Developmental Switch in B Lymphopoiesis." *Proceedings of the National Academy of Sciences of the United States of America* 88 (24): 11550–54.

———. 2001. "B Cell Development Pathways." *Annual Review of Immunology* 19 (1): 595–621.

Hardy, Richard R., Paul W. Kincade, and Kenneth Dorshkind. 2007. "The Protean Nature of Cells in the B Lymphocyte Lineage." *Immunity* 26 (6): 703–14.

Harman, Joe R., Ross Thorne, Max Jamilly, Marta Tapia, Nicholas T. Crump, Siobhan Rice, Ryan Beveridge, et al. 2021. "A KMT2A-AFF1 Gene Regulatory Network Highlights the Role of Core Transcription Factors and Reveals the Regulatory Logic of Key Downstream Target Genes." *Genome Research* 31 (7): 1159–73.

Hasaart, Karlijn A. L., Freek Manders, Marie-Louise van der Hoorn, Mark Verheul, Tomasz

Poplonski, Ewart Kuijk, Susana M. Chuva de Sousa Lopes, and Ruben van Boxtel. 2020. "Mutation Accumulation and Developmental Lineages in Normal and Down Syndrome Human Fetal Haematopoiesis." *Scientific Reports* 10 (1): 12991.

Hasle, H., I. H. Clemmensen, and M. Mikkelsen. 2000. "Risks of Leukaemia and Solid Tumours in Individuals with Down's Syndrome." *The Lancet* 355 (9199): 165–69.

Hasle, Henrik, Jan M. Friedman, Jørgen H. Olsen, and Sonja A. Rasmussen. 2016. "Low Risk of Solid Tumors in Persons with Down Syndrome." *Genetics in Medicine: Official Journal of the American College of Medical Genetics* 18 (11): 1151–57.

Hein, Daniel, Arndt Borkhardt, and Ute Fischer. 2020. "Insights into the Prenatal Origin of Childhood Acute Lymphoblastic Leukemia." *Cancer Metastasis Reviews* 39 (1): 161–71.

Hertzberg, Libi, Elena Vendramini, Ithamar Ganmore, Gianni Cazzaniga, Maike Schmitz, Jane Chalker, Ruth Shiloh, et al. 2010. "Down Syndrome Acute Lymphoblastic Leukemia, a Highly Heterogeneous Disease in Which Aberrant Expression of CRLF2 Is Associated with Mutated JAK2: A Report from the International BFM Study Group." *Blood* 115 (5): 1006–17.

Herzenberg, L. A., and L. A. Herzenberg. 1989. "Toward a Layered Immune System." *Cell* 59 (6): 953–54.

Hilton, J. M., D. A. Fitzgerald, and D. M. Cooper. 1999. "Respiratory Morbidity of Hospitalized Children with Trisomy 21." *Journal of Paediatrics and Child Health* 35 (4): 383–86.

Hingh, Yvette C. M. de, Petrus W. van der Vossen, Eugenie F. A. Gemen, André B. Mulder, Wim C. J. Hop, Frank Brus, and Esther de Vries. 2005. “Intrinsic Abnormalities of Lymphocyte Counts in Children with down Syndrome.” *The Journal of Pediatrics* 147 (6): 744–47.

Hipp, Nicolas, Hannah Symington, Cédric Pastoret, Gersende Caron, Céline Monvoisin, Karin Tarte, Thierry Fest, and Céline Delaloy. 2017. “IL-2 Imprints Human Naive B Cell Fate towards Plasma Cell through ERK/ELK1-Mediated BACH2 Repression.” *Nature Communications* 8 (1): 1443.

Hoebeke, I., M. De Smedt, F. Stolz, K. Pike-Overzet, F. J. T. Staal, J. Plum, and G. Leclercq. 2007. “T-, B- and NK-Lymphoid, but Not Myeloid Cells Arise from Human CD34(+)CD38(-)CD7(+) Common Lymphoid Progenitors Expressing Lymphoid-Specific Genes.” *Leukemia* 21 (2): 311–19.

Hollanda, Luciana M., Carmen S. P. Lima, Anderson F. Cunha, Dulcinéia M. Albuquerque, José Vassallo, Margareth C. Ozelo, Paulo P. Joazeiro, Sara T. O. Saad, and Fernando F. Costa. 2006. “An Inherited Mutation Leading to Production of Only the Short Isoform of GATA-1 Is Associated with Impaired Erythropoiesis.” *Nature Genetics* 38 (7): 807–12.

Holmes, Roxanne, and Juan Carlos Zúñiga-Pflücker. 2009. “The OP9-DL1 System: Generation of T-Lymphocytes from Embryonic or Hematopoietic Stem Cells in Vitro.” *Cold Spring Harbor Protocols* 2009 (2): db.prot5156.

Huggard, Dean, Derek G. Doherty, and Eleanor J. Molloy. 2020. “Immune Dysregulation in Children With Down Syndrome.” *Frontiers in Pediatrics* 8 (February): 73.

Hunger, Stephen P., and Charles G. Mullighan. 2015. “Acute Lymphoblastic Leukemia in Children.” *The New England Journal of Medicine* 373 (16): 1541–52.

Huyhn, A., M. Dommergues, B. Izac, L. Croisille, A. Katz, W. Vainchenker, and L. Coulombel. 1995. “Characterization of Hematopoietic Progenitors from Human Yolk Sacs and Embryos.” *Blood* 86 (12): 4474–85.

Hystad, Marit E., June H. Myklebust, Trond H. Bø, Einar A. Sivertsen, Edith Rian, Lise Forfang, Else Munthe, et al. 2007. “Characterization of Early Stages of Human B Cell Development by Gene Expression Profiling.” *Journal of Immunology* 179 (6): 3662–71.

Ichii, Michiko, Kenji Oritani, and Yuzuru Kanakura. 2014. “Early B Lymphocyte Development: Similarities and Differences in Human and Mouse.” *World Journal of Stem Cells* 6 (4): 421–31.

Ichii, Michiko, Kenji Oritani, Takafumi Yokota, Daniel C. Schultz, Jennifer L. Holter, Yuzuru Kanakura, and Paul W. Kincade. 2010. “Stromal Cell-Free Conditions Favorable for Human B Lymphopoiesis in Culture.” *Journal of Immunological Methods* 359 (1-2): 47–55.

Ichii, Michiko, Kenji Oritani, Takafumi Yokota, Qingzhao Zhang, Karla P. Garrett, Yuzuru Kanakura, and Paul W. Kincade. 2010. “The Density of CD10 Corresponds to Commitment and Progression in the Human B Lymphoid Lineage.” *PloS One* 5 (9): e12954.

Igarashi, Kazuhiko, Tomohiro Kurosaki, and Rahul Roychoudhuri. 2017. “BACH Transcription Factors in Innate and Adaptive Immunity.” *Nature Reviews. Immunology* 17 (7): 437–50.

Iida, Ryuji, Kaori Shinoda, Yuki Hayano, Yoshinori Nagai, Kiyoshi Takatsu, and Taku Kouro. 2016. "Fetal Lymphoid Progenitors Become Restricted to B-1 Fates Coincident with IL-7Rα Expression." *PloS One* 11 (10): e0165676.

Illouz, Tomer, Arya Biragyn, Maria Florencia Iulita, Lisi Flores-Aguilar, Mara Dierssen, Ilario De Toma, Stylianos E. Antonarakis, et al. 2021. "Immune Dysregulation and the Increased Risk of Complications and Mortality Following Respiratory Tract Infections in Adults With Down Syndrome." *Frontiers in Immunology* 12 (June): 621440.

Inlay, Matthew A., Thomas Serwold, Adriane Mosley, John W. Fathman, Ivan K. Dimov, Jun Seita, and Irving L. Weissman. 2014. "Identification of Multipotent Progenitors That Emerge prior to Hematopoietic Stem Cells in Embryonic Development." *Stem Cell Reports* 2 (4): 457–72.

Itoh, K., H. Tezuka, H. Sakoda, M. Konno, K. Nagata, T. Uchiyama, H. Uchino, and K. J. Mori. 1989. "Reproducible Establishment of Hemopoietic Supportive Stromal Cell Lines from Murine Bone Marrow." *Experimental Hematology* 17 (2): 145–53.

Itoh-Nakadai, Ari, Reina Hikota, Akihiko Muto, Kohei Kometani, Miki Watanabe-Matsui, Yuki Sato, Masahiro Kobayashi, et al. 2014. "The Transcription Repressors Bach2 and Bach1 Promote B Cell Development by Repressing the Myeloid Program." *Nature Immunology* 15 (12): 1171–80.

Iturri, Lorea, Laina Freyer, Anne Biton, Pascal Dardenne, Yvan Lallemand, and Elisa Gomez Perdiguero. 2021. "Megakaryocyte Production Is Sustained by Direct Differentiation from Erythromyeloid Progenitors in the Yolk Sac until Midgestation." *Immunity* 54 (7): 1433–46.e5.

Ivanovs, Andrejs, Stanislav Rybtsov, Richard A. Anderson, Marc L. Turner, and Alexander Medvinsky. 2014. “Identification of the Niche and Phenotype of the First Human Hematopoietic Stem Cells.” *Stem Cell Reports* 2 (4): 449–56.

Ivanovs, Andrejs, Stanislav Rybtsov, Elizabeth S. Ng, Edouard G. Stanley, Andrew G. Elefanty, and Alexander Medvinsky. 2017. “Human Haematopoietic Stem Cell Development: From the Embryo to the Dish.” *Development* 144 (13): 2323–37.

Ivanovs, Andrejs, Stanislav Rybtsov, Lindsey Welch, Richard A. Anderson, Marc L. Turner, and Alexander Medvinsky. 2011. “Highly Potent Human Hematopoietic Stem Cells First Emerge in the Intraembryonic Aorta-Gonad-Mesonephros Region.” *The Journal of Experimental Medicine* 208 (12): 2417–27.

Ivarsson, Martin A., Liyen Loh, Nicole Marquardt, Eliisa Kekäläinen, Lena Berglin, Niklas K. Björkström, Magnus Westgren, Douglas F. Nixon, and Jakob Michaëlsson. 2013. “Differentiation and Functional Regulation of Human Fetal NK Cells.” *The Journal of Clinical Investigation* 123 (9): 3889–3901.

Jackson, Thomas R., Rebecca E. Ling, and Anindita Roy. 2021. “The Origin of B-Cells: Human Fetal B Cell Development and Implications for the Pathogenesis of Childhood Acute Lymphoblastic Leukemia.” *Frontiers in Immunology* 12 (February): 637975.

Jacobsen, Sten Eirik W., and Claus Nerlov. 2019. “Haematopoiesis in the Era of Advanced Single-Cell Technologies.” *Nature Cell Biology* 21 (1): 2–8.

Jardine, Laura, Simone Webb, Issac Goh, Mariana Quiroga Londoño, Gary Reynolds, Michael Mather, Bayanne Olabi, et al. 2021. “Blood and Immune Development in Human Fetal Bone Marrow and Down Syndrome.” *Nature* 598 (7880): 327–31.

Jassinskaja, Maria, Emil Johansson, Trine Ahn Kristiansen, Hugo Åkerstrand, Kristoffer Sjöholm, Simon Hauri, Johan Malmström, Joan Yuan, and Jenny Hansson. 2017. “Comprehensive Proteomic Characterization of Ontogenic Changes in Hematopoietic Stem and Progenitor Cells.” *Cell Reports* 21 (11): 3285–97.

Jassinskaja, Maria, Kristýna Pimková, Emil Johansson, Ewa Sitnicka Quinn, and Jenny Hansson. 2019. “In-Depth Proteomic Characterization of Lineage-Biased Hematopoietic Progenitor Cells in the Fetus and Adult.” *Blood* 134 (November): 3703.

Jensen, Christina T., Shabnam Kharazi, Charlotta Böiers, Min Cheng, Anna Lübking, Ewa Sitnicka, and Sten Eirik W. Jacobsen. 2008. “FLT3 Ligand and Not TSLP Is the Key Regulator of IL-7-Independent B-1 and B-2 B Lymphopoiesis.” *Blood* 112 (6): 2297–2304.

Jensen, Christina T., Shabnam Kharazi, Charlotta Böiers, Karina Liuba, and Sten Eirik W. Jacobsen. 2007. “TSLP-Mediated Fetal B Lymphopoiesis?” *Nature Immunology*.

Johnson, Sonja E., Nisha Shah, Angela Panoskaltsis-Mortari, and Tucker W. LeBien. 2005. “Murine and Human IL-7 Activate STAT5 and Induce Proliferation of Normal Human pro-B Cells.” *Journal of Immunology* 175 (11): 7325–31.

Karamitros, Dimitris, Bilyana Stoilova, Zahra Aboukhalil, Fiona Hamey, Andreas Reinisch, Marina

Samitsch, Lynn Quek, et al. 2018. “Single-Cell Analysis Reveals the Continuum of Human Lympho-Myeloid Progenitor Cells.” *Nature Immunology* 19 (1): 85–97.

Karlsson, B., J. Gustafsson, G. Hedov, S. A. Ivarsson, and G. Annerén. 1998. “Thyroid Dysfunction in Down’s Syndrome: Relation to Age and Thyroid Autoimmunity.” *Archives of Disease in Childhood* 79 (3): 242–45.

Kearney, Lyndal, David Gonzalez De Castro, Jenny Yeung, Julia Procter, Sharon W. Horsley, Minenori Eguchi-Ishimae, Caroline M. Bateman, et al. 2009. “Specific JAK2 Mutation (JAK2R683) and Multiple Gene Deletions in Down Syndrome Acute Lymphoblastic Leukemia.” *Blood* 113 (3): 646–48.

Khabirova, Eleonora, Laura Jardine, Tim H. H. Coorens, Simone Webb, Taryn D. Treger, Justin Engelbert, Tarryn Porter, et al. 2022. “Single-Cell Transcriptomics Reveals a Distinct Developmental State of KMT2A-Rearranged Infant B-Cell Acute Lymphoblastic Leukemia.” *Nature Medicine* 28 (4): 743–51.

Klusmann, Jan-Henning, Ursula Creutzig, Martin Zimmermann, Michael Dworzak, Norbert Jorch, Claudia Langebrake, Arnulf Pekrun, Katarina Macakova-Reinhardt, and Dirk Reinhardt. 2008. “Treatment and Prognostic Impact of Transient Leukemia in Neonates with Down Syndrome.” *Blood* 111 (6): 2991–98.

Knapp, David J. H. F., Colin A. Hammond, Tony Hui, Marijn T. J. van Loenhout, Fangwu Wang, Nima Aghaeepour, Paul H. Miller, et al. 2018. “Single-Cell Analysis Identifies a CD33+ Subset of Human Cord Blood Cells with High Regenerative Potential.” *Nature Cell Biology* 20 (6): 710–20.

Kohn, Lisa A., Qian-Lin Hao, Rajkumar Sasidharan, Chintan Parekh, Shundi Ge, Yuhua Zhu, Hanna K. A. Mikkola, and Gay M. Crooks. 2012. “Lymphoid Priming in Human Bone Marrow Begins before Expression of CD10 with Upregulation of L-Selectin.” *Nature Immunology* 13 (10): 963–71.

Kondo, M., I. L. Weissman, and K. Akashi. 1997. “Identification of Clonogenic Common Lymphoid Progenitors in Mouse Bone Marrow.” *Cell* 91 (5): 661–72.

Kong, Xiao-Fei, Lisa Worley, Darawan Rinchai, Vincent Bondet, Puthen Veettil Jithesh, Marie Goulet, Emilie Nonnotte, et al. 2020. “Three Copies of Four Interferon Receptor Genes Underlie a Mild Type I Interferonopathy in Down Syndrome.” *Journal of Clinical Immunology* 40 (6): 807–19.

Korbel, Jan O., Tal Tirosh-Wagner, Alexander Eckehart Urban, Xiao-Ning Chen, Maya Kasowski, Li Dai, Fabian Grubert, et al. 2009. “The Genetic Architecture of Down Syndrome Phenotypes Revealed by High-Resolution Analysis of Human Segmental Trisomies.” *Proceedings of the National Academy of Sciences of the United States of America* 106 (29): 12031–36.

Korenberg, J. R., X. N. Chen, R. Schipper, Z. Sun, R. Gonsky, S. Gerwehr, N. Carpenter, C. Daumer, P. Dignan, and C. Disteche. 1994. “Down Syndrome Phenotypes: The Consequences of Chromosomal Imbalance.” *Proceedings of the National Academy of Sciences of the United States of America* 91 (11): 4997–5001.

Kristiansen, Trine A., Elin Jaensson Gyllenbäck, Alya Zriwil, Tomas Björklund, Jeremy A. Daniel,

Ewa Sitnicka, Shamit Soneji, David Bryder, and Joan Yuan. 2016. “Cellular Barcoding Links B-1a B Cell Potential to a Fetal Hematopoietic Stem Cell State at the Single-Cell Level.” *Immunity* 45 (2): 346–57.

Krow-Lucal, Elisabeth R., and Joseph M. McCune. 2014. “Distinct Functional Programs in Fetal T and Myeloid Lineages.” *Frontiers in Immunology* 5 (July): 314.

Kubota, Yasuo, Kumiko Uryu, Tatsuya Ito, Masafumi Seki, Tomoko Kawai, Tomoya Isobe, Tadayuki Kumagai, et al. 2019. “Integrated Genetic and Epigenetic Analysis Revealed Heterogeneity of Acute Lymphoblastic Leukemia in Down Syndrome.” *Cancer Science* 110 (10): 3358–67.

Kuijk, Ewart, Francis Blokzijl, Myrthe Jager, Nicolle Besselink, Sander Boymans, Susana M. Chuva de Sousa Lopes, Ruben van Boxtel, and Edwin Cuppen. 2019. “Early Divergence of Mutational Processes in Human Fetal Tissues.” *Science Advances* 5 (5): eaaw1271.

Kumar, Brahma V., Thomas J. Connors, and Donna L. Farber. 2018. “Human T Cell Development, Localization, and Function throughout Life.” *Immunity* 48 (2): 202–13.

Kurdi, Ahmed T., Ribal Bassil, Marta Olah, Chuan Wu, Sheng Xiao, Mariko Taga, Michael Frangieh, et al. 2016. “Tiam1/Rac1 Complex Controls Il17a Transcription and Autoimmunity.” *Nature Communications* 7 (October): 13048.

Kusters, M. A. A., R. H. J. Verstegen, E. F. A. Gemen, and E. de Vries. 2009. “Intrinsic Defect of the Immune System in Children with Down Syndrome: A Review.” *Clinical and Experimental*

Immunology 156 (2): 189–93.

Kyttälä, Satu, Ivonne Habermann, Takashi Minami, Gerhard Ehninger, and Alexander Kiani. 2009. "Regulation of Down Syndrome Critical Region 1 Expression by Nuclear Factor of Activated T Cells in Megakaryocytes." *British Journal of Haematology* 144 (3): 395–408.

Labuhn, Maurice, Kelly Perkins, Sören Matzk, Leila Varghese, Catherine Garnett, Elli Papaemmanuil, Marlen Metzner, et al. 2019a. "Mechanisms of Progression of Myeloid Preleukemia to Transformed Myeloid Leukemia in Children with Down Syndrome." *Cancer Cell* 36 (2): 123–38.e10.

———. 2019b. "Mechanisms of Progression of Myeloid Preleukemia to Transformed Myeloid Leukemia in Children with Down Syndrome." *Cancer Cell* 36 (2): 123–38.e10.

Lai, Anne Y., and Motonari Kondo. 2006. "Asymmetrical Lymphoid and Myeloid Lineage Commitment in Multipotent Hematopoietic Progenitors." *The Journal of Experimental Medicine* 203 (8): 1867–73.

Lambert, Katharina, Keagan G. Moo, Azlann Arnett, Gautam Goel, Kaitlin J. Flynn, Cate Speake, Alice E. Wiedeman, et al. 2021. "Permutational Immune Analysis Reveals Architectural Similarities between Inflammaging, Down Syndrome and Autoimmunity." *bioRxiv*. https://doi.org/10.1101/2021.09.13.460115.

Lambert, Katharina, Keagan G. Moo, Azlann Arnett, Gautam Goel, Alex Hu, Kaitlin J. Flynn, Cate Speake, et al. 2022. "Deep Immune Phenotyping Reveals Similarities between Aging, Down

Syndrome, and Autoimmunity." *Science Translational Medicine* 14 (627): eabi4888.

Lane, Andrew A., Bjoern Chapuy, Charles Y. Lin, Trevor Tivey, Hubo Li, Elizabeth C. Townsend, Diederik van Bodegom, et al. 2014. "Triplication of a 21q22 Region Contributes to B Cell Transformation through HMGN1 Overexpression and Loss of Histone H3 Lys27 Trimethylation." *Nature Genetics* 46 (6): 618–23.

Lappalainen, Tuuli, Michael Sammeth, Marc R. Friedländer, Peter A. C. 't Hoen, Jean Monlong, Manuel A. Rivas, Mar Gonzàlez-Porta, et al. 2013. "Transcriptome and Genome Sequencing Uncovers Functional Variation in Humans." *Nature* 501 (7468): 506–11.

Laurent, Anouchka P., Rishi S. Kotecha, and Sébastien Malinge. 2020. "Gain of Chromosome 21 in Hematological Malignancies: Lessons from Studying Leukemia in Children with Down Syndrome." *Leukemia* 34 (8): 1984–99.

Laurenti, Elisa, Sergei Doulatov, Sasan Zandi, Ian Plumb, Jing Chen, Craig April, Jian-Bing Fan, and John E. Dick. 2013. "The Transcriptional Architecture of Early Human Hematopoiesis Identifies Multilevel Control of Lymphoid Commitment." *Nature Immunology* 14 (7): 756–63.

Laurenti, Elisa, and Berthold Göttgens. 2018. "From Haematopoietic Stem Cells to Complex Differentiation Landscapes." *Nature* 553 (7689): 418–26.

LeBien, Tucker W. 2000. "Fates of Human B-Cell Precursors." *Blood* 96 (1): 9–23.

LeBien, Tucker W., and Thomas F. Tedder. 2008. "B Lymphocytes: How They Develop and

Function." *Blood* 112 (5): 1570–80.

Lee, Jaeyop, Gaëlle Breton, Arafat Aljoufi, Yu Jerry Zhou, Sarah Puhr, Michel C. Nussenzweig, and Kang Liu. 2015. "Clonal Analysis of Human Dendritic Cell Progenitor Using a Stromal Cell Culture." *Journal of Immunological Methods* 425 (October): 21–26.

Lee, P., R. Bhansali, S. Izraeli, N. Hijiya, and J. D. Crispino. 2016. "The Biology, Pathogenesis and Clinical Aspects of Acute Lymphoblastic Leukemia in Children with Down Syndrome." *Leukemia* 30 (9): 1816–23.

Leipold, Michael D., Evan W. Newell, and Holden T. Maecker. 2015. "Multiparameter Phenotyping of Human PBMCs Using Mass Cytometry." *Methods in Molecular Biology* 1343: 81–95.

Letourneau, Audrey, Federico A. Santoni, Ximena Bonilla, M. Reza Sailani, David Gonzalez, Jop Kind, Claire Chevalier, et al. 2014. "Domains of Genome-Wide Gene Expression Dysregulation in Down's Syndrome." *Nature* 508 (7496): 345–50.

Lewis, Kyle, Momoko Yoshimoto, and Takanori Takebe. 2021. "Fetal Liver Hematopoiesis: From Development to Delivery." *Stem Cell Research & Therapy* 12 (1): 139.

Li, Chenying, Lei Dong, Rui Su, Ying Bi, Ying Qing, Xiaolan Deng, Yile Zhou, et al. 2020. "Homoharringtonine Exhibits Potent Anti-Tumor Effect and Modulates DNA Epigenome in Acute Myeloid Leukemia by Targeting SP1/TET1/5hmC." *Haematologica* 105 (1): 148–60.

Li, Zhongyou, Tao Yu, Masae Morishima, Annie Pao, Jeffrey LaDuca, Jeffrey Conroy, Norma Nowak, Sei-Ichi Matsui, Isao Shiraishi, and Y. Eugene Yu. 2007. “Duplication of the Entire 22.9 Mb Human Chromosome 21 Syntenic Region on Mouse Chromosome 16 Causes Cardiovascular and Gastrointestinal Abnormalities.” *Human Molecular Genetics* 16 (11): 1359–66.

Ling, Te, Yehudit Birger, Monika J. Stankiewicz, Nissim Ben-Haim, Tomer Kalisky, Avigail Rein, Eitan Kugler, et al. 2019. “Chromatin Occupancy and Epigenetic Analysis Reveal New Insights into the Function of the GATA1 N Terminus in Erythropoiesis.” *Blood* 134 (19): 1619–31.

Liu, Binbin, Sarah Filippi, Anindita Roy, and Irene Roberts. 2015. “Stem and Progenitor Cell Dysfunction in Human Trisomies.” *EMBO Reports* 16 (1): 44–62.

Liu, Chen, Yandong Gong, Han Zhang, Hua Yang, Yang Zeng, Zhilei Bian, Qian Xin, et al. 2021. “Delineating Spatiotemporal and Hierarchical Development of Human Fetal Innate Lymphoid Cells.” *Cell Research* 31 (10): 1106–22.

Liu, Nan, Victoria V. Hargreaves, Qian Zhu, Jesse V. Kurland, Jiyoung Hong, Woojin Kim, Falak Sher, et al. 2018. “Direct Promoter Repression by BCL11A Controls the Fetal to Adult Hemoglobin Switch.” *Cell* 173 (2): 430–42.e17.

Liu, Yibin, Paulina Siejka-Zielińska, Gergana Velikova, Ying Bi, Fang Yuan, Marketa Tomkova, Chunsen Bai, Lei Chen, Benjamin Schuster-Böckler, and Chun-Xiao Song. 2019. “Bisulfite-Free Direct Detection of 5-Methylcytosine and 5-Hydroxymethylcytosine at Base Resolution.” *Nature Biotechnology* 37 (4): 424–29.

Lott, Ira T., and Mara Dierssen. 2010. “Cognitive Deficits and Associated Neurological Complications in Individuals with Down’s Syndrome.” *Lancet Neurology* 9 (6): 623–33.

Luetke-Eversloh, Merlin, Monica Killig, and Chiara Romagnani. 2013. “Signatures of Human NK Cell Development and Terminal Differentiation.” *Frontiers in Immunology* 4 (December): 499.

Lyle, Robert, Frédérique Béna, Sarantis Gagos, Corinne Gehrig, Gipsy Lopez, Albert Schinzel, James Lespinasse, et al. 2009. “Genotype-Phenotype Correlations in Down Syndrome Identified by Array CGH in 30 Cases of Partial Trisomy and Partial Monosomy Chromosome 21.” *European Journal of Human Genetics: EJHG* 17 (4): 454–66.

MacKinney, A. A., Jr. 1978. “Effect of Aging on the Peripheral Blood Lymphocyte Count.” *Journal of Gerontology* 33 (2): 213–16.

Maclean, Glenn A., Tobias F. Menne, Guoji Guo, Danielle J. Sanchez, In-Hyun Park, George Q. Daley, and Stuart H. Orkin. 2012. “Altered Hematopoiesis in Trisomy 21 as Revealed through in Vitro Differentiation of Isogenic Human Pluripotent Cells.” *Proceedings of the National Academy of Sciences of the United States of America* 109 (43): 17567–72.

Maguer-Satta, Véronique, Marion Chapellier, Emmanuel Delay, and Elodie Bachelard-Cascales. 2011. “CD10: A Tool to Crack the Role of Stem Cells in Breast Cancer.” *Proceedings of the National Academy of Sciences of the United States of America*.

Majeti, Ravindra, Christopher Y. Park, and Irving L. Weissman. 2007. “Identification of a Hierarchy of Multipotent Hematopoietic Progenitors in Human Cord Blood.” *Cell Stem Cell* 1 (6):

635–45.

Malfroy, B., W. J. Kuang, P. H. Seeburg, A. J. Mason, and P. R. Schofield. 1988. “Molecular Cloning and Amino Acid Sequence of Human Enkephalinase (neutral Endopeptidase).” *FEBS Letters* 229 (1): 206–10.

Malinge, Sébastien, Meghan Bliss-Moreau, Gina Kirsammer, Lauren Diebold, Timothy Chlon, Sandeep Gurbuxani, and John D. Crispino. 3 2012. “Increased Dosage of the Chromosome 21 Ortholog Dyrk1a Promotes Megakaryoblastic Leukemia in a Murine Model of Down Syndrome.” *The Journal of Clinical Investigation* 122 (3): 948–62.

Malouf, Camille, and Katrin Ottersbach. 2018. “The Fetal Liver Lymphoid-Primed Multipotent Progenitor Provides the Prerequisites for the Initiation of t(4;11) MLL-AF4 Infant Leukemia.” *Haematologica* 103 (12): e571–74.

Månsson, Robert, Anne Hultquist, Sidinh Luc, Liping Yang, Kristina Anderson, Shabnam Kharazi, Suleiman Al-Hashmi, et al. 2007. “Molecular Evidence for Hierarchical Transcriptional Lineage Priming in Fetal and Adult Stem Cells and Multipotent Progenitors.” *Immunity* 26 (4): 407–19.

Mantri, Sruthi, Andreas Reinisch, Beruh T. Dejene, Deirdre J. Lyell, David L. DiGiusto, Rajni Agarwal-Hashmi, Ravindra Majeti, Kenneth I. Weinberg, and Matthew H. Porteus. 2020. “CD34 Expression Does Not Correlate with Immunophenotypic Stem Cell or Progenitor Content in Human Cord Blood Products.” *Blood Advances* 4 (21): 5357–61.

Manz, Markus G., Toshihiro Miyamoto, Koichi Akashi, and Irving L. Weissman. 2002.

"Prospective Isolation of Human Clonogenic Common Myeloid Progenitors." *Proceedings of the National Academy of Sciences of the United States of America* 99 (18): 11872–77.

Mårild, Karl, Olof Stephansson, Lena Grahnquist, Sven Cnattingius, Gabriella Söderman, and Jonas F. Ludvigsson. 2013. "Down Syndrome Is Associated with Elevated Risk of Celiac Disease: A Nationwide Case-Control Study." *The Journal of Pediatrics* 163 (1): 237–42.

Marshall, C. J., and A. J. Thrasher. 2001. "The Embryonic Origins of Human Haematopoiesis." *British Journal of Haematology* 112 (4): 838–50.

Martin, Matthew A., and Mickie Bhatia. 2005. "Analysis of the Human Fetal Liver Hematopoietic Microenvironment." *Stem Cells and Development* 14 (5): 493–504.

McGrath, Kathleen E., Jenna M. Frame, Katherine H. Fegan, James R. Bowen, Simon J. Conway, Seana C. Catherman, Paul D. Kingsley, Anne D. Koniski, and James Palis. 2015. "Distinct Sources of Hematopoietic Progenitors Emerge before HSCs and Provide Functional Blood Cells in the Mammalian Embryo." *Cell Reports* 11 (12): 1892–1904.

McGrath, Kathleen E., Jenna M. Frame, and James Palis. 2015. "Early Hematopoiesis and Macrophage Development." *Seminars in Immunology* 27 (6): 379–87.

McHale, Cliona M., and Martyn T. Smith. 2004. "Prenatal Origin of Chromosomal Translocations in Acute Childhood Leukemia: Implications and Future Directions." *American Journal of Hematology* 75 (4): 254–57.

McLean, S., C. McHale, and H. Enright. 2009. “Hematological Abnormalities in Adult Patients with Down’s Syndrome.” *Irish Journal of Medical Science* 178 (1): 35–38.

Mebius, R. E., T. Miyamoto, J. Christensen, J. Domen, T. Cupedo, I. L. Weissman, and K. Akashi. 2001. “The Fetal Liver Counterpart of Adult Common Lymphoid Progenitors Gives Rise to All Lymphoid Lineages, CD45+CD4+CD3- Cells, as Well as Macrophages.” *Journal of Immunology* 166 (11): 6593–6601.

Medvinsky, A., and E. Dzierzak. 1996. “Definitive Hematopoiesis Is Autonomously Initiated by the AGM Region.” *Cell* 86 (6): 897–906.

Mejia-Ramirez, Eva, and Maria Carolina Florian. 2020. “Understanding Intrinsic Hematopoietic Stem Cell Aging.” *Haematologica* 105 (1): 22–37.

Mestas, Javier, and Christopher C. W. Hughes. 2004. “Of Mice and Not Men: Differences between Mouse and Human Immunology.” *Journal of Immunology* 172 (5): 2731–38.

Migliaccio, G., A. R. Migliaccio, S. Petti, F. Mavilio, G. Russo, D. Lazzaro, U. Testa, M. Marinucci, and C. Peschle. 1986. “Human Embryonic Hemopoiesis. Kinetics of Progenitors and Precursors Underlying the Yolk Sac----Liver Transition.” *The Journal of Clinical Investigation* 78 (1): 51–60.

Mishra, Deepshikha, Sunita Singh, and Gopeshwar Narayan. 2016. “Role of B Cell Development Marker CD10 in Cancer Progression and Prognosis.” *Molecular Biology International* 2016 (November): 4328697.

Montagna, D., R. Maccario, A. G. Ugazio, L. Nespoli, E. Pedroni, P. Faggiano, and G. R. Burgio. 1988. “Cell-Mediated Cytotoxicity in Down Syndrome: Impairment of Allogeneic Mixed Lymphocyte Reaction, NK and NK-like Activities.” *European Journal of Pediatrics* 148 (1): 53–57.

Montecino-Rodriguez, Encarnacion, and Kenneth Dorshkind. 2012. “B-1 B Cell Development in the Fetus and Adult.” *Immunity* 36 (1): 13–21.

Montecino-Rodriguez, Encarnacion, Michael Fice, David Casero, Beata Berent-Maoz, Chad L. Barber, and Kenneth Dorshkind. 2016. “Distinct Genetic Networks Orchestrate the Emergence of Specific Waves of Fetal and Adult B-1 and B-2 Development.” *Immunity* 45 (3): 527–39.

Montecino-Rodriguez, Encarnacion, Hyosuk Leathers, and Kenneth Dorshkind. 2006. “Identification of a B-1 B Cell-Specified Progenitor.” *Nature Immunology* 7 (3): 293–301.

Mori, Hiroshi, Susan M. Colman, Zhijian Xiao, Anthony M. Ford, Lyn E. Healy, Craig Donaldson, Jill M. Hows, Cristina Navarrete, and Mel Greaves. 2002. “Chromosome Translocations and Covert Leukemic Clones Are Generated during Normal Fetal Development.” *Proceedings of the National Academy of Sciences of the United States of America* 99 (12): 8242–47.

Morrison, S. J., A. M. Wandycz, H. D. Hemmati, D. E. Wright, and I. L. Weissman. 1997. “Identification of a Lineage of Multipotent Hematopoietic Progenitors.” *Development* 124 (10): 1929–39.

Mowery, Cody T., Jaime M. Reyes, Lucia Cabal-Hierro, Kelly J. Higby, Kristen L. Karlin, Jarey H. Wang, Robert J. Kimmerling, et al. 2018. “Trisomy of a Down Syndrome Critical Region Globally

Amplifies Transcription via HMGN1 Overexpression." *Cell Reports* 25 (7): 1898–1911.e5.

Müller, A. M., A. Medvinsky, J. Strouboulis, F. Grosveld, and E. Dzierzak. 1994. "Development of Hematopoietic Stem Cell Activity in the Mouse Embryo." *Immunity* 1 (4): 291–301.

Müller, Lena, Petra Aigner, and Dagmar Stoiber. 2017. "Type I Interferons and Natural Killer Cell Regulation in Cancer." *Frontiers in Immunology* 8 (March): 304.

Muller-Sieburg, Christa E., Rebecca H. Cho, Lars Karlsson, Jing-F Huang, and Hans B. Sieburg. 2004. "Myeloid-Biased Hematopoietic Stem Cells Have Extensive Self-Renewal Capacity but Generate Diminished Lymphoid Progeny with Impaired IL-7 Responsiveness." *Blood* 103 (11): 4111–18.

Mundschau, Gina, Sandeep Gurbuxani, Alan S. Gamis, Marianne E. Greene, Robert J. Arceci, and John D. Crispino. 2003. "Mutagenesis of GATA1 Is an Initiating Event in Down Syndrome Leukemogenesis." *Blood* 101 (11): 4298–4300.

Muskens, Ivo S., Shaobo Li, Thomas Jackson, Natalina Elliot, Helen M. Hansen, Swe Swe Myint, Priyatama Pandey, et al. 2021. "The Genome-Wide Impact of Trisomy 21 on DNA Methylation and Its Implications for Hematopoiesis." *Nature Communications* 12 (1): 1–15.

Namikawa, R., M. O. Muench, J. E. de Vries, and M. G. Roncarolo. 1996. "The FLK2/FLT3 Ligand Synergizes with Interleukin-7 in Promoting Stromal-Cell-Independent Expansion and Differentiation of Human Fetal pro-B Cells in Vitro." *Blood* 87 (5): 1881–90.

Nikolaev, Sergey I., Marco Garieri, Federico Santoni, Emilie Falconnet, Pascale Ribaux, Michel Guipponi, Aoife Murray, et al. 2014. “Frequent Cases of RAS-Mutated Down Syndrome Acute Lymphoblastic Leukaemia Lack JAK2 Mutations.” *Nature Communications* 5 (August): 4654.

Notta, Faiyaz, Sergei Doulatov, Elisa Laurenti, Armando Poeppl, Igor Jurisica, and John E. Dick. 2011. “Isolation of Single Human Hematopoietic Stem Cells Capable of Long-Term Multilineage Engraftment.” *Science* 333 (6039): 218–21.

Notta, Faiyaz, Sasan Zandi, Naoya Takayama, Stephanie Dobson, Olga I. Gan, Gavin Wilson, Kerstin B. Kaufmann, et al. 2016. “Distinct Routes of Lineage Development Reshape the Human Blood Hierarchy across Ontogeny.” *Science* 351 (6269): aab2116.

Nutt, S. L., B. Heavey, A. G. Rolink, and M. Busslinger. 1999. “Commitment to the B-Lymphoid Lineage Depends on the Transcription Factor Pax5.” *Nature* 401 (6753): 556–62.

Nutt, Stephen L., and Barbara L. Kee. 2007. “The Transcriptional Regulation of B Cell Lineage Commitment.” *Immunity* 26 (6): 715–25.

O’Byrne, Sorcha, Natalina Elliott, Siobhan Rice, Gemma Buck, Nicholas Fordham, Catherine Garnett, Laura Godfrey, et al. 2019. “Discovery of a CD10-Negative B-Progenitor in Human Fetal Life Identifies Unique Ontogeny-Related Developmental Programs.” *Blood* 134 (13): 1059–71.

O’Byrne, Sorcha Isabella, Natalina Elliott, Gemma Buck, Siobhan Rice, David O’Connor, Jana Oswald, Hannah Fuchs, et al. 2019. “Trisomy 21 Driven Pro-Inflammatory Signalling in Fetal Bone Marrow May Play a Role in Perturbed B-Lymphopoiesis and Acute Lymphoblastic Leukemia

of Down Syndrome." *Blood* 134 (Supplement_1): 1206–1206.

O'Doherty, Aideen, Sandra Ruf, Claire Mulligan, Victoria Hildreth, Mick L. Errington, Sam Cooke, Abdul Sesay, et al. 2005. "An Aneuploid Mouse Strain Carrying Human Chromosome 21 with Down Syndrome Phenotypes." *Science* 309 (5743): 2033–37.

O'Riordan, M., and R. Grosschedl. 2000. "Transcriptional Regulation of Early B-Lymphocyte Differentiation." *Immunological Reviews* 175 (June): 94–103.

Oberlin, Estelle, Bouchra El Hafny, Laurence Petit-Cocault, and Michèle Souyri. 2010. "Definitive Human and Mouse Hematopoiesis Originates from the Embryonic Endothelium: A New Class of HSCs Based on VE-Cadherin Expression." *The International Journal of Developmental Biology* 54 (6-7): 1165–73.

Oliveira-Mateos, Cristina, Anaís Sánchez-Castillo, Marta Soler, Aida Obiols-Guardia, David Piñeyro, Raquel Boque-Sastre, Maria E. Calleja-Cervantes, et al. 2019. "The Transcribed Pseudogene RPSAP52 Enhances the Oncofetal HMGA2-IGF2BP2-RAS Axis through LIN28B-Dependent and Independent Let-7 Inhibition." *Nature Communications* 10 (1): 1–18.

Olova, Nelly, Felix Krueger, Simon Andrews, David Oxley, Rebecca V. Berrens, Miguel R. Branco, and Wolf Reik. 2018. "Comparison of Whole-Genome Bisulfite Sequencing Library Preparation Strategies Identifies Sources of Biases Affecting DNA Methylation Data." *Genome Biology* 19 (1): 1–19.

Olson, L. E., J. T. Richtsmeier, J. Leszl, and R. H. Reeves. 2004. "A Chromosome 21 Critical Region

Does Not Cause Specific Down Syndrome Phenotypes." *Science* 306 (5696): 687–90.

Orkin, S. H. 2000. "Diversification of Haematopoietic Stem Cells to Specific Lineages." *Nature Reviews. Genetics* 1 (1): 57–64.

Orkin, Stuart H., and Leonard I. Zon. 2008. "Hematopoiesis: An Evolving Paradigm for Stem Cell Biology." *Cell* 132 (4): 631–44.

Owens, Dominic D. G., Giorgio Anselmi, A. Marieke Oudelaar, Damien J. Downes, Alessandro Cavallo, Joe R. Harman, Ron Schwessinger, et al. 2022. "Dynamic Runx1 Chromatin Boundaries Affect Gene Expression in Hematopoietic Development." *Nature Communications* 13 (1): 773.

Palis, James. 2016. "Hematopoietic Stem Cell-Independent Hematopoiesis: Emergence of Erythroid, Megakaryocyte, and Myeloid Potential in the Mammalian Embryo." *FEBS Letters* 590 (22): 3965–74.

Pang, Wendy W., Elizabeth A. Price, Debashis Sahoo, Isabel Beerman, William J. Maloney, Derrick J. Rossi, Stanley L. Schrier, and Irving L. Weissman. 2011. "Human Bone Marrow Hematopoietic Stem Cells Are Increased in Frequency and Myeloid-Biased with Age." *Proceedings of the National Academy of Sciences of the United States of America* 108 (50): 20012–17.

Paolini, Rossella, Giovanni Bernardini, Rosa Molfetta, and Angela Santoni. 2015. "NK Cells and Interferons." *Cytokine & Growth Factor Reviews* 26 (2): 113–20.

Papavassiliou, Paulie, Chariyawan Charalsawadi, Kelly Rafferty, and Colleen Jackson-Cook. 2015. "Mosaicism for Trisomy 21: A Review." *American Journal of Medical Genetics. Part A* 167A (1): 26–39.

Papúchová, Henrieta, Torsten B. Meissner, Qin Li, Jack L. Strominger, and Tamara Tilburgs. 2019. "The Dual Role of HLA-C in Tolerance and Immunity at the Maternal-Fetal Interface." *Frontiers in Immunology* 10 (December): 2730.

Park, L. S., U. Martin, K. Garka, B. Gliniak, J. P. Di Santo, W. Muller, D. A. Largaespada, et al. 2000. "Cloning of the Murine Thymic Stromal Lymphopoietin (TSLP) Receptor: Formation of a Functional Heteromeric Complex Requires Interleukin 7 Receptor." *The Journal of Experimental Medicine* 192 (5): 659–70.

Parrish, Yasmin Khan, Ineavely Baez, Terry-Ann Milford, Abigail Benitez, Nicholas Galloway, Jaqueline Willeman Rogerio, Eva Sahakian, et al. 2009. "IL-7 Dependence in Human B Lymphopoiesis Increases during Progression of Ontogeny from Cord Blood to Bone Marrow." *Journal of Immunology* 182 (7): 4255–66.

Pellegrini, F. P., M. Marinoni, V. Frangione, A. Tedeschi, V. Gandini, F. Ciglia, L. Mortara, R. S. Accolla, and L. Nespoli. 2012. "Down Syndrome, Autoimmunity and T Regulatory Cells." *Clinical and Experimental Immunology* 169 (3): 238–43.

Pelleri, Maria Chiara, Elena Cicchini, Chiara Locatelli, Lorenza Vitale, Maria Caracausi, Allison Piovesan, Alessandro Rocca, et al. 2016. "Systematic Reanalysis of Partial Trisomy 21 Cases with or without Down Syndrome Suggests a Small Region on 21q22.13 as Critical to the Phenotype."

Human Molecular Genetics 25 (12): 2525–38.

Pereira, Patricia Lopes, Laetitia Magnol, Ignasi Sahún, Véronique Brault, Arnaud Duchon, Paola Prandini, Agnès Gruart, et al. 2009. “A New Mouse Model for the Trisomy of the Abcg1-U2af1 Region Reveals the Complexity of the Combinatorial Genetic Code of down Syndrome.” *Human Molecular Genetics* 18 (24): 4756–69.

Perez-Andres, Martin, Christina Grosserichter-Wagener, Cristina Teodosio, Jacques J. M. van Dongen, Alberto Orfao, and Menno C. van Zelm. 2011. “The Nature of Circulating CD27+CD43+ B Cells.” *The Journal of Experimental Medicine*.

Perry, S. Scott, Robert S. Welner, Taku Kouro, Paul W. Kincade, and Xiao-Hong Sun. 2006. “Primitive Lymphoid Progenitors in Bone Marrow with T Lineage Reconstituting Potential.” *Journal of Immunology* 177 (5): 2880–87.

Pietras, Eric M., Damien Reynaud, Yoon-A Kang, Daniel Carlin, Fernando J. Calero-Nieto, Andrew D. Leavitt, Joshua M. Stuart, Berthold Göttgens, and Emmanuelle Passegué. 2015. “Functionally Distinct Subsets of Lineage-Biased Multipotent Progenitors Control Blood Production in Normal and Regenerative Conditions.” *Cell Stem Cell* 17 (1): 35–46.

Popescu, Dorin-Mirel, Rachel A. Botting, Emily Stephenson, Kile Green, Simone Webb, Laura Jardine, Emily F. Calderbank, et al. 2019. “Decoding Human Fetal Liver Haematopoiesis.” *Nature* 574 (7778): 365–71.

Prasher, V. P. 1994. “Down Syndrome, Dementia and Macrocytosis.” *British Journal of*

Developmental Disabilities 40 (79): 131–34.

Pridans, Clare, Melissa L. Holmes, Matthew Polli, James M. Wettenhall, Aleksandar Dakic, Lynn M. Corcoran, Gordon K. Smyth, and Stephen L. Nutt. 2008. "Identification of Pax5 Target Genes in Early B Cell Differentiation." *Journal of Immunology* 180 (3): 1719–28.

Puel, A., S. F. Ziegler, R. H. Buckley, and W. J. Leonard. 1998. "Defective IL7R Expression in T(-)B(+)NK(+) Severe Combined Immunodeficiency." *Nature Genetics* 20 (4): 394–97.

Pui, C. H., G. K. Rivera, M. L. Hancock, S. C. Raimondi, J. T. Sandlund, H. H. Mahmoud, R. C. Ribeiro, W. L. Furman, C. A. Hurwitz, and W. M. Crist. 1993. "Clinical Significance of CD10 Expression in Childhood Acute Lymphoblastic Leukemia." *Leukemia* 7 (1): 35–40.

Rackaityte, Elze, and Joanna Halkias. 2020. "Mechanisms of Fetal T Cell Tolerance and Immune Regulation." *Frontiers in Immunology* 11 (April): 588.

Rahmani, Z., J. L. Blouin, N. Creau-Goldberg, P. C. Watkins, J. F. Mattei, M. Poissonnier, M. Prieur, Z. Chettouh, A. Nicole, and A. Aurias. 1989. "Critical Role of the D21S55 Region on Chromosome 21 in the Pathogenesis of Down Syndrome." *Proceedings of the National Academy of Sciences of the United States of America* 86 (15): 5958–62.

Rainis, Liat, Tsutomu Toki, John E. Pimanda, Ester Rosenthal, Keren Machol, Sabine Strehl, Berthold Göttgens, Etsuro Ito, and Shai Izraeli. 2005. "The Proto-Oncogene ERG in Megakaryoblastic Leukemias." *Cancer Research* 65 (17): 7596–7602.

Ram, G., and J. Chinen. 2011. “Infections and Immunodeficiency in Down Syndrome.” *Clinical and Experimental Immunology* 164 (1): 9–16.

Ramond, Cyrille, Claire Berthault, Odile Burlen-Defranoux, Ana Pereira de Sousa, Delphine Guy-Grand, Paulo Vieira, Pablo Pereira, and Ana Cumano. 2014. “Two Waves of Distinct Hematopoietic Progenitor Cells Colonize the Fetal Thymus.” *Nature Immunology* 15 (1): 27–35.

Ranzoni, Anna Maria, Andrea Tangherloni, Ivan Berest, Simone Giovanni Riva, Brynelle Myers, Paulina M. Strzelecka, Jiarui Xu, et al. 2021. “Integrative Single-Cell RNA-Seq and ATAC-Seq Analysis of Human Developmental Hematopoiesis.” *Cell Stem Cell* 28 (3): 472–87.e7.

Rechavi, Erez, Atar Lev, Yu Nee Lee, Amos J. Simon, Yoav Yinon, Schlomo Lipitz, Ninette Amariglio, Boaz Weisz, Luigi D. Notarangelo, and Raz Somech. 2015. “Timely and Spatially Regulated Maturation of B and T Cell Repertoire during Human Fetal Development.” *Science Translational Medicine* 7 (276): 276ra25.

Reeves, R. H., N. G. Irving, T. H. Moran, A. Wohn, C. Kitt, S. S. Sisodia, C. Schmidt, R. T. Bronson, and M. T. Davisson. 1995. “A Mouse Model for Down Syndrome Exhibits Learning and Behaviour Deficits.” *Nature Genetics* 11 (2): 177–84.

Renoux, Virginie M., Alya Zriwil, Claudia Peitzsch, Jakob Michaëlsson, Danielle Friberg, Shamit Soneji, and Ewa Sitnicka. 2015. “Identification of a Human Natural Killer Cell Lineage-Restricted Progenitor in Fetal and Adult Tissues.” *Immunity* 43 (2): 394–407.

Reth, Michael, and Peter Nielsen. 2014. “Chapter Four - Signaling Circuits in Early B-Cell

Development." In *Advances in Immunology*, edited by Frederick W. Alt, 122:129–75. Academic Press.

Reya, T., S. J. Morrison, M. F. Clarke, and I. L. Weissman. 2001. "Stem Cells, Cancer, and Cancer Stem Cells." *Nature* 414 (6859): 105–11.

Reynaud, Damien, Nathalie Lefort, Elodie Manie, Laure Coulombel, and Yves Levy. 2003. "In Vitro Identification of Human pro-B Cells That Give Rise to Macrophages, Natural Killer Cells, and T Cells." *Blood* 101 (11): 4313–21.

Rice, Siobhan, Thomas Jackson, Nicholas T. Crump, Nicholas Fordham, Natalina Elliott, Sorcha O'Byrne, Maria del Mar Lara Fanego, et al. 2021. "A Human Fetal Liver-Derived Infant MLL-AF4 Acute Lymphoblastic Leukemia Model Reveals a Distinct Fetal Gene Expression Program." *Nature Communications* 12 (1): 1–13.

Roberts, Irene, Kate Alford, Georgina Hall, Gaetan Juban, Helen Richmond, Alice Norton, Grant Vallance, et al. 2013. "GATA1-Mutant Clones Are Frequent and Often Unsuspected in Babies with Down Syndrome: Identification of a Population at Risk of Leukemia." *Blood* 122 (24): 3908–17.

Roberts, Irene, and Shai Izraeli. 2014. "Haematopoietic Development and Leukaemia in Down Syndrome." *British Journal of Haematology* 167 (5): 587–99.

Rodig, Scott J., Jeffery L. Kutok, Jennifer C. Paterson, Hiroaki Nitta, Wenjun Zhang, Bjoern Chapuy, Lynette K. Tumwine, et al. 2010. "The Pre-B-Cell Receptor Associated Protein VpreB3 Is

a Useful Diagnostic Marker for Identifying c-MYC Translocated Lymphomas." *Haematologica* 95 (12): 2056–62.

Rodriguez-Meira, Alba, Jennifer O'Sullivan, Haseeb Rahman, and Adam J. Mead. 2020. "TARGET-Seq: A Protocol for High-Sensitivity Single-Cell Mutational Analysis and Parallel RNA Sequencing." *STAR Protocols* 1 (3): 100125.

Rodriguez-Zhurbenko, Nely, Tam D. Quach, Thomas J. Hopkins, Thomas L. Rothstein, and Ana M. Hernandez. 2019. "Human B-1 Cells and B-1 Cell Antibodies Change With Advancing Age." *Frontiers in Immunology* 10 (March): 483.

Rosnet, O., M. G. Mattéi, O. Delattre, and C. Schiff. 1999. "VPREB3: cDNA Characterization and Expression in Human and Chromosome Mapping in Human and Mouse." *Cytogenetics and Cell Genetics* 87 (3-4): 205–8.

Rosnet, Olivier, Carla Blanco-Betancourt, Karine Grivel, Kirsten Richter, and Claudine Schiff. 2004. "Binding of Free Immunoglobulin Light Chains to VpreB3 Inhibits Their Maturation and Secretion in Chicken B Cells." *The Journal of Biological Chemistry* 279 (11): 10228–36.

Rothenberg, Ellen V. 2014. "Transcriptional Control of Early T and B Cell Developmental Choices." *Annual Review of Immunology* 32 (January): 283–321.

Rowe, R. Grant, Leo D. Wang, Silvia Coma, Areum Han, Ronald Mathieu, Daniel S. Pearson, Samantha Ross, et al. 2016. "Developmental Regulation of Myeloerythroid Progenitor Function by the Lin28b-Let-7-Hmga2 Axis." *The Journal of Experimental Medicine* 213 (8): 1497–1512.

Roy, Anindita, Georg Bohn, Katerina Goudevenou, Gillian Cowan, Neha Bhatnagar, David O'Connor, Oliver Tunstall, et al. 2014. "Developmental Stage Specific B-Progenitor Expansion in Normal Fetal Bone Marrow Is Absent in Down Syndrome: Implications for Infant ALL." *Blood* 124 (21): 4331.

Roy, Anindita, Vojtech Bystry, Georg Bohn, Katerina Goudevenou, Tomas Reigl, Maria Papaioannou, Adam Krejci, et al. 2017. "High Resolution IgH Repertoire Analysis Reveals Fetal Liver as the Likely Origin of Life-Long, Innate B Lymphopoiesis in Humans." *Clinical Immunology* 183 (October): 8–16.

Roy, Anindita, Guanlin Wang, Deena Iskander, Sorcha O'Byrne, Natalina Elliott, Jennifer O'Sullivan, Gemma Buck, et al. 2021. "Transitions in Lineage Specification and Gene Regulatory Networks in Hematopoietic Stem/progenitor Cells over Human Development." *Cell Reports* 36 (11): 109698.

Russell, Lisa J., Melania Capasso, Inga Vater, Takashi Akasaka, Olivier A. Bernard, Maria Jose Calasanz, Thiruppavaii Chandrasekaran, et al. 2009. "Deregulated Expression of Cytokine Receptor Gene, CRLF2, Is Involved in Lymphoid Transformation in B-Cell Precursor Acute Lymphoblastic Leukemia." *Blood* 114 (13): 2688–98.

Ryan, D. H., B. L. Nuccie, I. Ritterman, J. L. Liesveld, C. N. Abboud, and R. A. Insel. 1997. "Expression of Interleukin-7 Receptor by Lineage-Negative Human Bone Marrow Progenitors with Enhanced Lymphoid Proliferative Potential and B-Lineage Differentiation Capacity." *Blood* 89 (3): 929–40.

Sago, H., E. J. Carlson, D. J. Smith, J. Kilbridge, E. M. Rubin, W. C. Mobley, C. J. Epstein, and T. T. Huang. 1998. “Ts1Cje, a Partial Trisomy 16 Mouse Model for Down Syndrome, Exhibits Learning and Behavioral Abnormalities.” *Proceedings of the National Academy of Sciences of the United States of America* 95 (11): 6256–61.

Sailani, M. Reza, Federico A. Santoni, Audrey Letourneau, Christelle Borel, Periklis Makrythanasis, Youssef Hibaoui, Konstantin Popadin, et al. 2015. “DNA-Methylation Patterns in Trisomy 21 Using Cells from Monozygotic Twins.” *PloS One* 10 (8): e0135555.

Sánchez-Albisua, Iciar, Wolfgang Storm, Iris Wäscher, and Martin Stern. 2002. “How Frequent Is Coeliac Disease in Down Syndrome?” *European Journal of Pediatrics* 161 (12): 683–84.

Sanjuan-Pla, Alejandra, Iain C. Macaulay, Christina T. Jensen, Petter S. Woll, Tiago C. Luis, Adam Mead, Susan Moore, et al. 2013. “Platelet-Biased Stem Cells Reside at the Apex of the Haematopoietic Stem-Cell Hierarchy.” *Nature* 502 (7470): 232–36.

Sankaran, Vijay G., and Stuart H. Orkin. 2013. “The Switch from Fetal to Adult Hemoglobin.” *Cold Spring Harbor Perspectives in Medicine* 3 (1): a011643.

SanMiguel, Jennifer M., Kira Young, and Jennifer J. Trowbridge. 2020. “Hand in Hand: Intrinsic and Extrinsic Drivers of Aging and Clonal Hematopoiesis.” *Experimental Hematology* 91 (November): 1–9.

Sanz, Eva, Melchor Alvarez-Mon, Carlos Martínez-A, and Antonio de la Hera. 2003. “Human Cord

Blood CD34+Pax-5+ B-Cell Progenitors: Single-Cell Analyses of Their Gene Expression Profiles." *Blood* 101 (9): 3424–30.

Sanz, Eva, Norman Muñoz-A, Jorge Monserrat, Ana Van-Den-Rym, Pedro Escoll, Ismael Ranz, Melchor Alvarez-Mon, and Antonio de-la-Hera. 2010. "Ordering Human CD34+CD10-CD19+ Pre/pro-B-Cell and CD19- Common Lymphoid Progenitor Stages in Two pro-B-Cell Development Pathways." *Proceedings of the National Academy of Sciences of the United States of America* 107 (13): 5925–30.

Sanz, Ignacio, Chungwen Wei, Scott A. Jenks, Kevin S. Cashman, Christopher Tipton, Matthew C. Woodruff, Jennifer Hom, and F. Eun-Hyung Lee. 2019. "Challenges and Opportunities for Consistent Classification of Human B Cell and Plasma Cell Populations." *Frontiers in Immunology* 10 (October): 2458.

Savino, Angela Maria, and Shai Izraeli. 2016. "On Mice and Humans: The Role of Thymic Stromal Lymphopoietin in Human B-Cell Development and Leukemia." *Haematologica*.

Saxena, Nivedita Shankar, Kara L. Davis, Matthew Arthur Inlay, Astraea Junger, Yujun Yang, Mark L. Krampf, Beruh Dejene, Garry P. Nolan, Irving L. Weissman, and Kenneth I. Weinberg. 2016. "High Resolution Mapping of Human Lymphopoiesis Reveals a Common Lymphoid Progenitor (CLP) Population." *Blood* 128 (22): 1473–1473.

Scheeren, Ferenc A., Anja U. van Lent, Maho Nagasawa, Kees Weijer, Hergen Spits, Nicolas Legrand, and Bianca Blom. 2010. "Thymic Stromal Lymphopoietin Induces Early Human B-Cell Proliferation and Differentiation." *European Journal of Immunology* 40 (4): 955–65.

Scheller, Marina, Anne Kathrin Ludwig, Stefanie Göllner, Christian Rohde, Stephen Krämer, Sina Stäble, Maike Janssen, et al. 2021. “Hotspot DNMT3A Mutations in Clonal Hematopoiesis and Acute Myeloid Leukemia Sensitize Cells to Azacytidine via Viral Mimicry Response.” *Nature Cancer* 2 (5): 527–44.

Schoch, Justine, Tilman R. Rohrer, Michael Kaestner, Hashim Abdul-Khaliq, Ludwig Gortner, Urban Sester, Martina Sester, and Tina Schmidt. 2017. “Quantitative, Phenotypical, and Functional Characterization of Cellular Immunity in Children and Adolescents With Down Syndrome.” *The Journal of Infectious Diseases* 215 (10): 1619–28.

Seita, Jun, and Irving L. Weissman. 2010. “Hematopoietic Stem Cell: Self-Renewal versus Differentiation.” *Wiley Interdisciplinary Reviews. Systems Biology and Medicine* 2 (6): 640–53.

Seo, Wooseok, Tomokatsu Ikawa, Hiroshi Kawamoto, and Ichiro Taniuchi. 2012. “Runx1-Cbfβ Facilitates Early B Lymphocyte Development by Regulating Expression of Ebf1.” *The Journal of Experimental Medicine* 209 (7): 1255–62.

Shapiro, B. L. 1999. “The Down Syndrome Critical Region.” *Journal of Neural Transmission. Supplementum* 57: 41–60.

Shen, Xiaohua, Yingchun Liu, Yu-Jung Hsu, Yuko Fujiwara, Jonghwan Kim, Xiaohong Mao, Guo-Cheng Yuan, and Stuart H. Orkin. 2008. “EZH1 Mediates Methylation on Histone H3 Lysine 27 and Complements EZH2 in Maintaining Stem Cell Identity and Executing Pluripotency.” *Molecular Cell* 32 (4): 491–502.

Shen, Yong, Jeffrey M. Verboon, Yuannyu Zhang, Nan Liu, Yoon Jung Kim, Samantha Marglous, Satish K. Nandakumar, et al. 2021. “A Unified Model of Human Hemoglobin Switching through Single-Cell Genome Editing.” *Nature Communications* 12 (1): 4991.

Shlush, Liran I. 2018. “Age-Related Clonal Hematopoiesis.” *Blood* 131 (5): 496–504.

Sigvardsson, Mikael. 2018. “Molecular Regulation of Differentiation in Early B-Lymphocyte Development.” *International Journal of Molecular Sciences* 19 (7). https://doi.org/10.3390/ijms19071928.

Simon, J. H., C. K. Tebbi, A. I. Freeman, M. L. Brecher, D. M. Green, and A. A. Sandberg. 1987. “Acute Megakaryoblastic Leukemia Associated with Mosaic Down’s Syndrome.” *Cancer* 60 (10): 2515–20.

Smith, Matthew A., Michelle Maurin, Hyun Il Cho, Brian Becknell, Aharon G. Freud, Jianhua Yu, Sheng Wei, et al. 2010. “PRDM1/Blimp-1 Controls Effector Cytokine Production in Human NK Cells.” *Journal of Immunology* 185 (10): 6058–67.

Soares-da-Silva, Francisca, Laina Freyer, Ramy Elsaid, Odile Burlen-Defranoux, Lorea Iturri, Odile Sismeiro, Perpétua Pinto-do-Ó, Elisa Gomez-Perdiguero, and Ana Cumano. 2021. “Yolk Sac, but Not Hematopoietic Stem Cell-Derived Progenitors, Sustain Erythropoiesis throughout Murine Embryonic Life.” *The Journal of Experimental Medicine* 218 (4). https://doi.org/10.1084/jem.20201729.

Solari, Claudia, María Victoria Petrone, Camila Vazquez Echegaray, María Soledad Cosentino, Ariel Waisman, Marcos Francia, Lino Barañao, Santiago Miriuka, and Alejandra Guberman. 2018. "Superoxide Dismutase 1 Expression Is Modulated by the Core Pluripotency Transcription Factors Oct4, Sox2 and Nanog in Embryonic Stem Cells." *Mechanisms of Development* 154 (December): 116–21.

Sood, Raman, Yasuhiko Kamikubo, and Paul Liu. 2017. "Role of RUNX1 in Hematological Malignancies." *Blood* 129 (15): 2070–82.

Stamoulis, Georgios, Marco Garieri, Periklis Makrythanasis, Audrey Letourneau, Michel Guipponi, Nikolaos Panousis, Frédérique Sloan-Béna, et al. 2019. "Single Cell Transcriptome in Aneuploidies Reveals Mechanisms of Gene Dosage Imbalance." *Nature Communications* 10 (1): 1–11.

Stankiewicz, Monika J., and John D. Crispino. 2009. "ETS2 and ERG Promote Megakaryopoiesis and Synergize with Alterations in GATA-1 to Immortalize Hematopoietic Progenitor Cells." *Blood* 113 (14): 3337–47.

Su, Ruijun, Terry-Ann Milford, Ineavely Baez, Abby Jones Weldon, Sinisa Dovat, and Kimberly J. Payne. 2010. "Expression of the IL-7R Identifies a Human Common Lymphoid Progenitor (CLP) In Cord Blood Lymphopoiesis." *Blood* 116 (21): 1603–1603.

Sullivan, Kelly D., Donald Evans, Ahwan Pandey, Thomas H. Hraha, Keith P. Smith, Neil Markham, Angela L. Rachubinski, et al. 2017. "Trisomy 21 Causes Changes in the Circulating Proteome Indicative of Chronic Autoinflammation." *Scientific Reports* 7 (1): 14818.

Sullivan, Kelly D., Hannah C. Lewis, Amanda A. Hill, Ahwan Pandey, Leisa P. Jackson, Joseph M. Cabral, Keith P. Smith, et al. 2016. “Trisomy 21 Consistently Activates the Interferon Response.” *eLife* 5 (July). https://doi.org/10.7554/eLife.16220.

Sun, Joseph C., and Lewis L. Lanier. 2009. “Natural Killer Cells Remember: An Evolutionary Bridge between Innate and Adaptive Immunity?” *European Journal of Immunology* 39 (8): 2059–64.

Suo, Chenqu, Emma Dann, Issac Goh, Laura Jardine, Vitalii Kleshchevnikov, Jong-Eun Park, Rachel A. Botting, et al. 2022. “Mapping the Developing Human Immune System across Organs.” *Science* 376 (6597): eabo0510.

Symmons, Orsolya, Marcello Chang, Ian A. Mellis, Jennifer M. Kalish, Jihwan Park, Katalin Suszták, Marisa S. Bartolomei, and Arjun Raj. 2019. “Allele-Specific RNA Imaging Shows That Allelic Imbalances Can Arise in Tissues through Transcriptional Bursting.” *PLoS Genetics* 15 (1): e1007874.

Taguchi, Tomoko, Hisami Takenouchi, Yusuke Shiozawa, Jun Matsui, Noriko Kitamura, Yoshitaka Miyagawa, Yoko U. Katagiri, et al. 2007. “Interleukin-7 Contributes to Human pro-B-Cell Development in a Mouse Stromal Cell-Dependent Culture System.” *Experimental Hematology* 35 (9): 1398–1407.

Tavian, M., M. F. Hallais, and B. Péault. 1999. “Emergence of Intraembryonic Hematopoietic Precursors in the Pre-Liver Human Embryo.” *Development* 126 (4): 793–803.

Taylor, K. H., J. Liu, J. Guo, J. W. Davis, H. Shi, and C. W. Caldwell. 2006. “Promoter DNA Methylation of CD10 in Lymphoid Malignancies.” *Leukemia* 20 (10): 1910–12.

Thilaganathan, B., D. Tsakonas, and K. Nicolaides. 1993. “Abnormal Fetal Immunological Development in Down’s Syndrome.” *British Journal of Obstetrics and Gynaecology* 100 (1): 60–62.

Thompson, Benjamin J., Rahul Bhansali, Lauren Diebold, Daniel E. Cook, Lindsay Stolzenburg, Anne-Sophie Casagrande, Thierry Besson, et al. 2015. “DYRK1A Controls the Transition from Proliferation to Quiescence during Lymphoid Development by Destabilizing Cyclin D3.” *The Journal of Experimental Medicine* 212 (6): 953–70.

Toki, Tsutomu, Fumiki Katsuoka, Rika Kanezaki, Gang Xu, Hidekachi Kurotaki, Jiying Sun, Takuya Kamio, et al. 2005. “Transgenic Expression of BACH1 Transcription Factor Results in Megakaryocytic Impairment.” *Blood* 105 (8): 3100–3108.

Tsuneto, Motokazu, Koji Tokoyoda, Ekaterina Kajikhina, Anja E. Hauser, Takahiro Hara, Shizue Tani-Ichi, Koichi Ikuta, and Fritz Melchers. 2013. “B-Cell Progenitors and Precursors Change Their Microenvironment in Fetal Liver during Early Development.” *Stem Cells* 31 (12): 2800–2812.

Tunstall, Oliver, Neha Bhatnagar, Beki James, Alice Norton, Aengus S. O’Marcaigh, Tim Watts, Anne Greenough, et al. 2018. “Guidelines for the Investigation and Management of Transient Leukaemia of Down Syndrome.” *British Journal of Haematology* 182 (2): 200–211.

Tunstall-Pedoe, Oliver, Anindita Roy, Anastasios Karadimitris, Josu de la Fuente, Nicholas M. Fisk, Phillip Bennett, Alice Norton, Paresh Vyas, and Irene Roberts. 2008. “Abnormalities in the Myeloid Progenitor Compartment in Down Syndrome Fetal Liver Precede Acquisition of GATA1 Mutations.” *Blood* 112 (12): 4507–11.

Uckun, F. M., K. Herman-Hatten, M. L. Crotty, M. G. Sensel, H. N. Sather, L. Tuel-Ahlgren, M. B. Sarquis, et al. 1998. “Clinical Significance of MLL-AF4 Fusion Transcript Expression in the Absence of a Cytogenetically Detectable t(4;11)(q21;q23) Chromosomal Translocation.” *Blood* 92 (3): 810–21.

Ulloa, Bianca A., Samima S. Habbsa, Kathryn S. Potts, Alana Lewis, Mia McKinstry, Sara G. Payne, Julio Flores, et al. 2021. “Definitive Hematopoietic Stem Cells Minimally Contribute to Embryonic Hematopoiesis.” *bioRxiv*. https://doi.org/10.1101/2021.05.02.442359.

Valentini, Diletta, Valentina Marcellini, Simona Bianchi, Alberto Villani, Marzia Facchini, Isabella Donatelli, Maria Rita Castrucci, Emiliano Marasco, Chiara Farroni, and Rita Carsetti. 2015. “Generation of Switched Memory B Cells in Response to Vaccination in Down Syndrome Children and Their Siblings.” *Vaccine* 33 (48): 6689–96.

Vanhee, Stijn, Hugo Åkerstrand, Trine Ahn Kristiansen, Sebak Datta, Giorgia Montano, Stefano Vergani, Stefan Lang, et al. 2019. “Lin28b Controls a Neonatal to Adult Switch in B Cell Positive Selection.” *Science Immunology* 4 (39): eaax4453.

Vardiman, James W., Jüergen Thiele, Daniel A. Arber, Richard D. Brunning, Michael J. Borowitz, Anna Porwit, Nancy Lee Harris, et al. 2009. “The 2008 Revision of the World Health Organization

(WHO) Classification of Myeloid Neoplasms and Acute Leukemia: Rationale and Important Changes." *Blood* 114 (5): 937–51.

Vazquez, Monica I., Jovani Catalan-Dibene, and Albert Zlotnik. 2015. "B Cells Responses and Cytokine Production Are Regulated by Their Immune Microenvironment." *Cytokine* 74 (2): 318–26.

Velten, Lars, Simon F. Haas, Simon Raffel, Sandra Blaszkiewicz, Saiful Islam, Bianca P. Hennig, Christoph Hirche, et al. 2017. "Human Haematopoietic Stem Cell Lineage Commitment Is a Continuous Process." *Nature Cell Biology* 19 (4): 271–81.

Viswanathan, Srinivas R., John T. Powers, William Einhorn, Yujin Hoshida, Tony L. Ng, Sara Toffanin, Maureen O'Sullivan, et al. 2009. "Lin28 Promotes Transformation and Is Associated with Advanced Human Malignancies." *Nature Genetics* 41 (7): 843–48.

Vo, Linda T., Melissa A. Kinney, Xin Liu, Yuannyu Zhang, Jessica Barragan, Patricia M. Sousa, Deepak K. Jha, et al. 2018. "Regulation of Embryonic Haematopoietic Multipotency by EZH1." *Nature* 553 (7689): 506–10.

Vosshenrich, Christian A. J., Ana Cumano, Werner Müller, James P. Di Santo, and Paulo Vieira. 2003. "Thymic Stromal-Derived Lymphopoietin Distinguishes Fetal from Adult B Cell Development." *Nature Immunology* 4 (8): 773–79.

———. 2004. "Pre-B Cell Receptor Expression Is Necessary for Thymic Stromal Lymphopoietin Responsiveness in the Bone Marrow but Not in the Liver Environment." *Proceedings of the*

National Academy of Sciences of the United States of America 101 (30): 11070–75.

Vukadin, Lana, Jung-Hyun Kim, Tara Bly Hackwelder, Nathan Ungerleider, Erik Flemington, and Eun-Young Erin Ahn. 2019. “Hematological Disorders in Human Patients with Son Mutations.” *Blood* 134 (November): 3709.

Wagenblast, Elvin, Joana Araújo, Olga I. Gan, Sarah K. Cutting, Alex Murison, Gabriela Krivdova, Maria Azkanaz, et al. 2020. “Mapping the Cellular Origin and Early Evolution of Leukemia in Down Syndrome.” *bioRxiv*. https://doi.org/10.1101/2020.11.29.402800.

———. 2021. “Mapping the Cellular Origin and Early Evolution of Leukemia in Down Syndrome.” *Science* 373 (6551). https://doi.org/10.1126/science.abf6202.

Wagenblast, Elvin, Maria Azkanaz, Sabrina A. Smith, Lorien Shakib, Jessica L. McLeod, Gabriela Krivdova, Joana Araújo, et al. 2019. “Functional Profiling of Single CRISPR/Cas9-Edited Human Long-Term Hematopoietic Stem Cells.” *Nature Communications* 10 (1): 4730.

Wagenblast, Elvin, Gabriela Krivdova, Olga I. Gan, Johann K. Hitzler, John E. Dick, and Eric R. Lechman. 2018. “Functional and Molecular Consequences of Trisomy 21 on Human Fetal Hematopoiesis.” *Blood* 132 (Supplement 1): 1317–1317.

Wang, Dahai, Mayuri Tanaka-Yano, Eleanor Meader, Melissa A. Kinney, Vivian Morris, Edroaldo Lummertz da Rocha, Nan Liu, et al. 2022. “Developmental Maturation of the Hematopoietic System Controlled by a Lin28b-Let-7-Cbx2 Axis.” *Cell Reports* 39 (1): 110587.

Wang, Saifeng, Bryan Chim, Yijun Su, Pavel Khil, Madeline Wong, Xiantao Wang, Amir Foroushani, et al. 2019. “Enhancement of LIN28B-Induced Hematopoietic Reprogramming by IGF2BP3.” *Genes & Development* 33 (15-16): 1048–68.

Wang, Xinxin, Zuly E. Parra, and Robert D. Miller. 2012. “A VpreB3 Homologue in a Marsupial, the Gray Short-Tailed Opossum, Monodelphis Domestica.” *Immunogenetics* 64 (8): 647–52.

Waugh, Katherine A., Paula Araya, Ahwan Pandey, Kimberly R. Jordan, Keith P. Smith, Ross E. Granrath, Santosh Khanal, et al. 2019. “Mass Cytometry Reveals Global Immune Remodeling with Multi-Lineage Hypersensitivity to Type I Interferon in Down Syndrome.” *Cell Reports* 29 (7): 1893–1908.e4.

Waugh, Katherine A., Ross Minter, Jessica Baxter, Congwu Chi, Kathryn D. Tuttle, Neetha P. Eduthan, Matthew D. Galbraith, et al. 2022. “Interferon Receptor Gene Dosage Determines Diverse Hallmarks of Down Syndrome.” *bioRxiv*. https://doi.org/10.1101/2022.02.03.478982.

Wechsler, Joshua, Marianne Greene, Michael A. McDevitt, John Anastasi, Judith E. Karp, Michelle M. Le Beau, and John D. Crispino. 2002. “Acquired Mutations in GATA1 in the Megakaryoblastic Leukemia of Down Syndrome.” *Nature Genetics* 32 (1): 148–52.

Weerd, Nicole A. de, and Thao Nguyen. 2012. “The Interferons and Their Receptors--Distribution and Regulation.” *Immunology and Cell Biology* 90 (5): 483–91.

Wiemels, J. L., G. Cazzaniga, M. Daniotti, O. B. Eden, G. M. Addison, G. Masera, V. Saha, A. Biondi, and M. F. Greaves. 1999. “Prenatal Origin of Acute Lymphoblastic Leukaemia in

Children." *The Lancet* 354 (9189): 1499–1503.

Wiemels, Joseph L., Ivo S. Muskens, Shaobo Li, Priyatama Pandey, Ritu Roy, Helen M. Hansen, Kimberly D. Siegmund, et al. 2019. "The Genome-Wide Impact of Trisomy 21 on DNA Methylation and Its Implications for Hematologic Malignancies." *Blood* 134 (Supplement_1): 2510–2510.

Wong, Jason B., Susannah L. Hewitt, Lynn M. Heltemes-Harris, Malay Mandal, Kristen Johnson, Klaus Rajewsky, Sergei B. Koralov, Marcus R. Clark, Michael A. Farrar, and Jane A. Skok. 2019. "B-1a Cells Acquire Their Unique Characteristics by Bypassing the Pre-BCR Selection Stage." *Nature Communications* 10 (1): 4768.

Xie, Huafeng, Jian Xu, Jessie H. Hsu, Minh Nguyen, Yuko Fujiwara, Cong Peng, and Stuart H. Orkin. 2014. "Polycomb Repressive Complex 2 Regulates Normal Hematopoietic Stem Cell Function in a Developmental-Stage-Specific Manner." *Cell Stem Cell* 14 (1): 68–80.

Xu, G., R. Kanezaki, T. Toki, S. Watanabe, Y. Takahashi, K. Terui, I. Kitabayashi, and E. Ito. 2006. "Physical Association of the Patient-Specific GATA1 Mutants with RUNX1 in Acute Megakaryoblastic Leukemia Accompanying Down Syndrome." *Leukemia* 20 (6): 1002–8.

Xu, Jian, Daniel E. Bauer, Marc A. Kerenyi, Thuy D. Vo, Serena Hou, Yu-Jung Hsu, Huilan Yao, Jennifer J. Trowbridge, Gail Mandel, and Stuart H. Orkin. 2013. "Corepressor-Dependent Silencing of Fetal Hemoglobin Expression by BCL11A." *Proceedings of the National Academy of Sciences of the United States of America* 110 (16): 6518–23.

Xue, Hai-Hui, Julie Bollenbacher-Reilley, Zheng Wu, Rosanne Spolski, Xuefang Jing, Yi-Chen Zhang, J. Philip McCoy, and Warren J. Leonard. 2007. “The Transcription Factor GABP Is a Critical Regulator of B Lymphocyte Development.” *Immunity* 26 (4): 421–31.

Yang, G-X, Z-X Lian, Y-H Chuang, S-A Shu, Y. Moritoki, R. Lan, K. Wakabayashi, et al. 2007. “Generation of Functionally Distinct B Lymphocytes from Common Myeloid Progenitors.” *Clinical and Experimental Immunology* 150 (2): 349–57.

Yang, Quanhe, Sonja A. Rasmussen, and J. M. Friedman. 2002. “Mortality Associated with Down’s Syndrome in the USA from 1983 to 1997: A Population-Based Study.” *The Lancet* 359 (9311): 1019–25.

Yang, Zhong-Fa, Karen Drumea, James Cormier, Junling Wang, Xuejun Zhu, and Alan G. Rosmarin. 2011. “GABP Transcription Factor Is Required for Myeloid Differentiation, in Part, through Its Control of Gfi-1 Expression.” *Blood* 118 (8): 2243–53.

Yang, Zhongfa, Yu Zhu, Rachel Gerstein, and Alan G. Rosmarin. 2015. “GABP Transcription Factor Is Required for B Lymphocyte Maturation and Plasma Cell Development.” *Blood* 126 (23): 1179–1179.

Yokomizo, Tomomasa, Takako Ideue, Saori Morino-Koga, Cheng Yong Tham, Tomohiko Sato, Naoki Takeda, Yoshiaki Kubota, et al. 2022. “Independent Origins of Fetal Liver Haematopoietic Stem and Progenitor Cells.” *Nature* 609 (7928): 779–84.

Yoshida, Toshimi, Samuel Yao-Ming Ng, Juan Carlos Zuniga-Pflucker, and Katia Georgopoulos.

2006. “Early Hematopoietic Lineage Restrictions Directed by Ikaros.” *Nature Immunology* 7 (4): 382–91.

Young, Kira, Sneha Borikar, Rebecca Bell, Lauren Kuffler, Vivek Philip, and Jennifer J. Trowbridge. 2016. “Progressive Alterations in Multipotent Hematopoietic Progenitors Underlie Lymphoid Cell Loss in Aging.” *The Journal of Experimental Medicine* 213 (11): 2259–67.

Young, Kira, Elizabeth Eudy, Rebecca Bell, Matthew A. Loberg, Tim Stearns, Devyani Sharma, Lars Velten, Simon Haas, Marie-Dominique Filippi, and Jennifer J. Trowbridge. 2021. “Decline in IGF1 in the Bone Marrow Microenvironment Initiates Hematopoietic Stem Cell Aging.” *Cell Stem Cell* 28 (8): 1473–82.e7.

Yu, Shuyang, Kairong Cui, Raja Jothi, Dong-Mei Zhao, Xuefang Jing, Keji Zhao, and Hai-Hui Xue. 2011. “GABP Controls a Critical Transcription Regulatory Module That Is Essential for Maintenance and Differentiation of Hematopoietic Stem/progenitor Cells.” *Blood* 117 (7): 2166–78.

Yu, Tao, Zhongyou Li, Zhengping Jia, Steven J. Clapcote, Chunhong Liu, Shaomin Li, Suhail Asrar, et al. 2010. “A Mouse Model of Down Syndrome Trisomic for All Human Chromosome 21 Syntenic Regions.” *Human Molecular Genetics* 19 (14): 2780–91.

Yuan, Joan, Cuong K. Nguyen, Xiuhuai Liu, Chrysi Kanellopoulou, and Stefan A. Muljo. 2012. “Lin28b Reprograms Adult Bone Marrow Hematopoietic Progenitors to Mediate Fetal-like Lymphopoiesis.” *Science* 335 (6073): 1195–1200.

Zaslavsky, Alexander, Stella T. Chou, Keri Schadler, Allyson Lieberman, Maxim Pimkin, Yeo Jung Kim, Kwan-Hyuck Baek, William C. Aird, Mitchell J. Weiss, and Sandra Ryeom. 2013. "The Calcineurin-NFAT Pathway Negatively Regulates Megakaryopoiesis." *Blood* 121 (16): 3205–15.

Zhang, Yong, Tao Liu, Clifford A. Meyer, Jérôme Eeckhoute, David S. Johnson, Bradley E. Bernstein, Chad Nusbaum, et al. 2008. "Model-Based Analysis of ChIP-Seq (MACS)." *Genome Biology* 9 (9): R137.

Zhou, Jianbiao, Siok-Bian Ng, and Wee-Joo Chng. 2013. "LIN28/LIN28B: An Emerging Oncogenic Driver in Cancer Stem Cells." *The International Journal of Biochemistry & Cell Biology* 45 (5): 973–78.

Zhou, Yan, Yue-Sheng Li, Srinivasa Rao Bandi, Lingjuan Tang, Susan A. Shinton, Kyoko Hayakawa, and Richard R. Hardy. 2015. "Lin28b Promotes Fetal B Lymphopoiesis through the Transcription Factor Arid3a." *The Journal of Experimental Medicine* 212 (4): 569–80.

Zhu, Can, Ge Chen, Ying Zhao, Xiao-Ming Gao, and Jun Wang. 2018. "Regulation of the Development and Function of B Cells by ZBTB Transcription Factors." *Frontiers in Immunology* 9 (March): 580.

Zhu, Yanling, Tianyu Wang, Jiaming Gu, Ke Huang, Tian Zhang, Zhishuai Zhang, He Liu, et al. 2020. "Characterization and Generation of Human Definitive Multipotent Hematopoietic Stem/progenitor Cells." *Cell Discovery* 6 (1): 89.

Zipursky, Alvin. 2003. "Transient Leukaemia--a Benign Form of Leukaemia in Newborn Infants

with Trisomy 21." *British Journal of Haematology* 120 (6): 930–38.

Zizka, Zdenek, Pavel Calda, Tomas Fait, Lucia Haakova, Jan Kvasnicka, and Hana Viskova. 2006. "Prenatally Diagnosable Differences in the Cellular Immunity of Fetuses with Down's and Edwards' Syndrome." *Fetal Diagnosis and Therapy* 21 (6): 510–14.

Zuna, Jan, Katerina Muzikova, Anthony M. Ford, Ana Teresa Maia, Ondrej Krejci, Katerina Tousovska, Irina Oravkinova, Mel Greaves, and Jan Trka. 2003. "Pre-Natal, Clonal Origin of Acute Lymphoblastic Leukaemia in Triplets." *Leukemia & Lymphoma* 44 (12): 2099–2102.